

**Maintenance of glutamate homeostasis
in *Bacillus subtilis*
by complex regulatory systems and genomic adaptation**

Dissertation

to acquire the doctoral degree in mathematics and natural science
“Doctor rerum naturalium”
at the Georg-August Universität Göttingen

in the doctoral degree program
Microbiology & Biochemistry
at the Georg-August University School of Science (GAUSS)



submitted by

Miriam Dormeyer

from Hildesheim

Göttingen 2017



Thesis Advisory Committee

PD Dr. Fabian M. Commichau

Institute of Microbiology and Genetics; Department of General Microbiology

Prof. Dr. Jörg Stülke

Institute of Microbiology and Genetics; Department of General Microbiology

Prof. Dr. Christiane Gatz

Schwann-Schleiden Research Center; Department of Plant Molecular Biology and Physiology

Members of the examination board

Referee:

Prof. Dr. Stefanie Pöggeler

Institute of Microbiology and Genetics; Department of Genetics of Eukaryotic Microorganisms

Co-Referee:

Dr. Manfred Konrad

Max-Planck-Institute for Biophysical Chemistry; Enzyme Biochemistry Group

2nd Co-Referee:

Prof. Dr. Stefan Klumpp

Institute for Nonlinear Dynamics; Theoretical Biophysics Group

Date of oral examination: 12th of October 2017



Statement of authorship

I hereby declare that the doctoral thesis entitled “Maintenance of glutamate homeostasis in *Bacillus subtilis* by complex regulatory systems and genomic adaptation” has been written independently and with no other sources and aids than quoted.

Miriam Dormeyer

Danksagung

Vielen Dank Fabian, dass ich meine Doktorarbeit in deiner Abteilung anfertigen durfte und für die hilfreichen Diskussionen. Ich habe in der Zeit wirklich sehr viel gelernt, aber auch sehr viel Spaß gehabt. Besonders habe ich mich gefreut, dass ich auf so viele Tagungen mitkommen durfte, so viel gesehen und so viele besondere Menschen kennen gelernt habe! Jedes Mal hatte ich gehörigen Respekt vor den Präsentationen, aber es hat sich wirklich gelohnt. Die zahllosen durchgefeierten Nächte in Göttingen, in Montecatini, am Mittelmeer in Tirrenia, in Bad Bergzabern, an der Ostsee in Usedom und in Berlin werde ich wohl nie vergessen! Aber Achtung: wer feiern kann, kann auch arbeiten und genau so war es richtig! Jörg, auch dir gebührt besonderer Dank, immer wenn ich doch sehr an mir gezweifelt habe, hast du mich in meiner Arbeit und meinem Handeln bestärkt. Aber ich finde, dass du nicht nur als Professor und Redner herausragende Fähigkeiten hast, sondern wie ich erfahren durfte, bist du wahrscheinlich für jede europäische Großstadt ein kompetenter Stadtführer! Besonders an den, ab Dezember wöchentlichen, Führungen über den Göttinger Weihnachtsmarkt habe ich immer gern teilgenommen! Auch möchte ich Ihnen, Frau Gatz für Ihr Interesse und Ihre tatkräftige Teilnahme an meinen TAC meetings danken. Schon während meiner Bachelorarbeit, habe ich Ihre offene und neugierige Art sehr geschätzt. Sabine, dir möchte ich von ganzem Herzen danken. Du hast mich immer ermutigt und hattest immer ein offenes Ohr! Danke, dass du immer so schnell durch meine unendlich langen Klonierungs- und LacZ-Listen durchgestiegen bist, ggf. Lücken und Ungereimtheiten meinerseits gefüllt hast und oft alles schneller umgesetzt hast, als ich auswerten konnte! Ich werde unsere herausragende Zusammenarbeit und vor allem dich sehr vermissen! Cedric, dir kann ich gar nicht genug danken. Mit dir kann man jeden Blödsinn machen, Probleme wegtanzen und einfach man selbst sein. Danke, dass du immer da warst und mir gerade auch in den letzten Wochen mit deinen Nerven aus Stahl so zur Seite gestanden hast! Du bist ein wunderbarer Mensch und ich freue mich jeden Tag, dass wir nach der Weihnachtsfeier im Zug aus Goslar noch so albern über deinen Einzug bei mir rumgewitzelt haben. Da hatten wir die erste wirklich gute Idee, der noch viele folgten. Lorena, wir haben schon so unfassbar vieles gemeinsam erlebt, danke, dass du immer für mich da bist! Es war eine große Ehre für mich in deine Fußstapfen treten zu dürfen! In diesem Zuge möchte ich auch Katrin danken! Katrin, ich kenne niemanden der mit so viel Geduld und Spaß Wissen vermitteln kann, wie du. Egal ob ich ein technisches oder fachliches Problem hatte, so hattest du schon die Lösung parat. Und ehrlich mal, Christina und Katrin, was hatten wir für einen Spaß in Berlin! Christina, dir als unserer Labormutti möchte ich auch danken. Du hast mir mit einer Engelsgeduld jeden Primer, den ich doch noch vergessen hatte, aus dem Freezer geholt. Danke auch dafür, dass ich mit jedem erdenklichen Problem zu dir kommen durfte und du mich immer bestärkt hast! Anika, ich freue mich wirklich, dass wir Freunde geworden sind! Du hast mir Cedric schmackhaft geredet und mich hast du Cedric schmackhaft geredet UND hast uns dann auch noch gemeinsam auf vielen Weinabenden ertragen. Ich bin mir übrigens ganz sicher, dass diese ganzen Jive Flaschen in meinem Schrank dir gehören! Aber auch fachlich schätze ich deine Meinung sehr, du denkst oft um die Ecke und hast mir oft geholfen, vielen Dank dafür! Ein großer Dank geht natürlich auch an die HIF, besonders an Joni, Johannes und Michael für die vielen interessanten Fachsimpeleien. Dabei möchte ich dir, Joni, für die gesanglichen Beiträge danken, die dank deiner Lautstärke bestimmt nicht nur wir genießen durften. Es hat wirklich viel Spaß gemacht mit euch zu arbeiten! Dabei ist natürlich auch die LIF gemeint! Ich werde euch alle

vermissen. Auch den Kollegen aus Jülich möchte ich meinen Dank aussprechen! Danke Dietrich, Alex, Eugen, Eugen, Agnes, Nadja, Anika und Loreen, dass ihr mich so herzlich aufgenommen habt! Ich hatte sehr viel Spaß bei euch! Auch wenn es nicht immer leicht war in Jülich nach 20:00 Uhr noch etwas zu essen oder gar zu trinken zu finden, nicht wahr Alex? Das muss gut geplant sein! Ansonsten geht's ab zu Eugen, der hat immer White Russian und Muffins parat. Danke dafür, Eugen!

Mama, Papa, Oma, Opa, Marion und meinen Brüdern möchte ich für ihre Unterstützung während meines ganzen Studiums danken! Ihr seid immer für mich da gewesen, habt mich immer ermutigt und unterstützt, egal was ich mir in den Kopf gesetzt hatte. Gerade in den letzten Jahren habe ich gelernt, dass dies ohne euch nicht möglich gewesen wäre! Otto, ich freue mich so sehr, dass Opa dich uns vorgestellt hat! Für mich gehörst du zur Familie! Danke, dass du mich auf deine einzigartig charmante Art immer unterstützt und zum Lächeln gebracht hast. Sarah, danke dass du mich so wunderbar vom Laboralltag abgelenkt hast, ohne dich hätte ich so manches Abenteuer verpasst. Dann hätte ich mich nämlich auf den mittlerweile 12000 km Road-Trip nicht so oft verfahren! Du bist ein ganz besonderer Mensch, lass dich bloß nicht von deinem Weg abbringen. Steffi, dir möchte ich auch danken, wir beide sind schon so ein Dreamteam und das werden wir auch bleiben, nicht nur beim Kickern. Ich freu mich schon auf's nächste Oktoberfest! Mein Dank gilt auch dem Rest der Rasselbande, die mich auf meinem Weg begleitet und unterstützt hat.

Table of Contents

Table of Contents

STATEMENT OF AUTHORSHIP	III
DANKSAGUNG	IV
TABLE OF CONTENTS	VI
LIST OF PUBLICATIONS	IX
ABBREVIATIONS	X
GENERAL	X
UNITS	XI
PREFIXES	XI
NUCLEOSIDES	XI
AMINO ACID NOMENCLATURE	XI
SUMMARY	XII
1. INTRODUCTION	1
1.1. <i>BACILLUS SUBTILIS</i>	1
1.2. GLOBAL REGULATORS	1
1.2.1. CARBON CATABOLITE REPRESSION IN <i>B. SUBTILIS</i>	1
1.2.2. THE GLOBAL NITROGEN REGULATOR TNRA	4
1.2.3. REGULATION OF TRANSITION STATE GENES	5
1.3. GLUTAMATE HOMEOSTASIS IN <i>B. SUBTILIS</i>	5
1.3.1. GLUTAMINE SYNTHETASE GLNA	7
1.3.2. GLUTAMATE SYNTHASE GLTAB	7
1.3.3. GLUTAMATE DEHYDROGENASES GUDB/ROCG	9
1.4. HIGH FREQUENCY MUTAGENESIS OF <i>GUDB^{CR}</i> GENE	12
1.4.1. COLLISIONS OF THE REPLICATION AND TRANSCRIPTION MACHINERIES	12
1.4.2. TRANSCRIPTION-COUPLED STATIONARY-PHASE MUTAGENESIS	17
1.4.3. DNA/RNA STRAND SLIPPAGE	18
1.5. VISUALIZATION OF EMERGING MUTATIONS	19
1.6. OBJECTIVES	21
2. MATERIALS & METHODS	22

2.1. MATERIALS	22
2.1.1. BACTERIAL STRAINS AND PLASMIDS	22
2.1.2. GROWTH MEDIA	22
2.2. METHODS	23
2.2.1. GENERAL METHODS	23
2.2.2. CULTIVATION OF BACTERIA	23
2.2.3. GENETIC MODIFICATION OF BACTERIA	24
2.2.4. PREPARATION AND DETECTION OF DNA	24
2.2.5. PREPARATION & DETECTION OF PROTEINS	28
2.2.6. DETECTION OF MUTATION FREQUENCIES	31
2.2.7. BACTERIAL ADENYLATE CYCLASE-BASED TWO-HYBRID SYSTEM	32
2.2.8. MICROFLUIDIC ANALYSIS	33
3. RESULTS	35
3.1. THE MECHANISMS OF <i>GUDB^{CR}</i> MUTAGENESIS	35
3.1.1. THE CELL DENSITY INFLUENCES THE TR MUTAGENESIS	35
3.1.2. TWO MACHINERIES ARE INVOLVED IN INTRA- AND INTERGENIC TR MUTAGENESIS	35
3.1.3. PUTATIVE FACTORS	40
3.2. THE ACTIVATOR/REPORTER SYSTEM	44
3.2.1. ANALYSIS OF EMERGING MUTATIONS	45
3.2.2. MUTATIONS ON THE LEVEL OF SINGLE CELLS	46
3.2.3. INVESTIGATION OF SUBSTITUTIONS	48
3.2.4. INVESTIGATION OF AMPLIFICATIONS	48
3.2.5. INDUSTRIAL APPLICATION OF THE ACTIVATOR/REPORTER SYSTEM	52
3.3. GLTC-INDEPENDENT TRANSCRIPTION OF <i>GLTAB</i> GENES	58
3.3.1. A SELECTION AND SCREENING SYSTEM	58
3.3.2. ANALYSIS OF SUPPRESSOR MUTANTS	59
3.3.3. HIERARCHY OF MUTATIONS	63
3.4. GLTC – A DEVIL IN DISGUISE	64
3.4.1. THE ROCG-GLTC-DNA COMPLEX	64
3.4.2. ONLY <i>B. SUBTILIS</i> GDHS HAVE METABOLIC AND REGULATORY TREATS	69
3.4.3. THE DIFFERENCE OF <i>GUDB⁺</i> AND ROCG	69
4. DISCUSSION	72
4.1. WHAT DOES <i>B. SUBTILIS</i> NEED TO ACHIEVE HIGHEST FITNESS LEVELS?	72
4.2. REGULATION OF THE <i>GLTAB</i> GENES	73
4.2.1. ACTIVATION OF <i>GLTAB</i> GENE EXPRESSION	73
4.2.2. PREVENTION OF <i>GLTAB</i> GENE EXPRESSION	73

Table of Contents

4.2.3.	THE INTERPLAY OF BOX III AND ROCG TO ENSURE <i>GLTAB</i> GENE REGULATION	75
4.2.4.	THE HIGH IMPACT OF CO-FACTORS	77
4.2.5.	THE IMPORTANCE OF UNTAGGED PROTEINS	79
4.3.	TWO GDHS, ONE GLTC, TWO EVOLUTIONARY ROUTES?	80
4.3.1.	DIFFERENT REGULATION OF GLTC VARIANTS VIA ROCG AND GUDB	80
4.3.2.	THE PHYSIOLOGICAL ASPECT OF GLTC REGULATION VIA ROCG AND GUDB	81
4.3.3.	THE EVOLUTIONARY ASPECT OF GLTC REGULATION VIA ROCG AND GUDB	82
4.4.	TR MUTAGENESIS, SEVERAL MACHINERIES?	86
5.	REFERENCES	89
6.	APPENDIX	101
6.1.	SUPPLEMENTARY INFORMATION	101
6.2.	MATERIALS	104
6.2.1.	CHEMICALS	104
6.2.2.	ANTIBODIES	104
6.2.3.	ENZYMES	104
6.2.4.	COMMERCIAL SYSTEMS	104
6.2.5.	EQUIPMENT	105
6.2.6.	DISPENSABLE EQUIPMENT	105
6.3.	OLIGONUCLEOTIDES	106
6.3.1.	OLIGONUCLEOTIDES CONSTRUCTED IN THIS WORK	106
6.3.2.	OTHER OLIGONUCLEOTIDES USED IN THIS WORK	114
6.4.	BACTERIAL STRAINS	116
6.4.1.	<i>B. SUBTILIS</i> STRAINS CONSTRUCTED IN THIS WORK	116
6.4.2.	<i>B. SUBTILIS</i> STRAINS USED IN THIS WORK	126
6.4.3.	<i>E. COLI</i> STRAINS USED IN THIS WORK	128
6.5.	PLASMIDS	129
6.5.1.	PLASMIDS CONSTRUCTED IN THIS WORK	129
6.5.2.	PLASMIDS USED IN THIS WORK	131
6.6.	BIOINFORMATIC SOFTWARE	132
7.	CURRICULUM VITAE	133

List of publications

Dormeyer, M., Egelkamp, R., Thiele, M.J., Hammer, E., Gunka, K., Stannek, L., Völker, U. & Commichau, F. M. (2015). Another engineering tool in the *Bacillus subtilis* toolbox: inducer-free activation of gene expression by selection-driven promoter decryptification. *Microbiology* **161**: 354-361

Commichau, F. M., Alzinger, A., Sande, R., Bretzel, W., Reuß, D. R., **Dormeyer, M.**, Chevreux, B., Daniel, R., Akeroyd, M., Wyss, M., Hohmann, H.-P. & Prágai, Z. (2015). Engineering *Bacillus subtilis* for the conversion of the antimetabolite 4-hydroxy-L-threonine to pyridoxine. *Metab Eng* **29**: 196-207.

Dormeyer, M., Lübke, A.L., Müller, P., Lentjes, S., Reuß, D.R., Thürmer, A., Stülke, J., Daniel, R., Brantl, S., Commichau, F.M. (2017). Hierarchical mutational events compensate for glutamate auxotrophy of a *Bacillus subtilis* *gltC* mutant. *Environ Microbiol Rep* **3**: 279-289.

Abbreviations

General

% (vol/vol)	% (volume/volume)	LFH	long flanking homology
% (wt/vol)	% (weight/volume)	MMR	multiple mutation reaction/ mismatch repair
AP	alkaline phosphatase	NAD ⁺	nicotinamide-adeninedinucleotide
APS	ammonium persulfate	NADH ₂	nicotinamide-adeninedinucleotide (reduced form)
ATP	adenosine triphosphate	Ni ²⁺ -NTA	nickel-nitriloacetic acid
<i>B.</i>	<i>Bacillus</i>	OD _x	optical density, measured at wave length $\lambda = x$ nm
CCR	carbon catabolite repression	P	promoter
CDP*	disodium 2-chloro-5-(4- methoxyspiro{1,2-dioxetane-3,2'- (5'chloro)tricyclo[3.3.1.1 ^{3,7}]decan}- 4-yl)phenyl phosphate	PAA	polyacrylamide
CE	crude extract	PAGE	polyacrylamide gel electrophoresis
del	deletion	PBS	phosphate buffered saline
dH ₂ O	deionized water	PCR	polymerase chain reaction
DIG	digoxigenin	pH	power of hydrogen
DMSO	dimethyl sulfoxide	PLP	pyridoxal-5'-phosphate
DNA	deoxyribonucleic acid	rev	reverse
dNTP	deoxyribonucleosidtriphosphate	RNA	ribonucleic acid
dpi	days past inoculation	RNase	ribonuclease
<i>E.</i>	<i>Escherichia</i>	rpm	rounds per minute
<i>et al.</i>	<i>et alia</i>	RT	room temperature
Fig.	figure	SD	shine dalgarno
FT	flow through	SDS	sodium dodecyl sulfate
fwd	forward	SM	suppressor mutant
gDNA	genomic DNA	SP	sporulation medium
GFP	green fluorescence protein	Tab.	table
<i>goi</i>	gene of interest	TAE	tris-(hydroxymethyl)- aminomethan
HR	homologous recombination	TEMED	N,N,N',N'-tetramethylethyldiamine
ins	insertion	TF	transcription factor
IPTG	isopropyl-1-thio- β -D-galactoside	w/o	without
kan	kanamycin	WT	wild type
LB	lysogenic broth	X-Gal	5-bromo-4-chloro-indolyl- galactopyranoside

Units

°C	degree Celsius
A	ampere
bar	bar
Da	dalton
g	gram
h	hour
l	liter
m	meter
min, m	minute
Mol	mol
M	molar
s	second
V	volt
bp	base pairs

Prefixes

M	mega
k	kilo
m	milli
μ	micro
n	nano
p	pico

Nucleosides

A	adenine
C	cytosine
G	guanine
T	thymine
U	uracil

Amino acid nomenclature

A	Ala	alanine
C	Cys	cysteine
D	Asp	aspartate
E	Glu	glutamate
F	Phe	phenyl alanine
G	Gly	glycine
H	His	histidine
I	Ile	isoleucine
K	Lys	lysine
L	Leu	leucine
M	Met	methionine
N	Asn	asparagine
P	Pro	proline
Q	Gln	glutamine
R	Arg	arginine
S	Ser	serine
T	Thr	threonine
Y	Tyr	tyrosine
V	Val	valine
W	Trp	trpytophan

Summary

The Gram-positive model organism *Bacillus subtilis* lives in the soil and must cope with a constantly changing environment. Glutamate plays an important role in cellular metabolism, because it is the major amino group donor and it serves as a precursor for proline, which is an osmoprotectant in *B. subtilis*. The reactions involved in anabolism and catabolism of glutamate represent an important metabolic node, linking carbon to nitrogen metabolism. The glutamine synthetase (GS) and the glutamate synthase (GOGAT) forming the GS-GOGAT cycle, are responsible for nitrogen assimilation in *B. subtilis*. The GS uses ATP to produce glutamine from ammonium and glutamate and the GOGAT catalyzes the conversion of glutamine and α -ketoglutarate to two molecules of glutamate. The glutamate dehydrogenase (GDH) is strictly catabolically active and oxidizes glutamate to ammonium and α -ketoglutarate. To ensure a constantly high level of glutamate, the anabolic and catabolic reactions involved in glutamate metabolism have to be tightly controlled by signals derived from nitrogen and carbon metabolism. Perturbation of glutamate homeostasis causes a severe growth defect of *B. subtilis*. To adjust glutamate synthesis to the cellular demand for glutamate, expression of the GOGAT encoding *gltAB* genes is strictly controlled. This is achieved by controlling the DNA-binding activity of the transcription factor GltC, which regulates expression of the *gltAB* genes. It was found *in vivo* that the GDH RocG in *B. subtilis* can bind GltC in the presence of glutamate and thereby prevents the expression of the *gltAB* genes and the emergence of a futile cycle of glutamate synthesis and degradation. *In vitro*, it was found that GltC, which prevents the RNAP from transcribing the *gltAB* genes acts as a glutamate-dependent repressor. In this work, it is shown

that RocG triggers the repressor function of GltC resulting in the formation of a RocG-GltC complex that binds to the promoter of the *gltAB* genes. This model combines the two existing models for the regulation of the *gltAB* genes to one consistent model. The disturbance of this highly complex regulation results in a severe growth defect. For instance, a RocG deficient strain cannot degrade glutamate, resulting in the accumulation of glutamate. The accumulation of glutamate is prevented in rapidly emerging suppressor mutants (SM) that have mutated the *gudB^{CR}* gene. In the *B. subtilis* laboratory strain 168, the *gudB^{CR}* gene harbors a tandem repeat (TR) and encodes for a second inactive GDH. The excision of one TR unit leads to the activation of the *gudB* gene encoding the active GDH GudB that can fully replace RocG. In this work, the influence of several factors on the TR mutagenesis of the *gudB* gene is investigated. In contrast to a RocG deficient strain, a GltC deficient strain cannot produce the GOGAT and consequently it does not synthesize glutamate. In this work, a selection and screening system is used to show that several classes of mutations can compensate for glutamate auxotrophy. Class I mutants harbored promoter-up mutations in the promoter of the *gltAB* genes. In class II mutants the *gltR* gene acquired a single mutation and the resulting GltR24 protein replaces GltC. The majority of SMs were class III mutants, harboring multiple copies of the *gltAB* genes to increase the cellular amount of the GOGAT.

To conclude, a genetic approach was employed to generate a novel and consistent model describing the control of glutamate biosynthesis in *B. subtilis*. This work also revealed that *B. subtilis* mutants with defects in glutamate metabolism flexibly respond to perturbation of glutamate homeostasis at the level of the genome.

1. Introduction

1.1. *Bacillus subtilis*

The soil bacterium *Bacillus subtilis* belongs to the phylum Firmicutes. It is a model organism for Gram-positive bacteria. As it is generally regarded as safe (GRAS status), it serves also as model organism for pathogenic bacteria like *Bacillus anthracis*. For *B. subtilis* many well established tools for genetic manipulation are available (Blötz *et al.*, 2017) and already in 1997, the complete genome of *B. subtilis* was sequenced (Kunst *et al.*, 1997). Moreover, information about all genes, as well as regulatory and metabolic interconnections within *B. subtilis* are easily accessible via the online tool *SubtiWiki* (www.subtiwiki.uni-goettingen.de) (Michna *et al.*, 2016). This immense number of working tools and information makes *B. subtilis* attractive for many researchers. In *SubtiWiki* alone are about 170 labs listed working with *B. subtilis* (Michna *et al.*, 2016). For example, *B. subtilis* is used to investigate the basic question about what is needed for life. To solve this question, the *B. subtilis* genome is already reduced by 36 % and extensively analyzed via an multiomics approach (Reuß *et al.*, 2017). Furthermore, novel targets for antibiotics could be identified in *B. subtilis*. For instance, the essential function of c-di-AMP only occurring in Gram-positive bacteria was discovered, making several novel enzymes attractive as new targets for antibiotics (Gundlach *et al.*, 2017). However, *B. subtilis* is also of great interest for industry. It is the main producer of poly- γ -glutamic acid (natto) and the efficiency of natto production is continuously improved (Zhang *et al.*, 2014; Feng *et al.*, 2015; Cai *et al.*, 2017). Moreover, its ability to take up ammonia from the environment makes *B. subtilis* suitable as plant growth promoter in food production using systems with lettuce and fish (Cerozi and Fitzsimmons, 2016). In conclusion,

B. subtilis plays a central role in academic and industrial science.

1.2. Global regulators

To cope with changing environmental conditions, there are plenty of transcriptional regulators taking care of optimal gene expression to ensure the most efficient usage of nutrients and enable fast growth. For instance, there are transcription factors regulating the expression of only one gene as it is the case for the transcriptional activator GltC of the *gltAB* glutamate synthase genes. Moreover, in many cases several enzymes must be active simultaneously. For instance, during nitrogen limitation TnrA activates gene expression of all enzymes taking part in ammonium assimilation and further processing. Another example is CcpA (catabolite control protein A), which represses in the presence of glucose, the activity of catabolic pathways for the utilization of other carbon sources to increase the efficiency of energy production. These comprehensive and overlapping regulations are done by global regulators like CcpA, CodY, TnrA, and GlnR (Fig. 1.1) (Sonenshein, 2007).

1.2.1. Carbon catabolite repression in *B. subtilis*

In natural environments *B. subtilis* is exposed to a variety of carbon and nitrogen sources. Some carbon sources are highly energetic and easier to metabolize. *B. subtilis* selectively uses the most efficient carbon sources to ensure high growth rates. As long as the preferred carbon source glucose is present, carbon catabolite repression (CCR) inhibits expression of genes involved in the usage of other secondary carbon sources (Stülke and Hillen, 2000). The constitutively expressed *trans*-acting factor CcpA is the major CCR regulator in *B. subtilis* and binds in the presence of glucose to the catabolite

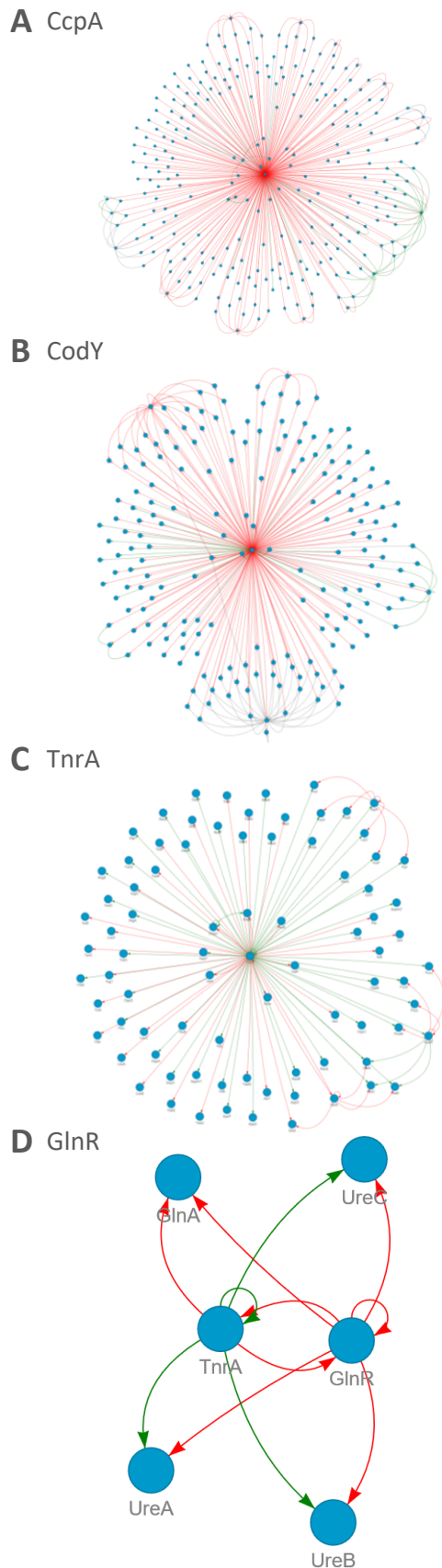


Fig. 1.1 Regulons of CcpA, CodY, TnrA and GlnR
Regulons consist of 278, 228, 88, and 6 genes for CcpA (A), CodY (B), TnrA (C) and GlnR (D), respectively. Positive (green) and negative (red) regulation is indicated by arrows. Data derived from *SubtiWiki* (Michna *et al.*, 2016).

responsive element (*cre*), a *cis*-acting palindromic sequence (Miwa *et al.*, 1994; Stülke and Hillen, 2000). Thereby, genes involved in the utilization of secondary carbon sources are repressed (Blencke *et al.*, 2003). CCR is present in most bacterial species, though its mechanism is slightly different between species, the outcome is the same and about 5-10 % of bacterial genes are regulated by CCR, indicating its importance (Görke and Stülke, 2008). In *B. subtilis* and *E. coli* this phenomenon is well studied, and mediated in different manners by the phosphoenolpyruvate-carbohydrate phosphotransferase system (PTS). The core of the PTS consists of the enzyme I (EI), the enzyme II (EII) having the subunits A, B, and C, and the histidine kinase HPr (Fig. 1.2). To prevent glucose from diffusion out of the cell, it is phosphorylated during its uptake by the EII protein complex. Glucose-6-phosphate is catabolized to two molecules of phosphoenolpyruvate via the glycolysis. One molecule is used to feed into the PTS, thereby the EI protein is phosphorylated and in turn phosphorylates the histidine residue of HPr. HPr-(His-P) in turn phosphorylates the EIIA subunit and this phosphate group is subsequently transferred to the EIIB subunit to phosphorylate a new glucose molecule (Fig. 1.2) (Görke and Stülke, 2008).

The phosphorylation state of HPr depends on the metabolic conditions within the cell, allowing a fast reaction on the protein level to changing conditions. HPr can be phosphorylated either on the Ser46 via EI within the PTS or on the His15 via the histidine kinase/phosphorylase (HPrK). In the presence of good carbon sources as glucose, the HPrK phosphorylates HPr on the serine residue (Nessler *et al.*, 2003). Acting as an effector HPr-(Ser-P) binds to two CcpA proteins and causes a conformational change enabling CcpA to bind to the *cre* site (Görke and Stülke, 2008). This activation of the CCR is enhanced by the presence of glucose-6-phosphate and fructose-

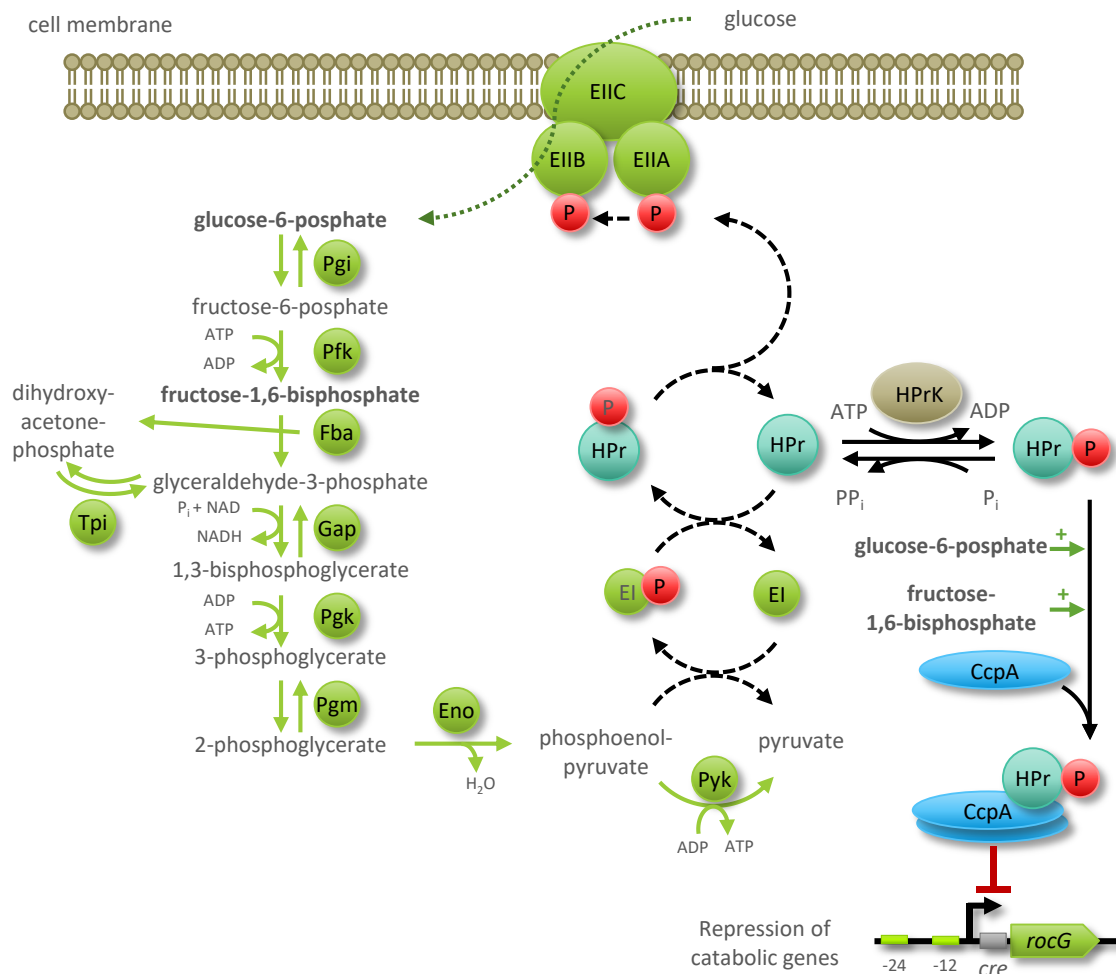


Fig. 1.2 Interplay of PTS, glycolysis and CcpA regulation

Glucose uptake is mediated by the EII protein complex and thereby phosphorylated. Glucose-6-phosphate is degraded via glycolysis into two molecules of phosphoenolpyruvate. One of them is used to phosphorylate the EI protein and the phosphate group is transferred by the phosphorylation chain via the HPr kinase (HPr(His-P)), the EIIA and EIIB complex to a novel glucose molecule. Under high concentration of ATP and fructose-1,6-bisphosphate other carbohydrates than glucose are not necessary for *B. subtilis*, therefore the HPr kinase/phosphorylase (HPrK) phosphorylates HPr. The resulting HPr(Ser-P) activates in the presence of glucose-6-phosphate and fructose-1,6-bisphosphate the CcpA protein, a global regulator of CCR. Binding of CcpA to *cre* sites represses or induces genes important for CCR, as for instance the expression of the *rocG* gene is prevented and glutamate cannot be used as carbon source in the presence of glucose (Belitsky *et al.*, 2004). When the environmental conditions change and low ATP and high inorganic P_i concentrations are present in the cell, HPrK dephosphorylates HPr(Ser-P) to stop CCR. Abbreviations for enzymes from glycolysis: Pgi - phosphoglucose isomerase, Pfk - phosphofruktokinase, Fba - fructose-1,6-bisphosphate aldolase, Tpi - triosephosphate isomerase, Gap - glyceraldehyde-3-phosphate dehydrogenase, Pgg - phosphoglycerate kinase, Pgm - phosphoglycerate mutase, Eno - enolase; Pyk - pyruvate kinase. Dashed arrows: phosphotransfer within the PTS; green arrows: glycolysis. Adapted from (Deutscher *et al.*, 2006; Görke and Stülke, 2008).

1,6-bisphosphate (Schumacher *et al.*, 2007; Deutscher, 2008). The active CcpA transcription factor can act as a transcriptional repressor or activator depending on the location of the *cre* site (Görke and Stülke, 2008). One example is the CcpA mediated repression of the *rocG* gene encoding for a glutamate dehydrogenase, thereby CcpA binds to the *cre* site behind the transcription start site preventing transcription initiation (see also Ch. 1.3.3). Under conditions that do not initiate CCR in *B. subtilis*, for instance

in the absence of glucose, but the presence of succinate (Blencke *et al.*, 2003), HPrK dephosphorylates HPr(His-P) and thereby actively stops CcpA mediated CCR (Fig. 1.2). Besides the CcpA dependent repression, common mechanisms for CCR in *B. subtilis* are inducer prevention and antitermination mediated by PTS-regulatory domains and the presence of HPr(His-P) (Stülke *et al.*, 1998; Stülke and Hillen, 2000). Though differently, both mechanisms lead to the activation of catabolic

operons of secondary carbon sources. This shows the immense reach of the CCR to render *B. subtilis* metabolism to be most efficient.

1.2.2. The global nitrogen regulator TnrA

TnrA is the global transcription factor of nitrogen metabolism, regulates 88 genes (Fig. 1.1 C), and was shown to bind to 42 regions on the chromosome *in vivo* (Mirouze *et al.*, 2015). Besides TnrA, the major components of the nitrogen regulatory network are the transcriptional repressor GlnR and the glutamine synthetase (GS) (Fisher, 1999). GlnR and TnrA form an own new family of transcription factors, the TnrA/GlnR family (Schumacher *et al.*, 2015). TnrA is active during nitrogen limitation to activate genes involved in utilization of secondary nitrogen sources as nitrate, nitrite, and urea, whereas GlnR is active during nitrogen excess inactivating those genes (Fig. 1.1 D) (Fisher, 1999; Detsch and Stülke, 2003). Remarkably, in *glnA* deficient strains the GlnR- and TnrA-regulated genes are expressed constitutively, indicating the importance of GS in GlnR and TnrA functionality (Fisher and Wray, 2008).

TnrA was originally identified in a transposon screen to find mutants unable to express the *nrgAB* genes (Wray *et al.*, 1996). The *nrgAB* genes are indeed activated by TnrA under nitrogen limitation to take care of ammonium uptake into the cell (Gunka and Commichau, 2012). The *nrgAB* genes encode for the AmtB ammonium transporter and the GlnK regulatory P_{II} like protein, respectively. At high pH ammonia diffuses into the cell independent of any uptake system, but at low pH the equilibrium is shifted to ammonium, which needs to be actively imported into the cell. AmtB is the major ammonium transporter in *B. subtilis* and GlnK co-localizes with AmtB at the cell membrane, but is not necessary for ammonium transport (Fig. 1.3

A) (Detsch and Stülke, 2003). *In vitro* studies showed that TnrA binds to AmtB-bound GlnK depending on the absence of ATP (Heinrich *et al.*, 2006; Kayumov *et al.*, 2011). Recent studies suggested that the ammonium channel is blocked under excess of nitrogen (Schumacher *et al.*, 2015). Under nitrogen limitation, GlnK stabilizes TnrA in its dimeric form, supporting the TnrA mediated activation of genes required for nitrogen acquisition (Fig. 1.1 C, D, Fig. 1.3) (Heinrich *et al.*, 2006; Kayumov *et al.*, 2011; Schumacher *et al.*, 2015). In the absence of glutamine and the presence of ammonium, the *glnRA* operon is expressed. The synthesized GS is present in its ATP-bound dodecameric form and catalyzes the ATP-dependent condensation of glutamate with ammonium to glutamine (Fig. 1.3 A), but is unable to bind TnrA (Hauf *et al.*, 2016).

However, *in vitro* and *in vivo* investigations showed that under excess of nitrogen GS is locked in its feedback-inhibited state (FBI) by glutamine (Murray *et al.*, 2013; Hauf *et al.*, 2016). TnrA can bind to FBI-GS, which leads to a conformational change of the GS to a tetrameric form inactivating its metabolic function and the DNA binding properties of TnrA (Fig. 1.3 E) (Wray *et al.*, 1996; Wray *et al.*, 2001; Schumacher *et al.*, 2015). As TnrA positively regulates its own expression (Fig. 1.1 C, D) (Fisher, 1999), the *tnrA* gene is not expressed under excess of nitrogen. Furthermore, the feedback-inhibited GS functions as chaperone and enhances the dimer formation and DNA-binding activity of GlnR. This leads to self-repression of the *glnRA* genes and additional repression of the transcription factor TnrA (Fig. 1.3 B, E) (Brown and Sonenshein, 1996; Wray *et al.*, 2001; Fisher and Wray, 2008; Schumacher *et al.*, 2015). To conclude, the conformational state of the trigger enzyme GS reflects the energy and nitrogen state of the cell via competitive, alternative binding by ATP and glutamine. This results in activation or

inactivation of the global regulator of nitrogen metabolism TnrA, respectively (Hauf *et al.*, 2016).

1.2.3. Regulation of transition state genes

The global regulator CodY modulates the transition from exponential growth to stationary growth and sporulation by sensing the GTP pool within the cell, allowing adaptation to nutrient limitation (Ch. 1.1) (Ratnayake-Lecamwasam *et al.*, 2001). Being activated by the presence of GTP or branched-chain amino acids (BCAAs), CodY represses regulatory genes for sporulation, genes encoding for amino acid and sugar transporters and genes for BCAA synthesis (Molle *et al.*, 2003; Shivers and Sonenshein, 2004). In a recent study in *Listeria monocytogenes*, CodY was shown to directly repress the *glnR* and activate the *gdhA* genes encoding for a transcriptional repressor involved in nitrogen metabolism and the glutamate dehydrogenase, respectively (Lobel and Herskovits, 2016). Furthermore, the CodY-dependent activation and inhibition of genes occurs in rich and minimal medium, in the presence and absence of BCAAs in *L. monocytogenes* (Lobel and Herskovits, 2016). Based on RNA-Seq analyses, it was shown that genes involved in nitrogen and arginine metabolism were up-regulated in rich medium except the *gdhA* gene which was down-regulated. In minimal medium, the *gdhA* gene was still repressed and the glutamine synthase gene *glnA* still activated, but none of the other genes but the genes encoding for the glutamate decarboxylase were regulated anymore by CodY (Lobel and Herskovits, 2016). Even though there is a regulatory impact of CodY on 228 genes for *B. subtilis* (Fig. 1.1), this study in *L. monocytogenes* reveals a much greater impact on global and overlapping regulation of

metabolic and lifestyle regulating genes as investigated so far.

1.3. Glutamate homeostasis in *B. subtilis*

Glutamate is of great importance as it is the most abundant metabolite in all organisms and its homeostasis is strictly controlled (Gunka and Commichau, 2012). It stands right at the intersection between nitrogen and carbon metabolism, serves as nitrogen storage molecule (Brunhuber and Blanchard, 1994) and acts as the major amino group donor in the cell for over than 37 transaminase reactions, including the formation of nucleotides and amino acids (Oh *et al.*, 2007). Thereby, it serves also as precursor of the *B. subtilis* osmoprotectant proline (Fig. 1.3) (Brill *et al.*, 2011). Under conditions of carbon limitation glutamate is catabolized to α -ketoglutarate and serves as carbon source. This is for instance important for the virulence of *Staphylococcus aureus* during abscess formation, because the major nutrition is based on proline and metabolites of the arginine degradation pathway which are highly abundant in the animal derived collagen (Halsey *et al.*, 2017). Moreover, glutamate is involved in the formation of biofilms, as glutamate oscillations can be used to investigate growth synchronizations through electrical signaling between two distinct *B. subtilis* biofilms (Liu *et al.*, 2015; Liu *et al.*, 2017). Besides, the glutamate dehydrogenases RocG and GudB are of great industrial interest as they use the cheap cofactors NAD⁺ and NADH instead of NADP⁺ and NADPH (Spaans *et al.*, 2015). The enzyme is well studied with regards to the specific glutamate binding pocket and initial attempts were made using molecular evolutionary engineering to render the substrate specificity towards other metabolites as oxaloacetate and to increase the temperature stability of a GDH that can be functionally

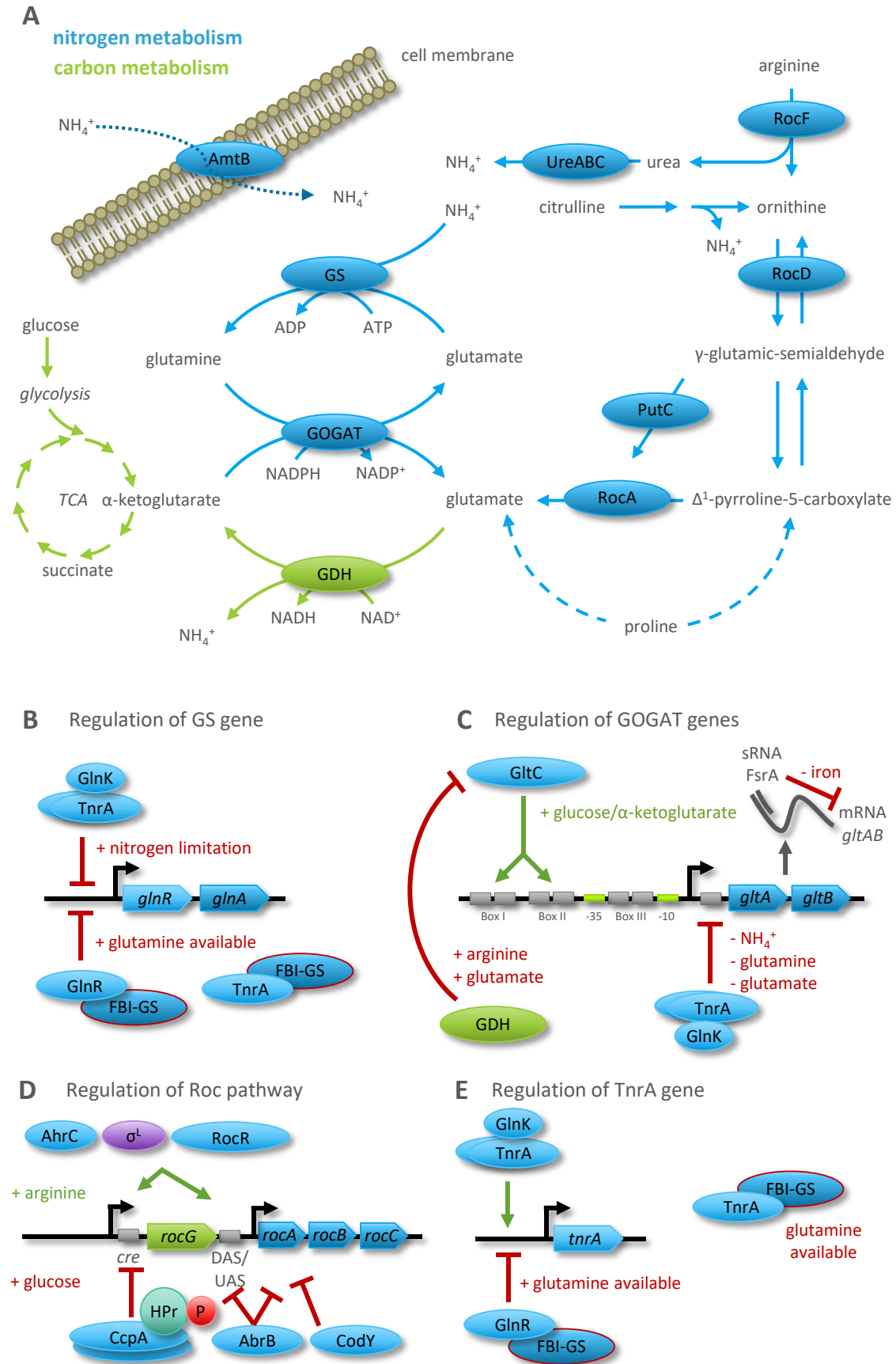


Fig. 1.3 Glutamate metabolism and regulation in *B. subtilis*

A: Overview of the nitrogen metabolism in *B. subtilis*. In the GS-GOGAT cycle, ammonium is assimilated via the glutamine synthetase (GS) and glutamate is produced by the glutamate synthase (GOGAT). Glutamate degradation is mediated by the glutamate dehydrogenase (GDH) GldB or RocG. Enzymes involved in ammonium uptake and arginine degradation: **AmtB** – Ammonium uptake

protein, **RocF** – arginase, **UreABC** – urease, **RocD** – ornithine transaminase, **RocA** – Δ^1 -pyrroline-5-carboxylate dehydrogenase. Blue arrows indicate metabolic pathways belonging to the nitrogen metabolism and green arrows for the carbon metabolism. The dashed line indicates, where proline degradation pathway feeds into the arginine degradation pathway. **B**: Regulation of the *glnA* gene encoding for the GS. **C**: Regulation of the *gltAB* genes encoding for the GOGAT. **D**: Regulation of the Roc pathway, including *rocG* gene encoding for the GDH RocG. **E**: Regulation of the *tnrA* gene encoding for TnrA. **B,C,D,E**: **GlnK** – P_{ii} -like regulatory protein, **TnrA** – global regulator of nitrogen metabolism genes, **GlnR** – transcriptional repressor, **FBI-GS** – feedback inhibited GS, **GltC** – transcription factor of the *gltAB* genes, **FsrA** – non-coding RNA helping the cell to economize its iron consumption, **AhrC** – transcriptional regulator of arginine metabolic genes, σ^L – sigma factor L important for utilization of arginine, **RocR** – transcriptional activator of arginine utilization operons, **CcpA-HPr-P** – active CCR-mediating complex, **AbrB** – transcriptional regulator of transition state genes, **CodY** – transcriptional pleiotropic repressor.

expressed by *E. coli* (Khan *et al.*, 2005b; Khan *et al.*, 2005a).

In Fig. 1.3, a general overview of the glutamate metabolism is given. The central reaction circuits represent the ammonium assimilation in form of glutamine via the glutamine synthetase (GS), the biosynthesis of two molecules of glutamate from α -ketoglutarate and glutamine via the glutamate synthase (GOGAT), and the degradation of glutamate via the glutamate dehydrogenases (GDH) (Gunka and Commichau, 2012). As the maintenance of the glutamate homeostasis is crucial for *B. subtilis* fitness, the corresponding synthesis and degradation pathways are strongly regulated on gene expression and protein activity level as depicted in Fig. 1.3.

1.3.1. Glutamine synthetase GlnA

In *B. subtilis* only the GS can assimilate ammonium into usable cellular metabolites (Fisher, 1999). The ATP-dependent reaction from glutamate and ammonium to glutamine (Fig. 1.3 A) is only required in the presence of ammonium and in the absence of good nitrogen sources. Therefore, the expression of the *glnRA* operon encoding for the transcriptional repressor GlnR and the glutamine synthetase is strictly regulated by nitrogen sources (Fig. 1.3 B, Ch. 1.2.2). In the absence of its substrate ammonium, GS activity is not needed, therefore the *glnRA* operon is repressed by TnrA. In the presence of its product glutamine the GS is feedback inhibited, and binds to its repressor GlnR which prevents expression by binding to two adjacent operators of the *glnRA* promoter (Fisher and Wray, 2008). Having a metabolic and a regulatory function, the GS is

a trigger enzyme which constantly monitors the glutamine level of the cell (Ch. 1.2.2) (Commichau and Stülke, 2008).

1.3.2. Glutamate synthase GltAB

In contrast to other bacteria as for instance *E. coli*, glutamate is exclusively synthesized in *B. subtilis* via the glutamate synthase GltAB (GOGAT) and not via an anabolically active GDH (Gunka and Commichau, 2012). The GOGAT catalyzes the NADPH-fueled reaction from glutamine to α -ketoglutarate producing two molecules of glutamate (Suzuki and Knaff, 2005). Hence, GOGAT activity is strongly required in medium that does not provide good nitrogen sources as glutamine, which is the favored nitrogen source of *B. subtilis*, followed by arginine and ammonium (Atkinson and Fisher, 1991; Detsch and Stülke, 2003). It is suggested that the GOGAT is directly fed with α -ketoglutarate via an interaction of the GltB subunit with the isocitrate dehydrogenase which is part of the core TCA cycle metabolon, consisting of the citrate synthase, the isocitrate dehydrogenase and the malate dehydrogenase (Meyer *et al.*, 2011). The *gltAB* operon encoding for the α - and β -subunits of the heterodimeric GOGAT is under the control of a highly regulated promoter exhibiting only a very narrow basal activity. The promoter of the *gltAB* genes harbors three transcription factor binding boxes partly overlapping the -35 and -10 regions of the *gltAB* promoter and a TnrA binding box behind the transcriptional start site (Fig. 1.4). TnrA represses the *gltAB* gene expression under conditions of nitrogen limitation as described in Ch. 1.2.2

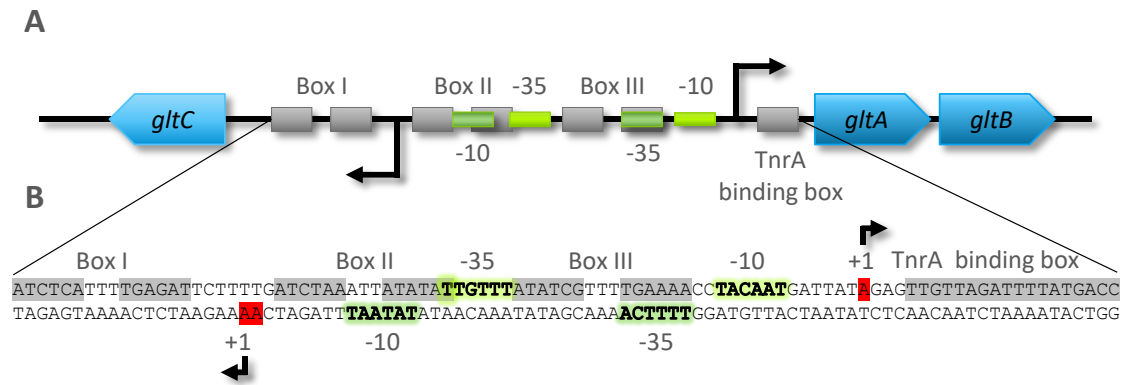


Fig. 1.4 Promoter region of the *gltAB* and *gltC* genes

A: Schematic view of the promoter region. The grey rectangles represent transcription factor binding sites: Box I, Box II, and Box III are GltC binding boxes and the remaining box is a TnrA binding box. The bright green promoter region belongs to the *gltAB* genes and the dark green promoter region belongs to the *gltC* gene. A black arrow indicates the transcriptional start site and genes are blue. **B:** Detailed DNA sequence of the indicated area from the schematic view of the promoter (A). Here, transcriptional start sites are additionally marked in red.

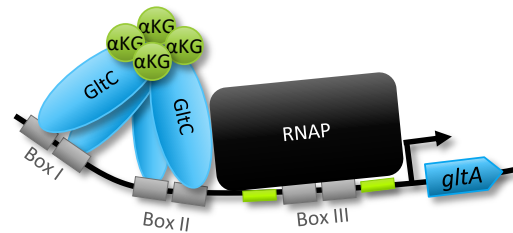
(Belitsky *et al.*, 2000). It was shown that the *gltAB* gene expression is strictly dependent on the transcriptional activator GltC (Fig. 1.3 C) (Bohannon and Sonenshein, 1989). GltC, encoded by the *gltC* gene, belongs to the family of LysR type transcriptional regulators (LTTR), which is the most abundant type in the prokaryotic kingdom (Maddocks and Oyston, 2008). LTTRs act in many cases as activators for divergently transcribed genes and repress their own transcription, as it is also the case for GltC regulating the *gltAB* genes and the *gltC* gene (Fig. 1.4) (Bohannon and Sonenshein, 1989). In general, LTTRs are active in a tetrameric form consisting of two dimers depending on the presence of a specific inducer and bind multiple sites in the promoter region (Maddocks and Oyston, 2008). In 2007, two experimentally different studies explained the regulatory connection of the GltC activity to the nitrogen and carbon metabolism. In an *in vitro* approach the expression of the *gltAB* genes was reconstituted using a tag-free version of the GltC protein (Picossi *et al.*, 2007). Interestingly, *in vitro* foot printing analyses revealed that GltC alone weakly binds to box I. The presence of α -ketoglutarate stimulated the binding of GltC to box I and II leading to a drastically increased

binding of the RNAP to the promoter region (Fig. 1.5 A). In contrast, the presence of glutamate stimulated the DNA bending and binding of GltC to box I and III, blocking the spacer region between the -35 and -10 regions of the *gltAB* promoter and thereby preventing the RNAP from binding to the promoter (Fig. 1.5 B) (Picossi *et al.*, 2007). The *in vitro* investigation of the GltC variant T99A, which was *in vivo* active even in the presence of arginine or ornithine (Belitsky and Sonenshein, 2004), revealed that this mutant variant does not need α -ketoglutarate to activate the expression of the *gltAB* genes. However, the presence of glutamate still slightly reduces the GltC(T99A)-dependent expression of the *gltAB* genes. Regarding the high and constant levels of intracellular glutamate (100-200 mM) and the small and varying levels of α -ketoglutarate (Fisher and Magasanik, 1984; Whatmore *et al.*, 1990; Hu *et al.*, 1999) within the cell, the authors suggested α -ketoglutarate to be physiologically the major regulator of GltC activity (Picossi *et al.*, 2007).

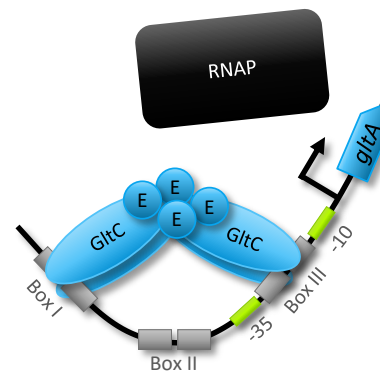
B. subtilis is unable to grow in the absence of good carbon sources as glucose when ammonium is the only source of nitrogen (Commichau *et al.*, 2007b). Therefore, another study investigated the impact of the nitrogen

metabolism on the *gltAB* gene expression *in vivo*. In the presence of ammonium, the *gltAB* genes are not repressed by TnrA (Belitsky *et al.*, 2000). There was no growth detectable unless the cells were provided with either glutamate or glucose, indicating a problem in the biosynthesis of glutamate. Identification of emerging suppressor mutants on medium with succinate and ammonium as sole carbon and nitrogen sources, respectively, revealed several loss-of-function mutations within the *rocG* gene encoding for a GDH in *B. subtilis* (Commichau *et al.*, 2007b). All mutants regained the ability of *gltAB* expression (Commichau *et al.*, 2007b). This was in good agreement with a study investigating *gltAB* gene expression in mutants with various defects in the Roc pathway (Fig. 1.3), which finally identified RocG as important for arginine, ornithine, or proline mediated repression of the *gltAB* genes (Belitsky and Sonenshein, 2004). Finally, a direct protein-protein interaction between RocG and GltC was shown by *in vivo* crosslinking as RocG was coeluted with GltC (Commichau *et al.*, 2007a; Herzberg *et al.*, 2007). The binding of RocG to GltC and thereby preventing it from binding to the DNA (Fig. 1.5) was also shown for GudB, the second GDH in *B. subtilis* (Stannek *et al.*, 2015b). Furthermore, the effector of a functional interaction between GltC and RocG or GudB *in vivo* was identified to be glutamate (Stannek *et al.*, 2015b). Besides regulations regarding the nutrient status of the cell, sufficient iron must be available for a functional GOGAT harboring an iron-sulfur cluster at its active site (van den Heuvel *et al.*, 2002; Suzuki and Knaff, 2005). To economize the iron consumption in the cell, the small non-coding RNA FrsA represses “low-priority” iron-containing enzymes as the GOGAT (Fig. 1.3) (Miethke *et al.*, 2006; Smaldone *et al.*, 2012; Gunka and Commichau, 2012).

A *In vitro* model: *gltAB* gene expression



B *In vitro* model: no *gltAB* gene expression



C *In vivo* model: no *gltAB* gene expression

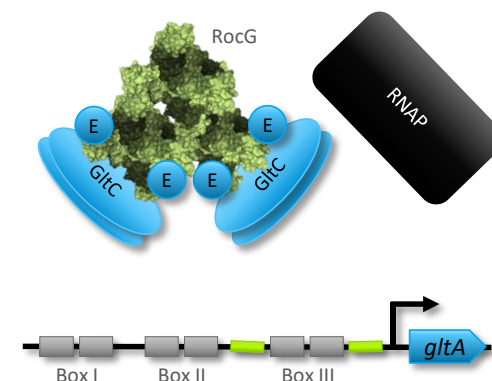


Fig. 1.5 *In vitro* and *in vivo* derived models for GltC dependent regulation of the *gltAB* genes.

GltC – transcriptional activator of *gltAB* genes, RNAP – RNA polymerase, α KG – α -ketoglutarate, E – glutamate, RocG – glutamate dehydrogenase. (adapted from Picossi *et al.*, 2007; Commichau *et al.*, 2007a)

1.3.3. Glutamate dehydrogenases

GudB/RocG

Under growth conditions without an appropriate carbon source, glutamate can be converted via the oxidative deamination of L-glutamate into ammonium and α -ketoglutarate, feeding into the TCA cycle (Brunhuber and Blanchard, 1994). The GDHs in *B. subtilis* use NAD^+ as co-factor and

have a very low affinity for ammonium (Gunka *et al.*, 2010), which is typical for strictly catabolic GDHs. Other GDHs as for instance the *E. coli* GDH GdhA which is catabolically and anabolically active, uses NADP⁺ and has a higher affinity for ammonium (Brunhuber and Blanchard, 1994; Reitzer, 2003; Sharkey and Engel, 2008). *B. subtilis* harbors *rocG* and *gudB* two paralogous genes encoding for GDHs, which share 74 % amino acid sequence identity (Belitsky and Sonenshein, 1998). The *rocG* gene expression is strongly regulated by different nitrogen and carbon sources, whereas the promoter of the *gudB* gene is constitutively expressed (Fig. 1.6).

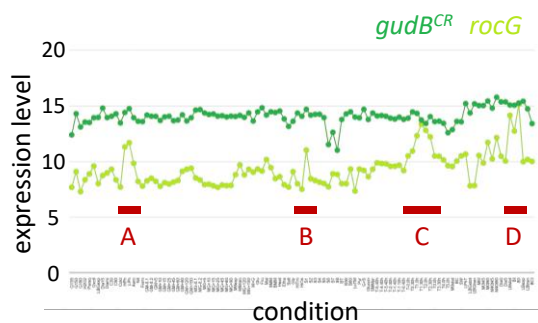


Fig. 1.6 Transcript levels of the *gudB^{CR}* and the *rocG* genes under different growth conditions.

The transcript level overview of the *gudB^{CR}* and the *rocG* gene in *B. subtilis* under different growth conditions is derived from SubtiWiki (Michna *et al.*, 2016). The transcript level from the *gudB^{CR}* gene is constant whereas the transcript level from *rocG* gene depends on the different conditions (Nicolas *et al.*, 2012): **A:** high & low phosphate defined media containing arginine (Müller *et al.*, 1997). **B:** Sporulation after 1 h in sporulation medium (Sterlini and Mandelstam, 1969). **C:** 0.3 h, 1 h, 1.3 h (maximum), 2 h, 2.3 h and 3 h after glucose exhaustion in modified M9 medium (Hardiman *et al.*, 2007). **D:** Stationary growth in LB and sporulation after 0 h in sporulation medium (Sterlini and Mandelstam, 1969).

A *B. subtilis* strain deficient of the σ^L sigma factor is not able to use arginine or ornithine as sole nitrogen sources. The genes involved in arginine catabolism were shown to be under the control of the σ^L sigma factor and a corresponding transcriptional activator RocR encoded by the *rocR* gene (Calogero *et al.*, 1994; Gardan *et al.*, 1995). In contrast, the *rocR* gene is under the control of a σ^A sigma factor, not induced by arginine, and autoregulated (Gardan *et al.*, 1995). However, the regulation of the *rocG* gene

and the *rocABC* operon is special, because the binding site of the RocR protein is located downstream of the *rocG* gene. It acts as downstream activating sequence (DAS) for the expression of the *rocG* gene and as upstream activating sequence (UAS) for the expression of the *rocABC* operon (Fig. 1.3) (Belitsky and Sonenshein, 1999). DNase I footprinting experiments defined the bidirectional enhancer element as doubled 8 bp inverted repeat separated by one base which leads to a curved DNA facilitating the interaction of RocR with the σ^L -RNAP (Ali *et al.*, 2003).

As previously mentioned a GDH makes glutamate accessible as a carbon source. This is only necessary in the absence of a good carbon source. Therefore, the promoter is repressed in the presence of glucose by CcpA, the global regulator of CCR (Belitsky and Sonenshein, 1999; Belitsky, 2004). Hence, under this conditions the RocG protein cannot inhibit the GOGAT activity (Commichau *et al.*, 2007a) and GOGAT in turn can synthesize glutamate. In perfect agreement with this is the observation that a Δ *ccpA* strain deficient of CCR, grows poorly on medium with ammonium and glucose as sole nitrogen and carbon sources, respectively (Faires *et al.*, 1999). In this mutant strain CcpA does not repress *rocG* gene expression, but it is also not induced by RocR. Interestingly, it was shown that a readthrough effect of the upstream located *sivA* gene is responsible for a low level of *rocG* gene expression, which is normally shielded by CcpA (Belitsky *et al.*, 2004). Consequently, RocG inhibits GOGAT and glutamate cannot be synthesized, resulting in a growth defect of Δ *ccpA* strains on medium with ammonium and glucose (Belitsky *et al.*, 2004). Furthermore, a CcpA binding site leading to a roadblock mechanism was identified within the *sigL* gene encoding for the σ^L sigma factor and another putative binding site was identified behind the

promoter region of the *rocDEF* genes (Choi and Saier, 2005). This indicates that the regulation of the σ^L sigma factor, the arginine catabolism genes and especially the *rocG* gene, all belonging to the nitrogen metabolism are strongly linked to global regulators of the carbon metabolism. Another repression of the *rocG* gene and the *rocABC* operon is mediated by the transition state regulator AbrB, under conditions of good nutrient supply, when cells are in exponential growth phase (Chumsakul *et al.*, 2011). Furthermore, sensing the arginine pool in the cell, the transcriptional regulator of the arginine catabolism AhrC activates in the presence of arginine expression of the *rocABC*, the *rocDEF*, and the *rocG* genes and represses genes involved in arginine biosynthesis (Czaplewski *et al.*, 1992; Gardan *et al.*, 1995; Klingel *et al.*, 1995; Commichau *et al.*, 2007b).

To summarize, RocG is expressed in the presence of arginine or ornithine or to a lesser extent proline or citrulline in the absence of glucose (Belitsky and Sonenshein, 1998; Belitsky *et al.*, 2004).

However, there is a second GDH in *B. subtilis* and growth experiments with $\Delta gudB$ and $\Delta rocG$ knock-out mutants of the *B. subtilis* NCIB 3610 wild type strain and biochemical analyses of the two proteins revealed that GudB is the major contributor for glutamate degradation (Noda-Garcia *et al.*, 2017). In contrast to the less domesticated *B. subtilis* strains as the NCIB 3610, the major GDH GudB of the laboratory *B. subtilis* strains 160, 166, and 168 is not functional and very instable (Zeigler *et al.*, 2008). This cryptic *gudB^{CR}* gene harbors a directly repeated sequence of 9 bp, termed tandem repeat (TR), within its coding region resulting in a duplication of three amino acids (VKA-VKA) in the positions 93-95 and 96-98 of the catalytically active center of the GudB protein. In strains deficient of the *rocG* gene, suppressor mutants (SM) emerge

rapidly on selective medium, that have precisely excised one part of the TR from the *gudB^{CR}* gene (Belitsky and Sonenshein, 1998). The resulting *gudB⁺* gene encodes the functional GDH GudB⁺ that restores the glutamate homeostasis. The mutation rate of the *gudB^{CR}* gene is about 10^{-4} and the highest reported so far (Gunka *et al.*, 2012).

It is assumed that the *gudB* gene was inactivated during domestication of the laboratory wild type strain 168, because in contrast to the soil, *B. subtilis*' natural environment, a lack of exogenous glutamate in laboratory culture media might have provided a selective growth advantage for mutants that have inactivated the *gudB* gene (Gunka *et al.*, 2013). The acquisition of an inactive *gudB^{CR}* gene conferred a selective growth advantage. However, presence of a constitutively expressed *gudB* gene seems not to be disadvantageous, as recent studies revealed that the NCIB 3610 wild type strain shows no growth defect on medium with glucose and ammonium as carbon and nitrogen sources, respectively (Noda-Garcia *et al.*, 2017). Contradictory, this medium does not provide glutamate for the cell, which consequently must be synthesized. Its constant degradation by the GDH GudB should lead to a futile cycle. However, in this study, it was shown that an exchange of the open reading frames of the *gudB* and the *rocG* gene leads to an impaired growth phenotype (Noda-Garcia *et al.*, 2017). This indicates, that high levels of GudB are not dangerous, but high levels of RocG are a serious problem for the cell. The RocG protein can form stable enzymatically active hexamers under a broader range of pH and with more varying concentrations of glutamate. Whereas the GudB protein is only present in its active hexameric form at distinct pH and high glutamate concentrations (Noda-Garcia *et al.*, 2017). Furthermore, the authors observed that GudB

and RocG are allosterically regulated by ATP and α -ketoglutarate even though the regulation is rather minor (Noda-Garcia *et al.*, 2017). Taken together, the *rocG* gene expression is tightly regulated but the resulting GDH RocG is stable and active under a broad range of conditions. In contrast, the *gudB* gene is constitutively expressed, but the resulting GDH GudB is only stable under defined environmental conditions. However, the stability of the RocG and GudB complexes might be influenced further by their secondary function as so called moonlighting or trigger enzymes (Commichau and Stülke, 2008). As it is the case for the GS (Ch.1.2.2), the trigger enzymes have besides their metabolic function a regulatory function. To prevent the emergence of a futile cycle of glutamate synthesis and degradation, GltC activity is inhibited by binding to the GDH RocG or GudB (Commichau *et al.*, 2007a; Stannek *et al.*, 2015b), which of course could also be important for RocG or GudB stability. However, two paralogous enzymes so differently regulated are likely to provide *B. subtilis* a selective growth advantage in adaptation to specific growth conditions.

1.4. High frequency mutagenesis of *gudB^{CR}* gene

1.4.1. Collisions of the replication and transcription machineries

The question rises, how the mutagenesis of the *gudB^{CR}* gene reaches such a high rate and specificity? DNA is most prone to mutations when exposed as single stranded DNA (ssDNA) during replication, transcription, or when present as non-B-DNA like structure (Kim and Jinks-Robertson, 2012; Gaillard *et al.*, 2013; Wang and Vasquez, 2017). Every action upon the DNA is a potential and inevitable risk for the cell, but also a source of evolution. For instance, during replication 10-50 % of the replication

forks encounter a DNA lesion or strand break (Cox, 1998) plus the general base substitution error of the replication machinery is between 10^{-7} and 10^{-8} (Kunkel, 2004) and even without selection 10 % of all cells in a culture contain a duplication somewhere in the genome (Andersson and Hughes, 2009). The first hint to unravel the mechanism of TR mutagenesis in the *gudB^{CR}* gene is its connection to the transcription machinery, because deletion of the transcription repair coupling factor Mfd leads to a severe decrease of the mutation rate of the *gudB^{CR}* gene (Gunka *et al.*, 2012). Besides the simple exposure of ssDNA during transcription, there exist several crosslinks to the emergence of mutations as for instance transcription-replication collisions, transcription associated mutagenesis (TAM), and it is also known that transcription has a major role in stationary phase mutagenesis (Kim and Jinks-Robertson, 2012; Gaillard *et al.*, 2013).

Severe is a collision between the replication and transcription machinery, which is likely to happen as both occur simultaneously on one DNA strand (Fig. 1.7). The conflicts can occur in two manners, either co-directional or head-on. Co-directional conflicts occur when the replisome overtakes the RNAP (Fig. 1.7 A), which processes depending on the organism up to 10 times slower compared to the replisome (Gaillard *et al.*, 2013). Upon this type of collision, the replisome slows until transcription of the leading strand gene is completed or aborted. It was shown for *E. coli in vitro* that remaining RNA can be used by the replisome as primer resulting later on in a DNA gap (Pomerantz and O'Donnell, 2008). A collapse of the replication fork is unlikely but can happen *in vivo*, because a second replisome might convert a gap or nick into a double strand break (DSB) (French, 1992; Kreuzer, 2005; Pomerantz and O'Donnell, 2010b; Merrikh *et al.*, 2011) (Fig. 1.8). More severe are head-on collisions of the replisome and the RNAP

transcribing a lagging strand gene (Fig. 1.7 B). It was shown *in vitro* that the replication stalls upon both co-directional and head-on conflict, but the duration is much longer encountering a head-on conflict (Pomerantz and O'Donnell, 2010b). If replisome encounters a highly transcribed gene with several RNAPs transcribing it simultaneously, it is very likely that the transcription machinery is completely dislodged and the replication fork collapses (Srivatsan *et al.*, 2010; Pomerantz and O'Donnell, 2010b). This results in DNA damages as gaps or nicks in ssDNA or DSB (Fig. 1.8). It is also possible that the respective gene is less transcribed and the replication fork only pauses until the RNAP is dislodged from the DNA (Pomerantz and O'Donnell, 2010b). The removal of the RNAP might be facilitated by the transcription repair coupling factor Mfd (Fig. 1.8), which is an ATP dependent DNA translocase, or ppGpp, which can destabilize RNAP open promoter complexes (Trautinger *et al.*, 2005; Pomerantz and O'Donnell, 2010a; Pomerantz and O'Donnell, 2010b). To avoid collisions in eukaryotes, replication and transcription are spatiotemporally separated to a certain extent, even though the speed of replication and transcription are almost the same in eukaryotes (Helmrich *et al.*, 2013). This separation cannot take place in prokaryotes. To avoid head-on collisions and putative DNA damage, most essential or highly transcribed genes as the ribosomal RNA genes are encoded on the leading strand (Rocha and Danchin, 2003; Guy and Roten, 2004; Merrikh, 2017), where only less severe codirectional conflicts appear. Interesting but only investigated in *B. subtilis*, genes present on the lagging strand are substantially shorter and not organized in operons compared to genes encoded on the leading strand (Paul *et al.*, 2013). Consequently, the chance of completing the transcription of a short and separately organized

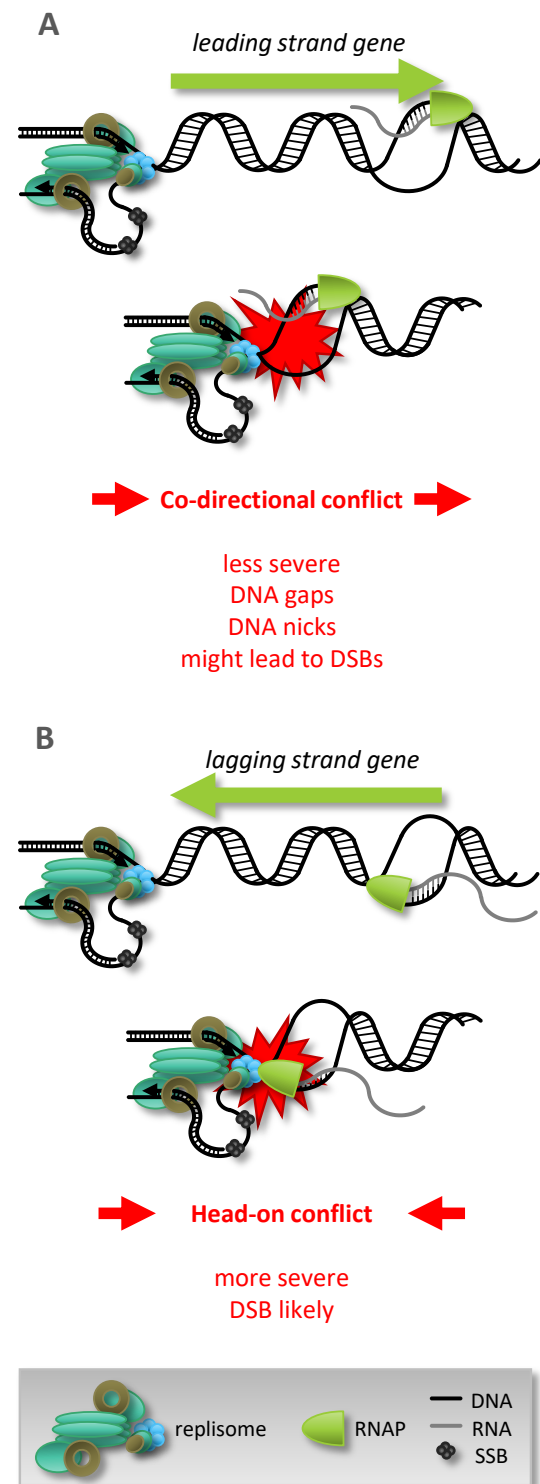


Fig. 1.7 Replication-transcription collisions
The legend is grey: replisome, RNAP, DNA, RNA, and single strand binding proteins (SSB) **A:** Co-directional conflict of the replisome and the RNAP transcribing a leading strand gene, resulting in less severe DNA damages. **B:** Head-on conflict of the replisome and the RNAP transcribing a lagging strand gene, resulting in more severe DNA damages.

gene before colliding with the replisome is increased. However, head-on collisions have also a positive effect, because they accelerate gene evolution. In *B. subtilis*, the core genes encoded

on the lagging strand represent a variety of stress response genes (Paul *et al.*, 2013). Hence genes, that are not essential for life, but for adaptation to environmental stresses. In such harsh situations, these genes are under a high selective pressure and a fast evolution might be advantageous. Most of these genes are highly expressed when they are needed. In a recent study it was shown, that highly transcribed genes even encounter an increased rate of mutation when encoded on the lagging strand (Sankar *et al.*, 2016). Interestingly, the *gudB^{CR}* gene is encoded on the leading strand and consequently not subject to head-on collisions (Fig. 3.5. on p. 40). However, it was shown that the genomic localization of the *gudB^{CR}* gene is irrelevant for its mutability (Gunka *et al.*, 2012), because the ectopic introduction of the *gudB^{CR}* gene into the *amyE* gene locus leads to identical mutation rates compared to the native situation. Even as the *gudB^{CR}* gene was transferred from the left to the right replicore and as a result exposed to putative head-on collisions (Fig. 3.5 on p. 40). However, it is constitutively transcribed and as previously mentioned transcribed genes were shown to have a higher mutation rate compared to genes that are not transcribed (Sankar *et al.*, 2016).

1.4.1.1. Replication restart upon head-on collision

A head-on collision of the replication and transcription machinery ends both, the transcription aborts and the replication fork collapses. Additionally, double strand breaks (DSB) or single stranded DNA gaps or nicks might occur. To reconstitute the replisome, these damages must be repaired.

Initially, DSB are recognized by RecN belonging to the structural maintenance of chromosomes (SMC) family of proteins, which play important roles in chromosome dynamics especially during

segregation and in DNA repair (Sanchez *et al.*, 2006; Graumann and Knust, 2009). A $\Delta recN$ strain shows increased susceptibility to DNA damaging agents. However, the initiation of RecA nucleation still occurs indicating that RecN has an important but not essential role for homologous recombination (HR) (Kidane and Graumann, 2005; Lenhart *et al.*, 2012). During the early stages of DSB repair, PnpA the polynucleotide phosphorylase (PNPase) binds ssDNA mediated by RecN, even if the ssDNA is coated by single strand binding (SSB) proteins (Fig. 1.8 D-F). There, PnpA performs initial pre-processing of non-ligatable termini and 3' \rightarrow 5' exonuclease activity on 3'-tailed duplex DNA (Cardenas *et al.*, 2011), to provide blunt ends required by the AddAB helicase-nuclease complex (Yeeles and Dillingham, 2010).

The main processing of dsDNA breaks and the accompanied loading of RecA, the major DNA recombinase, is well known for *E. coli*, but differentially discussed for *B. subtilis* (Lenhart *et al.*, 2014; Million-Weaver *et al.*, 2015). In *E. coli* it is mediated by RecORF or RecBCD helicase-nuclease pathway (Xu and Marians, 2003; Dillingham and Kowalczykowski, 2008). In *B. subtilis*, the RecBCD helicase-nuclease complex homolog AddAB is present. HR initiates preferably on crossover hotspot instigator (χ , χ) sites (Yeeles and Dillingham, 2010; Wigley, 2013). The majority of χ -sites in bacteria are oriented towards the origin of replication, to promote recombination from collapsed replication forks (Yeeles and Dillingham, 2010; Lenhart *et al.*, 2012). However, this is not exclusively the case as for instance the *gudB^{CR}* gene in *B. subtilis* harbors two χ -sites in opposite directions. The AddAB complex binds to blunt ended dsDNA breaks, unwinds the DNA duplex, and degrades the DNA in an ATP-dependent manner until it reaches the χ -sequence (Krajewski *et al.*, 2014). Even though the

χ -sequence (AGCGG) of *B. subtilis* is only 5 bp long, the resulting AddAB- χ -complex is more stable compared to the *E. coli* RecBCD- χ -complex having an 8 bp long χ -sequence (GCTGGTGG) (Chédin *et al.*, 2006). Firmly bound to the χ -sequence, the AddAB 3'-5' exonuclease activity stops, but the 5'-3' exonuclease activity further processes the DNA generating a growing loop at the 3'-end (Chédin *et al.*, 2006) (Fig. 1.8 F). The *E. coli* RecBCD helicase-nuclease complex was shown to degrade the dsDNA with a speed of 900 bp/s until it reaches the χ -side, stops for 5 s and the 5'-3' exonuclease activity processes the DNA further with a speed of 140 bp/s; the whole process persists for a distance over ~30 kbp (Spies *et al.*, 2003). However, both helicase-nuclease-complexes, the *B. subtilis* AddAB and the *E. coli* RecBCD complex produce ssDNA substrate for RecA. Active loading of RecA onto the DNA was only shown for RecBCD, but a similar mechanism is strongly suggested for AddAB (Anderson and Kowalczykowski, 1997; Chédin *et al.*, 2006; Million-Weaver *et al.*, 2015). Furthermore, it was shown that single deletions of the *addA*, *addB*, *addAB*, *recS*, *recJ*, or *recQ* genes are moderately sensitive to DNA damaging agents (Sanchez *et al.*, 2006), but the double mutant $\Delta addAB \Delta recJ$ shows a severe $\Delta recA$ like phenotype unable to cope with DNA damaging agents and perform HR. These findings indicate, that besides the helicase-nuclease AddAB, the 5'-3' endonuclease RecJ is important for successful loading of RecA onto the DNA (Sanchez *et al.*, 2006). RecJ acts in concert with the RecQ-like helicase RecQ or its paralog RecS (RecQ(S)-RecJ) and form an alternative end-processing pathway to generate 3'-tailed DNA (Sanchez *et al.*, 2006) (Fig. 1.8 F). There are several hints that RecQ act as safeguard for the genome, especially during replication. In contrast to the RecN-mediated recruitment of AddAB to dsDNA breaks, RecQ(S)-RecJ are constantly colocalized with the replisome

(Lecoite *et al.*, 2007; Costes *et al.*, 2010). It was shown, that a variety of DNA repair proteins including RecQ(S)-RecJ can bind to the C-terminus of SSB proteins. The replication fork consists of 1-2 kb of lagging strand template coated with SSB tetramers (Lohman and Ferrari, 1994), forming some sort of DNA maintenance hub. The constant co-localization of RecQ with the replication fork was first observed using RecQ with an N-terminal GFP fusion (Lohman and Ferrari, 1994). This interaction was disturbed by a stop less C-terminal CFP fusion, because RecQ-CFP was shown to localize throughout the nucleoids (Sanchez *et al.*, 2006). Besides the constant presence of RecQ at the replication fork, it unwinds forked dsDNA, DNA duplexes with a 3'-overhang and specifically blunt-ended dsDNA with structural features as for instance nicks, gaps, and holiday junctions (Qin *et al.*, 2014) indicating its importance in several DNA damages. After processing of the DNA, either by RecBCD, AddAB or RecQ(S)-RecJ, 3'-tailed DNA emerges coated by SSB proteins stabilizing ssDNA. In *B. subtilis* there are two paralogous SSB proteins present, SsbA and SsbB encoded by the *ssbA* and *ssbB* genes, respectively. Analysis of promoter expression revealed an increased expression of the *ssbA* gene during exponential growth and a lower in the stationary phase, suggesting a role of SsbA in replication. In contrast, there was no expression detectable for the *ssbB* gene in exponential growth, but an increased expression when cells entered the stationary phase (Lindner *et al.*, 2004). Furthermore, the transcription of the *ssbB* gene is strongly reduced in a $\Delta comK$ deletion mutant, suggesting a role of SsbB in genetic competence, which could be confirmed as the transformation efficiency of a $\Delta ssbB$ deficient strain is strongly reduced (Lindner *et al.*, 2004). SSB proteins were shown to reduce secondary structures and therewith promote RecA filamentation by rendering the ssDNA more

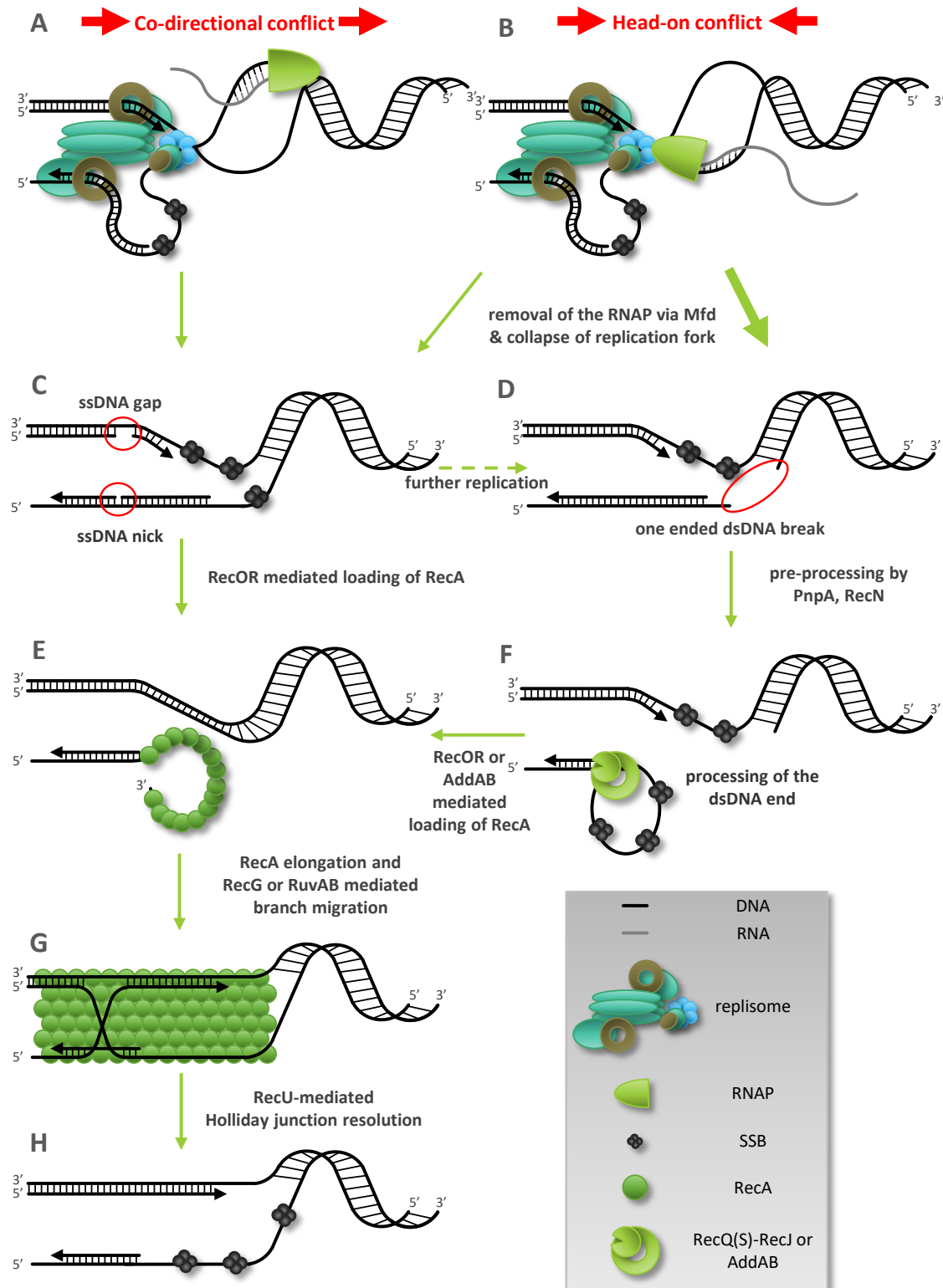


Fig. 1.8 Repair of replication-transcription conflicts

Scheme of the repair of collapsed replication forks. **A:** Co-directional conflict of replisome and RNAP. **B:** Head-on conflict of replisome and RNAP. **C:** Both collisions can lead to single strand gaps or nicks **D:** Head-on conflicts often lead to one ended DSB. **E:** RecA nucleates on 3'-tailed DNA ends with the help of either RecOR or AddAB, but this is not shown yet. **F:** The generation of the 3'-tailed DNA ends is mediated by the helicase-nuclease complexes of AddAB or RecQ(S)-RecJ. **G:** RecA elongates and branch migration is mediated by RecG and RuvAB. RecU controls the elongation of RecA and finally cleaves the Holiday junction. **H:** Rescued DNA, ready for PriA-mediated assembly of the replication fork.

accessible for RecA (Kowalczykowski and Krupp, 1987; Carrasco *et al.*, 2015). However, if either of

the two SSB proteins is bound to the ssDNA, RecA cannot nucleate and form filaments (Yadav *et al.*,

2014). In *E. coli*, the RecBCD helicase nuclease actively removes SSB proteins and loads RecA onto the 3'-tailed DNA in 5'-3' direction (Cox and Lehman, 1982). Besides RecBCD, in *E. coli* the RecOR/RecFOR pathway is important for RecA loading (Sakai and Cox, 2009). In contrast to the RecBCD/AddAB systems, the RecFOR system is much more conserved among bacterial species (Rocha *et al.*, 2005). *B. subtilis* RecO protein shares only about 25 % identity with the *E. coli* RecO protein (Fernández *et al.*, 1999), but can alone induce the RecA nucleation whereas the *E. coli* RecO needs RecR to overcome the SSB inhibition (Lenhart *et al.*, 2012). Interestingly, it was shown that AddAB and RecO might act in parallel to repair head-on collisions in *B. subtilis*, and still can compensate for each other's loss (Fig. 1.8 F-E) (Million-Weaver *et al.*, 2015). In a study published just two weeks later, it was shown that RecO and SsbA are crucial for RecA-mediated DNA strand exchange essential for recombination in both the RecQ(S)-RecJ and the AddAB pathway (Carrasco *et al.*, 2015). Their phenotypic study of the double mutants $\Delta addAB \Delta recO$ and $\Delta recJ \Delta recO$, which resemble the phenotype of an RecA deficient strain upon treatment with DNA damaging agents, were corroborated with *in vitro* ATP hydrolysis and RecA-mediated DNA strand exchange studies (Carrasco *et al.*, 2015). In a fluorescence localization study, RecR, besides RecO, is shown to be important for the formation of a RecA-GFP focus *in vivo* (Lenhart *et al.*, 2014). Albeit, the specific role RecF in *B. subtilis* is not completely understood it is suggested to facilitate the RecA elongation process (Cárdenas *et al.*, 2012; Lenhart *et al.*, 2014). Cárdenas and colleagues proposed a model for *B. subtilis* RecA filament assembly, in which the role of RecF is not completely clear, but it is assumed to promote the elongation process in the presence and absence of RecX (Cárdenas *et al.*, 2012). RecX alone facilitates the disassembly of the RecA

filament. However, once the RecA nucleation is established, RecA alone is able to elongate along the ssDNA (Carrasco *et al.*, 2008). For *E. coli*, it is shown that the filaments grow in 5'-3' direction with 120 to 1200 subunits min⁻¹, but the dissociation occurs mainly on the 5'-proximal end (Cox, 2007). The actual process of branch migration is controlled by the presence of SsbA and dATP which is the co-factor of RecA (Carrasco *et al.*, 2008). In *E. coli*, branch migration and the holiday junction cleavage is mediated by the RuvABC complex (Lenhart *et al.*, 2012). In *B. subtilis*, RuvAB recruits RecU which in turn modulates the activity of RecA, as it can inhibit the dATPase activity of RecA (Fig. 1.8 E-G) (Carrasco *et al.*, 2005; Sanchez *et al.*, 2005). Besides the Holiday junction resolvase RecU, *B. subtilis* harbors a second enzyme RecV that might cleaves Holiday junctions (Fig. 1.8 G-H) (Sanchez *et al.*, 2007). It is also discussed whether the branch migration translocase RecG is, besides the partitioning of chromosomes, also involved in DNA repair (Sanchez *et al.*, 2007). However, once the holiday junctions are cleaved and the DNA is repaired, PriA which is already directed to the replication fork via SSB interaction (Lecoite *et al.*, 2007), can restart the assembly of the replisome. Therefore, the primosome is assembled. PriA loads in combination with the DNA remodeling proteins DnaB and DnaD, the helicase loader DnaI onto the DNA which in turn loads the helicase DnaC and the primase DnaG (Bruand *et al.*, 2001b).

1.4.2. Transcription-coupled stationary-phase mutagenesis

Stationary-phase mutagenesis, which occurs also in *B. subtilis*, is induced when cells stop dividing and start to suffer from environmental conditions as nutrient limitations, hence conditions that are growth limiting but not lethal (Sung and Yasbin, 2002). A similar non-lethal

condition is present in *rocG* deficient *B. subtilis* cells. They cannot synthesize a functional GDH converting glutamate to α -ketoglutarate and stopping further production of glutamate by inhibiting the GOGAT (Ch. 1.3.2). The accumulating intermediates of the arginine degradation pathway are putatively toxic to the cell, which leads to a decrease in growth, but not to cell death. As previously mentioned the mutation frequency decline Mfd enzyme is involved in the decryptification process of the secondary GDH GudB. The *gudB^{CR}* gene is inactivated by a direct repeat within the region encoding for the active center of the resulting GDH (Belitsky and Sonenshein, 1998; Gunka *et al.*, 2012). The Mfd enzyme is thought to find lesions on the DNA during transcription. It binds to the DNA and the stalled RNAP and removes the nascent RNA (Fan *et al.*, 2016). Subsequently, the UvrA₂B complex removes the Mfd-RNAP complex and recruits UvrC functioning as DNA polymerase and ligase excising the lesion (Fan *et al.*, 2016). Mfd deficient strains show a decreased efficiency of HR and combined with other factors taking part in HR as RecB or RecG as the transformation rate is further reduced (Ayora *et al.*, 1996). Interestingly, the mutation frequency increases in a *mfd* deficient strain during exponential growth as the process mentioned above cannot take place as efficiently as in the presence of Mfd, but the mutation frequency severely decreases during stationary phase (Lenhart *et al.*, 2012). In studies analyzing stationary-phase mutation rates it was shown that Mfd is epistatic to UvrA and MutY, indicating involvement of Mfd in both nucleotide excision repair and base excision repair, suggesting a coordinating role to speed evolution in highly transcribed regions (Gómez-Marroquín *et al.*, 2016). Furthermore, the *B. subtilis* DNA polymerase Poll lacking proofreading activity is involved in the DNA synthesis of stationary-phase mutations (Gómez-Marroquín *et al.*,

2016), but in contrast to *E. coli* RecA is not involved in stationary-phase mutagenesis (Sung and Yasbin, 2002).

The stationary-phase mutagenesis is also termed adaptive mutagenesis, which reminds on the Larmarckian theory, but instead of cells evolving a certain gene it is suggested that during differentiation a small hyper mutable subpopulation emerges sacrificing itself by establishing high mutation rates (Sung and Yasbin, 2002).

1.4.3. DNA/RNA strand slippage

During collisions of the replication and transcription machinery TRs are prone to mutate, but they are also subject to strand slippage during replication or transcription. Such slippage of one TR unit towards the other TR unit leads to the formation of loops or hair pins. These are subsequently excised resulting in an extension or contraction of the DNA (Zhou *et al.*, 2014). The efficiency of these mechanisms relies on the similarity of the repeats, their unit length and also the repeat number in general (Zhou *et al.*, 2014). The DNA slippage model was first proposed in 1966 and has not been changed much (Streisinger *et al.*, 1966). It could be also applicable for the *gudB^{CR}* gene TR mutagenesis. The core of the DNA strand-slippage model is the removal of the emerging loop by a DNase. To the current knowledge the decryptification of the *gudB^{CR}* gene is linked to transcription, therefore, rather RNases, as for instance those of the RNase H family, are of special interest.

The RNase H family consists of endo-ribonucleases responsible for the cleavage of RNA in RNA-DNA hybrid molecules. The RNases H contribute to the maintenance of the genetic code, as they are associated with DNA replication, transcription, and DNA repair (Fukushima *et al.*, 2007). For instance, they are

involved in the removal of primers of Okazaki fragments (Ogawa and Okazaki, 1984; Fukushima *et al.*, 2007) and are important for the removal of single rNTPs accidentally incorporated by the DNA polymerase. The incorporation of rNTPs into DNA strands happens statistically every 2.3 kbp due to an excess of rNTPs compared to dNTPs at the replication fork (Yao *et al.*, 2013). They are also important for RNA-DNA hybrid removal upon collisions of the transcription and replication machinery in prokaryotes and eukaryotes (Helmrich *et al.*, 2011; Merrikh *et al.*, 2012).

B. subtilis encodes four RNase H genes *rnhB*, *rnhC*, *ypeP*, and *ypdQ*. All of the resulting RNases H can specifically hydrolyze the phosphodiester bonds of RNA-DNA hybrids, except the RNase H encoded by the *ypdQ* gene (Fukushima *et al.*, 2007). The *rnhB* and *rnhC* genes encode for RNase HII and RNase HIII, respectively (Ohtani *et al.*, 1999) and the *ypeP* gene encoding an RNase H with only some minor activity. The RNases H are divided into different classes according to the RNases H from *E. coli*. Class 1 consists of the *E. coli* RNase HI, and class 2 of RNases HII and RNases HIII. In other organisms having two paralogs of RNase HII, the ones most identical to the *E. coli* RNase HII are designated as RNase HII, whereas the other paralog is classified as RNase HIII (Tadokoro and Kanaya, 2009). RNases HI and RNases HIII differ also from RNase HII as they cannot cleave a DNA/DNA duplex that contains a rNTP at the DNA-RNA junction, but RNase HII can (Haruki *et al.*, 2002; Tadokoro and Kanaya, 2009). There are also differences between the RNases H regarding substrate recognition. The RNase HIII has an elongated N-terminus harboring a structure similar to the one of TATA-box binding proteins (Tadokoro and Kanaya, 2009).

Interestingly, it has been shown that single deletion mutants of the *ypeP*, *rnhB*, and *rnhC*

genes grow as the wild type (Fukushima *et al.*, 2007). However, a $\Delta rnhB \Delta rnhC$ double mutant exhibits a temperature dependent reduction in growth compared to a wild type, which is even severe in a $\Delta rnhB \Delta rnhC \Delta ypeP$ triple mutant (Fukushima *et al.*, 2007; Yao *et al.*, 2013).

1.5. Visualization of emerging mutations

Reporter gene fusions with proteins involved in DNA repair are a common technique to investigate the DNA repair machinery (Kidane *et al.*, 2004; Sanchez *et al.*, 2006). It sounds quite logical to investigate DNA repair machineries for nucleotide or base excision repair, HR, or other repair pathways using reporter gene fusions, but a major problem is to practically target a cell having a DNA lesion and needing a certain repair pathway. To circumvent this problem DNA damaging agents as mitomycin C (MMC), 4-nitroquinoline-1-oxide (4NQO) or methyl methane sulfonate (MMS) are often used leading to stalling or collapse of the replication fork (Sanchez *et al.*, 2006). MMC even results in DSB. Other systems to investigate DSB repair are the arabinose inducible *I-Sce-I* endonuclease or the xylose inducible HO endonuclease system from *Saccharomyces cerevisiae*. Both systems can be used to generate DSBs at certain cut sites (Haber, 2002; Kidane and Graumann, 2005; Lesterlin *et al.*, 2014). However, the investigation of natural occurring DNA damages during replication or transcription is rather difficult. One attempt to visualize the emergence of mutations that escaped mismatch repair (MMR) in *E. coli*, used a plasmid derived functional MutL-GFP fusion in an *E. coli* strain deficient of its native *mutL* gene (Elez *et al.*, 2010). MutL is recruited by MutS to the site harboring the misincorporated base and further recruits MutH, an endonuclease cleaving the new DNA. Is the newly synthesized strand already methylated by the Dam methylase, MutH cannot distinguish between the two

strands anymore and the mismatch cannot be repaired (Schofield and Hsieh, 2003; Kunkel and Erie, 2005). Using MutL-GFP, foci occur when MutL accumulates and MutH does not appear or cannot detect the newly synthesized DNA because of premature methylation resulting in a mutation. The problem of this experiment is the low rate of non-repaired mismatches, in fact only 0.45% of the investigated cells contained a MutL derived GFP focus. Consistent with the previous assumption, a deletion of *mutH* or the removal of proofreading activity of the DNA polymerase increased the fraction of cells harboring a GFP focus up to 52% (Elez *et al.*, 2010). To conclude, this study investigated the occurrence of mutations randomly distributed over the whole genome and derived from a defective MMR machinery. The low level of foci formation in cells having a functional MMR machinery is not sufficient for practical analyses using for instance double mutants to investigate the influence of

other DNA repair proteins. A system enabling the investigation of a specific mutation in a specific locus on the level of single cells with a functional DNA repair machinery, would substantially contribute to understanding of repair machineries. This can be achieved by the usage of an activator/reporter system (Dormeyer, 2014).

The activator/reporter system provides a mutable unit in form of a transcriptional activator artificially inactivated by a direct repeat within region of the gene important for DNA binding of the resulting protein. The activation of the transcription factor by the precise excision of one repeat unit is comparable to the native situation of the *gudB^{CR}* gene. The major difference is that the activation of the *gudB^{CR}* gene is only detectable by the growth advantage conferred by the acquisition of a functional GDH in the absence of RocG. The activation of the

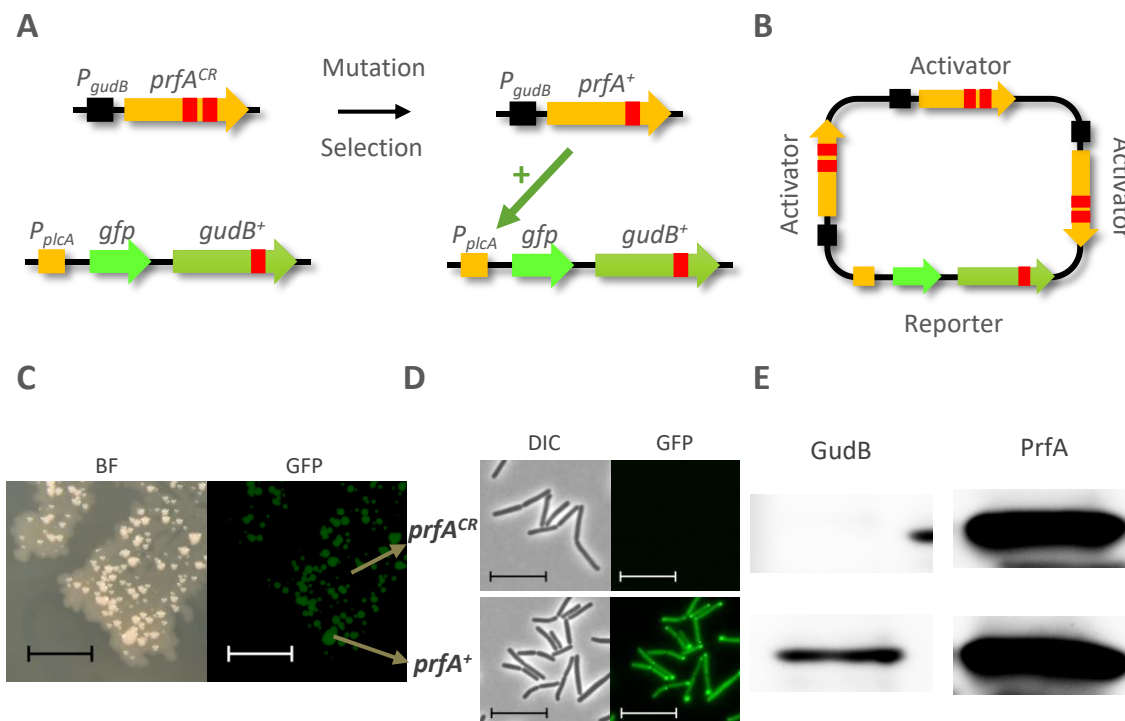


Fig. 1.9 Overview of the activator/reporter system

A: Scheme of the activator/reporter system. The activator unit consists of the constitutively active *gudB* promoter and the artificially inactivated transcription factor gene *prfA^{CR}*. Upon TR excision *PrfA⁺* activates the *plcA* derived promoter of the reporter unit harboring the *gfp* reporter gene and the *gudB⁺* gene conferring a growth advantage on selective medium. **B:** Scheme of several activator units introduced into the *B. subtilis* genome increasing the chance of a mutation to occur. **C:** Activator/reporter strain and emerged SMs on a selective SP plate after 6 dpi RT. Scale 2 mm. **D:** Cell cultures of the activator/reporter strain (above) and its SM (below) at OD_{600} 1. Scale 5 μ m. **E:** Western blot analysis of the activator/reporter strain and its SM using α -RocG antibody for the detection of GudB and α -PrfA for the detection of PrfA. (Adapted from Dormeyer, 2014)

transcription factor results in the expression of the reporter unit consisting of an active *gudB⁺* gene conferring a growth advantage as just described and the *gfp* reporter gene for visualization. The *gudB⁺* gene allows easy detection of SMs on plate, whereas the *gfp* gene allows easy detection on the level of single cells. A similar system exists using an artificial operon, that is under the control of an inactive promoter and expresses upon TR excision the *gudB⁺* gene and the *gfp* reporter gene (Dormeyer *et al.*, 2014). However, in this system the mutation rate is very low. To enhance the rate of mutations in the activator/reporter system, it is planned to introduce several activator units enabling successful detection of emerging mutations on the level of single cells. The activator/reporter system is only functional in *B. subtilis* when the activator unit does not interfere with native genes from *B. subtilis* and when the reporter unit does not exhibit a basal expression that is sufficient to cope with the lack of GDH. Therefore, a transcription factor promoter pair from *L. monocytogenes* is used for the activator/reporter system. The major virulence regulator PrfA encoded by *prfA*, which is fused to the constitutively active promoter of the *gudB^{CR}* gene, forms the activator unit. The reporter unit is under the control of the promoter from the *plcA* gene encoding for virulence factor in *L. monocytogenes*. So far, the activator/reporter system was shown to be functional (Dormeyer, 2014). The activator unit is constitutively expressed and in contrast to the GudB^{CR} protein also detectable in its inactive form via Western blot (Gunka *et al.*, 2012; Dormeyer, 2014). However, until now the emergence of the TR mutation in the *prfA^{CR}* gene remains to be shown on the level of single cells.

1.6. Objectives

The aim of this thesis is to get a better understanding of how glutamate homeostasis is maintained in *B. subtilis*. The GDHs from the laboratory *B. subtilis* strain 168 are of special interest. During growth on rich medium a *rocG* deficient strain lacking the GDH RocG rapidly forms suppressor mutants that have activated the inactive *gudB^{CR}* gene by the precise excision of a TR unit (Ch. 1.4). The high frequency of the decryptification suggests the existence of a specific mutational machinery to be involved in the mutagenesis process. Previously, it was shown that the transcription-repair coupling factor Mfd is involved in the mutagenesis of the *gudB^{CR}* gene. The influence of transcription on TR mutagenesis in general will be investigated using promoters of different strength. Transcription may lead to mutations when the transcription machinery collides with the replication machinery. Therefore, it will be investigated whether the emergence of the mutation is influenced by the orientation of a gene harboring the TR and by factors participating in the repair of the collision (Ch. 1.4.1.1). Moreover, GltC mutants lacking the transcriptional activator of the GltAB encoding *gltAB* genes are auxotrophic for glutamate. It was previously shown that suppressor mutants accumulate, which have acquired the *gltR24* mutation enabling the encoded TF GltR24 variant to compensate for the loss of GltC (Belitsky and Sonenshein, 1997). In this thesis, it is planned to assess whether the DNA-binding activity of GltR24 is controlled by the GDHs, as it is the case for GltC. It is also planned to visualize emerging mutations in suppressor mutants at the level of single cells.

2. Materials & Methods

2.1. Materials

Materials, chemicals, commercial kits, and oligo nucleotides are listed in Ch. 6.

2.1.1. Bacterial strains and plasmids

Bacterial strains and plasmids are listed in Ch. 6.

2.1.2. Growth media

Media, solutions, and buffers were prepared with dH₂O and autoclaved for 20 min at 121 °C and 1 bar excessive pressure. Thermolabile substances were dissolved and sterilized by filtration. All solutions are prepared with water, unless otherwise indicated.

2.1.2.1. Bacterial growth media

E. coli was grown in LB and BHI medium, whereas *B. subtilis* was grown in LB, SP and different C-minimal media, supplemented with varying additives as indicated. Media were solidified using 1.5 % (w/v) agar for complex media and 1.5 % (w/v) Bacto agar for C-minimal media.

Complex media

SP medium

8 g Nutrient broth
0.25 g MgSO₄ · 7 H₂O
1 g KCl

Ad 1 l with dH₂O, autoclave

Afterwards:

1 ml CaCl₂ (0.5 M)
1 ml MnCl₂ (10 Mm)
2 ml Ferric ammonium citrate (2.2 mg/ml)

LB medium

10 g Tryptone
5 g Yeast extract
10 g NaCl

Ad 1 l with dH₂O

Starch medium

7.5 g Nutrient broth
5 g Starch

Ad 1 l with dH₂O

Minimal media

1x C-minimal medium

20 ml 5x C-salts
1 ml Tryptophan (5 mg/ml)
1 ml Ferric ammonium citrate (2.2 mg/ml)
1 ml III' salts

Ad 100 ml with dH₂O

Possible additives:

2 ml Potassium glutamate (40%) for CE medium
2 ml Sodium succinate (30%) for CS medium
1 ml Glucose (50%) for C-Glc medium

10x MN medium

136 g K₂HPO₄ · 3 H₂O
60 g KH₂PO₄
10 g Sodium citrate · 2 H₂O

Ad 1 l with dH₂O

MNGE medium

1 ml 10x MN medium
800 µl Glucose (50%)
50 µl Potassium glutamate (40%)
50 µl Ferric ammonium citrate (2.2 mg/ml)
100 µl Tryptophan (5 mg/ml)
30 µl MgSO₄ · 7 H₂O
+/- 100 µl CAA (10%)

Ad 10 ml with dH₂O

Additives

5x C-salts

20 g KH₂PO₄
80 g K₂HPO₄ · 3 H₂O
16.5 g (NH₄)₂SO₄

III' salts0.232 g $\text{MnSO}_4 \cdot 4 \text{H}_2\text{O}$ 12.3 g $\text{MgSO}_4 \cdot 7 \text{H}_2\text{O}$ Ad 1 l with dH₂O**Inducers & indicators****IPTG**

Stock solution: 0.5 M

Working concentration: 0.5 mM

X-Gal

Stock solution: 40 mg/ml (in DMF)

Working concentration: 40 µg/ml

Xylose

Stock solution: 50%

Working concentration: 1%

2.1.2.2. Antibiotics

All antibiotics were dissolved in dH₂O except chloramphenicol, erythromycin and tetracycline which were dissolved in 70% EtOH. For selection of the *ermC* resistance cassette, erythromycin and lincomycin were used in combination.

Selective concentrations for *B. subtilis*

Chloramphenicol	5 µg/ml
Erythromycin	2 µg/ml
Kanamycin	10 µg/ml
Lincomycin	25 µg/ml
Spectinomycin	150 µg/ml
Tetracycline	12.5 µg/ml
Zeocin	35 µg/ml

Selective concentrations for *E. coli*

Ampicillin	100 µg/ml
Kanamycin	10 µg/ml

2.2. Methods**2.2.1. General methods**

All general methods used in this work:

- Chain terminator sequencing (Sanger *et al.*, 1977)

- Determination of optical density (Sambrook *et al.*, 1989)
- Determination of protein concentrations (Bradford, 1976)
- Gel electrophoresis of DNA (Laemmli, 1970)
- Ligation of DNA fragments (Sambrook *et al.*, 1989)
- Plasmid isolation from *E. coli* (Sambrook *et al.*, 1989)
- Precipitation of nucleic acids (Sambrook *et al.*, 1989)

2.2.2. Cultivation of bacteria

Unless otherwise indicated, *E. coli* was grown in flasks or reaction tubes with LB medium overnight at 37 °C and 200 rpm. *B. subtilis* was grown in flasks, reaction tubes or 96 well microtiter plates with LB, SP, CSE-Glc, C-Glc or MNGE medium at 37 or 28 °C at 200 rpm. Media were inoculated with bacteria from single colonies on plate or from -80 °C cryo-stocks. The growth was monitored measuring the optical density at 600 nm.

2.2.2.1. For Western blot or expression analysis

A 3 ml LB culture was inoculated from a single colony on plate and incubated at 37 °C and 200 rpm. This culture was used to inoculate overnight pre-cultures in desired media as LB, CSE-Glc or other. On the next morning, the main culture was inoculated to an OD₆₀₀ of 0.1 and incubated at 37 °C and 200 rpm until and OD₆₀₀ of 0.5 to 0.8 was reached. Now in the exponential phase, 1.5 ml of the cells were harvested and centrifuged for 3 min at 4 °C and 13 000 rpm. The resulting cell pellet was stored at -20 °C.

2.2.2.2. For overexpression of proteins in *E. coli*

An LB overnight culture of *E. coli* BL21 harboring an overexpression plasmid was used to inoculate 1000 ml BHI medium to an OD₆₀₀ of 0.1 and incubated at 37 °C and 200 rpm. Expression of the heterologous protein was induced when the culture reached an OD₆₀₀ of 0.5-0.7 with 0.1 mM IPTG followed by additional 3 h of incubation.

Cells were harvested by centrifugation for 15 min at 5000 rpm at 4 °C. The cell pellet was washed in 50 ml of 1x PBS buffer and centrifuged for 15 min at 8500 rpm and 4 °C. The resulting cell pellet was stored at -20 °C.

2.2.3. Genetic modification of bacteria

2.2.3.1. Transformation of *E. coli*

A common method for generating competent *E. coli* cells is the CaCl₂ method (Lederberg and Cohen, 1974). Positively charged Ca²⁺ ions bind the negatively charged DNA backbone to phosphate groups belonging to the inner core of lipopolysaccharides on the outer cell membrane, enabling an easy access for the DNA into the cell during a heat shock.

Therefore, an overnight preculture of the desired *E. coli* strain was used to inoculate 10 ml LB in a 100 ml shake flask to an OD₆₀₀ of 0.05. The culture was grown at 37 °C and 200 rpm to an OD₆₀₀ of 0.3 and harvested by centrifugation at 4°C and 5 000 rpm for 6 min. The resulting cell pellet was resuspended in 5 ml ice-cold 50 mM CaCl₂ solution. The harvesting procedure was repeated after 30 min incubation on ice, this time the cell pellet was resuspended in 1 ml 50 mM CaCl₂ and can be used for transformation.

10-100 ng DNA were mixed carefully with 100 µl of the competent *E. coli* cells. After 30 min incubation on ice the cells were heat shocked at 42 °C for 90 s and incubated on ice for 5 min. For recovery, 500 µl LB medium were added to the cell suspension followed by an incubation at 37 °C for 1 h with agitation. Finally, 50 µl and the concentrated rest of the cell suspension were plated on LB plates supplemented with appropriate antibiotics and incubated overnight at 37 °C.

2.2.3.2. Transformation of *B. subtilis*

B. subtilis becomes naturally competent upon nutrient starvation within the stationary growth phase. The tightly regulated transcription factor ComK induces the expression of genes important

for DNA uptake and recombination of homologous DNA fragments into the chromosome (Krüger and Stingl, 2011). The highest *comK* expression occurs in minimal medium with glucose as sole carbon source when exponential growth ceases (Hamoen *et al.*, 2003).

Therefore, an overnight culture of the desired *B. subtilis* strain was used to inoculate 10 ml MNGE medium with CAA to an OD₆₀₀ of 0.1 and grown in a 100 ml shaking flask at 37 °C and 200 rpm. At an OD₆₀₀ of 1.3 the culture was diluted with 10 ml MNGE w/o CAA and incubated for 1h. Subsequently, 400 µl cell suspension were transformed with 0.1-1 µg DNA. After 30 min incubation at 37 °C and 200 rpm, the cell suspension was supplemented with 100 µl expression mix (500 µl yeast extract (5 %), 250 µl CAA (10%), 250 µl dH₂O and 50 µl tryptophan (5 mg/ml)) and again for 1 h incubated. Finally, 50 µl & the concentrated rest of the cell suspension were plated on SP plates supplemented with appropriate antibiotics and incubated overnight at 37 °C (Kunst and Rapoport, 1995).

2.2.4. Preparation and detection of DNA

2.2.4.1. Plasmid isolation from *E. coli*

Plasmids were isolated from *E. coli* overnight cultures (5 ml LB) using the NucleoSpin Plasmid-Kit from Macherey-Nagel.

2.2.4.2. Isolation of gDNA from *B. subtilis*

To isolate gDNA from *B. subtilis*, cells were either grown in 5 ml LB or C-Glc overnight or 5 ml SP for 6 h. The gDNA was extracted using the peqGOLD Bacterial DNA Kit from PEQLAB.

2.2.4.3. Gel electrophoresis

For size analysis of DNA fragments or gDNA 1 % agarose gels having a size of 85 x 100 x 3-5 mm were used. 30 ml of the 1 % agarose solution was supplemented with 3 µl of HDGreen Plus Safe DNA Dye (Intas) before solidification at RT.

Afterwards the gel was overlaid with 1x TAE buffer and DNA samples mixed with DNA loading dye were loaded on the gel. 100-120 V were applied until the marker reached the lower third of the gel. For detection of the DNA within the gel a photo was taken under UV light (254 nm) using the GelDoc™ XR (Biorad). As size marker *EcoRI/HindIII* digested λ -phage DNA was used.

DNA loading dye (5x)

5 ml	100 % Glycerol
200 μ l	50 x TAE
10 mg	bromophenol blue
10 mg	xylene cyanole
4.5 ml	dH ₂ O

TAE buffer (50x)

242 g	Tris
57.1 ml	Acetic acid
100 ml	EDTA (0.5 M, pH 8.0)

Ad 1 l with dH₂O

2.2.4.4. Sequencing of DNA

DNA fragments and plasmids were sequenced externally by Microsynth (Balgach, Switzerland). The Göttingen Genomics Laboratory performed whole genome sequencing.

2.2.4.5. Cloning procedures

For cloning preparation, the PCR fragment and a receiving vector were cleaved using DNA restriction enzymes from ThermoFisher. The vector was subsequently dephosphorylated at its 5' end using alkaline phosphatase (FastAP). It is sufficient to dephosphorylate 1 ng DNA with 1 μ l FastAP for 30 min at 37 °C. 10-100 ng of the dephosphorylated vector was ligated to the 5-fold amount of PCR fragment using T4 DNA ligase for 1 h at RT in darkness or overnight at 16 °C.

2.2.4.6. Polymerase chain reaction

Plasmid DNA or gDNA were used as templates for polymerase chain reactions (PCR). For cloning Phusion™ and for check PCRs *Taq* polymerase was used.

100 μ l PCR batch for Phusion™ polymerase

20 μ l	5x Phusion HF reaction buffer
1,6 μ l	dNTPs (12,5 μ mol/ml)
4 μ l	fwd oligonucleotide (5 pM)
4 μ l	rev oligonucleotide (5 pM)
1 μ l	Phusion™ polymerase
68,4 μ l	dH ₂ O

For each sample:

1 μ l	Template (cDNA, Plasmid)
-----------	--------------------------

Thermocycler program for Phusion™

Initial denaturation	02:00 min	98 °C	1x
Denaturation	00:20 min	98 °C	} 30x
Annealing	01:00 min	T _m [-5 °C]	
Elongation	30 s/kbp	72 °C	
Final Elongation	10:00 min	72 °C	1x
Hold	∞	15 °C	1x

100 μ l PCR batch for *Taq* polymerase

10 μ l	10x <i>Taq</i> reaction buffer
4 μ l	dNTPs (12,5 μ mol/ml)
5 μ l	fwd oligonucleotide (5 pM)
5 μ l	rev oligonucleotide (5 pM)
3 μ l	<i>Taq</i> polymerase
63 μ l	dH ₂ O

For each sample:

10 μ l	Template <i>E. coli</i> clone in H ₂ O
------------	---

Thermocycler programs for *Taq* polymerase

Initial denaturation	05:00 min	96 °C	1x
Denaturation	00:45 min	96 °C	} 30x
Annealing	01:00 min	T _m [-5 °C]	
Elongation	60 s/kbp	72 °C	
Final Elongation	10:00 min	72 °C	1x
Hold	∞	15 °C	1x

2.2.4.7. Long flanking homology PCR

B. subtilis is capable of homologous recombination, which is important to repair and

maintain DNA integrity but also to integrate exogenous DNA fragments into its chromosome (horizontal gene transfer) even if the homologous sequences are as short as 70 bp (Khasanov *et al.*, 1992). This capability can be used as molecular tool to delete or introduce *goi* genes (Wach, 1996). Long flanking homology PCR is used to fuse two DNA fragments flanking a gene of interest in the *B. subtilis* genome to an antibiotic resistance cassette. The resulting linear DNA fragment is used to transform *B. subtilis* as described previously (p. 24). Resistance cassettes were amplified from plasmids pDG646, pDG780, pDG1726, pDG1513, pDG148 and pGEM-cat for resistance against erythromycin/ lincomycin, kanamycin, spectinomycin, tetracycline, phleomycin, and chloramphenicol, respectively (Guérout-Fleury *et al.*, 1995). 1 kbp PCR fragments were amplified from *B. subtilis* genome flanking the up- and downstream regions of the *goi* using oligonucleotides with overhangs homologous to the resistance cassette. During the first step of the LFH PCR, homologous regions aligned and thereby the 3' end of the upstream fragment was joined to the 5' end of the resistance cassette and the 3' end of the resistance cassette to the 5' end of the downstream fragment. In the second step, the resulting joined fragment was amplified using the outer oligonucleotides.

100 µl LFH PCR batch

20 µl	5x Phusion HF Reaction Buffer
4 µl	dNTPs (12,5 µmol/ml)
[8 µl	fwd oligonucleotide (5 pM)]
[8 µl	rev oligonucleotide (5 pM)]
1 µl	PhuS/Phusion™ Polymerase
1 µl	upstream fragment (100 ng/µl)
1 µl	downstream fragment (100 ng/µl)
1 µl	resistance cassette (150 ng/µl)

Ad 100 µl dH₂O

Thermocycler programs for LFH PCR step 1

Initial			
denaturation	01:00 min	98 °C	1x

Denaturation	00:15 min	98 °C	} 10x
Annealing	00:30 min	52 °C	
Elongation	02:15 min	72 °C	
Hold	∞	8 °C	1x

Thermocycler program for LFH PCR step 2 after addition of oligonucleotides

Denaturation	00:15 min	98 °C	} 10x
Annealing	00:30 min	52 °C	
Elongation	04:00 min +5 s/cycle	72 °C	
Final Elongation	10:00 min	72 °C	1x
Hold	∞	8 °C	1x

2.2.4.8. Combined chain reaction PCR

Site directed mutagenesis was performed with mutagenic oligonucleotides hybridizing more strongly to the DNA compared to external fwd and rev oligonucleotides amplifying the *goi* (Bi and Stambrook, 1998). The mutagenic oligonucleotide harbored a single nucleotide point mutation and was phosphorylated at its 5' end. During the CCR PCR a thermostable DNA ligase closed the emerging gap between the 5' end and the 3' end of elongated upstream oligonucleotide. For the CCR PCR strongly diluted plasmid DNA was used as template and Phusion™ polymerase as polymerase without 5'-3'-exonuclease activity.

100 µl CCR PCR batch

2 µl	fwd oligonucleotide
2 µl	rev oligonucleotide
4 µl	mutagenic oligonucleotide
1 µl	plasmid DNA (strongly diluted)
5 µl	10x ampligase
1 µl	Phusion™ polymerase
3 µl	ampligase
2 µl	dNTP
2 µl	BSA
30 µl	dH ₂ O

Thermocycler programs for CCR PCR

Initial			
denaturation	05:00 min	95 °C	1x

Denaturation	01:00 min	95 °C	} 30x
Annealing	01:00 min	T _m [-5 °C]	
Elongation	04:00 min	68 °C	
Final Elongation	10:00 min	68 °C	1x
Hold	∞	15 °C	1x

2.2.4.9. Southern blot

Blotting procedure

A Southern blot allows the detection of a specific DNA sequence within digested gDNA. Therefore 300 ng gDNA of *B. subtilis* were digested with 3 µl FastDigest restriction enzyme for 5 h at 37 °C and subsequently separated by gel electrophoresis (see p. 24). To blot the DNA onto a nylon membrane, the vacuum blot device VacuGene™ XL (GE Healthcare) was used. The agarose gel was cleaned between different buffers.

Blotting steps with 15 ml buffer:

15 min	depurination buffer	} 60 mbar
20 min	denaturation buffer	
20 min	neutralization buffer	
2-x h	20x SSPE	80 mbar

Afterwards, the membrane is dried with Whatman Paper and crosslinked to the DNA via 90 s UV light treatment.

Depurination buffer

5.2 ml conc. HCl
Ad 250 ml with dH₂O

Denaturation buffer

43.83 g NaCl
10 g NaOH
Ad 500 ml with dH₂O

Neutralization buffer

121.14 g Tris-base
87.66 g NaCl
Ad 1 l with dH₂O, adjust pH to 7.4

20x SSPE

175.3 g NaCl
26.6 g NaH₂PO₄ · 2 H₂O

Dissolve in 800 ml dH₂O

7.4 g Na₂EDTA

Dissolve in 100 ml dH₂O, adjust pH to 8-9 (with NaOH). Merge solutions and ad 1 l with dH₂O, adjust pH to 7.4

Hybridization of DNA and DIG-labelled probes

For hybridization of the digested gDNA with a specific DIG labelled probe, the nylon membrane is inserted into a hybridization tube containing 25 ml prehybridization buffer and incubated for 1 h at 68 °C rotating. 15 µl of the RNA probe is diluted in 500 µl prehybridization buffer and incubated for 10 min at 95 °C and further diluted in 4.5 ml prehybridization buffer. The initial prehybridization buffer is removed from the hybridization tube and the RNA probe containing buffer added. Incubation occurred at 68 °C overnight while turning, followed by several washing steps:

2x 10 min	15 ml P1	RT
2x 15 min	15 ml P2	68 °C
5 min	15 ml 1x DigP1	} RT
30 min	5 ml blocking solution 45 ml 1x DigP1	
30 min	5 ml blocking solution 45 ml 1x DigP1 5 µl Anti-digoxigenin AP Fab fragments	
3x 10 min	15 ml DigP1	
10 min	15 ml P3	

Afterwards, substrate (5 µl CDP* in 1 ml P3) applied for detection of the alkaline phosphatase coupled to the anti-digoxigenin fragments using the ChemoCam Imager (INTAS).

P1

100 ml 20x SSPE
10 ml SDS (10 %)
Ad 1 l with dH₂O

5x DigP1

58.04 g Maleic Acid
43.83 g NaCl
36 g NaOH

Ad 1 l with dH₂O, adjust pH to 7.5

P2

5 ml 20x SSPE
10 ml SDS

Ad 1 l with dH₂O, adjust pH to 7.4

P3

12.1 g Tris-base
5.8 g NaCl

Ad 1 l with dH₂O, adjust pH to 9.5

Blocking solution

5 g Blocking reagent

Ad 50 ml 1x DigP1

Pre-hybridization solution

7.5 ml 20x SSPE
3 ml Blocking solution
300 µl N-Lauroylsarcosine (10 %)
60 µl SDS solution (10 %)

Ad 30 ml with dH₂O

Production of RNA probes

The RNA probe had a size of 500 bp and annealed to a region that was not digested by the restriction enzyme used to digest the gDNA of *B. subtilis*. The rev oligonucleotide had a T7 extension at its 5' end, to allow an *in vitro* transcription.

In vitro transcription:

13 µl PCR product (200-500 ng)
2 µl 10x DIG RNA Labelling Mix
2 µl Transcription buffer
2 µl T7 RNA polymerase
1 µl Protector RNase Inhibitor

Incubation for 2 h at 37 °C

1 µl 0.5 M EDTA pH 8.0
2.5 µl 4 M LiCl
75 µl 96 % EtOH (cold)

The probe precipitates at -20 °C overnight was centrifuged for 30 min at 13000 rpm and washed with 500 µl 70 % EtOH. Afterwards, the supernatant was discarded and the pellet dried

before it was dissolved in 100 µl dH₂O and 1 µl protector RNase inhibitor.

2.2.5. Preparation & detection of proteins

2.2.5.1. Cell disruption

French pressure cell press

A cell pellet from an overexpression cultivation was resuspended in 15 ml 1x PBS buffer with 5 mM imidazole. The cell disruption took place in an ice-cold bomb with a pressure of 18000 PSI for three times. Subsequently, the cell lysate was centrifuged for 15 min at 8500 rpm and 4 °C. The supernatant was further centrifuged for 30 min at 35000 rpm and 4 °C. The resulting supernatant was free of cell debris and transferred to a novel falcon tube.

Preparation of crude extracts

For Western blot and β-galactosidase activity assay *B. subtilis* was grown to exponential phase (OD₆₀₀ 0.5-0.8) and 1.5 ml were harvested. To extract cell free crude extract, cells were treated with lysozyme and DNase I as described in the following.

Crude extracts for β-galactosidase activity assays

The cell pellet was resuspended in 400 µl Z-buffer/LD-Mix (20 µl LD-Mix in 4 ml Z-buffer with β-mercaptoethanol) and incubated for 10 min at 37 °C. Cell debris were removed by centrifugation at 13 000 rpm at 4 °C for 3 min.

Crude extracts for Western blots

The cell pellet was resuspended in 40 µl Z-buffer/LD-Mix (100 µl LD-Mix in 4 ml Z-buffer without β-mercaptoethanol) and incubated for 30 min at 37 °C and 600 rpm. Cell debris were removed by centrifugation at 13 000 rpm at 4 °C for 3 min.

LD-Mix

100 mg lysozyme
10 mg DNase I

Ad 10 ml with dH₂O

Z-buffer

534 mg	Na ₂ HPO ₄ · 2 H ₂ O
276 mg	NAH ₂ PO ₄
37 mg	KCl
50 µl	MgSO ₄ (1 M)
+/-175 µl	β-Mercaptoethanol (toxic)

Ad 50 ml with dH₂O

2.2.5.2. IMAC

The immobilized metal affinity chromatography (IMAC) is used to purify His₆-tagged proteins from crude extracts (Franken *et al.*, 2000). The histidine residues formed coordination bonds with Ni²⁺ ions immobilized via nitrilotriacetic acid to a sepharose matrix polymer. All other proteins not capable of binding to Ni²⁺ moved through the column and were collected in the flow through fraction (FT). Imidazole has a higher affinity to Ni²⁺ compared to the His₆-tag and is used to elute the tagged protein.

For a 1 l cell culture 2.5 ml Ni-NTA[®] Sepharose (50 %) were used, resulting in 1.25 ml column bed volume. The column was equilibrated with 12.5 ml 1x PBS buffer with 5 mM imidazole before the crude extract was loaded. Remaining untagged proteins were washed from the column by the addition of 10 ml 1x PBS buffer with 5 mM imidazole. The elution occurred with increasing imidazole concentrations (10 mM, 50 mM, 100 mM, 200 mM, and 500 mM imidazole in 1x PBS).

All fractions were analyzed via SDS PAGE, combined respectively, and dialyzed in 1x PBS buffer.

10x PBS buffer

80 g	NaCl
2 g	KCl
26.8 g	Na ₂ HPO ₄ · 7 H ₂ O
2.4 g	KH ₂ PO ₄

Ad 1 l with dH₂O, adjust pH to 7.4

SUMO purification

The pET SUMO system provides the possibility to generate proteins without tag and increase the solubility of these proteins during purification. Therefore, the respective genes are cloned into the vector pET SUMO adapt using the restriction enzymes *Bsa*I and *Xho*I. The cloning procedure takes place in *E. coli* DH5α. The resulting plasmid is transformed into *E. coli* BL21 and grown in a 30 ml LB o/n culture at 37 °C. For the overexpression 1 l BHI medium are inoculated to an OD₆₀₀ of 0.05 and grown to the exponential phase (OD₆₀₀ of 0.5 to 0.8). To induce gene expression, IPTG is added to the medium to a final concentration of 0.5 mM. The culture is grown for additional 4 h at 37 °C. For harvesting, the cells are centrifuged at 5 000 rpm for 15 min at 4 °C. The supernatant is discarded and the pellet resuspended in 50 ml ice-cold 1x PBS buffer containing 5 mM imidazole. A second centrifugation takes place at 8 500 rpm at 4 °C. The supernatant is discarded and the cell pellet frozen at -20 °C.

The cells are disrupted using the French pressure cell press (see Ch. 2.2.5.1). Subsequently the proteins are purified from the crude extract via IMAC. The purified proteins still contain the His-SUMO-tag which was cleaved of during dialysis by the addition of 1:50 (v/v) SUMO protease (0.8 mg/ml) in the dialysis tube overnight. To improve the cleavage reaction, the protein solution was incubated at 30 °C slowly turning for 1 h. Next, the proteins are purified again via IMAC, but this time the His-SUMO-tag and the His-tagged SUMO protease will bind to the matrix and the protein of interest will be in the flow through.

2.2.5.3. Dialysis

A dialysis is used to remove salt debris or for instance imidazole from purified proteins. Thereby, the proteins, secured in a dialysis tube, are dialyzed against a 1000-fold excess of the desired buffer as 1x PBS overnight at 6 °C.

2.2.5.4. SDS-PAGE

A sodium dodecyl sulfate polyacrylamide gel electrophoresis (SDS-PAGE) is used to separate proteins according to their molecular mass (Laemmli, 1970). The size separation relies on the speed of negatively charged denaturated proteins moving through the gel towards the anode (Garfin, 2009). The denaturation was performed for 10 min at 95 °C in 1x PAP. The gel consisted of a running gel having a denser PAA net (12%) to separate the proteins and a stacking gel with a lower PAA net (5%) to collect all proteins a running front. Gel electrophoresis was performed in 1x PLP buffer at 80-140 V and PageRuler™ Plus (ThermoFisher) was used as size standard.

5x PAP

1.3 ml	Tris-HCl, pH 6.8
1.6 ml	β-mercaptoethanol
2.5 ml	20 % SDS
5 ml	99.5 % Glycerol
0.02 g	bromophenol blue

Ad 10 ml with dH₂O

12 % running gel

4.9 ml	dH ₂ O
6 ml	30% Acryl-bisacrylamide
3.8 ml	1.5 M Tris (pH 8.8)
150 μl	10 % SDS
150 μl	10 % Ammonium persulfate
15 μl	TEMED

5 % stacking gel

10.25 ml	dH ₂ O
1.95 ml	30% Acryl-bisacrylamide
1.3 ml	1.5 M Tris (pH 6.8)
150 μl	10 % SDS
150 μl	10 % Ammonium persulfate
30 μl	TEMED

10x PLP

144 g	L-Glycine
30 g	Tris-base
10 g	SDS

Ad 1 l with dH₂O, adjust pH to 8.3

2.2.5.5. Coomassie staining

Proteins in an SDS gel were visualized using Coomassie stain (Meyer and Lamberts, 1965). First the gel is fixed for 10 min in fixation solution and subsequently stained for 15 min in Coomassie stain. As the SDS gel is now completely stained it is necessary to remove the background stain with Coomassie de-stain solution or water (Sasse and Gallagher, 2009).

Fixation solution

10 % (v/v)	Acetic acid
45 % (v/v)	Methanol

Coomassie stain

0.5 % (w/v)	Coomassie Brilliant Blue
10 % (v/v)	Acetic acid
45 % (v/v)	Methanol

Coomassie de-stain

5 % (v/v)	Acetic acid
20 % (v/v)	EtOH

2.2.5.6. Western blot

A Western blot is used to detect specific proteins via antibodies in cell free crude extracts or protein purifications (Burnette, 1981). Therefore, the proteins are separated via SDS PAGE and blotted for 2 h at 80 mA on a PVDF membrane using a semi dry blotting machine (transfer buffer). The PVDF membrane is previously activated for 30 s in 100 % methanol. To prevent the antibody from binding to unspecific protein binding sites of the PVDF membrane, these sites are blocked with blotto treatment for 2 h. The primary antibody detecting specific proteins is diluted in blotto (Anti-GFP 1:10000, Anti-Strep 1:10000, Anti-GudB 1:1000, Anti-RocG 1:15000, Anti HPr 1:10000, PrfA: 1:1000) and incubated with the PVDF membrane overnight at 6 °C while moving. During three 30 min washing steps in blotto, the excess of the primary antibody was removed. The secondary antibody (anti-rabbit, 1:100000 in

blotto) detecting the primary antibody was incubated for 30 min and removed by three 20 min wash steps in blotto. The PVDF membrane was subsequently washed with dH₂O and incubated in buffer III for 5 min. As the secondary antibody is coupled to an alkaline phosphatase, CDP* served as substrate (1:100 in buffer III) and the emerging chemiluminescence was detected using the ChemoCam Imager (Intas).

Transfer buffer

15.1 g Tris-base
 72.1 g Glycin
 750 ml Methanol
 Ad 5 l with dH₂O

Blotto

100 ml 10x TBS
 25 g Skim milk powder
 1 ml Tween20
 Ad 1 l with dH₂O

10x Buffer III

121.14 g Tris-base
 58.44 g NaCl
 Ad 1 l with dH₂O, adjust pH to 9.5 (with NaOH)

10x TBS buffer

60 g Tris-base
 90 g NaCl
 Ad 1 l with dH₂O, adjust pH to 7.6 (with HCl)

2.2.5.7. Enzyme activity assays

β-Galactosidase activity assay

The conversion of o-nitrophenyl-β-D-galactopyranoside (ONPG) to galactose and o-nitrophenyl catalyzed by the β-galactosidase reflects directly the activity of the investigated promoter (Miller, 1972). As o-nitrophenyl absorbs light at 420 nm, its production can be measured directly.

The samples were prepared as described in Ch. 2.2.5.1. 100 μl of the crude extract were added to 700 μl Z-buffer (with β-mercaptoethanol) and pre-incubated for 5 min at 28 °C. 20 μl of the crude extract are used for the Bradford assay. The time dependent reaction starts with the addition of 200 μl ONPG, 800 μl Z-buffer serve as control. The reaction is stopped by the addition of 500 μl Na₂CO₃ as soon as yellow color is detectable. The absorption of the produced o-nitrophenyl is measured at 420 nm. The β-galactosidase activity was measured using the formula:

$$\frac{Units}{mg\ protein} = \frac{1500 \cdot A420}{\Delta t \cdot A595 \cdot 1.7 \cdot 4.4} = \frac{2000 \cdot A420}{\Delta t \cdot A595}$$

ONPG

4 mg ONPG
 Ad 1 ml with Z-buffer without β-mercaptoethanol

Stop solution

26.5 g Na₂CO₃
 Ad 1 ml with Z-buffer without β-mercaptoethanol

Glutamate dehydrogenase activity assay

This method is adapted from Aghajanian *et al.*, 2003. The conversion of glutamate to α-ketoglutarate and ammonium is NAD⁺ dependent. The resulting production of NADH can be monitored at an OD₃₄₀. As enzyme reactions are very fast it is important to add the component starting the reaction (glutamate) at last. The assay was performed in 1x PBS using 100 mM glutamate, 6 μM tag-free RocG and 1 mM NAD⁺.

2.2.6. Detection of Mutation frequencies

2.2.6.1. Comparison of mutation frequencies

To compare mutation frequencies of mutations that result in the acquisition of a GDH as for

instance the *gudB^{CR}* gene, the intragenic/intergenic TR strains, or the activator/reporter system strains, cells were grown in two selective media. For selection against a functional GDH C-Glc minimal medium and to select for a functional GDH SP medium was used.

First, cells are streaked on C-Glc pates and incubated o/n at 37 °C. The pates are used to inoculate 5 ml C-Glc o/n cultures, which are subsequently used to inoculate a 10 ml C-Glc o/d culture to an OD₆₀₀ of 0.1. The cells were harvested in the exponential phase at an OD₆₀₀ of 0.5 to 0.8. 1x C-salts were used to wash the cells twice and adjust the OD₆₀₀ to 0.4. 100 µl of the cell suspension (4 · 10⁶ cells in total) were plated on an area of 25 cm² on a SP plate and incubated at 37 °C. Photos were taken at 1, 2, 3 and 4 dpi. To compare different mutants, huge square plates (24.5 x 24.5 cm) were used. Additionally, the culture was tested for active GDHs by plating the cell suspension additionally on CE minimal medium. The CE plates were analyzed at 2 dpi.

Fiji and R were used to analyze the images. First, the images are processed in Fiji to ensure a proper identification of the SM colonies. The background is subtracted using a rolling ball radius of 10, the filter gaussian blur is applied using a sigma (radius) of 0.5 and triangle dark is chosen as auto threshold. Subsequently the file is converted to a binary picture and the watershed algorithm is used to separate colonies grown together. In Fiji squares of 3.79 x 3.79 cm were analyzed for each mutant at each day. A grid structure was applied to ensure monitoring the same spot over time. Using the analyze particles option, the area of every single particle in each picture was measured and saved in a list.

This list was further processed in the statistical program R. Only particles with a size above 10⁴ pixels were counted as SM. The output is a

list with strain, dpi, and number of emerged SMs with an area above 10⁴ pixels.

To confirm the data, all pictures were examined and possible contaminations falsifying the SM count were corrected manually.

2.2.6.2. Fluctuation experiment

The fluctuation experiment is used to determine actual mutation rates (Luria and Delbrück, 1943; Lea and Coulson, 1949). Here, the selective pressures are adjusted exclusively to select for and against the acquisition of GDHs. The method was adapted from Gunka *et al.*, 2012.

5, 10, 15, 25, 50, 75 and 100 µl of 500 µl resuspended cell suspension of a single colony from C-Glc plates of the desired *B. subtilis* strain are used to inoculate 4 ml of C-Glc minimal medium. These cultures were grown o/d at 37 °C and 200 rpm to an OD₆₀₀ of 1 (10⁸ cells/ml) and diluted in 0.9 % NaCl up to 10⁻⁴ (10000 cells/ml). 22 flasks with 10 ml SP medium were inoculated with exact 100 µl of the dilution (100 cells in total) and grown o/n at 37 °C and 200 rpm to an OD₆₀₀ of 1. Serial dilutions in 0.9 % NaCl up to 10⁻⁶ are made of all cultures and of at least 6 cultures the dilutions are made up to 10⁻⁸. On CE medium, the dilutions 10⁻⁴, 10⁻⁵, and 10⁻⁶ are plated to identify the SMs and on C-Glc medium the dilutions 10⁻⁶, 10⁻⁷, and 10⁻⁸ to determine the cell titer. After two days of incubation at 37 °C, all cells are counted and the median number of SMs was determined.

A web based application was used to determine the final mutation rate (Gunka *et al.*, 2012).

2.2.7. Bacterial adenylate cyclase-based two-hybrid system

The bacterial adenylate cyclase based two-hybrid system (BACTH) is used to show *in vivo* protein-protein interactions. It takes advantage

of the reconstitution of the catalytic domain the of *Bordetella pertussis* adenylate cyclase (Karimova *et al.*, 1998). The adenylate cyclase consists of the T18 and T25 domains, that form a functional enzyme when they are near each other. To test the interaction of two proteins of interest, the domains of the adenylate cyclase are fused to the N- and C-terminus of the proteins of interest transformed into the *E. coli* strain BTH101 (see Ch. 2.2.3.1) and dropped on LB agar plates containing amp, kan, X-Gal and IPTG (Karimova *et al.*, 1998).

Association of the two proteins of interest leads to the formation of a functional adenylate cyclase and consequently cAMP synthesis. cAMP triggers the transcriptional activation of the lactose operon and the synthesis of the β -galactosidase. The formation of blue colonies indicates the conversion of X-Gal and the interaction of the proteins of interest. Pictures were taken after 24 h and 48 h.

2.2.8. Microfluidic analysis

To analyze growing cells over a long period of time, a microfluidic approach is used. Therefore, a single-use polydimethylsiloxane (PDMS) microfluidic chip (Fig. 2.1 A) is fabricated as previously described (Grünberger *et al.*, 2013). The chips used in this study were modified from Binder *et al.*, 2014 for *B. subtilis*. Two different chip designs were used. The chambers used for the mutation analysis have a size of 90 x 80 μm (Fig. 2.1 B) with open inlets in Ch. 3.2.1 the height is 778 nm and in Ch. 3.2.4 it is 702 nm. Each chip contains 400 growth chambers in parallel arrays (8 x 50) (Fig. 2.1 C). The microfluidic chip is mounted onto a motorized microscope (Nikon Eclipse Ti) equipped with an incubator and a camera as previously described (Binder *et al.*, 2014; Grünberger *et al.*, 2015). The temperature is kept constantly at 37 °C. To prepare the cells for investigation of SM occurrence in rich SP medium, o/n precultures are made in C-Glc medium. C-Glc medium is prone to micro

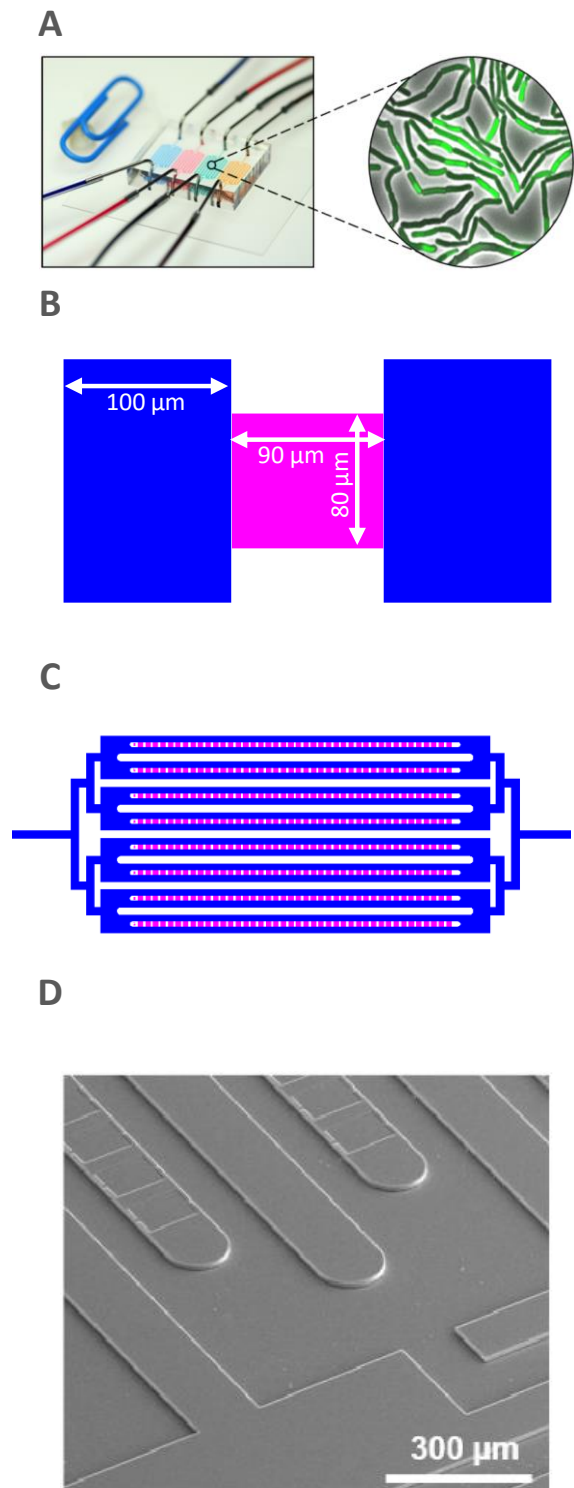


Fig. 2.1 Microfluidic chips

A: A microfluidic cultivation chip ready as it is mounted on a microscope (adapted from Burmeister, 2016) **B:** Scheme of the supply channel (blue) and the open growth chambers (pink) used in this study. **C:** overview of the chip structures (blue: main channels, pink: growth chambers). **D:** SEM images of chip structures. The main channel diverges to two channels harboring growth chambers (adapted from Burmeister, 2016).

precipitations, therefore, it is sterile filtered twice using an 0.2 and 0.1 μm filter. The remaining C-Glc medium is stored at 4 °C o/n and

filtered again using the 0.1 μm filter. The o/n preculture is used inoculated 10 ml C-Glc to an OD_{600} of 0.1. Once the culture reached an OD_{600} of 0.3 to 0.5 the cells were infused manually to the chip using a 1 ml syringe (Probst *et al.*, 2015). When 1-5 cells were trapped in each chamber, fresh SP medium was applied to the setup with a constant flow of 300 nl/min for 1 to 3 days. DIC and GFP images were taken every 10 min with an exposure time of 50 ms and 200 ms respectively using the YFPHQ filter.

The resulting images were analyzed in FIJI using the *microbeJ* plug in (Ducret *et al.*, 2016), thereby cell length and mean fluorescence values of each cell are determined.

3. Results

3.1. The mechanisms of *gudB^{CR}* mutagenesis

3.1.1. The cell density influences the TR mutagenesis

The high rate of *gudB^{CR}* gene activation in *B. subtilis* was studied already extensively (Gunka *et al.*, 2012; Gunka *et al.*, 2013), but a simple system to compare different mutation frequencies was always missing.

Therefore, an easy and reproducible method to compare mutation frequencies under constant

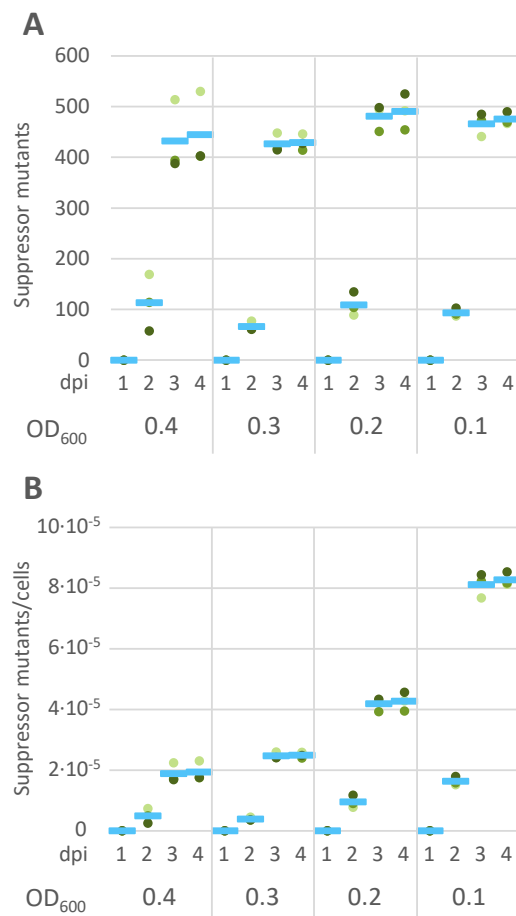


Fig. 3.1 Cell density dependence of TR mutagenesis. Comparison of mutation frequencies of *rocG::Tn10* (GP747). The strain was grown to an OD₆₀₀ of 0.5 to 0.6, washed twice in 1x C-salts, thereby the OD₆₀₀ was adjusted to 0.1, 0.2, 0.3, or 0.4 and 100 μ l were used for plating. $0.57 \cdot 10^6$, $1.15 \cdot 10^6$, $1.72 \cdot 10^6$, and $2.3 \cdot 10^6$ cells were plated, respectively. **A:** Number of mutants of the respective strains in dependence of time (1, 2, 3, and 4 dpi). **B:** The number of suppressor mutant per cells used for plating in dependence of time.

conditions was established. Cells were grown to the exponential phase (OD₆₀₀ 0.5 to 0.8) at 37°C in C-Glc minimal medium conferring a disadvantage upon the emergence of a SM harboring the *gudB⁺* gene. After two washing steps in 1x C-salts, $4 \cdot 10^6$ cells are plated (100 μ l of a cell suspension with the OD₆₀₀ of 0.4) on 25 cm² SP medium and incubated at 37 °C. Images are taken every 24 h. An area of 14.36 cm² is cut from the original image, consequently there are $2.3 \cdot 10^6$ cells investigated for the emergence of SMs, assuming an even plating efficiency. A strain lacking the *rocG* gene (GP747) will rapidly accumulate suppressor mutants (SMs) that have acquired the *gudB⁺* gene. This strain exhibits about 500 SM after 4 dpi in the experimental context described above. Interestingly, the same amount of SMs emerged from $0.57 \cdot 10^6$, $1.15 \cdot 10^6$, and $1.72 \cdot 10^6$ cells (Fig. 3.1 A). Hence, the mutation frequency increases with decreasing cell density (Fig. 3.1 B). For the future use of this experimental set up the lowest dilution having an OD₆₀₀ of 0.4 was used, because it is more difficult to guarantee an even bacterial lawn using higher dilutions.

3.1.2. Two machineries are involved in intra- and intergenic TR mutagenesis

3.1.2.1. Temperature dependencies of intra- and intergenic TRs

Next, the temperature dependence was assessed. Therefore, the *B. subtilis* strains GP747 (*rocG::Tn10 spc*), BP404 and BP405 are all grown at different temperatures (30, 37, and 42 °C) once streaked on SP medium as described above. The BP404 strain harbors a promoter in front of the *gudB^{CR}* gene inactivated by the introduction of a repeated sequence (Gunka *et al.*, 2012; Dormeyer *et al.*, 2014). Once the intergenic TR is

excised, the -35 and -10 regions have a perfect spacer and the RNAP can bind to the promoter to activate *gudB⁺* gene expression. The BP405 strain is isogenic to the BP404, but harbors an active promoter and an inactive *gudB^{CR}* gene. Removing the intragenic TR from the *gudB^{CR}* gene, results also in the acquisition of a functional *gudB⁺* gene expression. As expected, intra- and intergenic TR

have different mutation frequencies (Gunka *et al.*, 2012). The intragenic TR as present in the native locus or an artificial locus are removed in general with an increased efficiency compared to an intergenic TR (Fig. 3.2). As expected all three strains grow similar compared to each other at the different temperatures (Fig. 3.2 B).

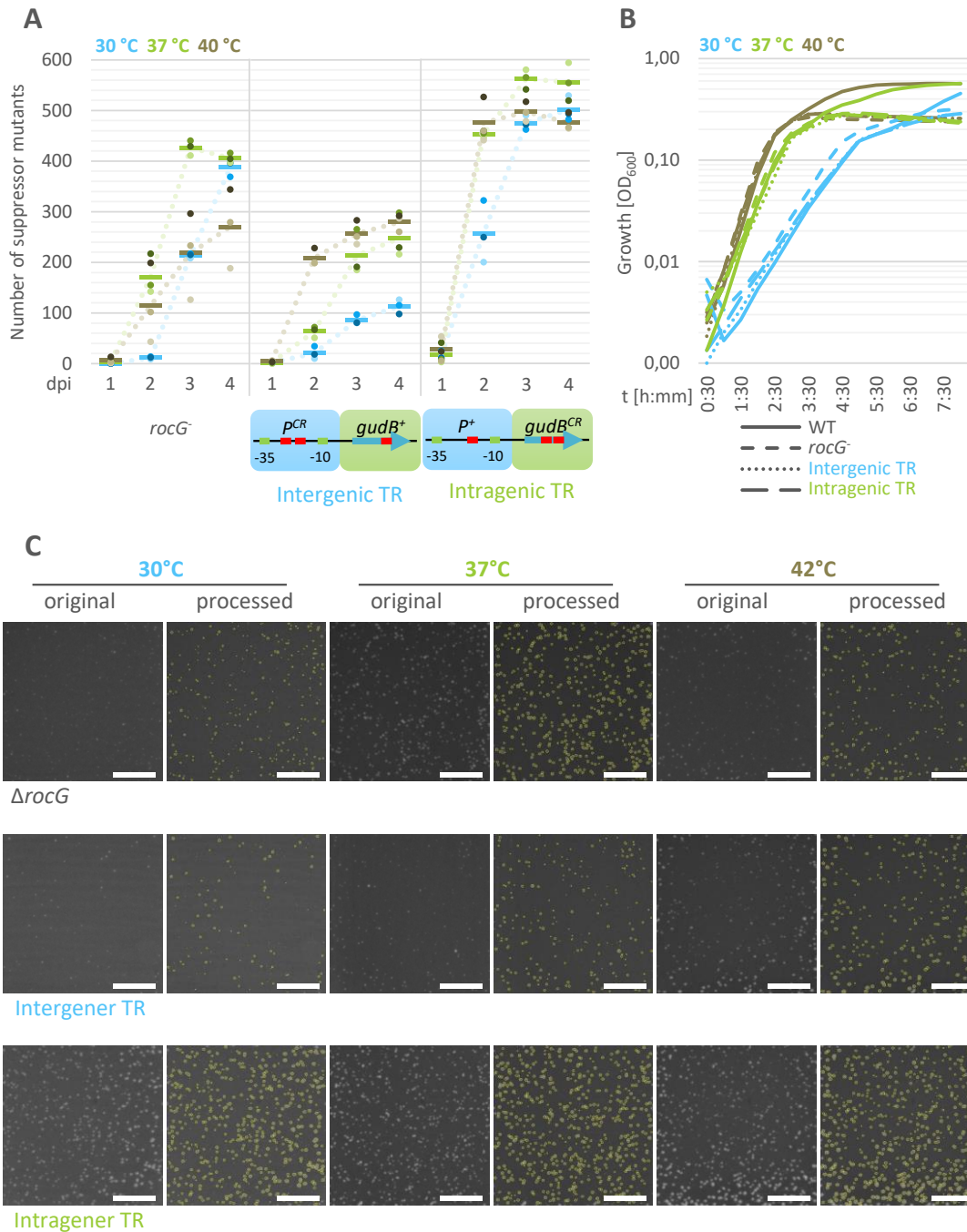


Fig. 3.2 Temperature dependence of TR mutagenesis
 Comparison of mutation frequencies of *rocG::Tn10* (GP747), a strain harboring an intragenic TR (BP404) and an intergenic TR (BP405) on SP medium. The strains were grown at different temperatures (30, 37, and 42 °C). **A**: Number of mutants of the respective strains in dependence of time (1, 2, 3, and 4 dpi). **B**: Growth curve of the strains including the WT (168) in SP medium. **C**: Representative pictures of the cells from A at 3 dpi before and after processing with Fiji. Scale bar 1 cm. The yellow marks indicate SMs found by Fiji.

In general, they grow faster with increasing temperatures. The wild type (168) reaches a higher OD₆₀₀ in the stationary phase compared to the strains deficient of a functional GDH (GP747, BP404, BP405). These differences are detectable after 2 to 3 h of growth at 42 and 37 °C but barely emerge after 7 h of growth at 30 °C. Besides the general differences of mutation frequencies of inter- and intragenic TRs, they are also differently dependent on temperatures. For intergenic TR, the highest mutation frequency is achieved at 42 °C. In contrast, at this temperature the mutation frequency is lowest for intragenic TRs. 37 °C leads to the highest mutation frequencies for intragenic TRs. The lowest mutation frequency is detected at 30 °C for intergenic TRs. Interestingly, the difference in mutation frequency from 30 to 37 °C is remarkable obvious, indicating a much stronger dependence of intergenic TR on the temperature.

3.1.2.2. Promoter strength

The mutation frequencies of inter- and intragenic TRs are drastically different and additionally differences regarding the temperature dependencies were observed (Fig. 3.2). This suggests different machineries being involved in TR mutagenesis. As mutations can occur during replication and transcription, and the native *gudB^{CR}* gene is highly expressed (Gunka *et al.*, 2012), the role of transcription on the excision of intragenic TRs was assessed. Promoters with a different strength were used to control the transcription rate. The promoter strengths decrease in the order $P_{alf1} > P_{gudB} > P_{alf2} > P_{alf4} > P_{-}$ (no promoter) (Stannek, 2015). The promoters were fused to a *gudB^{CR}* gene and transformed into a strain deficient of the native GDHs. These strains were subsequently compared regarding the mutation frequencies of the intragenic *gudB^{CR}* gene. The strongest promoter P_{alf1} exhibited the most SMs on SP

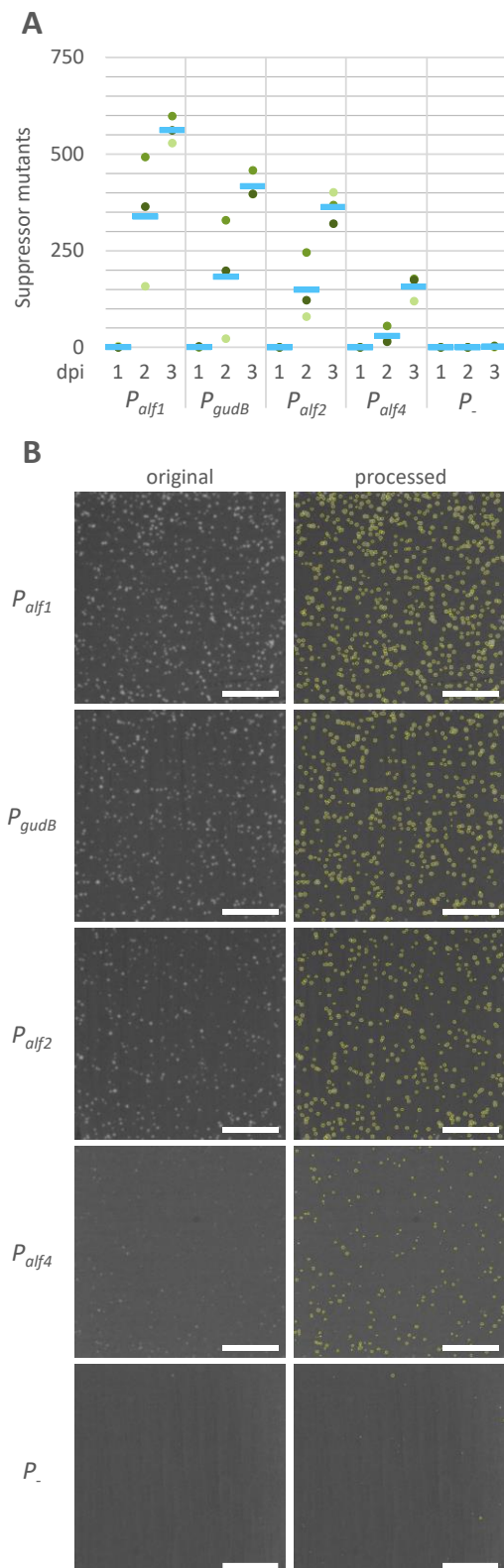


Fig. 3.3 Mutation frequency is dependent on promoter strength
Comparison of mutation frequencies of strains having *gudB^{CR}* fused to promoters with decreasing activity (BP672, BP671, BP674, BP675, BP673, respectively). **A**: Number of mutants of the respective strains in dependence of time (1, 2, 3, and 4 dpi). **B**: Representative pictures of the cells from A at 3 dpi before and after processing with Fiji. Scale bar 1 cm. The yellow marks indicate SMs found by Fiji.

medium. The mutation frequency of the *gudB^{CR}* gene in different strains correlates perfectly with the promoter strength. It decreases constantly with decreasing promoter strength and vanishes for the promoter-less *gudB^{CR}* gene fusion (Fig. 3.3).

Thus, the transcription has a great impact on the mutation frequency of intragenic TRs. However, intergenic TRs are also excised and they are exclusively in contact with the replication machinery, whereas intragenic TRs are in contact with both. To assess the role of replication in the TR mutagenesis, intra- and intergenic TR constructions were introduced in different orientations into the *B. subtilis* genome in the *amyE* gene locus. In a previous study (Gunka *et al.*, 2012), parts of this experiment were already investigated. In this study, a *gudB^{CR}* gene was ectopically inserted into the *amyE* locus, but in the same direction as its native version. It had the same mutation frequency as its native version (Gunka *et al.*, 2012). However, to distinguish between the first and the second TR, one TR unit was marked by the introduction of two G to T substitutions in the third and last position of the 9 bp long TR unit rendering it imperfect (see Fig. 3.4, marked in yellow). These mutations correspond the wobble bases of the valine and alanine, respectively, and have been shown to reduce the mutation frequency of intragenic TRs (Gunka *et al.*, 2012). Additionally, the positions of marked and unmarked TR unit are changed to exclude influences by the position of the imperfect TR unit.

In perfect agreement with the previous study, in intragenic TRs co-directional to the replication fork always the first TR was found to be mutated. When the gene harboring the intragenic TR is flipped and the direction of transcription and replication converge, still the first TR in direction of transcription was found to be mutated. The

occurred mutations were either the distinct and complete first TR unit or a deletion of three base triplets shifted in frame. These accurate deletions are required, because other than in frame deletions might not lead to a functional GudB⁺ protein. Hence, there might be other mutations occurring, but those are not detected because they do not lead to a functional GudB⁺ protein conferring a growth advantage.

This is different for the intergenic TR, there the mutations were not strictly in frame and in form of triplets or restricted to the area of the two TR units. Even though most SM harbored a 9 bp deletion within the promoter region, one mutant was found harboring only an 8 bp deletion. Furthermore, the promoter used in this study is an artificial promoter and the spacer region between the -10 and -35 is not important for any regulatory purposes as it is for other genes like the *gltAB* genes (see Ch. 1.3.2). However, it is of crucial importance to bring the -35 and -10 in optimal proximity of 17 bp to each other to support the sigma factor binding of the RNAP to the promoter region. As expected the additionally introduced 9 bp had to be removed for that purpose, but only the number of base pairs is important not the location. In general, the second TR in direction of replication mutates, but there is one construct that does not exhibit any SMs when streaked on selective SP medium.

To conclude, the excision of intragenic TRs is strongly dependent on the transcription machinery. The transcription machinery is not involved in the excision of intergenic TRs, as in general the first TR in the direction of replication is excised and one would not expect the transcription machinery act upon an intergenic element in general. It remains elusive why the last construct of the intergenic TR does not lead to any SM. However, an influence of the replication machinery cannot be excluded.

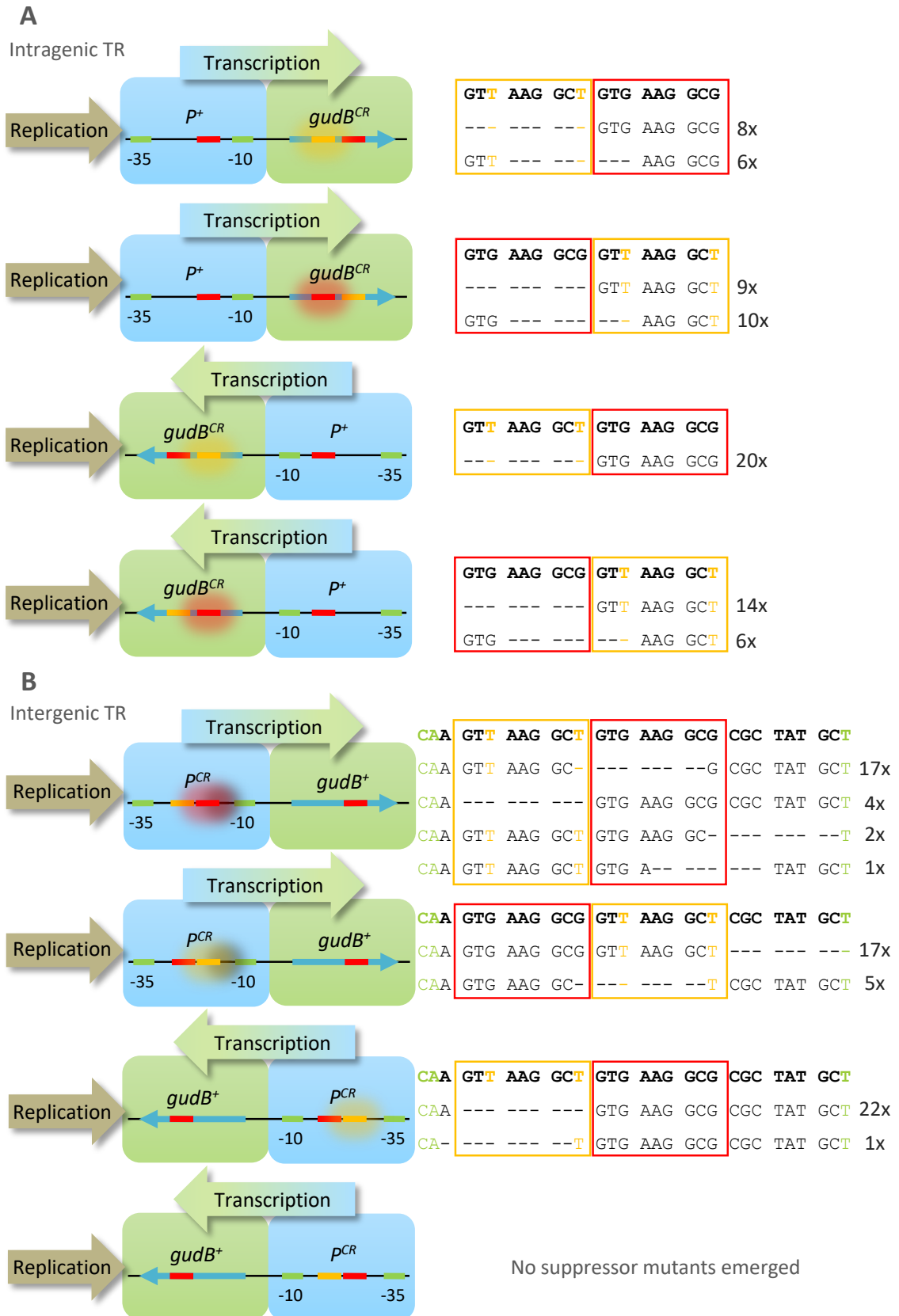


Fig. 3.4 Excision of TR units depending on the genomic orientation
 Strains harboring different orientations of intra- and intergenic TRs with distinguishable units were streaked on selective SP medium and incubated at 37 °C. Emerging SMs were isolated and sequenced. The sequencing results are displayed on the right side of the figure. The original sequence is emphasized in bold letters. A: Strains harboring intragenic TRs: BP20, BP21, GP1179, and GP1197 as parental strains (from top to down respectively). B: Strains harboring intergenic TRs: BP638, BP639, BP636, and BP637 (from top to down respectively).

3.1.3. Putative factors

The previous experiments in Ch. 3.1.2.1 and 3.1.2.2 strongly suggest two independent machineries relying either on replication or on transcription to be involved in inter- or intragenic TR mutagenesis. Therefore, several genes involved in repair of replication and transcription conflicts were investigated regarding their influence on the natural *gudB^{CR}* gene encountering co-directional conflicts with the replisome and the ectopically introduced *P^{CR}-gudB⁺* and *P⁺-gudB^{CR}* encountering head-on conflicts (Fig. 3.5). In general, the SMs were detected on plates in comparison to the parental strain. All experiments were performed at least three times under the same conditions.

The influence of the Mfd protein was shown previously (Gunka *et al.*, 2012) in the TR mutagenesis of intragenic TR involved in co-directional conflicts. Next, its impact on inter- and intragenic TR encountering head-on conflicts was investigated. Interestingly no clear change in the amount of SM was detected for head-on conflicts (Fig. 3.7 B). However, this could be also due to the changed experimental conditions, because the previous study determined distinct mutation rates using the fluctuation experiment (Lea and Coulson, 1949; Gunka *et al.*, 2012).

First, the influences of the RNases HII and HIII were investigated encoded by the *rnhB* and *rnhC* genes, respectively. The RNases HII and HIII are known to cleave RNA from RNA-DNA hybrids (Fukushima *et al.*, 2007) that can occur during replication and transcription conflicts. Interestingly, the SM emerged from strains lacking the *rocG* gene and either the *rnhB* or *rnhC* gene were much smaller and weaker compared to SM derived from a *rocG⁻* strain. In the native *rocG⁻* background there are less SM detectable for the *rnhB* mutant compared to the

Co-directional conflicts of replisome with leading strand genes

Head-on conflicts of replisome with lagging strand genes

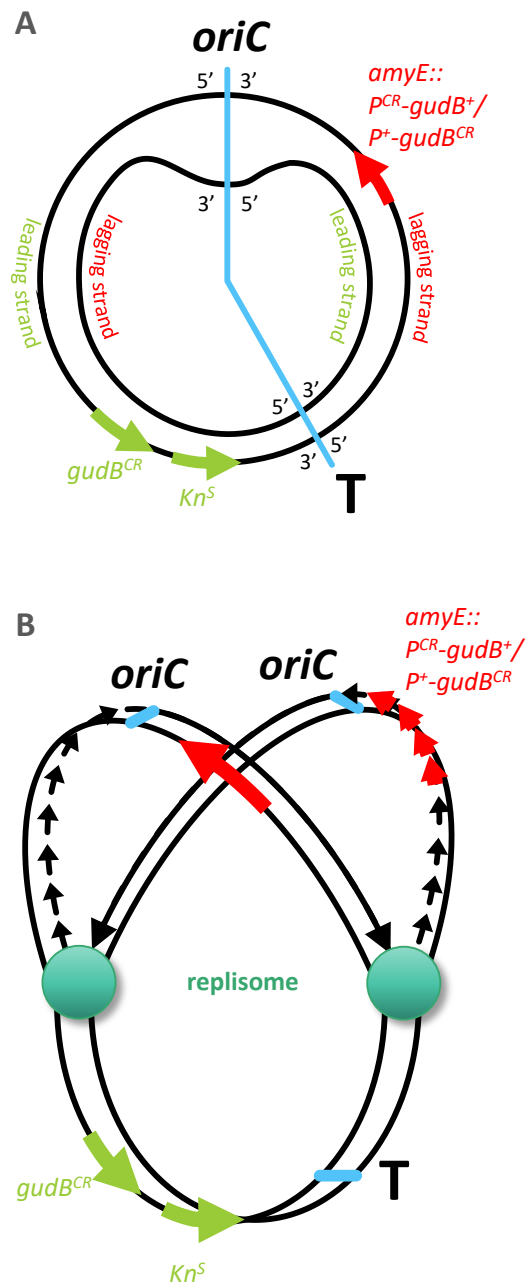


Fig. 3.5 Genomic localization of the investigated genes Overview of the *B. subtilis* genome with its origin of replication (*oriC*) and its terminator (*T*). Also annotated are the native *gudB^{CR}* gene, the ectopically in the *amyE* gene introduced *P^{CR}-gudB⁺*/*P⁺-gudB^{CR}* (Thiele, 2013), and the *Kn^S* gene (Bruand *et al.*, 2001a). A: Flat view. B: Split view with replisomes.

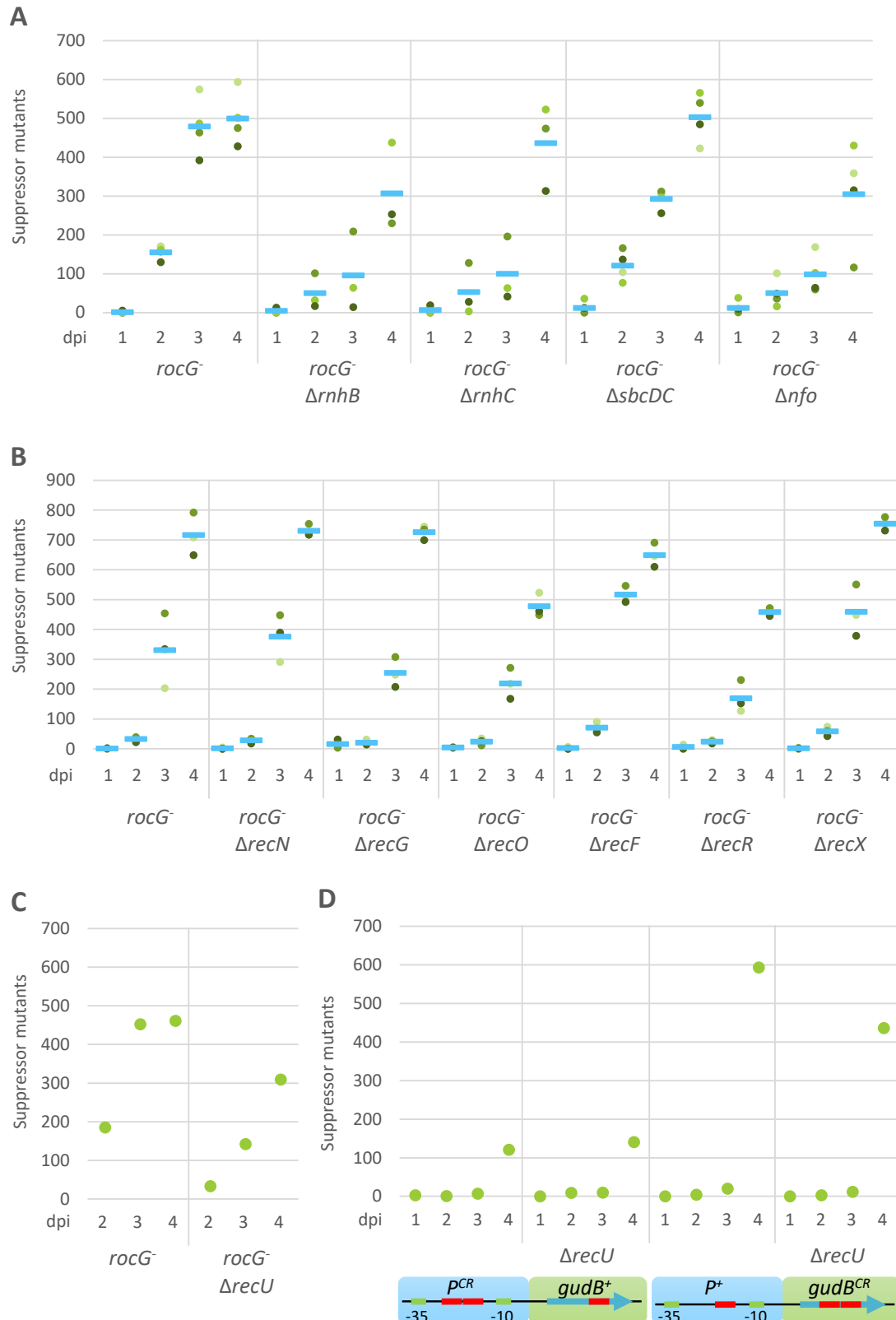


Fig. 3.6 Factors involved in TR mutagenesis I

Comparison of mutation frequencies of the natural *gudB^{CR}* gene encountering a co-directional conflict in GP747 (*rocG*::Tn10 = *rocG*) or of the artificial constructs Δ *gudB* *rocG*⁻ *P^{CR}-gudB⁺*/ Δ *gudB* *rocG*⁻ *P⁺-gudB^{CR}* encountering head-on conflicts (BP404/BP405) harboring secondary deletions of factors putatively involved in TR mutagenesis, determined as described in Ch. 2.2.6.1. The strain was grown to an OD₆₀₀ of 0.5 to 0.6, washed twice in 1x C-salts, thereby the OD₆₀₀ was adjusted to 0.4 and 100 μ l were used for plating ($2.3 \cdot 10^6$ cells). Number of mutants of the respective strains in dependence of time (1, 2, 3, and 4 dpi). **A:** *rocG*⁻ (GP747), *rocG*⁻ Δ *rnhB* (BP424), *rocG*⁻ Δ *rnhC* (BP431), *rocG*⁻ Δ *sbcDC* (GP896), *rocG*⁻ Δ *nfo* (GP1501). **B:** *rocG*⁻ (GP747), *rocG*⁻ Δ *recN* (BP629), *rocG*⁻ Δ *recG* (BP630), *rocG*⁻ Δ *recO* (BP631), *rocG*⁻ Δ *recF* (BP644), *rocG*⁻ Δ *recR* (BP645), *rocG*⁻ Δ *recX* (BP646). **C:** *rocG*⁻ (GP747), *rocG*⁻ Δ *recU* (GP892). **D:** *P^{CR}-gudB⁺* (BP404), *P^{CR}-gudB⁺* Δ *recU* (BP771), *P⁺-gudB^{CR}* (BP405), *P⁺-gudB^{CR}* Δ *recU* (BP770).

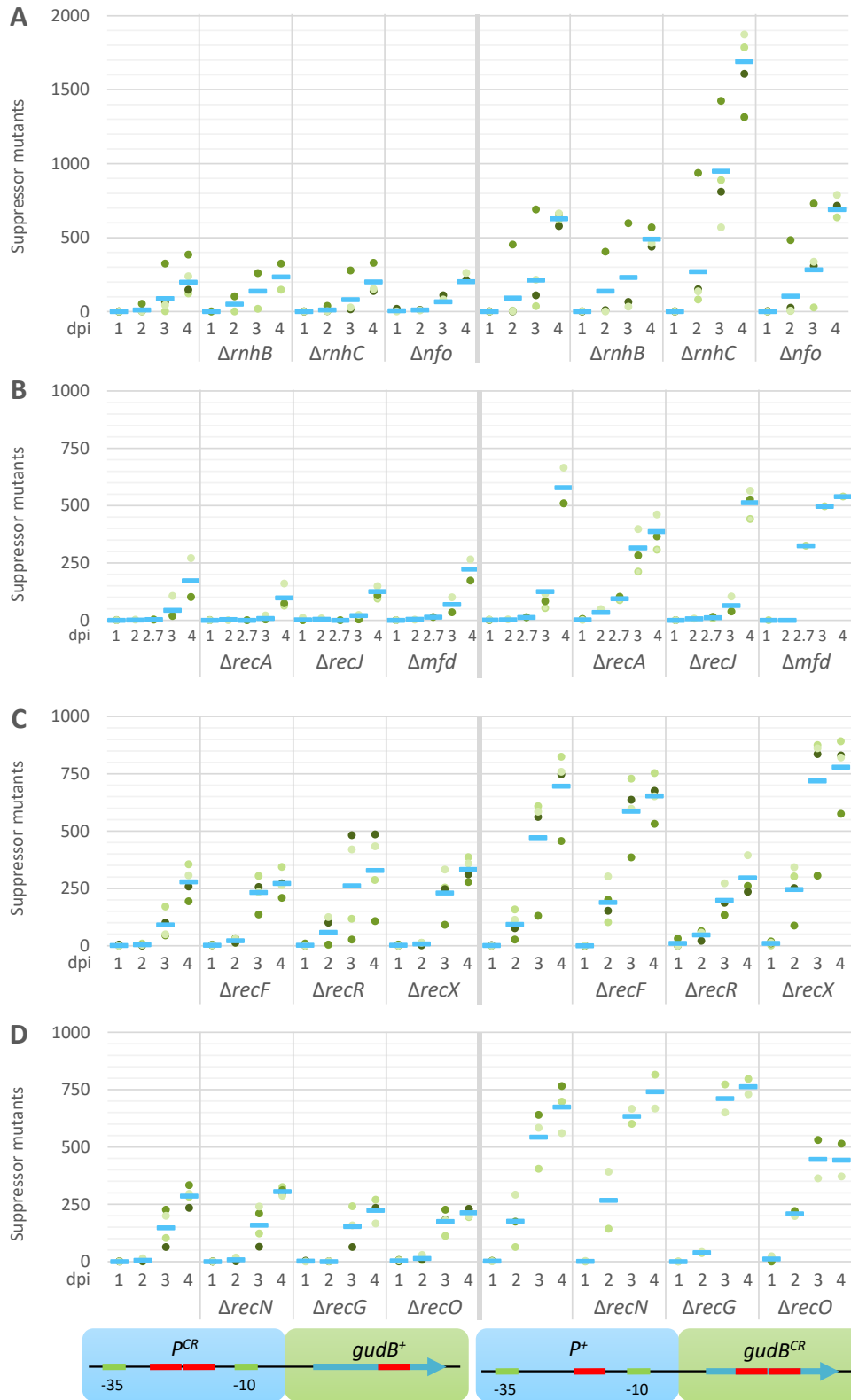


Fig. 3.7 Factors involved in TR mutagenesis II

Comparison of mutation frequencies of the artificial constructs $\Delta gudB rocG$ *P^{CR}-gudB⁺*/ $\Delta gudB rocG$ *P⁺-gudB^{CR}* encountering head-on conflicts (BP404/BP405) harboring secondary deletions of factors putatively involved in TR mutagenesis, determined as described in Ch. 2.2.6.1. The strain was grown to an OD₆₀₀ of 0.5 to 0.6, washed twice in 1x C-salts, thereby the OD₆₀₀ was adjusted to 0.4 and 100 μ l were used for plating (2.3 \cdot 10⁶ cells). Number of mutants of the respective strains in dependence of time (1, 2, 3, and 4 dpi). **A:** *P^{CR}-gudB⁺* (BP404), *P^{CR}-gudB⁺ Δ rnhB* (BP769), *P^{CR}-gudB⁺ Δ rnhC* (BP763), *P^{CR}-gudB⁺ Δ nfo* (BP765), *P⁺-gudB^{CR}* (BP405), *Δ rnhB P⁺-gudB^{CR}* (BP768), *Δ rnhC P⁺-gudB^{CR}* (BP762), *Δ nfo P⁺-gudB^{CR}* (BP764). **B:** *P^{CR}-gudB⁺* (BP404), *P^{CR}-gudB⁺ Δ recA* (BP753), *P^{CR}-gudB⁺ Δ recJ* (BP751), *P^{CR}-gudB⁺ Δ mfd* (BP755), *P⁺-gudB^{CR}* (BP405), *Δ recA P⁺-gudB^{CR}* (BP754), *Δ recJ P⁺-gudB^{CR}* (BP752), *Δ mfd P⁺-gudB^{CR}* (BP756). **C:** *P^{CR}-gudB⁺* (BP404), *P^{CR}-gudB⁺ Δ recF* (BP708), *P^{CR}-gudB⁺ Δ recR* (BP710), *P^{CR}-gudB⁺ Δ recX* (BP712), *P⁺-gudB^{CR}* (BP405), *Δ recF P⁺-gudB^{CR}* (BP709), *Δ recR P⁺-gudB^{CR}* (BP711), *Δ recX P⁺-gudB^{CR}* (BP713). **D:** *P^{CR}-gudB⁺* (BP404), *P^{CR}-gudB⁺ Δ recN* (BP702), *P^{CR}-gudB⁺ Δ recG* (BP704), *P^{CR}-gudB⁺ Δ recO* (BP706), *P⁺-gudB^{CR}* (BP405), *Δ recN P⁺-gudB^{CR}* (BP703), *Δ recG P⁺-gudB^{CR}* (BP705), *Δ recO P⁺-gudB^{CR}* (BP707).

parental strain and the *rnhC* mutant (Fig. 3.6 A). However, encountering a head-on conflict, an impact of RNase HIII on the mutation frequency of intra- and intergenic TRs is not detectable (Fig. 3.7 A). Interestingly, the RNase HIII seems to be involved in the repair of head-on collisions of intragenic TRs, because a deletion results in a dramatic increase of SMs (Fig. 3.7 A). It makes perfectly sense that neither of the RNase Hs are involved in the repair of intergenic TRs, because RNA-DNA hybrids only occur within genes. It is also likely that there are less conflicts in co-directional orientation compared to head-on orientation and therefore the RNases are less required. As previously stated, RNases H remove RNA-DNA hybrids to ensure a proper replication restart. A deletion of the RNases H would lead to a disruption of this process and the probability of a DNA damage increases. This is reflected by the distinct increase in SMs for the $\Delta rnhC$ strain harboring the intragenic TR in head-on direction (Fig. 3.7 A), but not by the decrease in mutation frequency in the $\Delta rnhB$ strain harboring the intragenic TR in co-directional orientation.

A detailed description of the repair mechanisms upon collisions of the replication and transcription machinery is given in Ch. 1.4.1.1. To investigate the contribution of the initial recognition of DSB in TR mutagenesis, $\Delta recN$ deletion mutants harboring an intragenic TR in co-directional and an inter- and intragenic TR in head-on direction were investigated but no influence was detected (Fig. 3.6 B, Fig. 3.7 D). The main processing of the DSB was investigated using a $\Delta recJ$ deletion mutant harboring inter- and intragenic TRs in head-on direction, but did not lead to obviously changed amounts of SMs compared to the parental strains. However, the lack of the RecJ endonuclease might be compensated by the AddAB helicase/nuclease complex. Albeit, the *recA* gene encodes for the major factor in homologous recombination, its

deletion leads only to a slight decrease in the amount of the SMs in strains harboring an intragenic TR in head-on direction. The deletion of the *recO* and *recR* genes had a drastic impact on the amount of SMs in strains harboring an intragenic TR in either direction (Fig. 3.6 B, Fig. 3.7 C, D). If RecO and RecR are required for successful deletion of one TR unit, it is very likely that also RecA is involved in the TR mutagenesis. In a previous study the impact of different factors building the replication fork in *B. subtilis* was investigated (Bruand *et al.*, 2001a). There, a kanamycin resistance cassette was artificially inactivated (*Kn^S* gene) by a TR and introduced near the native *gudB^{CR}* gene (Fig. 3.5) in a co-directional manner and no influence of RecA in TR mutagenesis could be detected. However, the deletion of the *recA* gene in mutants that already have an increased mutation frequency as the *dnaD23*, the *dnaG20*, the *dnaN5*, the *dnaX51*, or the *dnaE1* mutants revealed that these mutants differentially enhance the emergence of SMs in a RecA-dependent or independent manner (Bruand *et al.*, 2001a). Indicated by this study and by the observations made in the previous Ch. 3.1.2, there are several pathways leading to the excision of one TR. Even though the simple deletion of the *recA* gene has no influence or only a slight influence on TR mutagenesis in this experimental context (Fig. 3.7 B), the general involvement of RecA in TR mutagenesis cannot be ruled out.

To further investigate the importance of RecA in the TR mutagenesis, RecG mediating branch migration, RecF promoting the RecA elongation, and RecX facilitating the disassembly of the RecA filament are tested. However, the three proteins do not have any influence on TR mutagenesis (Fig. 3.6 B, Fig. 3.7 C, D). However, further testing the influence of RecU, which mediates RecA elongation and cleaves Holliday junctions, reveals its involvement in the TR mutagenesis of

intragenic TR in either direction (Fig. 3.6 C, D). Though, deletion of the *sbcDC* genes does not have any influence on intragenic TR mutagenesis encountering co-directional conflicts (Fig. 3.6 A). The *sbcDC* genes encode nucleases and are upregulated upon SOS-response, which is induced upon RecA-mediated autocleavage of the transcriptional repressor LexA (Lenhart *et al.*, 2012). This finding suggests that RecA itself might be important for TR mutagenesis, but not its function in activating the SOS response. This makes perfectly sense, as RecA-mediated DNA strand exchange requires the LexA binding site for the binding of a second DNA strand.

Interestingly, the 2-deoxyribose-phosphate (AP) endonuclease Nfo seems to be involved in TR mutagenesis encountering co-directional conflicts. Its normal task is to remove remaining AP sites from the DNA which remain after base excision repair, for instance (Lenhart *et al.*, 2012). Furthermore, bacterial two hybrid (BACTH) analyses were performed to find interactions between the different factors tested. However, the BACTH analyses revealed only self-interactions between RNase HII, RNase HIII, RecA, RecR and RecJ (Fig. 6.2, p. 102).

To conclude, RecO, RecR and RecU support the excision of TR units in the applied experimental conditions indicating also an involvement of RecA which could not be shown. However, to identify the different pathways involved in TR mutagenesis, a larger screen should be performed using the ectopically introduced P^{CR} -*gudB*⁺ and P^+ -*gudB*^{CR} encountering head-on conflicts (Fig. 3.5) and inverted versions encountering co-directional conflicts (Gunka *et al.*, 2012). Furthermore, the experiments should be performed at different temperatures, as many of the genes involved in those pathways are temperature sensitive as the RNases H (Bruand *et al.*, 2001a; Fukushima *et al.*, 2007; Yao

et al., 2013). Here, the experiments were performed at least three times, but in some cases fluctuations were quite high and more repetitions would lead to more sophisticated results. Consequently, the experiments are rather indicators and the actual impact of the different factors on the decryptification process should be further corroborated using also other methods.

3.2. The activator/reporter system

The activator/reporter system was established to visualize the emergence of distinct mutations on the level of single cells (Dormeyer, 2014). Therefore, a transcriptional activator is used not interfering with any promoter in *B. subtilis*. The used activator is PrfA, the major virulence gene regulator in *L. monocytogenes* (Chakraborty *et al.*, 1992). PrfA activates the expression of the genes *hly*, *mpl*, and *plcA* encoding for listeriolysin O, a metalloproteinase precursor, and a broad substrate-range phospholipase, respectively (Domann *et al.*, 1991; Mengaud *et al.*, 1991; de las Heras *et al.*, 2011). The activation of the *hly* and the *plcA* promoter occurred in less than 30 min in *B. subtilis* after induction of *prfA* gene expression and already small amounts of PrfA lead to strong activation of the *hly* and the *plcA*

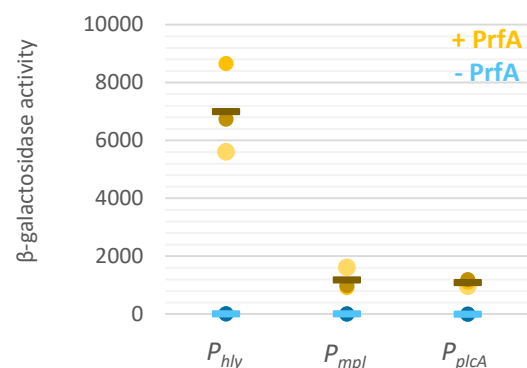


Fig. 3.8 PrfA inducible promoters of *L. monocytogenes*. Activity of the *hly*, *mpl*, and *plcA* promoter were determined in *B. subtilis* strains: BP100 (P_{hly} -*lacZ*), BP101 (P_{mpl} -*lacZ*) and BP102 (P_{plcA} -*lacZ*) with either pBQ200 (- PrfA) or pBP103 (+ PrfA). Cells were grown to an OD₆₀₀ of 0.5-0.8 and β -galactosidase activity was measured.

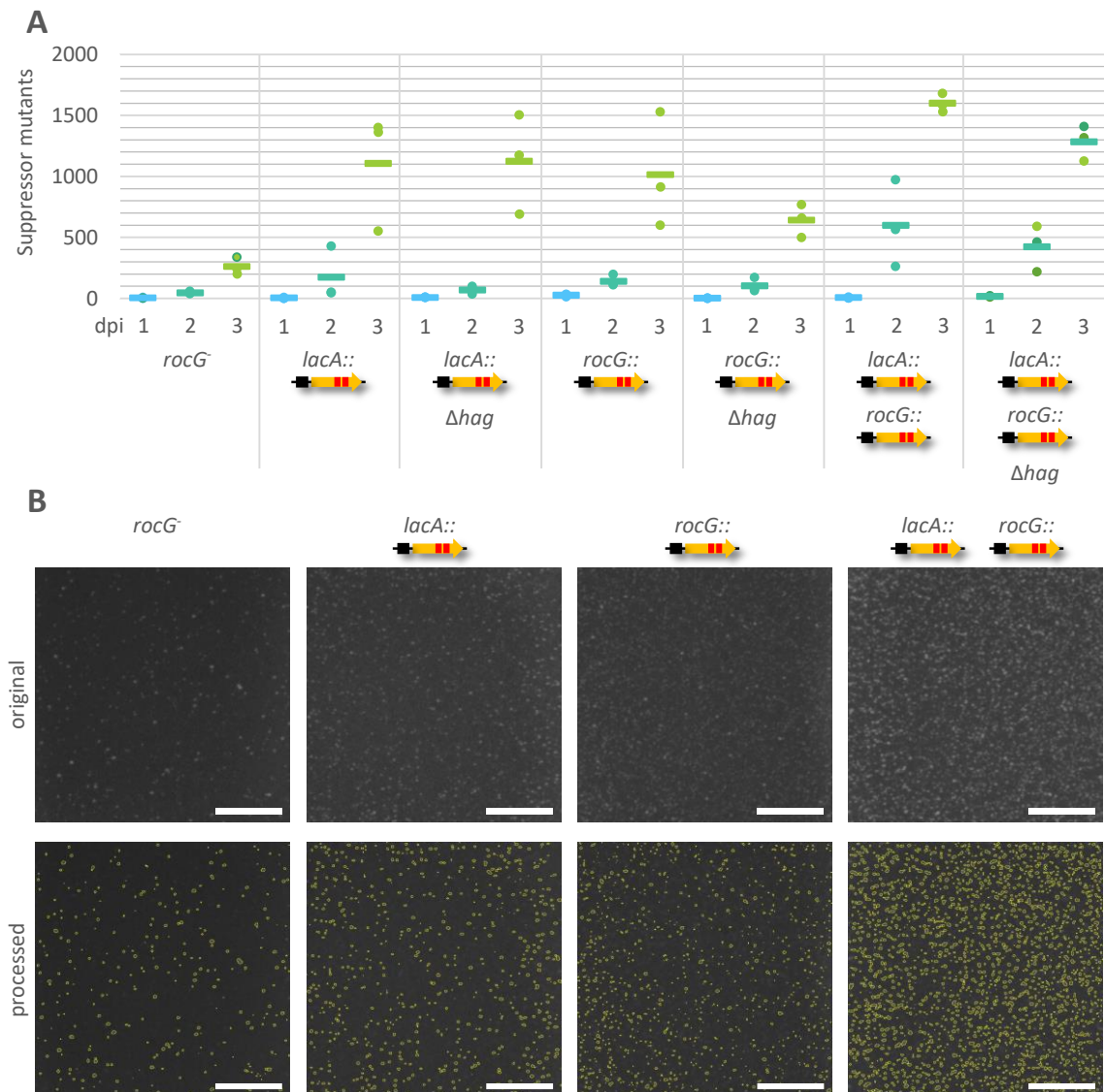


Fig. 3.9 Mutation frequencies of the activator/reporter strains on plate.

A: Number of suppressor mutants on SP medium emerged from initially $2.3 \cdot 10^6$ plated cells in dependence of time. GP747 (*rocG*::Tn10) as control, Activator/reporter strains: BP520 (*lacA*::activator unit), BP692 (*rocG*::activator unit), BP696 (*lacA/rocG*::activator unit) and their immobile Δ *hag* versions BP624, BP625, BP697, respectively. **B:** Original photos taken of the plate at 3 dpi showing the emerged suppressor colonies on SP medium, these are marked with yellow in the processed version. Scale bar 1 cm.

promoter in *B. subtilis* (Sheehan *et al.*, 1995). The promoter activities under constant presence of PrfA in *B. subtilis* were identified using the *prfA* gene fused to the strong *P_{degQ36}* promoter of the pBQ200 plasmid (Ballin, 2012). None of the promoters showed basal expression in the absence of PrfA (Fig. 3.8). The activity of the *hly* promoter was 7-fold higher compared to the *mpl* and *plcA* promoter. In the activator/reporter system such high expression of the reporter unit harboring the GDH GudB might lead to imbalance of the glutamate pool resulting in a growth disadvantage. Therefore, the *hly*

promoter was not chosen for the reporter unit. The *mpl* and *plcA* promoters exhibited similar and high activity, but as it is known that transcription upon the presence of PrfA occurs much more rapidly for the *plcA* promoter in *B. subtilis* (Sheehan *et al.*, 1995), it was chosen as suitable promoter for the reporter unit.

3.2.1. Analysis of emerging mutations

In previous studies the activator/reporter system harboring only one activator unit was proven as functional (Dormeyer, 2014). Additionally, the plasmid pBP407 was constructed allowing the

integration of several activator units with a subsequent removal of the antibiotic resistance gene. The plasmid pBP407 is a powerful tool as it provides a basis for an LFH PCR using flanks of the integration locus of the activator unit. The cre/lox system is subsequently used to remove the resistance gene flanked by lox sites. Here, this plasmid was used to integrate the activator unit into the *rocG* gene locus, thereby combining the deletion of a native GDH and the integration of an additional activator unit (BP692). BP692 was transformed with the *lacA*::activator unit, to combine both activator units in one *B. subtilis* strain (BP696). Compared to the native $\Delta rocG$ strain, all activator/reporter strains exhibit an at least two-fold increased mutation frequency (Fig. 3.9). The strains harboring a single activator unit exhibit a similar mutation frequency. This was expected as the mutation frequency is most likely independent on the locus of the activator unit. In contrast, the introduction of a second activator unit as shown in Fig. 3.9 could successfully increase the mutation frequency at 2 dpi and moderately at 3 dpi. Performing the fluctuation experiment according to the method of the median, the actual mutation rate of the strain BP696 is $1.8 \cdot 10^{-6}$ (Ch. 2.2.6.2).

3.2.2. Mutations on the level of single cells

The investigation of emerging mutations on the level of single cells was performed in a microfluidic system (Grünberger *et al.*, 2014). The advantages of this system are the constant supply of fresh medium ensuring constant growth conditions and the possibility to monitor a high number of growth chambers over a long period of time increasing the chance of finding an emerging mutation. The growth chambers used for the experiments were 778 nm high ensuring the investigation of a single layer of cells. Considering the different growth media,

B. subtilis varies in length from 5 μm in rich medium (LB, SP), with great fluctuations forming indistinguishable chains up to 41 μm long, to only 2 μm long cells in C-Glc minimal medium. The width of *B. subtilis* changed also but to a lesser extent. Consequently, in certain media there was still enough space for *B. subtilis* to move and as a result the cells were relocated in each frame. To improve the tracking of single cells, the *hag* gene encoding for the flagellin monomer protein Hag was deleted. The Hag monomer is essential for the assembly of the flagellum (Mukherjee and Kearns, 2014) and Δhag mutants are not motile anymore. The mutation frequency of the activator/reporter system strains was not significantly influenced by the deletion of the *hag* gene (Fig. 3.9 A). The activator/reporter strain harboring two activator units and the Δhag deletion (BP697) was used for microfluidic analysis. When the not functional activator unit is activated by the excision of a TR unit, the expression of the reporter genes is induced leading to an increase in fluorescence and a growth advantage in SP medium. After 10 to 12 h of growth a mutation was detected by the increase in fluorescence (Fig. 3.10 A, B). The cell length served as indicator for growth. Interestingly, the mutation occurred when the cells were not growing fast (Fig. 3.10 C). The black cell line divided after 9 h and 15 h, so the cells are in stationary growth phase or suffering due to the media composition. In contrast, the green cell line seemed to behave similar in the beginning but when the mutation occurred and the fluorescence increased in the cell it started to grow faster indicated by the jaggy line of cell length. This is explained by the growth advantage due to the presence of GudB⁺ enabling the use of glutamate, which is highly abundant in SP medium, as carbon source. Additionally, a third cell line was monitored (Fig. 3.10 A, blue arrow) which derived from initial division of the green cell line, after the mutation

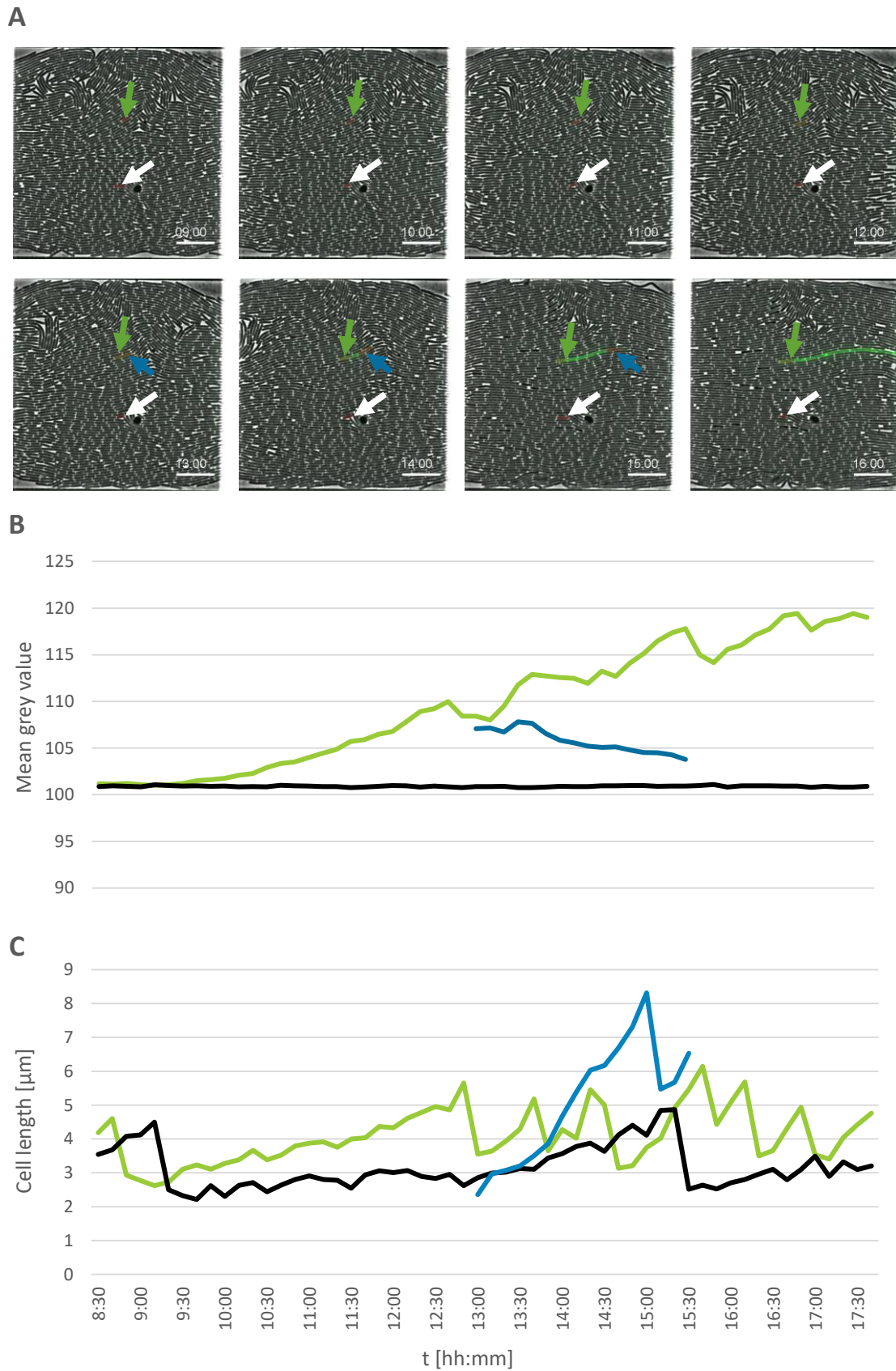


Fig. 3.10 The emergence of a mutation on the level of single cells.

A: Extract from a growth sequence of *B. subtilis* BP697 in SP medium in open microfluidic chambers with a size of 90 x 80 μm . The arrows indicate three different cell lines that were tracked over time, the colors correspond to the ones in B & C. Merged version of fluorescence and DIC photos. Time points are indicated [hh:mm]. Scale bar 15 μm . **B:** Fluorescence intensity for the three cell lines (see A) in form of the mean grey value over time [hh:mm]. **C:** Cell length [μm] for the three cell lines (see A) over time [hh:mm].

occurred. Contradictorily, a decrease instead of an increase in fluorescence was observed. The blue cell line also did not divide as fast as the green one, but at least faster compared to the black one. Unfortunately, only one division could be monitored as the cell was pressed out of the growth chamber by the green cell line. One explanation for the two different cell lines is that first one activator unit mutates and right afterwards the second activator unit leading to the strong *gfp* expression in the green cell line, whereas this second mutation did not occur in the blue cell line. Therefore, the blue cell line still has a growth advantage, but not as big as for the green cell line. Another explanation is that an amino acid starved cell exhibits stationary-phase mutagenesis (Sung and Yasbin, 2002) and is therefore also prone to deleterious or at least disadvantageous mutations explaining the growth disadvantage of the blue cell line.

3.2.3. Investigation of substitutions

The principle of the activator/reporter system is an inactive activator unit and a reporter unit strictly dependent on the activator. A TR within the sequence, important for the DNA binding, inactivated the transcription factor PrfA. This

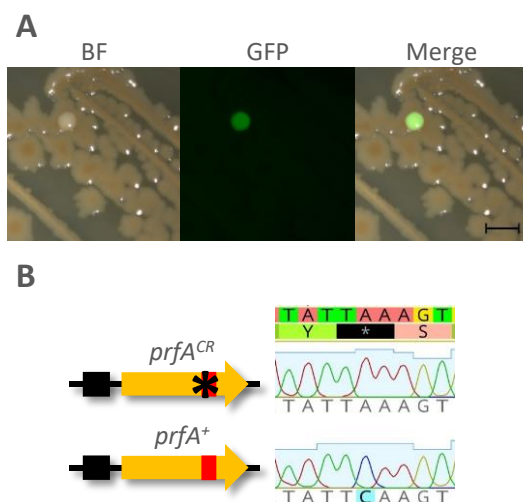


Fig. 3.11 Activator/reporter system with a substitution. **A:** Microscopic analysis of the SM BP827 emerged from BP824, the activator/reporter strain harboring an activator unit inactivated by a substitution leading premature stop codon. Scale bar 1 cm **B:** Sequence analysis of the activator unit in BP824 and BP827.

system allows the investigation of TR mutations, but the activator/reporter system can also be changed to investigate other mutations, as for instance substitutions. Instead of an artificially introduced sequence as for the TR investigation, a C530A mutation was introduced (Fig. 3.11 B) leading to a premature stop codon (S175X). The shortened PrfA variant was not active anymore. After incubation of the activator/reporter strain BP824 harboring the substitution in the *prfA* gene for several days on SP medium at 37 °C a SM emerged (Fig. 3.11 A). The resulting SM BP827 expressed the *gfp* gene compared to the parental strain indicating an activation of the activator unit and no other mutation leading to a growth advantage. Sequencing revealed the reversion of the premature stop codon to a serine codon again (Fig. 3.11 B).

Additionally, several insertions in position 527 +1, +2, 3, or +4 A and a deletion mutation of C530 were investigated, all mutations lead to premature stop codons, but in none of the strains SMs with an active PrfA could be detected.

3.2.4. Investigation of amplifications

Adaptation to constantly changing environmental conditions is crucial for every living organism. This adaptation does not only take place in the change of gene expression, of protein activity or the emergence of point mutations. Indeed, genome rearrangements by gene duplications and amplifications are a quite common possibility to adapt to changing environmental conditions (Andersson and Hughes, 2009). About 10 % of all cells in a culture grown in non-selective medium contain a gene duplication somewhere in the genome (Roth *et al.*, 1996).

To investigate amplifications with the activator/reporter system, identical sequences before and behind the reporter unit were

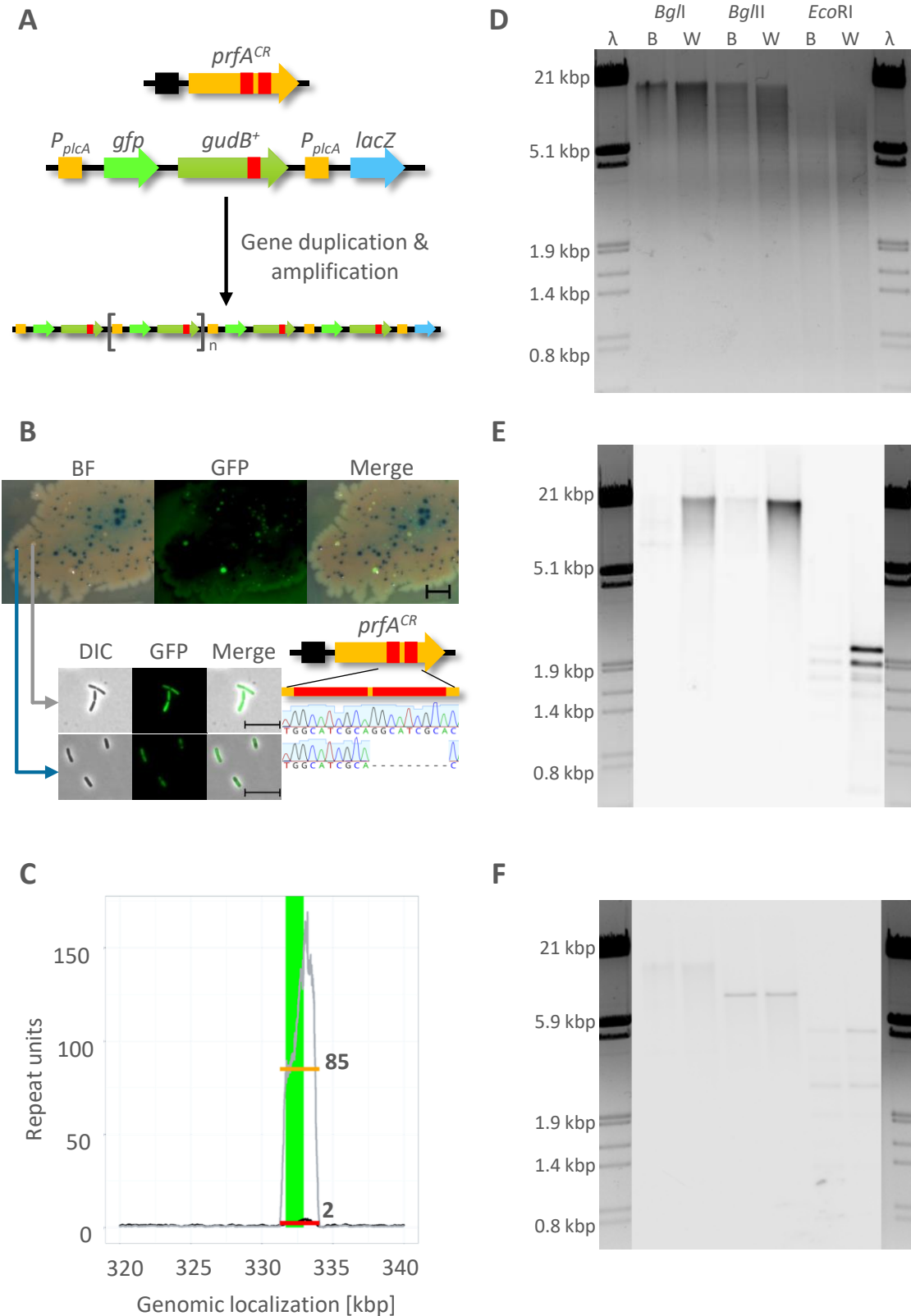


Fig. 3.12 Gene amplification of the reporter unit.

A: Schematic overview of the novel reporter unit and the amplification. **B:** Suppressor mutants emerged on SP plate after 5 dpi (scale bar 1 mm) and single cells of blue and white colonies (scale bar 10 μ m). **C:** Repeat units of BP628 (black, red) and a white SM of BP628 (grey, yellow) calculated from whole genome sequencing coverage data. **D:** 1 % agarose gel with 300 ng *BglI*, *BglII* and *EcoRI* digested gDNA of a blue and white SM of BP628 used for Southern blot (E, F). **E:** Southern blot with a *gudB⁺* specific probe (MD150/MD151). Expected sizes: *BglI* cuts in front of and right behind the reporter unit: min. 4.4 kbp (one unit), *BglII*: 57.7 kbp, *EcoRI* separates the amplification units: 2.4 kbp. **F:** Stripped and reprobed Southern blot with an *accD* specific probe (JN133/JN134) as loading control, only one copy of the *accD* gene is present in the genome). Expected sizes: *BglI*: 3.7 kbp, *BglII*: 8.2 kbp, *EcoRI*: 4.7 kbp.

required to provide a basis for recombination. Therefore, the *plcA* promoter fused to a *lacZ* reporter gene was transformed behind the reporter unit (Fig. 3.12 A). The two identical *plcA* promoters serve as basis for recombination. The *lacZ* reporter gene allows to discriminate between a TR mutation in the *prfA^{CR}* gene activating the expression of both reporter genes and a gene amplification of the region between the promoters activating only the expression of the *gfp* reporter gene.

On SP medium rapidly, blue (TR mutation) and white (gene amplification) SM colonies emerged (Fig. 3.12 B). Fluorescence analysis of single cells showed *gfp* gene expression in both strains, but only the blue SM exhibited an activated *prfA⁺* gene (Fig. 3.12 B).

To identify the distinct region of gene amplification, the genomes of the parental strain BP628 and a white SM were sequenced. The white SM exhibited a high coverage in the *gfp* and the *gudB⁺* gene. The number of amplified units was calculated from the mean coverage. Impressively, about 85 units were amplified until the basal expression of the *plcA* promoter was sufficient to compensate for the loss of a GDH in *B. subtilis*. This shows again (Fig. 3.8) that the basal expression of the *plcA* promoter is extremely low in the absence of *PrfA⁺*. Also, the parental BP628 strain exhibits a slightly increased coverage in the *gfp* and *gudB⁺* genes. There are already two units present, this observation could be verified via check PCR using primers directed towards the outside of the amplification unit (Fig. 3.13). The constructed reporter unit seems to form a highly mutable locus as the parental strain was handled with great care on medium disadvantageous for constant GDH expression.

A Southern blot confirmed the amplification experimentally. The signal for the *gudB* probe is

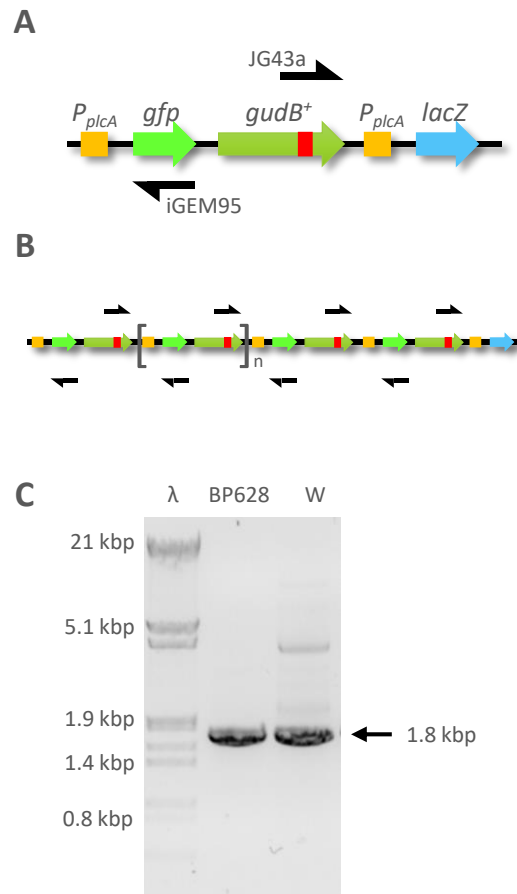


Fig. 3.13 Gene amplifications checked via PCR
A: Reporter unit with annotated primers JG43a and iGEM95, which do not lead to a fragment when only one reporter unit is present in the genome. **B:** The primers JG43a and iGEM95 lead to a product when gene amplification has taken place. **C:** PCR products using the primers JG43a and iGEM95 of the original BP628 and the respective white SM harboring gene amplifications.

strongly increased in the blue SM compared to the white SM, whereas the signal of the probe for the loading control gene *accD* was similar in both mutants (Fig. 3.12 E, F). As an amplification of the reporter unit is very likely to occur, the chance to monitor this event in a microfluidic growth chamber is also increased compared to a normal point mutation. Indeed, several of these events were found, but in contrast to the original activator/reporter system, the fluorescence intensity was constantly changing. Since an increase in amplification units also leads to an increase in fluorescence intensity the activator/reporter system allows to visualize the changing genome in real time.

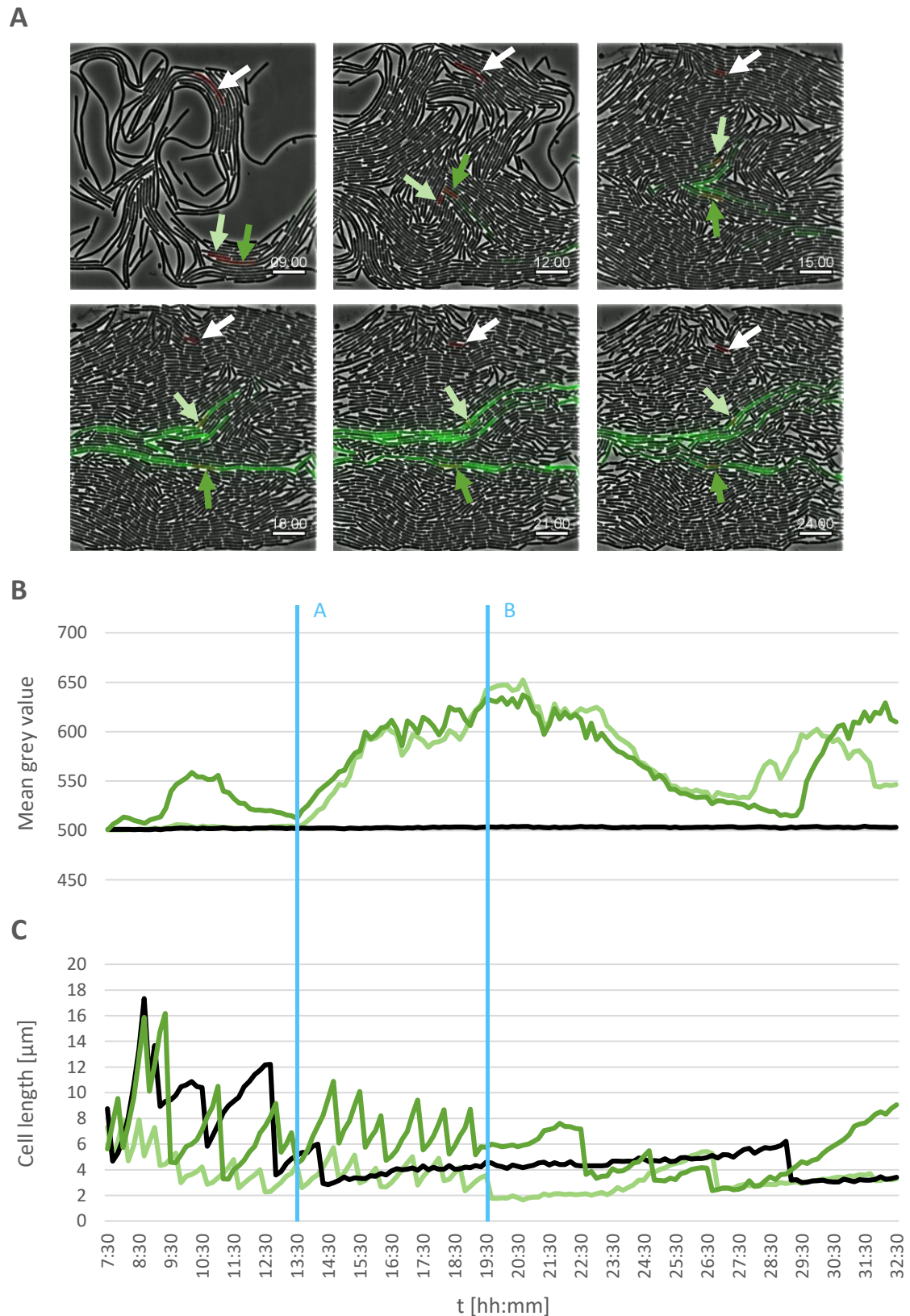


Fig. 3.14 Emerging amplifications visualized on the level of single cells.

A: Photos extracted from a growth sequence of *B. subtilis* BP628 in SP medium in open microfluidic chambers with a size of 90 x 80 μm . The arrows indicate three different cell lines that were tracked over time, the colors correspond to the ones in B & C. Merged version of fluorescence and DIC photos. Time points are indicated [hh:mm]. Scale bar 10 μm . **B:** Fluorescence intensity for the three cell lines (see A) in form of the mean grey value over time [hh:mm]. **C:** Cell length [μm] for the three cell lines (see A) over time [hh:mm].

In Fig. 3.14, three cell lines were tracked for 32 h and measured in length and fluorescence intensity. All the cells were growing nicely for 13.5 h, the dark green cell line even showed a slight in- and subsequent decrease in fluorescence intensity indicating spontaneous gene amplifications that were fast reverted again. Despite the lack of GDH *B. subtilis* grows in SP medium quite fast and emerging daughter cells can block the main supply channel leading to a delay in nutrient supply. This is a possible explanation for the stop in growth of the black cell line. However, at that time point the green cell lines showed a strong increase in fluorescence concomitant with an increase in growth indicated by the jaggy cell length graph (Fig. 3.14 B, C; timepoint A). The growth advantage results from the increased expression of the *gudB*⁺ gene which is also part of the amplification unit enabling the cell to use glutamate as carbon source. The fluorescence continuously increased for 6 h and reached a maximum after 19.5 h of growth in SP medium (Fig. 3.14 A, B; timepoint B). The cell growth also stopped at that time point. This growth delay resulted from a disadvantageous excess of GDHs in the cells. It emerged either because of the fast runaway nature of gene amplification or because of a change in the medium composition, for example, because the cells blocking the supply channel were flushed away. Rapidly, the number of amplification units was adjusted, the fluorescence decreased and the green cell lines started to grow again. This scenario was now monitored several times during the 32-h growth experiment, emphasizing the outstanding dynamic of a gene amplification region.

3.2.5. Industrial application of the activator/reporter system

There exist several expression systems for heterologous proteins (Vavrová *et al.*, 2010)

independent of expensive inducers which are based on spontaneous mutations or temperature changes as for instance the spontaneous TR mutation rendering a promoter region accessible for the RNAP (Dormeyer *et al.*, 2014) or low temperature expression systems (Welsch *et al.*, 2015). The major problems with using gene amplification to express heterologous genes is the need of a selective pressure and the counter selection by the possible disadvantage of the heterologous protein in the host cell. Usually amplification units harboring an antibiotic resistance and a heterologous gene is used. Gene amplification is forced by increasing the concentration of the respective antibiotic agent (Hohmann *et al.*, 2016).

The activator/reporter system was redesigned to express heterologous proteins and to minimize the problem of counter selection. As described previously (see Ch. 3.2.4), the reporter unit harboring a *P_{plcA}-lacZ* fusion is prone to gene amplification as it has two identical *plcA* promoter sequences. The use of glutamate rich medium as SP medium will favor the amplification once it occurred. Additionally, a xylose-inducible promoter of the *xyIA* gene was fused to the *prfA*⁺ gene (Fig. 3.15 A).

The *xyIA* promoter is advantageous, because it is repressed by XylR. Two non-competing chromosomal based versions of the *xyIR* repressor gene ensure a high abundance of the XylR repressor. The resulting inactivity of the activator unit allows the emergence of gene amplification of the reporter unit and is cheap and easily activated by the addition of xylose to the medium leading to a simultaneous expression of all amplified reporter units. On SP plates, only white SMs emerged from the strain BP691 harboring the novel overexpression system. Blue SMs would appear when the *lacZ* gene is expressed, but this is only the case when the promoter of the activator unit is leaky. One

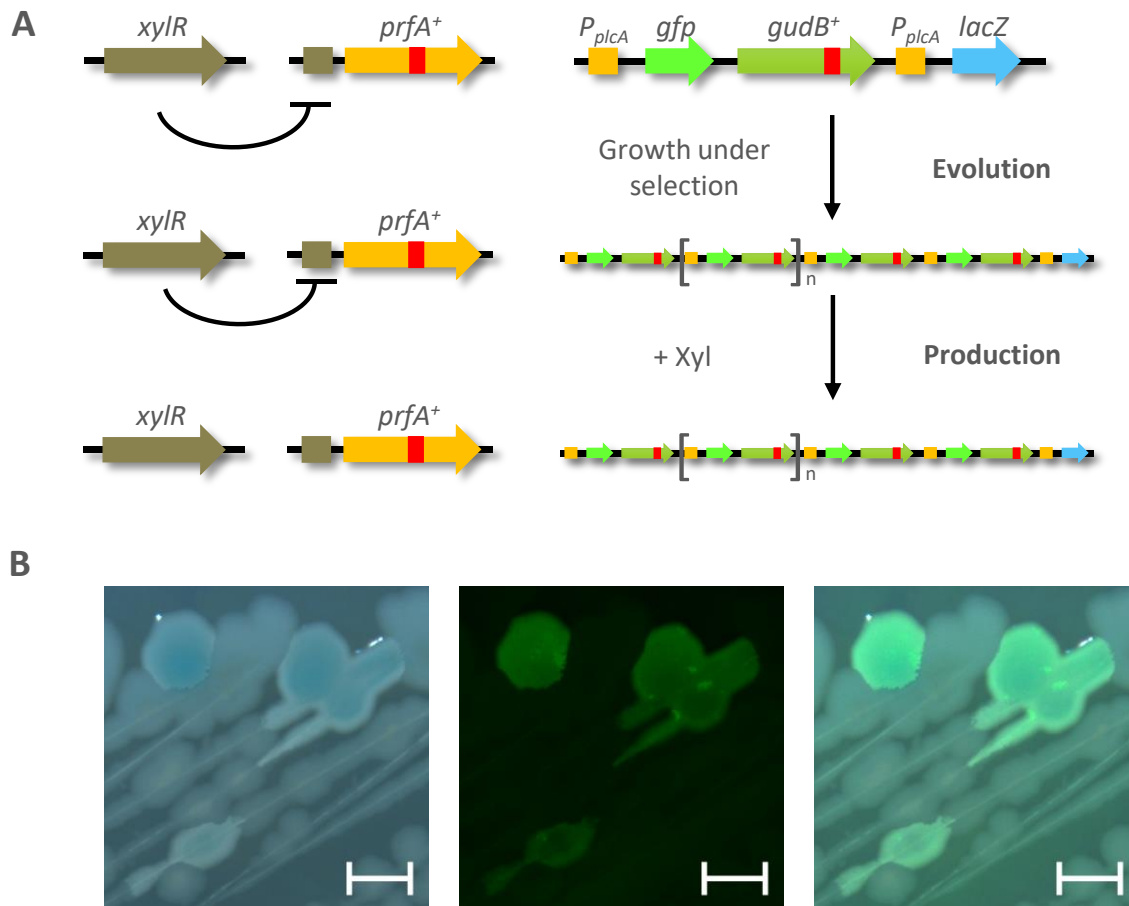


Fig. 3.15 Tool box: Gene amplification and subsequent induction of gene expression.

A: Schematic overview of the novel activator/reporter system using amplification of the reporter unit and subsequent induction of activator gene expression upon xylose addition to the medium to serve as basis for the overexpression of heterologous proteins.

B: Suppressor mutants of BP808 emerged on SP plate after 5 dpi (scale bar 1 mm).

of the white SMs was streaked and incubated for 5 d. The result of this first streaking is displayed in Fig. 3.15 B. There are still colonies consisting of the parental strain that do not express the *gfp* gene but also of the desired white SM exhibiting *gfp* expression. In the fluorescence photo, further small areas within the original SM are detectable by their increased fluorescence. These areas do not exhibit a visible growth advantage compared to their parental strain, but conceivably they do have a slight growth advantage. Even though these colonies are handled with great care and are streaked many times, there will never be a pure clone, because of the dynamic nature of an amplification region.

In Fig. 3.16, this dynamic nature of constant laboratory evolution is investigated. The parental BP691 strain and the resulting white SM

were streaked and cultured in different media for the whole experiment.

After 3 dpi both strains appear as homogeneous bacterial lawn on pure SP medium, but fluorescence analysis revealed a few areas of increased fluorescence indicated by the red arrow in Fig. 3.16. The fluorescence analysis of single cells reveals beyond doubt that the SM consists of a heterogeneous culture with fluorescent and non-fluorescent cells, compared to the parental strain consisting only of non-fluorescent cells. Apparently, the growth advantage of the actual number of amplification units within the SM of BP691 is optimal for pure SP medium and the acquisition of novel amplification units and an increased concentration of GDH does not lead to a distinct growth advantageous anymore.

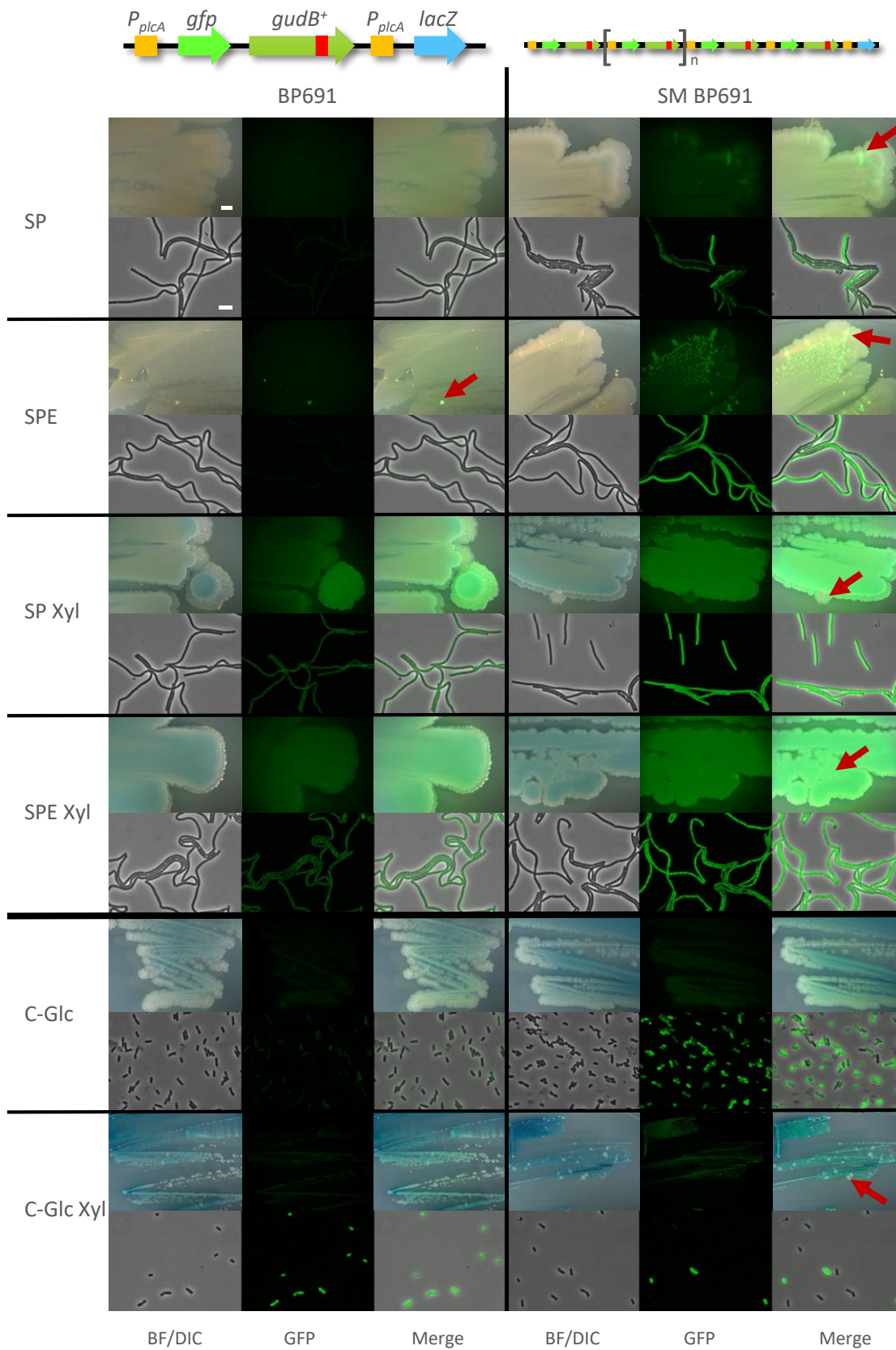


Fig. 3.16 Microscopic analysis of the dynamic nature of gene amplifications. BP691 and its SM were streaked on SP, SPE, SP Xyl, SPE Xyl, C-Glc and C-Glc Xyl medium plates (additional 0.8 % K⁺ glutamate and 1 % xylose final concentration) incubated for 1 dpi at 37 °C. These plates were used to inoculate an o/n culture using 5 ml of the respective medium. On the next day, the novel o/d culture was investigated at an OD₆₀₀ of 0.5-0.8 at the level of single cells. Scale bar: 5 µm. The initial plates were incubated for 2 dpi more at RT and analyzed. Scale bar 1 mm.

In the SPE, additional 0.8 % glutamate are added to the rich SP medium increasing the benefit of having more active GDHs. On this medium, SM of the parental BP691 strain are already detectable after 3 days (red arrow). On the SPE medium with the SM of BP691 areas with a growth advantage are already detectable on the bright field photo. In the fluorescence photo, these and even more areas show increased fluorescence. This number is much higher compared to the one for SP medium. It is also reflected on the level of single cells, because the culture consisted nearly exclusively of fluorescent cells.

In SP-Xyl and SPE-Xyl medium, the expression of the activator unit is induced and all amplified reporter units are expressed including the *lacZ* gene. The blue color of the colonies on plate results from the expression of the *lacZ* gene which serves as indicator for a successful induction of the *prfA* gene expression. The expression of the reporter unit is beneficial for the parental BP691 strain, because it lacks any GDH activity in the absence of xylose. Now it grows nicely on SP-Xyl and SPE-Xyl and no novel SMs are detectable neither on the bright field nor on the fluorescent photo. Also, the single cell analysis reveals a homogeneous culture consisting of exclusively fluorescent cells.

In contrast, the SM of BP691 exhibits a huge number of amplification units that are expressed simultaneously in the presence of xylose. The resulting increase of GFP proteins leads to a strong fluorescence signal especially on the level of single cells compared to the parental strain. Interestingly, the increased amount of GDHs in the cell might be disadvantageous on SP medium as SMs emerge having a growth advantage but do not express the *lacZ* gene anymore (red arrow) suggesting that the *prfA* gene or its promoter is inactivated to normalize the excess of GDHs within the cell. The situation is different on SPE-Xyl medium, because the danger of the

hyperactivity of GDHs and the resulting lack of glutamate for anabolic reactions in the cell is compensated by the presence of additional glutamate in the SP medium. Fluorescence analysis of SM of BP691 revealed even areas with a slightly increased fluorescence suggesting further amplification of the reporter unit even in the presence of the activator unit (red arrow).

SP and SPE medium exhibit *per se* a high concentration of glutamate favoring the acquisition of a GDH, but C-Glc minimal medium does not exhibit any glutamate and is normally used to select against emerging mutants with GDH activity. BP691, lacking any GDH, grows normally on C-Glc medium. The cell size in C-Glc medium is reduced in general for all *B. subtilis* cells due to the minimal set of nutrients in this medium. However, the SM of BP691 seems to suffer on C-Glc, which is especially visible on the level of single cells. Many cells do not express GFP anymore, a great fraction of cells expressing *gfp* exhibits an extremely small nearly roundish cell size and a lot of cell debris is detectable in the medium. The characteristics of this phenotype are even increased when adding xylose to the medium. The cultures of both strains barely reached the exponential phase OD_{600} in C-Glc-Xyl and both strains obviously suffered on plates. Interestingly, on the C-Glc-Xyl plate with the SM of BP691 white, non-fluorescent SM emerged (red arrow). These suppressor mutants must have inactivated the activator unit, because no blue color is detectable, and they must have decreased the amount of amplifications of the reporter unit until no *gfp* expression was detectable anymore. To conclude, laboratory evolution of the gene amplification units in the SM of BP691 is to a certain degree controllable using the desired medium compositions.

As the BP691 strain is now shown to be functional, the heterologous *pdxST* gene was

included in the reporter unit. The PdxS PLP synthase subunit and the PdxT glutaminase subunit build the PLP synthase complex to produce the B6 vitamers pyridoxal 5'-phosphate (PLP) in *B. subtilis* (Raschle *et al.*, 2005; Rosenberg *et al.*, 2017). B6 vitamers are of great industrial interest and many attempts to optimize the production of vitamin B6 were made (Kim *et al.*, 2010; Commichau *et al.*, 2014; 2015, Rosenberg *et al.*, 2017). As mentioned above, the Strep-tagged version of the *pdxST* genes was transformed in the reporter unit. The resulting strain BP808 was subsequently evolved on SP medium. The emergence of gene amplification was observed via fluorescence microscopy during the whole evolution and streaking process, to exclude the emergence of other mutations leading to a growth advantage by restoring the glutamate homeostasis. During the streaking process, the number of amplification units plateaued at the optimal balance between advantageous GDH supply and disadvantageous excess of the PdxST enzyme. As a result, there might be less amplification units present compared to the SM of the BP691 strain lacking the *pdxST* gene.

To analyze the overexpression of the reporter unit, BP691, BP808 and their SM were grown to the exponential phase. The cultures were split and half of them supplemented with 1 % xylose and grown for 4 h at 37 °C (Fig. 3.17). Microscopic analysis of cells from BP691 confirmed the results derived from the laboratory evolution experiment (Fig. 3.16). Slight fluorescence was detected for BP808 indicating already gene amplifications of the reporter unit. The addition of xylose to this strain resulted in a similar or even decreased fluorescence compared to the strain grown without xylose. Similarly, the SM of BP808 showed slight fluorescence in the absence of xylose and even decreased level of fluorescence after xylose addition. In general,

the SM of BP808 did not exhibit as much fluorescence compared to the SM of BP691. The reduced number of gene amplifications can be explained by the need to balance the disadvantageous effect of increased PdxST enzyme levels accompanied with higher levels of intermediates of the PLP synthesis pathway and the advantageous effect of the increased amount of GDHs (Andersson and Hughes, 2009). The induction of the amplified reporter gene expression leads to an increased disadvantage for the cell and consequently an even decreased number of amplifications.

This experiment shows that in the beginning there were amplifications of the reporter unit present, but after induction of their expression 4 h are sufficient for *B. subtilis* to reduce the amplification units again. Consequently, the production phase cannot be extended beyond this time point.

A possibility for counter selection and increasing the stability of the amplification units for a longer period is the addition of glutamate and xylose. However, there might be a high production of the PdxST complex at least for a short period of time. To test this hypothesis, the presence of proteins was verified performing a quantitative Western blot analysis (Fig. 3.17 B, C). GudB was detected for BP691 when xylose was added to the medium (Fig. 3.17 B). However, there is a very slight band present in the line for BP691 without xylose. Regarding slight *gfp* expression in the respective microscopic analysis in Fig. 3.17 A of the culture, the GudB band might result from some gene amplifications. The GudB signal is in general stronger for the SM of BP691 compared to the parental strain. The activation of the multiple reporter units is clearly visible comparing the lines with and without xylose. In all BP808 strains, the fluorescence intensity was decreased compared to the BP691 strains in the microscopic analysis. Accordingly, the Western

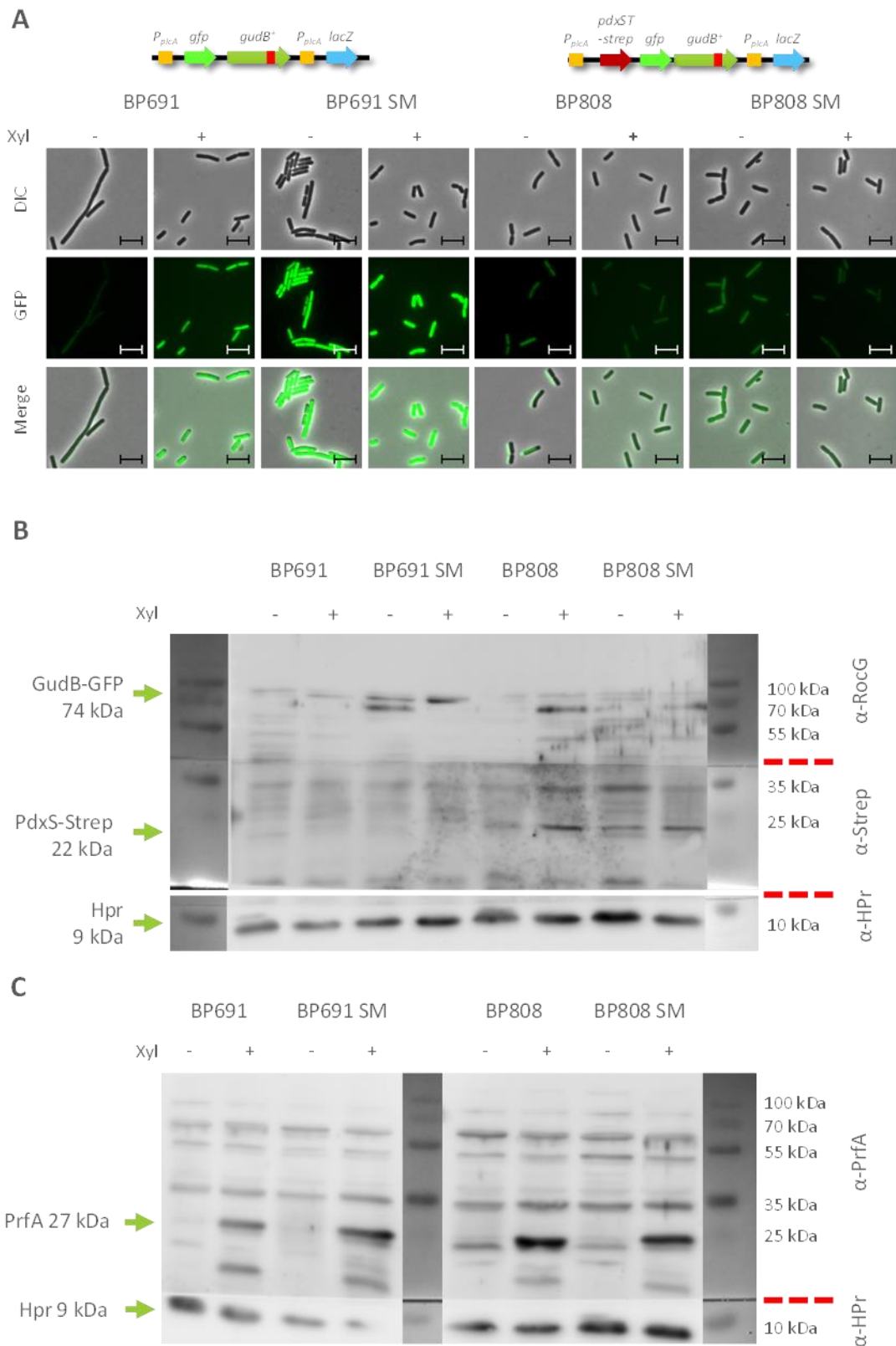


Fig. 3.17 Overexpression of heterologous proteins using the activator/reporter system.

A fresh colony of BP691, BP808 and respective SMs from an SP plate were used to inoculate 40 ml of SP medium, grown at 37 °C until an OD₆₀₀ of 0.5, split and half of the cultures were supplemented with 0.1 % xylose. After 4 h of growth, the cultures were harvested for microscopic and Western blot analysis. **A:** Microscopic fluorescence and DIC analysis of single cells. Scale bar 5 μm. **B:** Western blot analysis of GudB, PdxS-Strep and HPr (loading control). The membrane was cut in 3 parts (red lines) to allow the use of different antibodies. The signal of HPr was very strong, therefore a second exposure with only the upper two parts of the Western blot was performed. **C:** Western blot analysis of PrfA and HPr (loading control). For further loading control, both membranes (**B**, **C**) were stained with Coomassie (see supplementary information Fig. 6.3).

blot signals for GudB are also decreased in the BP808 strains. They are barely visible in BP808 grown in SP-Xyl and its SM grown in SP and SP-Xyl. In contrast, the signal for PdxS is nicely absent in the lines of BP691 and present in BP808 grown in SP-Xyl and its SM grown in SP and SP-Xyl. With respect to the uneven HPr loading control it is not possible to discuss the intensities of such faint bands, but the presence and absence of the PdxS enzyme shows already the functionality of the expression system in general. To show the induction of the activator unit, the presence of PrfA in the cells was tested. As expected, the respective Western blot is positive. All lines without xylose do not exhibit a band for PrfA and all lines with xylose do (Fig. 3.17 C). There is still plenty of room to improve and study the overexpression system based on the activator/reporter system, but the general idea of enriching a bacterial culture to a high OD₆₀₀ and subsequently induce extreme expression of the desired proteins for a short time accepting the cells to suffer and die or the amplification units to decrease is of high potential for hardly expressed proteins causing damage in the cell anyway.

3.3. GltC-independent transcription of *gltAB* genes

Glutamate is the most abundant metabolite in any living organism (Ch. 1.3). It is of great importance because glutamate builds the intersection between nitrogen and carbon metabolism. Its production is highly controlled (Picossi *et al.*, 2007; Commichau *et al.*, 2007a; Gunka and Commichau, 2012). Even though the glutamate homeostasis is intensively investigated, there are still controversies and unexplainable observations (Ch. 1.3.2). To unravel novel regulatory mechanisms to maintain glutamate homeostasis, *B. subtilis* strains auxotroph for glutamate were exposed to

selective medium lacking glutamate. As the glutamate homeostasis is of great importance for the cell, a variety of different SM was expected to be found.

3.3.1. A selection and screening system

A Δ *gltC* mutant strain auxotroph for glutamate was used for selection of SMs independent of GltC. Additionally, the strain harbored a *P_{gltA}-lacZ* fusion allowing the selection between different classes of SMs. Novel transcriptional activators would induce the expression of the *gltAB* genes as well as the expression of the promoter *lacZ* fusion. These mutants appear blue on plates supplemented with X-Gal and form the first class of suppressor mutations. In contrast, promoter-up mutations of the *gltAB* genes will not induce *lacZ* gene expression and appear white on plates supplemented with X-Gal. They form the second class of mutations. The third class consists of unexpected mutations belonging to neither novel activators, nor promoter-up mutations. The parental strain GP669 harboring a *P_{gltA}-lacZ* fusion (WT) and the respective Δ *gltC* strain BP640 were cultivated in C-Glc minimal medium under increasing glutamate concentration (0 % - 0.1 %), to define the optimal condition to grow poorly but steadily. BP640 (Δ *gltC*) grows under all glutamate concentration and even poorly in the absence of glutamate. Hence, the optimal condition for the isolation of GltC-independent mutations is C-Glc minimal medium without glutamate. To isolate SMs on plate, BP640 was grown to an OD₆₀₀ of 0.5 to 0.8 in CE-Glc and washed twice in C-Glc to remove the remaining glutamate from the cells. The resulting suspension was plated on C-Glc minimal medium plates supplemented with X-Gal. After incubation for 8 dpi at 37 °C, many white and some blue SM were detectable (Fig. 3.18. A). Six of the SM (3 white, 3 blue) were isolated and characterized. A drop dilution assay comparing

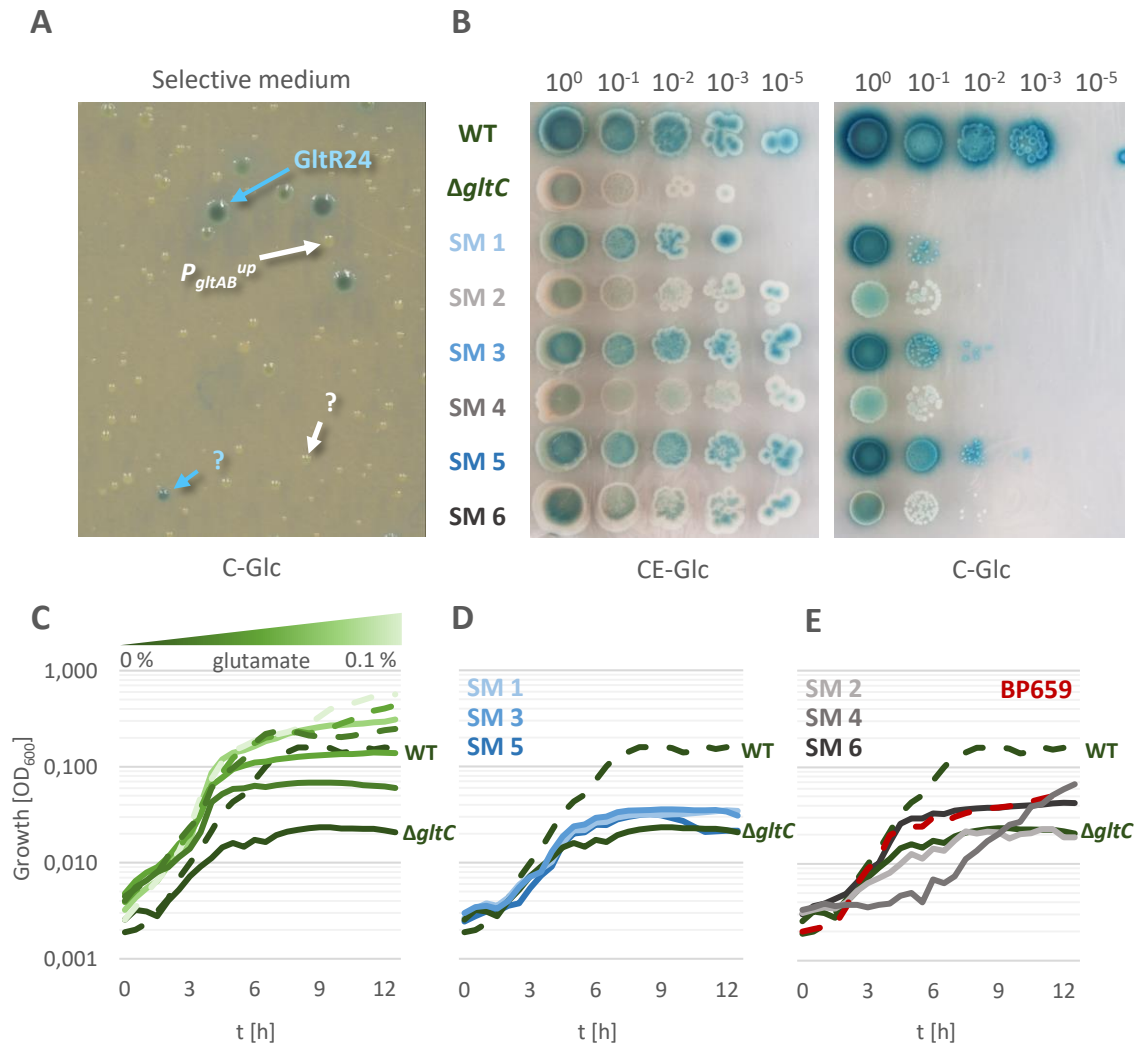


Fig. 3.18 Isolation of SMs independent of GltC using a selection and screening system

A: Selection and screening of SMs derived from BP640 ($\Delta gltC$) on C-Glc plates. **B:** Drop dilution assay to analyze growth of GP669 (WT), BP640 ($\Delta gltC$), SM1 – SM6 on non-selective (CE-Glc) and selective (C-Glc) medium, 3 dpi, 37 °C. **C-E:** Growth experiment C-E was split in the interest of clarity. GP669 (WT) and BP640 ($\Delta gltC$) serve as landmark for comparison in each graph. **C:** Growth curves of GP669 (WT, dashed line) and BP640 ($\Delta gltC$, solid line) under increasing glutamate concentrations indicated by the color index. **D:** Growth curve of the blue SMs 1, 3 and 5. **E:** Growth curve of white SMs 2, 4, 6 and the reconstituted strain BP659 ($P_{gltA(C-14G)}$). (Fig. adapted from Dormeyer *et al.*, 2017)

the growth of GP669 (WT), BP640 ($\Delta gltC$) and the isolated SM 1-6 on non-selective (CE-Glc) and selective (C-Glc) medium shows the growth advantage of the SMs in contrast to the parental strain BP640 ($\Delta gltC$). Interestingly, the white SM 2 and SM 4 have a similar phenotype compared to SM 6 which looks more bluish. Moreover, growth curves of all SM compared to BP669 (WT) and the parental strain BP640 were analyzed. The blue SMs 1, 3 and 5 exhibit a very similar and slightly improved growth compared to the parental strain BP640 (Fig. 3.18 D). In contrast, the white SMs 2, 4 and 6 grow all very different (Fig. 3.18 E). SM 2 does not show an improved

growth compared to the parental strain BP640. SM 4 shows an increased lag phase but starts growing very well after 6 h of incubation. SM 6 is the only SM growing initially as GP669 (WT) but reaches an early stationary phase.

3.3.2. Analysis of suppressor mutants

3.3.2.1. The transcriptional activator GltR24

In cells deficient of GltC, SM mutants emerge that harbor a G2087A mutation in the *gltR* gene (Belitsky and Sonenshein, 1997). This results in a single amino acid exchange (L219P) and renders

the resulting GltR24 transcription factor to activate the expression of the *gltAB* genes. Therefore, the *gltR* gene was sequenced in all SMs of BP640 from Ch. 3.3.1. The blue SMs 1, 3, and 5 contained the *gltR24* mutation (Dormeyer *et al.*, 2017). Testing the activity of the *gltAB* promoter in the GP669 (WT), the BP640 and the SM 3 (Fig. 3.19 A) in CSE-Glc minimal medium, a strong activity is detectable in the presence of GltC (GP669) and as expected no activity in its absence (BP640). The presence of GltR24 in SM 3 induces the *gltAB* gene expression again. This is in perfect agreement with the previous study (Belitsky and Sonenshein, 1997). However, only less than half of the activity is restored compared to the activity in the presence of GltC, leading to a lower amount of GOGAT and consequently of accessible glutamate in the cell. The SM cells suffer less, but they do not reach the health status of the GP669 (WT). This is reflected in the growth curve showing only a slight improve of growth for the blue SMs compared to the parental BP640 strain (Fig. 3.18 D).

It was also reported that GltR24 activity is reduced in the presence of proline (Belitsky and Sonenshein, 1997). However, in the present study this could not be shown (Fig. 3.19 A) for the *gltR24* SM 3, but the activity of GltC in GP669 (WT) was strongly reduced in the presence of proline.

The expression of the *gltAB* genes is tightly controlled. The transcriptional activator GltC activates the expression of the *gltAB* genes in the presence of glucose (Wacker *et al.*, 2003). However, when there is arginine, ornithine or to a lesser extend proline in the medium RocG is expressed (Belitsky and Sonenshein, 1998) which is known to repress the GltC activity in the presence of glutamate (Commichau *et al.*, 2007a; Stanek *et al.*, 2015b). It is possible that the observations made in the previous study are due to a RocG dependent regulation of GltR24.

Proline is only a weak inducer for the *rocG* gene expression, therefore the activity of the *gltAB* promoter was tested in medium supplemented with arginine, a strong inducer of *rocG* gene expression. Again, no regulation of GltR24 could be observed (Fig. 3.19 A). The controversy can be explained comparing the media compositions used in the previous and present study. Belitsky *et al.* used TSS medium containing glutamine as good nitrogen source. The presence of GltR24 leads to *gltAB* gene expression and the resulting GOGAT uses glutamine to produce glutamate for anabolic purposes. The addition of proline to the TSS medium serves a novel good source of glutamate for the cell. Now TnrA represses the expression of the *gltAB* genes by blocking the transcription start site, to conserve glutamine for anabolic purposes as glutamate can be produced from proline (Belitsky *et al.*, 1995; Belitsky *et al.*, 2000). However, when glutamate and ammonium or proline and ammonium, or all three are provided together as it is the case in Fig. 3.19, there is no TnrA-dependent repression of the *gltAB* genes (Belitsky *et al.*, 2000) and no decrease in GltR24 mediated activation of the *gltAB* gene expression.

Next, the activation potential of GltC, GltR and GltR24 was investigated. Therefore, all genes were transformed in the expression vector pBQ200 under the control of the strong promoter *P_{degQ36}*. Interestingly, having similar amounts of the respective proteins in the cell, there is a 6-fold increased activity of the *gltAB* promoter in the presence of GltR24, compared to the expression in SM 3 (Fig. 3.19 A, B). This suggests an improved binding of GltR24 to the promoter of *gltAB* genes compared to the binding of GltC. However, the binding is not regulated by the presence of proline or arginine in the medium. Interestingly, the GltC-

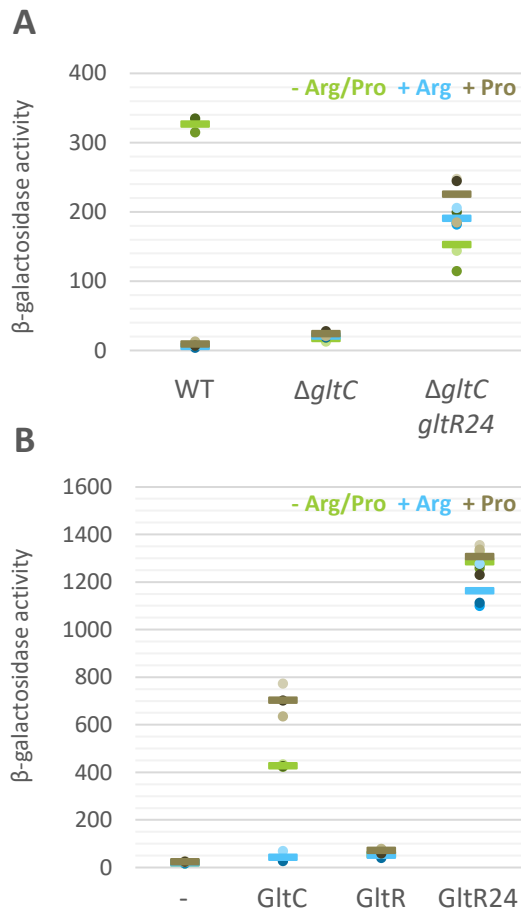


Fig. 3.19 Characterization of the GltR24 mutation. All strains were grown to the exponential phase (OD_{600} 0.5-0.8) in CSE-Glc minimal medium supplemented with 0.5 % arginine, 0.5 % proline (w/v) or none, harvested and β -galactosidase activity was measured. **A:** P_{gltA} activity of BP660 (WT), BP640 (Δ *gltC*) and SM 3 (*gltR24*). **B:** P_{gltA} activity of BP640 (Δ *gltC*) with the overexpression plasmids pBQ200 (empty), pGP907 (GltC), pBP418 (GltR) and pBP419 (GltC). (Fig. adapted from Dormeyer *et al.*, 2017)

dependent activity of the *gltAB* promoter is increased in the presence of proline. When arginine is present in the medium, GltC is inhibited by RocG (Commichau *et al.*, 2007a) and no expression of the *gltAB* genes is detectable. There is no activity of the *gltAB* promoter detectable in the presence of GltR as expected. To conclude, GltR24 has an increased promoter activation potential for the *gltAB* genes compared to GltC. However, in their native loci the *gltR24* gene seems to be expressed very poorly and the resulting amount of GltR24 does not activate the expression of the *gltAB* genes as good as the cellular level of GltC does.

3.3.2.2. GltC-independent promoter-up mutations

In the white SMs 2, 4, and 6 isolated in Ch. 3.3.1 there is no alternative transcriptional activator present as it is for the blue SMs 1, 3, and 5 in form of GltR24. Sequencing of the native *gltAB* promoter revealed a mutation within the promoter region of SM 6 (Fig. 3.20 A). The C to G substitution was located at position -14 right next to the -10 region and the GltC binding box III (Dormeyer *et al.*, 2017).

Whole genome sequencing revealed more mutations in this mutant: A substitution in the *clpC* gene (A700G), and a substitution in the promoter of *tapA* (C-73G). Both genes are not related to glutamate metabolism, as ClpC is involved in protein degradation and TapA in biofilm formation (Chu *et al.*, 2008). To elucidate whether the suppressor phenotype results from the promoter-up mutation, the SM 6 was reconstituted. Therefore, the strongly diluted gDNA of the SM 6 was used to amplify the Δ *GltC::aphA3* locus including the mutated $P_{gltA(C-14D)}$. The resulting PCR fragment was used to transform the parental strain GP669. Growth comparisons on selective and non-selective media revealed similar growth for the reconstituted BP659 and the original SM 6 on plate and in liquid C-Glc (Fig. 3.18 E, Fig. 3.20 B). Hence, the promoter-up mutation is sufficient to compensate for the loss of GltC.

For further characterization of this mutation, activity of the $P_{gltA(C-14G)}$ promoter determined in WT, Δ *gltC*, *rocG*⁻, and Δ *gltC rocG*⁻ strains (Fig. 3.20 C). In a Δ *gltC* mutant there is no wild type *gltA* gene expression detectable, in contrast the $P_{gltA(C-14G)}$ promoter mutation renders the promoter independent of GltC. Regarding the even increased expression of the promoter-up mutation in wild type cells, the promoter-up

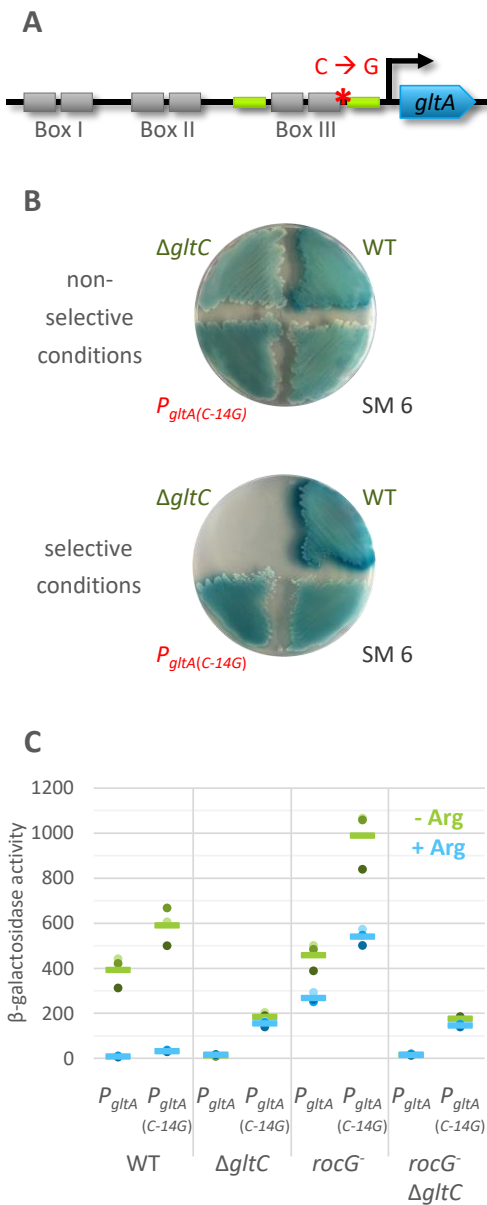


Fig. 3.20 GltC-independent promoter-up mutation **A:** Scheme of the *P*_{*gltA*(C-14G)} promoter-up mutation. **B:** Growth comparison of the reconstituted mutant BP659 (*P*_{*gltA*(C-14G)}), BP669 (WT), BP640 (Δ *gltC*) and the original *P*_{*gltA*(C-14G)} mutant SM 6 on selective C-Glc minimal medium and non-selective CE-Glc minimal medium as control. **C:** All strains were grown to the exponential phase (OD₆₀₀ 0.5-0.8) in CSE-Glc minimal medium supplemented with 0.5 % arginine (w/v) or none, harvested and β-galactosidase activity was measured. Promoter activities of *P*_{*gltA*} and *P*_{*gltA*(C-14G)} in different genotypes: WT (GP669, BP801), Δ *gltC* (BP640, BP802), *rocG*::Tn10 (BP803, BP805), *rocG*::Tn10 Δ *gltC* (BP804, BP806) respectively. (Fig. adapted from Dormeyer *et al.*, 2017)

mutation is rather partially independent of GltC, but not completely. The increased expression can be explained by an additional effect of the basal expression of *P*_{*gltA*(C-14G)} promoter and the presence of GltC (Fig. 3.20 C, the remaining data are explained in Ch. 3.4).

3.3.2.3. Gene amplifications of the *gltAB* genes

Whole genome sequencing of the remaining two white SMs revealed huge areas with increased coverage. Increased coverages arise when multiple gene copies exist in one genome, compare Ch. 3.2.4. Here, huge areas of 26 kbp (3 copies) and 36 kbp (10 copies) in SM 2 and 15 kbp (19 copies) in SM 4 were amplified. The number of copies of these areas was calculated dividing each coverage value of the gene amplification area by the mean coverage determined outside of the gene amplification region assuming the mean value to represent one copy of a gene. The exact breakpoints of the amplified areas were determined using reads of the whole genome sequencing data that were not aligned. In these reads, novel joint points of regions that are not next to each other in the natural genome were identified. Different copy numbers can be explained by the different sizes of the amplified area. The *gltAB* genes represent only a small part of the amplified regions and other genes located within the amplified region might confer a growth disadvantage when the resulting proteins are increased in the cell. Suggesting, that in SM 2 cells are found with a gene copy number increased to a point where the beneficial effect still predominates the disadvantageous effect of other gene products (Andersson and Hughes, 2009). In contrast, SM 4 harbors a smaller area of gene amplification and therefore a higher gene copy number can be reached.

As demonstrated in the previous chapter 3.2, cells harboring areas of gene amplifications will be under constant evolution. This is reflected in the growth curve experiment of the white SMs (Fig. 3.18 E). In the preculture the cells were cultivated in CE-Glc, in which amplifications of the *gltAB* genes are disadvantageous. Until the cells were washed twice in C-Glc medium to

avoid residual glutamate in the actual experiment, they were exposed to glutamate. This period is sufficient for *B. subtilis* to lose several gene copy numbers of *gltAB*, because they confer a growth disadvantage in the presence of glutamate. As a result, the promoter-up mutant grows constantly, whereas SM 2 and SM 4, harboring eventually reduced *gltAB* gene copy numbers suffer in the beginning of the growth curve. After 6 h of growth SM 4 starts to grow exponentially. This might be due to the acquisition of additional *gltAB* gene copies.

The *gltAB* gene amplification was also confirmed experimentally via Southern blot (Fig. 3.21 B, C, D). The signal derived from the *gltAB* specific probe showed high intensity in SM 2 and 4 compared to the parental strain BP640 and SM 6, harboring only one copy of the *gltAB* genes.

In contrast, the signals for SM 2 and 4 on the reprobed Southern blot, using the *accA* gene as reference for a single copy, were decreased. This finding does not only prove an increased *gltAB* gene copy number in SM 2 and 4. It is worth to mention, that the relative amount of *accA* in 300 ng gDNA is decreased for SM 2 and 4 compared to BP640 and SM 6. There were also large deletion regions in SM 2 of 28.1 kbp (genomic localization: 1954400 to 1982500) and in SM 4 of 5.1 kbp (genomic localization: 1950200 to 1955300). This taken together leads to a massive increase of 10 % (419.9 kbp) and 6 % (256.9 kbp) in size of the genomes of SM 2 and 4, respectively.

3.3.3. Hierarchy of mutations

A systematic quantification of blue and white SM emerged from the glutamate auxotroph Δ *gltC* mutant strain revealed an enormous excess of white compared to blue SMs independent of the availability of glutamate (Fig. 3.22). To identify whether the majority of white SMs are

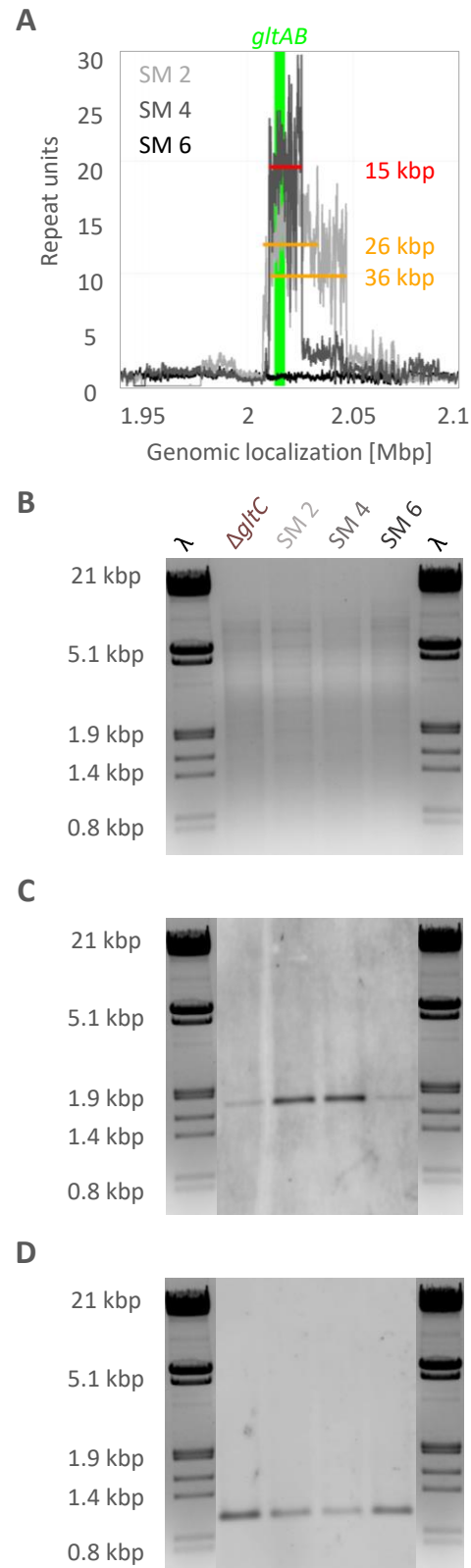


Fig. 3.21 Gene amplification of the *gltAB* gene locus
A: Repeat units of SM 2, 4, and 6 calculated from whole genome sequencing coverage data. **B:** 1 % agarose gel with 300 ng *Hind*III digested gDNA of BP640 (Δ *gltC*), SM 2, 4, and 6 used for Southern blot (C, D). **C:** Southern blot with a *gltAB* specific probe (MD216/MD217). Expected size: 1820 bp. **D:** Stripped and reprobed Southern blot with an *accA* specific probe (JN127/JN128) as loading control, only one copy of the *accA* gene is present in the genome). Expected size: 1227 bp. (Fig. adapted from Dormeyer *et al.*, 2017)

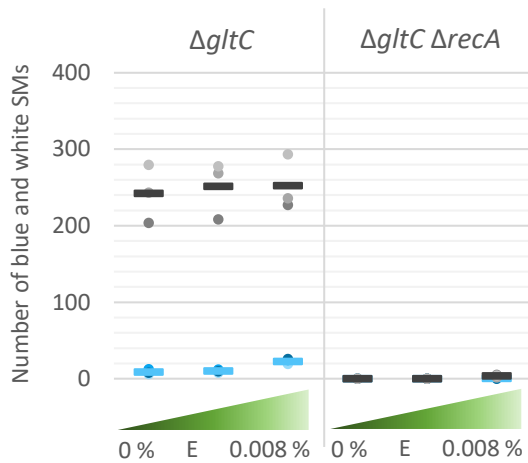


Fig. 3.22 Quantitative analysis of GltC-independent SMs BP640 was grown in CE-Glc to an OD_{600} of 0.5 to 0.8, washed twice in C-Glc, thereby the OD_{600} was adjusted to 0.4 and 100 μ l thereof ($4 \cdot 10^6$ cells) were plated on 25 cm^2 C-Glc plates with either 0%, 0.08% or 0.008% glutamate and analyzed after 8 dpi at 37 °C. (Fig. adapted from Dormeyer *et al.*, 2017)

promoter-up mutations or amplifications, the *gltAB* promoter region was sequenced. Only one white SM acquired a C-10T promoter-up mutation, which rendered the promoter constitutively active (Belitsky *et al.*, 2000; Commichau *et al.*, 2007a). Suggesting, that 9 out of 10 mutants harbor *gltAB* gene amplifications.

The RecA protein is involved in homologous recombination and DNA repair (Cox, 2007). Furthermore, gene amplification can be mediated by RecA (Shyamala *et al.*, 1990; Reams *et al.*, 2010; Reams *et al.*, 2012). Therefore, the *recA* gene was deleted in BP640 ($\Delta gltC$) and the SM quantification was repeated. Interestingly, the number of white SMs decreased, nearly vanished in the $\Delta recA$ strain (Fig. 3.22). Sequencing of 10 white SMs revealed exclusively C-10T substitutions in the *gltAB* promoter rendering the promoter independent of GltC as previously described. To conclude, most of the mutations emerged to compensate for the loss of GltC were amplifications. Substitutions, either in the promoter region of the *gltAB* genes or in the *gltR* gene emerged to a lesser extent.

3.4. GltC – A devil in disguise

3.4.1. The RocG-GltC-DNA complex

The regulation of the *gltAB* gene expression is extensively studied (Belitsky and Sonenshein, 1995; Belitsky *et al.*, 1995; Belitsky and Sonenshein, 1997; Belitsky *et al.*, 2000; Picossi *et al.*, 2007; Commichau *et al.*, 2007; Stannek *et al.*, 2015). However, there are two models co-existing that can explain the GltC mediated repression of the *gltAB* genes (Ch. 1.3.2). *In vitro*, Picossi *et al.* observed the binding of GltC to the GltC-binding box I and III in the presence of glutamate (Picossi *et al.*, 2007) thereby the binding of the RNAP is prevented and the *gltAB* genes are not transcribed. In another study, Commichau *et al.* observed *in vivo* the interaction of RocG and GltC (Commichau *et al.*, 2007a) preventing GltC from binding to the DNA.

In the previous experiment in Ch. 3.3.2.2, the *gltAB* promoter-up mutation C-14G was characterized. The mutation rendered the promoter only partially independent of GltC, because increased activity was detected in the presence of GltC (Fig. 3.20 C). The same was observed investigating promoter variants harboring either a mutation in the -35 (T-32A) or in the -10 (C-10T) region of the *gltAB* promoter (Fig. 3.23 A). These promoter variants are known to be constitutively active in the absence of GltC (Belitsky *et al.*, 1995; Commichau *et al.*, 2007a). The addition of arginine to the medium did not change the activity of the promoter variants in the $\Delta gltC$ background, but a GltC mediated repression of all promoter variants was observed in the wild type background (Fig. 3.20 C and Fig. 3.23 B). When arginine is in the medium the expression of the *rocG* gene is induced (Belitsky and Sonenshein, 1998). It is known from *in vivo* data that RocG binds, in the presence of glutamate, to GltC.

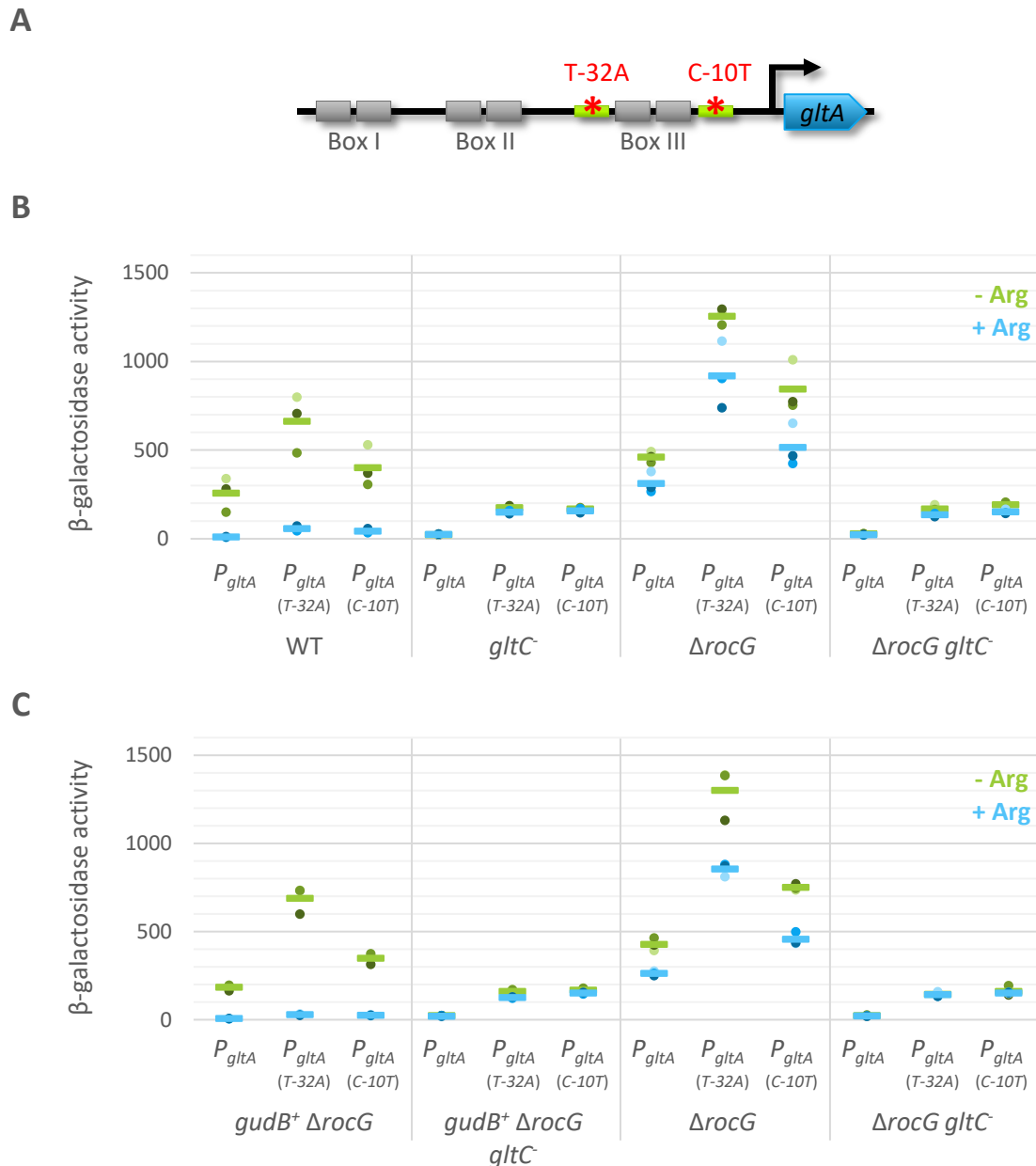


Fig. 3.23 Partially constitutive promoters

A: Promoter region of the *gltAB* genes with indicated mutations. **B, C:** All strains were grown to the exponential phase (OD₆₀₀ 0.5–0.8) in CSE-Glc minimal medium supplemented with 0.5% arginine (w/v) or none, harvested and β -galactosidase activity was measured. **B:** Promoter activities of P_{gltA} , $P_{gltA(T-32A)}$ and $P_{gltA(C-10T)}$ in different genotypes: WT (GP342, BP809, BP810), *gltC::Tn10* (GP650, GP689, GP692), $\Delta rocG$ (BP811, BP815, BP816), $\Delta rocG gltC::Tn10$ (BP812, BP813, BP814) respectively. **C:** Promoter activities of P_{gltA} , $P_{gltA(T-32A)}$ and $P_{gltA(C-10T)}$ in different genotypes: *gudB⁺ ΔrocG* (BP817, BP821, BP822), *gudB⁺ ΔrocG gltC::Tn10* (BP818, BP819, BP820), $\Delta rocG$ (BP811, BP815, BP816), $\Delta rocG gltC::Tn10$ (BP812, BP813, BP814) respectively.

The RocG-bound GltC might not be able to bind to the promoter region of the *gltAB* genes. Consequently, there should be activity detectable for the GltC-independent promoter variants in the wild type strain grown in medium containing arginine, but there is no expression detectable (Fig. 3.20 C and Fig. 3.23 B). To block the expression of GltC-independent promoter variants there is a repressor needed blocking the

promoter region and thereby preventing the RNAP from binding. This behavior was observed *in vitro* for GltC in the presence of glutamate (Picossi *et al.*, 2007). Suggesting a combined model where RocG binds to GltC that binds to the promoter of the *gltAB* genes. To corroborate this model, the activity of the promoter variants was determined in a RocG deficient strain. Indeed, the GltC mediated repression in the presence of

arginine in the medium was relieved in a RocG deficient strain (Fig. 3.20 C and Fig. 3.23 B). The activity of all promoter variants even increased in a RocG deficient strain compared to the wild type strain, suggesting a constant control of the *gltAB* gene expression by RocG. The increased activity vanished completely in a strain deficient of RocG and GltC.

This new model is also true for the second GDH in *B. subtilis* GudB⁺ (Fig. 3.23 C) that is also known to bind GltC in the presence of glutamate *in vivo* (Stannek *et al.*, 2015b).

To corroborate the new model with *in vitro* data, the promoter binding characteristics of GltC alone and in the presence RocG or GudB⁺ to the *gltAB* were planned to be investigated using surface plasmon resonance spectroscopy. Therefore, tag-free versions of all proteins were purified (Fig. 3.24 A) and the activity of the purified RocG was tested (Fig. 3.24 B). In the presence of glutamate RocG was active, indicated by the increase of NADH. In the presence of an excess of GltC the RocG activity was slightly reduced. As RocG is known to form a hexamer (Gunka *et al.*, 2010), it is possible that some of the RocG monomers are only required to inhibit GltC and do not fulfill their metabolic function.

3.4.1.1. Importance of the GltC binding boxes

To investigate the function of the GltC binding boxes regarding the novel model of *gltAB* gene regulation, mutants of the binding boxes II and III were investigated (Fig. 3.25 A). The box III T-28A promoter variant is known to show increased *gltAB* gene expression in the presence of GltC (Belitsky *et al.*, 1995). This is true in the presence of GltC compared to the activity of the native *gltAB* promoter (Fig. 3.25 B). Now, T-28A could be either a constitutively active promoter variant partly independent of GltC or a promoter variant

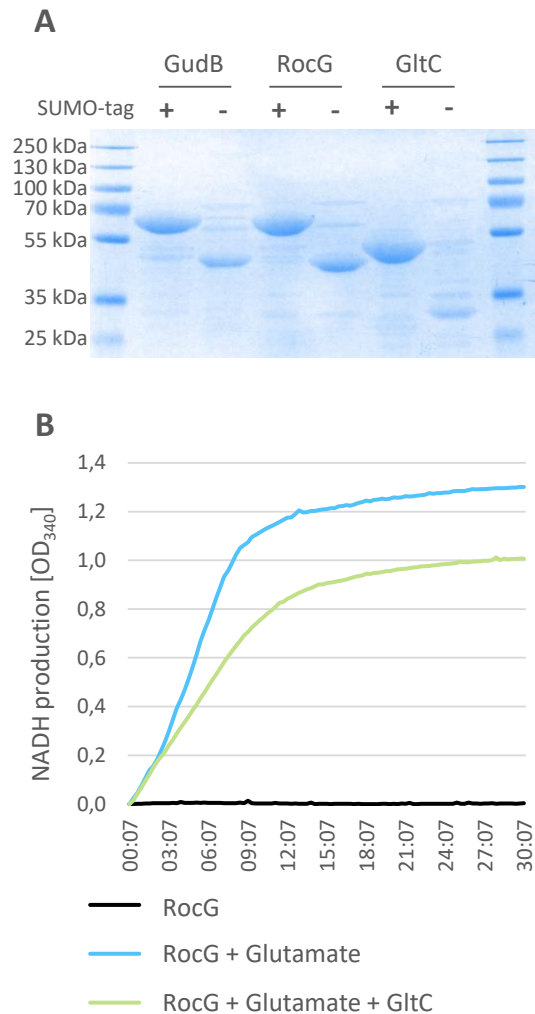


Fig. 3.24 Purification of GudB⁺, RocG and GltC
A: Purified GudB (47 kDa), RocG (46.5 kDa) and GltC (33.9 kDa) proteins with SUMO-tag (+ 13 kDa) and completely tag free. Protein purification of 1 l cultures grown in BHI medium from an OD₆₀₀ of 0.05 to 0.8, IPTG induction, 4 h growth at 37 °C. PBS buffer was used for protein extraction. **B:** GDH activity assay. Reaction was based in PBS buffer containing 1 mM NAD. The NADH production was measured for 6 μM RocG alone, 6 μM RocG with 0.1 M glutamate and 6 μM RocG with 0.1 M glutamate in the presence of 8 μM GltC. Mean of 3 technical replicates.

that prevents GltC from binding to the box III. Unfortunately, the T-28A mutation did not alter the binding characteristics of RocG because the activity of the *gltAB* promoter variant T-28A can be repressed upon addition of arginine to the medium and this repression can be relieved in a RocG deficient strain. As a result, the *gltAB* promoter variant T-28A does not prevent GltC from binding to the box III. The box II T-48C promoter variant is known to show a reduced *gltAB* gene expression (Belitsky *et al.*, 1995).

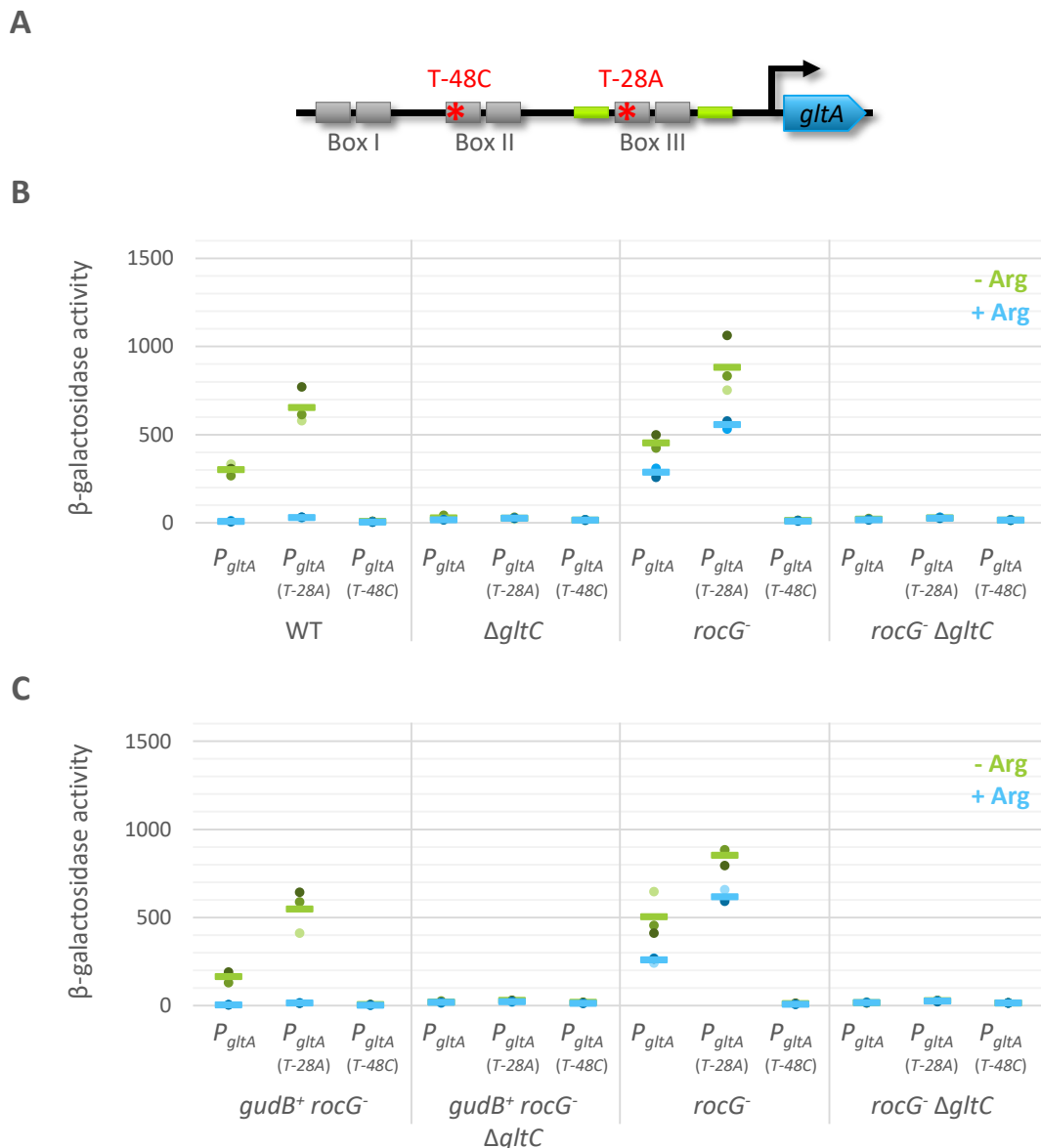


Fig. 3.25 Importance of GltC binding boxes III and II

A: Promoter region of the *gltAB* genes with indicated mutations. **B, C:** All strains were grown to the exponential phase (OD_{600} 0.5-0.8) in CSE-Glc minimal medium supplemented with 0.5 % arginine (w/v) or none, harvested and β -galactosidase activity was measured. **B:** Promoter activities of P_{gltA} , $P_{gltA(T-28A)}$ (Box III) and $P_{(T-48C)}$ (Box II) in different genotypes: WT (GP669, BP828, BP829), $\Delta gltC$ (BP640, BP832, BP835), $rocG::Tn10$ (BP803, BP833, BP836), $rocG::Tn10 \Delta gltC$ (BP804, BP834, BP837) respectively. **C:** Promoter activities of P_{gltA} , $P_{gltA(T-28A)}$ (Box III) and $P_{(T-48C)}$ (Box II) in different genotypes: $gudB^+ rocG::Tn10$ (BP830, BP838, BP839), $gudB^+ rocG::Tn10 \Delta gltC$ (BP842, BP840, BP841), $rocG::Tn10$ (BP803, BP833, BP836), $rocG::Tn10 \Delta gltC$ (BP804, BP834, BP837) respectively.

Indeed, this promoter variant does not exhibit any activity under any tested condition (Fig. 3.25 B) and thereby proves the box II to be essential for *gltAB* expression. All these findings were also true for the second GDH in *B. subtilis* $GudB^+$ (Fig. 3.25 C).

As the *gltAB* promoter variant T-28A does not prevent GltC from binding to the box III (Fig. 3.25), the function of the GltC binding box III was examined in more detail. Therefore, the

complete spacer sequence between the -35 and the -10 region was shuffled to obtain three different promoter variants (Fig. 3.26 A).

In the absence of arginine, the activity of the shuffle promoter variants is at least three- to five-fold increased compared to the promoter activity of the native *gltAB* promoter (Fig. 3.26 B). The GltC dependent repression of *gltAB* gene expression in the presence of arginine was successfully impaired in the shuffle promoter

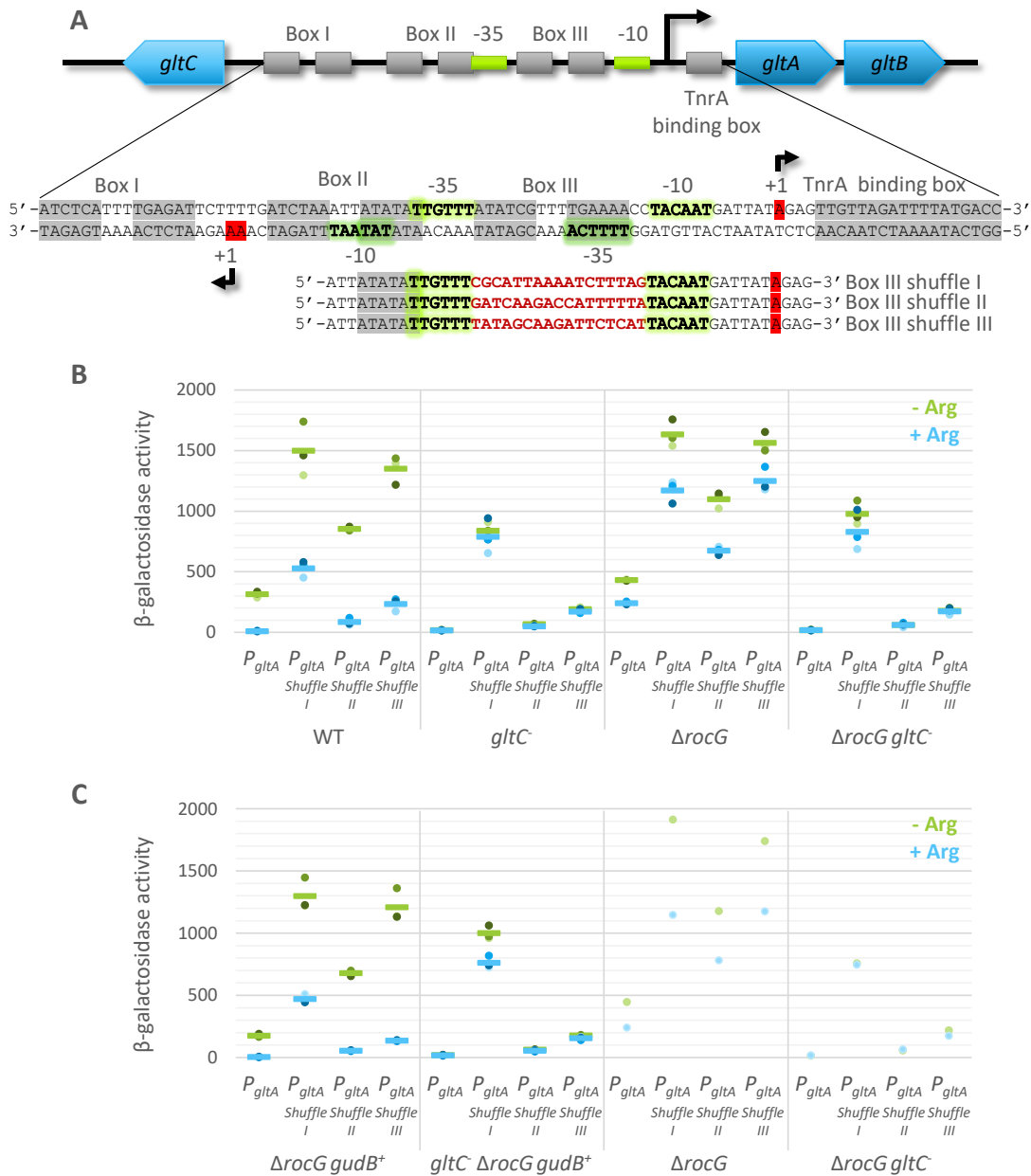


Fig. 3.26 Impact of GltC-binding box III on *gltAB* gene expression

A: Scheme of the *gltAB* and *gltC* promoter region with detailed sequence view. The GltC binding box III sequence was shuffled leading to three different shuffle variants (I-III) as displayed. The box III variants were fused to the *lacZ* gene in the ectopic *amyE* gene locus, hence the expression of the *gltC* gene within its native locus is not impaired. **B, C:** All strains were grown to the exponential phase (OD₆₀₀ 0.5-0.8) in CSE-Glc minimal medium supplemented with 0.5 % arginine (w/v) or none, harvested and β-galactosidase activity was measured. **B:** Promoter activities of *P_{gltA}*, *P_{gltA} shuffle I*, *P_{gltA} shuffle II*, *P_{gltA} shuffle III* in different genotypes: WT (GP669, BP862, BP863, BP864), *gltC::Tn10* (BP850, BP872, BP873, BP874), $\Delta rocG$ (BP885, BP875, BP876, BP877), $\Delta rocG gltC::Tn10$ (BP845, BP878, BP879, BP880), respectively. **C:** Promoter activities of *P_{gltA}*, *P_{gltA} shuffle I*, *P_{gltA} shuffle II*, *P_{gltA} shuffle III* in different genotypes: *gudB⁺ ΔrocG* (BP851, BP866, BP867, BP868), *gudB⁺ ΔrocG gltC::Tn10* (BP852, BP869, BP870, BP871), $\Delta rocG$ (BP885, BP875, BP876, BP877), $\Delta rocG gltC::Tn10$ (BP845, BP878, BP879, BP880), respectively.

variants. Strongest promoter activity in the presence of arginine was observed for the shuffle I promoter variant. It exhibited an expression slightly higher compared to the activity of the native promoter in the absence of arginine.

The promoter variants investigated in Fig. 3.23, are partially independent of GltC as their activity decreased in a GltC-deficient strain but did not abolish completely independent of the presence or absence of arginine. This can be also observed for the shuffle promoter variants, except for the shuffle II promoter, which does almost not

exhibit any activity in the absence of GltC (Fig. 3.26 B). Strikingly, the shuffle I promoter variant does only exhibit a slightly reduced activity in the absence of GltC in medium without arginine. Moreover, the activity in medium with arginine even slightly increases in a GltC-deficient strain compared to a wild type like strain.

Next, the impact of the GDH RocG on the promoter activities was accessed. In the absence of RocG and arginine the activity of all shuffle promoter variants including the native promoter were similar as in the wild type strain. Upon addition of arginine to the medium the activity of all promoters increased drastically compared to the wild type like situation. Indicating, that RocG still has an influence on all the promoter variants, even though the binding box III is altered. In the absence of both, GltC and RocG, the promoter activities were comparable to the ones in the GltC-deficient strain. All these observations were also true for the second GDH GudB in *B. subtilis*, even though the activities were slightly reduced in general in this strain, compared to the RocG situation (Fig. 3.26 A).

3.4.2. Only *B. subtilis* GDHs have metabolic and regulatory treats

RocG and GudB⁺ are known to be exclusively catabolically active and to bind GltC leading to the repression of the *gltAB* gene expression. Here, RocG, GudB⁺ and the also anabolically active GDH GdhA from *E. coli* are constitutively expressed in a *B. subtilis* strain deficient of native GDHs in the absence and presence of arginine (Fig. 3.27).

Even in the absence of a GDH, arginine mediated repression of 1/3 of the activity of the *gltAB* promoter is detectable. As expected RocG and GudB inactivate the activity of the *gltAB* promoter completely in the presence of arginine. Interestingly, the activity of the *gltAB* promoter

is even increased in the presence of large amounts of RocG compared to the empty vector control, suggesting an activating effect of RocG on the *gltAB* promoter. In contrast to the native GDHs of *B. subtilis*, the *E. coli* GDH GdhA has no regulatory effect on the activity of the *gltAB* promoter.

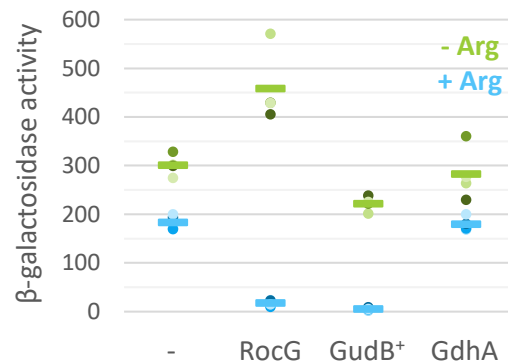


Fig. 3.27 Activity of the *gltAB* promoter upon an excess of GDHs

All strains were grown to the exponential phase (OD₆₀₀ 0.5-0.8) in CSE-Glc minimal medium supplemented with 0.5 % arginine (w/v) or none, harvested and β-galactosidase activity was measured. Activity of the *gltAB* promoter in GP28 Δ *gudB* *rocG*::Tn10 harboring either the empty vector control (pBQ200), constitutively expressed *rocG* (pGP529), *gudB*⁺ (pBP482) or *gdhA* (pGP934) was determined.

3.4.3. The difference of GudB⁺ and RocG

RocG and GudB⁺ share 74 % identity of the amino acid sequence (Belitsky and Sonenshein, 1998). RocG is only expressed upon the presence of arginine, ornithine, or proline in the medium, whereas GudB⁺ is constitutively expressed and regarded as major GDH in the *B. subtilis* NCIB 3610 strain. In the following, differences between GudB⁺ and RocG regarding the GltC interaction surfaces were investigated using GltC variants P88L, I160K and T99A (Belitsky and Sonenshein, 1995). To determine differences between GudB⁺ and RocG, the *gltC* variants and the native *gltC* were introduced in the *amyE* locus in a *B. subtilis* strain having either *rocG*⁺ or *gudB*⁺. The wild type and a *gudB*⁺ strain served as additional controls. All GltC variants induced strongly the activity of the *gltAB* promoter. The order of activation potential is GltC T99A > GltC

P88L > GltC I160K in CSE-Glc medium (Fig. 3.28), thus independent of GDHs. Upon addition of arginine to the medium the activity of the *gltAB* promoter was differently regulated by RocG and GudB⁺ in the presence of the different GltC variants. RocG repressed half of the impact of GltC P88L on the activity of the *gltAB* promoter, whereas GudB⁺ could not at all repress the activity of the GltC variant. This is similar for the GltC T99A variant. Only the GltC I160K was not

regulated by RocG, but regulated by GudB⁺. Regarding the protein sequence of GltC the P88L and T99A mutations are near of a putative dimerization region, whereas the I160K mutation is located within the two dimerization regions. Typical LysR type transcriptional regulators (LTTR) have a helix-turn-helix motif (HTH) and a co-factor binding domain (Maddocks and Oyston, 2008).

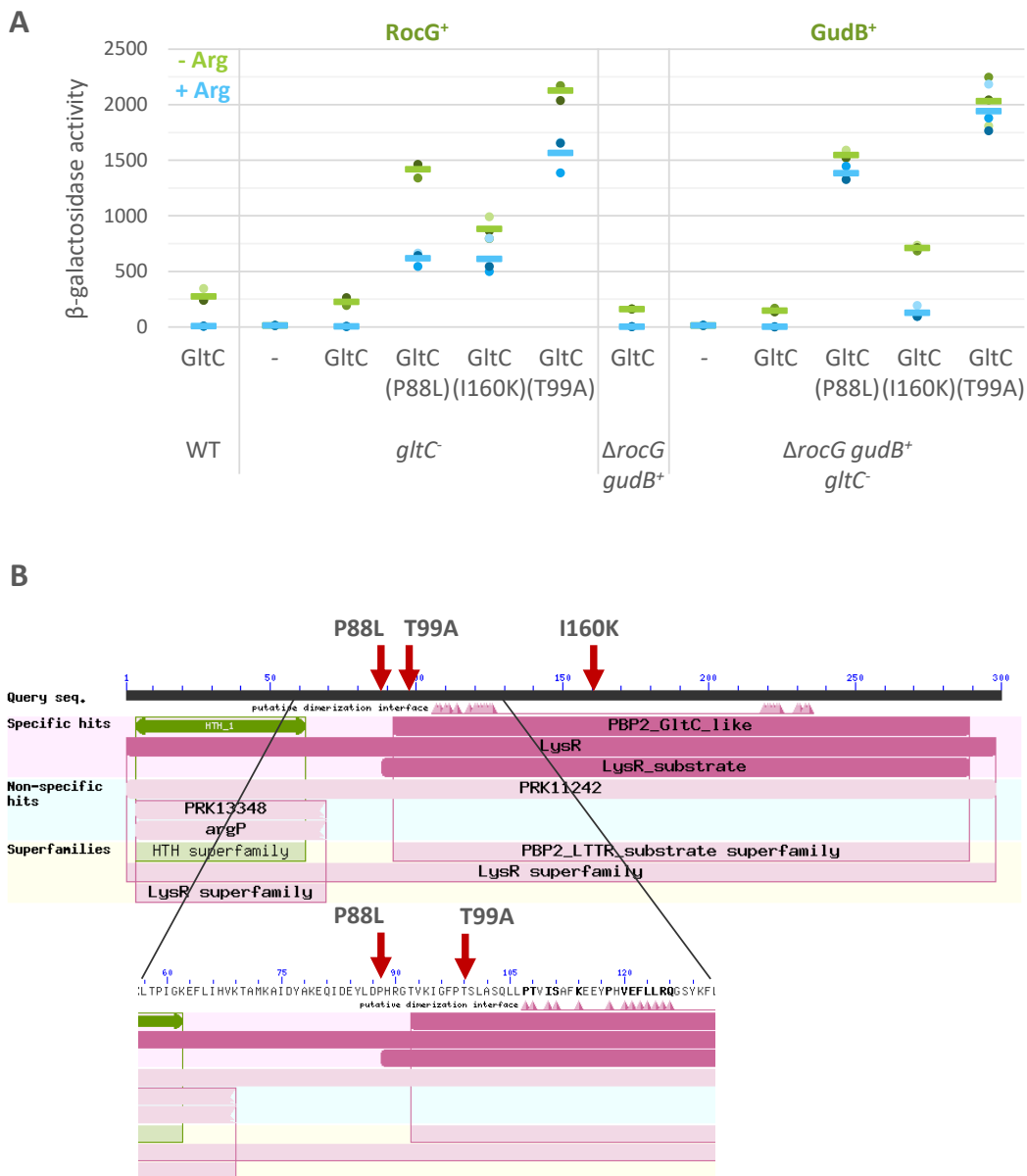


Fig. 3.28 Control of GltC variants by RocG and GudB
 All strains were grown to the exponential phase (OD₆₀₀ 0.5-0.8) in CSE-Glc minimal medium supplemented with 0.5 % arginine (w/v) or none, harvested and β -galactosidase activity was measured. *P_{gltA}* promoter activities was determined in different genotypes: As controls strains harboring *gltC* in its native locus in the WT background (GP669) and a $\Delta rocG$ *gudB*⁺ background (BP851). And the *gltC*::Tn10 mutant strain as well as the $\Delta rocG$ *gudB*⁺ *gltC*::Tn10 mutant strain harboring either no *gltC* (BP850, BP852), or the native GltC, a GltC P88L, I160K, or T99A mutant variant in the *amyE* locus (GP651, BP853, GP652, BP854, GP653, BP855, GP654, and BP856, respectively). B: DELTA-BLAST analysis of the GltC protein sequence. Mutated areas are indicated.

The HTH motif is characteristically located at the C-terminus for transcriptional activators and at the N-terminus for transcriptional repressors (Pérez-Rueda and Collado-Vides, 2000). In GltC, which is a LTR, the HTH is located at the N-terminus. It is also reported that a co-inducer binding cleft at the C-terminal domain is conserved spanning the residues 95 to 210 (Maddocks and Oyston, 2008). That RocG cannot

regulate the GltC variant harboring a mutation within this region is in perfect agreement with the previously stated model of RocG-GltC-DNA binding. The GudB mediated repression of GltC is still functional in the I160K variant, it is likely that the GltC-GudB interaction site is not in the co-inducer cleft, but in the area between the HTH motif and the dimerization region.

4. Discussion

4.1. What does *B. subtilis* need to achieve highest fitness levels?

For achieving a high fitness level, it is crucial to perfectly adapt and fast react to changing environmental conditions. Under the present environmental conditions, only the pathways for the most efficient nitrogen and carbon sources are expressed to produce a maximum of energy (Ch.1.2). To avoid unnecessary reactions and the resulting waste of energy, metabolic pathways are highly controlled and carefully adjusted. This is also the case for the glutamate metabolism forming the most important metabolic intersection in the cell (Gunka and Commichau, 2012). The biosynthesis and degradation of glutamate represents the connection between carbon and nitrogen metabolism, therefore maintaining the glutamate homeostasis is of great importance for *B. subtilis*.

In many studies, the strong dependence between glutamate synthesizing and degrading enzymes was shown. For example, on medium with succinate and ammonium the glutamate pool is too low and the cells suffer, because in the absence of glucose CcpA does not repress the *rocG* gene and RocG prevents the expression of the *gltAB* genes encoding for the GOGAT that synthesizes glutamate. On medium with succinate and ammonium suppressor mutants, which have inactivated the *rocG* gene, restored the glutamate homeostasis (Commichau *et al.*, 2007b). Another example, a $\Delta ccpA$ mutant growing on medium with glucose and ammonium cannot repress the expression of the *rocG* gene and encounters the same problem of a low glutamate pool (Wacker *et al.*, 2003; Commichau *et al.*, 2007b). An opposite example is a $\Delta rocG$ deletion mutant growing on medium with arginine, unable to use glutamate as carbon

source and to inhibit further production of glutamate. Most likely intermediates of the arginine degradation pathway accumulate to a toxic level. A suppressor mutation activating the cryptic *gudB^{CR}* gene compensates for the loss of the *rocG* gene (Belitsky and Sonenshein, 1998; Gunka *et al.*, 2013). Albeit it is not known what exactly is toxic for the cell, the fast degradation of glutamate by the GDHs is relevant to restore fitness.

But what is the advantage of having two homologous moonlighting enzymes with identical enzymatic and regulatory functions? At the first glance, there is not much of a difference between the GDHs RocG and GudB in *B. subtilis* as they share 74 % identity, having similar K_M values for glutamate, though GudB has a slightly higher turnover number, and both inhibit the GltC transcription factor (Belitsky and Sonenshein, 1998; Commichau *et al.*, 2007a; Noda-Garcia *et al.*, 2017). In an intraspecies competition experiment a *B. subtilis* strain, having RocG and GudB, had a significant growth advantage on medium with glucose, ammonium and glutamate, as carbon and nitrogen sources, compared to a strain having only RocG (Gunka *et al.*, 2013). The growth advantage most likely results from more efficient glutamate degradation with two GDHs. Similarly, in this study it was discovered that the loss of GltC and the resulting auxotrophy for glutamate can be compensated by the amplification of the *gltAB* genes increasing the amount of the GOGAT to reconstitute glutamate homeostasis (Ch. 3.3.2.3). However, it is doubtful that simply the amount of GDH is the reason for stably inheriting two homologous genes for the GDH function. Furthermore, a competition experiment in medium containing only glucose and ammonium as carbon and nitrogen sources revealed a disadvantage for cells encoding two genes encoding for GDHs (Gunka *et al.*, 2013). A closer

look to the biochemical and regulatory properties of RocG and GudB reveals differences between the GDHs: The *gudB* gene is constitutively expressed but the resulting protein can only form an enzymatically active hexamer under specific pH and glutamate concentrations. In contrast, the *rocG* gene is under strong regulation, but whenever it is expressed, the resulting GDH is stable and highly active. GudB confers the advantage of a fast reaction to suddenly increasing glutamate pools. It degrades a lot of glutamate until the concentration is below the small range in which GudB is active (Noda-Garcia *et al.*, 2017). RocG again provides the advantage of being always active, when expressed. Global regulators of carbon and nitrogen metabolism controlling the expression of the *rocG* gene, allow the cell to have a functional GDH present in the cell before the glutamate concentration rises to critical levels. Simultaneously, both enzymes can in principle prevent the *gltAB* gene expression to prevent a futile cycle of glutamate synthesis and degradation.

In this work, two regulatory models based on either *in vitro* or *in vivo* observations could be combined to one consistent model explaining the complex *gltAB* gene regulation in *B. subtilis* (Fig. 4.1 A & B), which was originally suggested by Dr. Katrin Gunka (Gunka, 2010) but never experimentally supported until now (Ch. 3.4.1). The model for the regulation and the complex evolution of the two GDHs RocG and GudB are discussed in the following chapters.

4.2. Regulation of the *gltAB* genes

4.2.1. Activation of *gltAB* gene expression

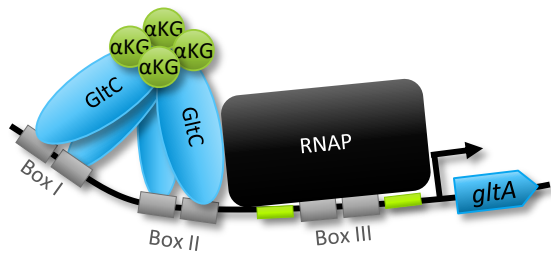
For activation of the *gltAB* gene expression, α -ketoglutarate forms a complex with at least four molecules GltC. The resulting complex binds

to box I and II in the *gltAB* promoter region and induces *gltAB* gene expression (Fig. 4.1 A and Fig. 4.2 A). Whereas the activating property on *gltAB* gene expression of GltC was discovered already 28 years ago (Bohannon and Sonenshein, 1989; Belitsky *et al.*, 1995), the concrete binding mechanism of GltC and its dependence on α -ketoglutarate was first shown *in vitro* via DNaseI footprinting analyses about 20 years later (Picossi *et al.*, 2007). This regulation was challenged in this study *in vivo*. A T-48A mutation inactivated the box II and no *gltAB* gene expression was detectable (Fig. 3.25), demonstrating its essentiality for *gltAB* gene expression (Belitsky *et al.*, 1995).

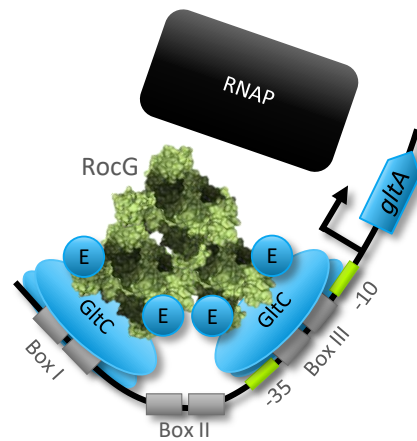
4.2.2. Prevention of *gltAB* gene expression

Initially, TnrA was the only factor known to repress the *gltAB* gene expression, but in a TnrA deficient strain still nitrogen dependent repression was observed. Intensive studies to find the other nitrogen dependent repressor in the absence of GltC were made (Belitsky *et al.*, 2000; Belitsky and Sonenshein, 2004). Years later, the mode of inactivation was still under debate and two distinct models were presented: An *in vitro* model showed the *gltAB* gene expression to be dependent on the different binding properties of GltC to the *gltAB* promoter in the absence and presence of glutamate (Picossi *et al.*, 2007). A second *in vivo* model showed the repression mechanism being mediated by RocG or GudB inactivating GltC by direct binding in the presence of glutamate (Herzberg *et al.*, 2007; Stanek *et al.*, 2015b). In this study (Ch. 3.4.1), a model combining those two ideas to one consistent model was shown. In minimal medium (CSER-Glc) containing glucose, ammonium, glutamate, and arginine many regulatory mechanisms are present. The presence of ammonium and

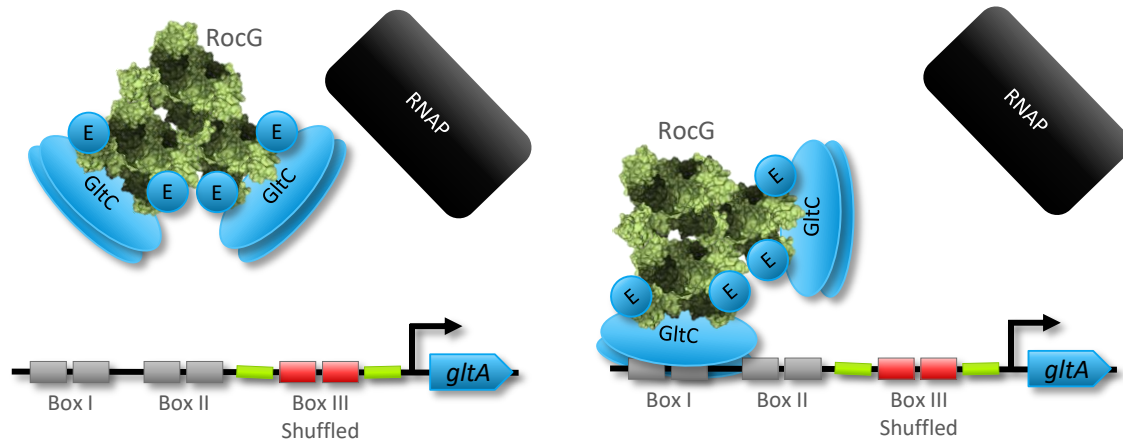
A Activation of *gltAB* gene expression



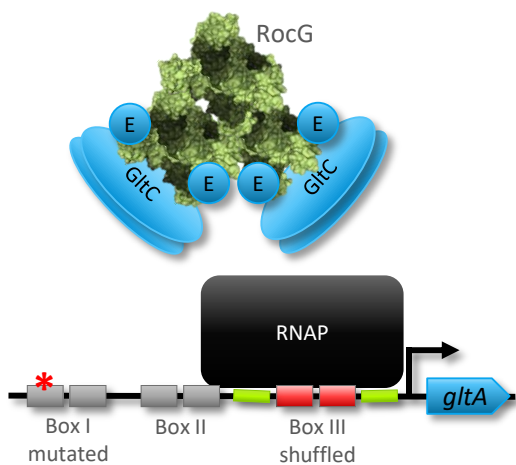
B Repression of *gltAB* gene expression



C Models for shuffled binding box III



D Identification of complex position in shuffled box III promoters



E Model for basic repression in the absence of RocG

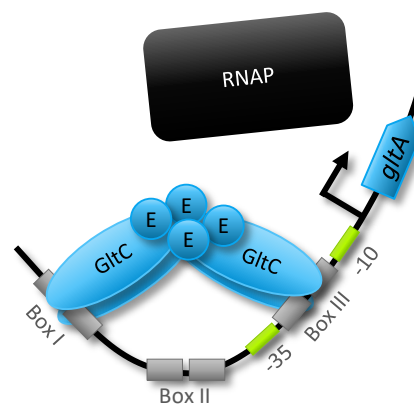


Fig. 4.1 Overview of the different regulation states at the *gltAB* promoter

A: Activation of the *gltAB* gene expression in the presence of α -ketoglutarate by binding of GltC to box I and II. **B:** Repression of the *gltAB* gene expression in the presence of glutamate by binding of the RocG-GltC complex to box I and III. **C:** Two models for the state at the *gltAB* promoter harboring a shuffled box III. Either the shuffled box III prevents complete binding of the glutamate mediated RocG-GltC complex to the promoter region or it binds only to the box I. **D:** Model for a possible experiment explaining the situation at the promoter containing the shuffled box III. **E:** Model for basic repression in the absence of RocG, when only GltC binds to box I and III in the presence of glutamate.

glutamate does not lead to nitrogen limiting conditions, therefore a TnrA is bound by the FBI-GS and cannot repress *gltAB* gene expression (Belitsky *et al.*, 2000; Gunka and Commichau, 2012). Further details for this are shown in Ch. 3.3.2.1. Albeit a TnrA-dependent repression of the *gltAB* genes in the presence of GltR24 was shown (Belitsky *et al.*, 2000), neither a TnrA-dependent nor a RocG-dependent repression could be observed in CSER-Glc medium in the presence of GltR24 in this work (Fig. 3.19). In conclusion, TnrA is not active in CSER-Glc medium.

However, the expression of the *rocG* gene is strongly induced in the presence of arginine via the transcriptional activators RocR and AhrC as well as the σ^t -equipped RNAP (Gunka and Commichau, 2012). In CSER-Glc medium the presence of arginine overbalances the CcpA-mediated repression of the *rocG* gene, which was shown as the 3.5-fold shift of the RocG/GltC ratio from 1.7 to 8 was sufficient to stop *gltAB* gene expression in the WT (see also WT in Fig. 3.23) (Commichau *et al.*, 2007a).

To verify the novel combined model for the regulation of *gltAB* gene expression, promoter-up mutations were used. These promoter variants of the *gltAB* genes are partially independent of GltC, meaning in the absence of GltC they were constitutively active and in the presence of GltC the promoter activity even increased. Regarding the model found *in vivo*, it was expected to detect *gltAB* gene expression in the presence of RocG, because RocG was shown to inhibit *gltAB* gene expression by binding to GltC and thereby preventing GltC from binding to the promoter and activating the transcription. However, there was no activity of the *gltAB* promoter variants detectable (Fig. 3.23), indicating an intact interaction of GltC and the promoter. This leads to the new combined model of *gltAB* gene regulation: glutamate supports the

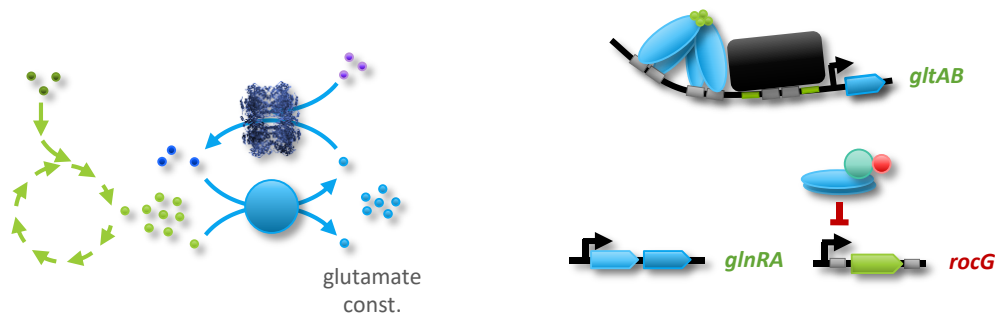
binding of GltC to RocG, which results in a conformational change of the present GltC complex allowing the binding to box I and III instead of box I and II. The GDH-GltC complex blocks the promoter region and prevents the RNAP from binding (Fig. 4.1 and Fig. 4.2).

4.2.3. The interplay of box III and RocG to ensure *gltAB* gene regulation

The GltC binding boxes I, II and III were identified simultaneously and the binding boxes I and II were quickly identified to be important for the expression of the *gltAB* genes (Belitsky *et al.*, 1995). However, the concrete role of the box III remained elusive until 2007, when *in vitro* studies showed its importance in the GltC-glutamate-mediated repression. Most point mutations within box III did not lead to an interesting phenotype as they were investigated under activating conditions (Belitsky *et al.*, 1995). Only the T-28A mutation was found in box III that increased the *gltAB* gene expression under activating conditions (Belitsky *et al.*, 1995). To test whether the mutant harbors a defective box III that might prevent the binding of the RocG-GltC complex, it was investigated in more detail. The increase of expression under activating conditions was reconstituted for the T-28A mutant, but apparently the binding of the GDH-GltC complex to box I and III was not disturbed, because in the presence of arginine no *gltAB* gene expression was detected (Fig. 3.25).

To find a box III variant that prevents binding from GltC, the entire box III sequence was shuffled. The shuffled box III variant I is most interesting, as no complete repression in the presence of arginine could be achieved (Fig. 3.26). However, the expression is still dependent on the presence and absence of RocG, GltC and arginine (Fig. 3.26). Unfortunately, the experimental setup used in this study does not reveal the mechanism why the RocG-GltC

A WT in CSE-Glc: + Glc + NH₄⁺ + glutamate



B WT in CSER-Glc: + Glc + NH₄⁺ + glutamate + arginine

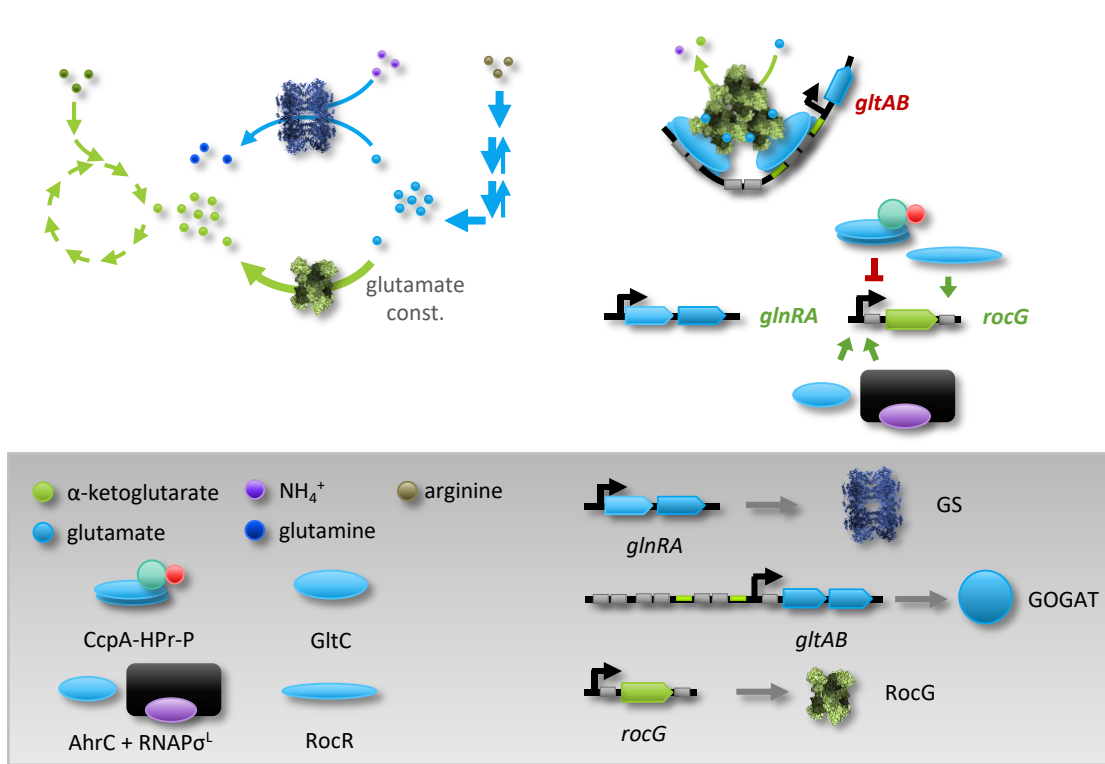


Fig. 4.2 Regulation of the metabolite flux in *B. subtilis*

A legend is displayed in gray at the end of the figure. **A:** *B. subtilis* WT grown in CSE-Glc medium containing glucose, ammonium, and glutamate as carbon and nitrogen sources, respectively. The *rocG* gene expression is repressed by CcpA, whereas the *gltAB* and the *glnRA* genes are expressed. This results in an intact GS-GOGAT cycle synthesizing glutamate. **B:** *B. subtilis* WT grown in CSER-Glc medium containing glucose, ammonium, glutamate, and arginine as carbon and nitrogen sources, respectively. In this situation, the expression of the *gltAB* genes is repressed by the presence of RocG and the *rocG* gene expression is induced by AhrC, RocR and σ^l-RNAP reducing the repressing effect of CcpA mediated CCR. Arginine is degraded via GS and RocG leading to the production of glutamine and α-ketoglutarate. Red gene: repressed, green gene: expressed.

complex cannot completely repress the *gltAB* gene expression in presence of the box III variant I. One possible solution is in line with the regulation model based on *in vivo* data (Commichau *et al.*, 2007a), where the RocG-GltC complex does not bind to the promoter region at all (Fig. 4.1 C). The other explanation would be a partial binding solely to box I (Fig. 4.1 C), might resulting in a competitive situation with

unbound GltC or simply interfering with the binding of the RNAP as the shuffle I promoter is also partially independent of GltC. To reveal the true situation, the shuffle I promoter could be combined with a box I mutation as T(-70)C or ΔT(-64), which are known to repress GltC-mediated *gltAB* gene expression (Belitsky *et al.*, 1995). Hence, in a Δ*gltC* mutant harboring the combined promoter variant *gltAB* gene

expression is still possible, because it is known that the shuffle I promoter is partially independent of GltC. In the WT harboring the combined promoter variant, *gltAB* gene expression in the absence of arginine should be comparable to the Δ *gltC* mutant, because an intact box I is required for GltC-mediated activation of the *gltAB* gene expression. In the presence of arginine, RocG is present in the cell and binds GltC. However, this should not alter the *gltAB* gene expression in cells harboring the combined promoter variant. The combination of a box I mutation and the shuffle I promoter variant is most likely completely independent of GltC, as it cannot bind to box I or box III. Nevertheless, such an experiment was not implemented yet and whether this theoretical outcome is correct remains elusive.

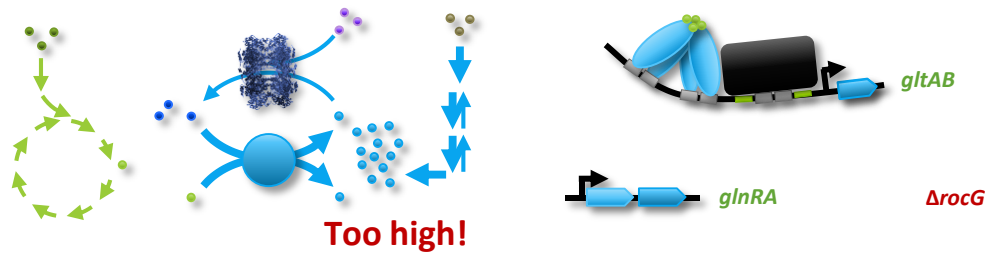
Besides the RocG dependent repression of the *gltAB* gene expression, there must be a RocG independent repression taking place in the absence of RocG. This repression is observed in all Δ *rocG* strains carrying either the WT promoter or one of the other investigated promoter variants (Fig. 3.23, Fig. 3.25 and Fig. 3.26). As previously mentioned, a Δ *rocG* mutant suffers on medium containing arginine, possibly due to toxic effects from accumulating intermediates of the arginine degradation pathway (Fig. 4.3). Additionally, the expression of the *gltAB* genes is not prevented. The resulting GOGAT synthesizes even more glutamate within the cell. It was previously suggested that α -ketoglutarate and glutamate bind in a competitive manner to GltC, albeit the presence of glutamate induces the formation of a GltC complex with glutamate that binds to box I and III *in vitro* (Picossi *et al.*, 2007). The high level of glutamate in a Δ *rocG* mutant might be sufficient to form such a complex of GltC with glutamate *in vivo* (Fig. 4.1 E). Additionally, glutamate was shown to further destabilize the open complex formation of the

gltAB promoter, as it does for open complexes of other promoters in *B. subtilis* (Picossi *et al.*, 2007). Hence, the RocG-independent regulation, is most likely solely mediated by the co-factor glutamate, albeit this mode of repression is much weaker compared to the RocG-mediated repression. A complex of only GltC and glutamate must span the long distance between box I and box III and bend the DNA, as previously suggested *in vitro* (Picossi *et al.*, 2007). This results in a certain tension which putatively destabilizes the complex resulting in less efficient repression of the *gltAB* genes compared to the RocG-mediated repression. Moreover, the RNAP and GltC could competitively bind to the DNA region of the promoter and box III, resulting in a decreased but not completely inactivated expression of the *gltAB* genes.

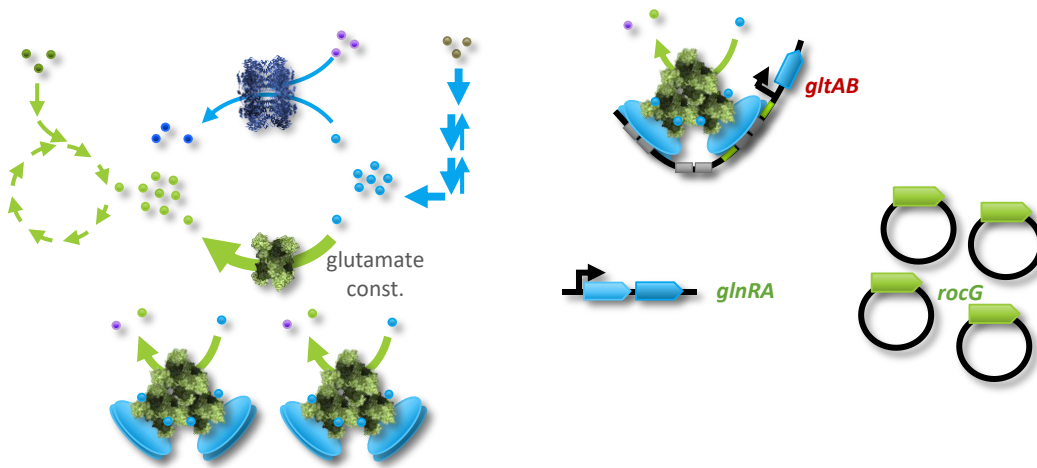
4.2.4. The high impact of co-factors

The co-factors α -ketoglutarate and glutamate substantially contribute to the regulation of the *gltAB* gene expression. This was demonstrated by the constitutive expression of plasmid based *rocG* gene creating an artificial situation for the cells growing on CSE-Glc medium. Normally, on medium with glucose, ammonium, and arginine, the *gltAB* genes are expressed because the *rocG* gene expression is repressed by CcpA. In the artificial situation RocG was present in high amounts, but contradictory an even increased level of *gltAB* promoter was detected (Fig. 3.27). The lack of RocG-mediated repression of the *gltAB* genes can be explained by the presence of co-factors. Glutamate was intensively degraded by RocG, most likely resulting in low levels of glutamate and increased levels of α -ketoglutarate (Fig. 4.3). Under these conditions, the competitive co-factor binding site for GltC is occupied with α -ketoglutarate (Picossi *et al.*, 2007). This is corroborated, by nearly wild type like *gltAB* gene expression levels in CSE-Glc

A $\Delta rocG$ in CSER-Glc: + Glc + NH_4^+ + glutamate + arginine



B *rocG* high in CSER-Glc: + Glc + NH_4^+ + glutamate + arginine



C *rocG* high in CSE-Glc: + Glc + NH_4^+ + glutamate

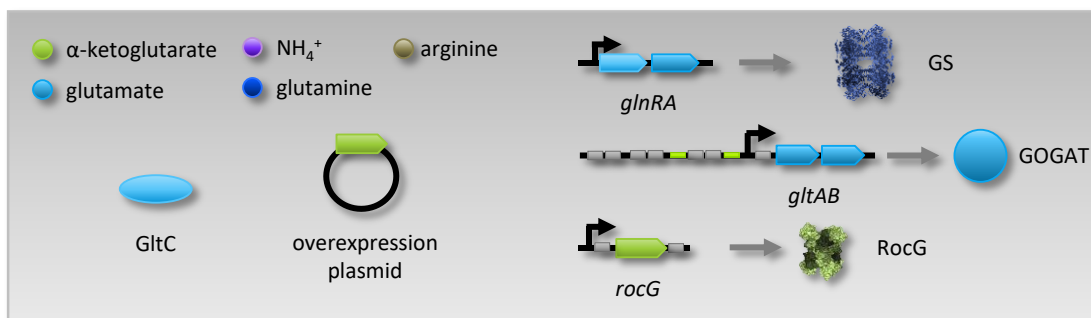
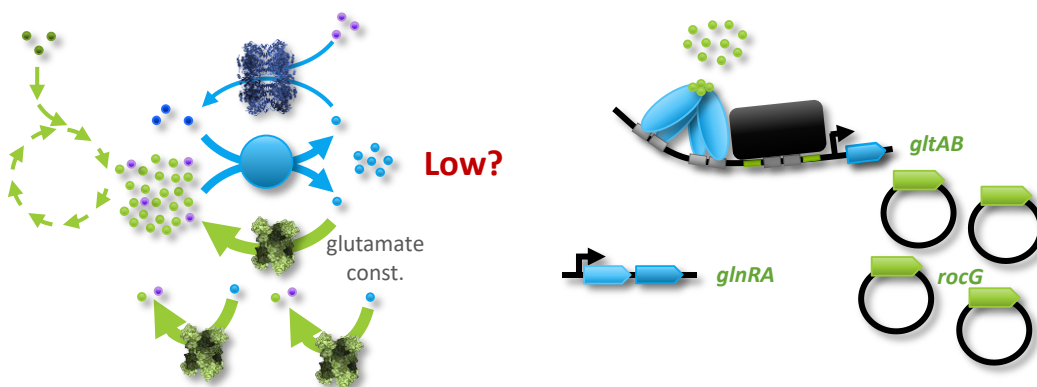


Fig. 4.3 Metabolic fluxes of metabolites in *B. subtilis* encountering artificial situations
 A legend is displayed in gray at the end of the figure. A: *B. subtilis* $\Delta rocG$ grown in CSER-Glc medium containing glucose, ammonium, glutamate and arginine as carbon and nitrogen sources, respectively. RocG cannot repress the *gltAB* gene expression. This results in

an intact GS-GOGAT cycle synthesizing glutamate additionally to the glutamate derived from the arginine degradation pathway. B: *B. subtilis* WT containing *rocG* overexpression plasmids grown in CSE-Glc medium containing glucose, ammonium, glutamate, and arginine as carbon and nitrogen sources, respectively. In this situation, the expression of the *gltAB* genes is repressed by the presence of RocG. Arginine is degraded via GS and RocG leading to the production of glutamine and α -ketoglutarate. C: *B. subtilis* WT containing *rocG* overexpression plasmids grown in CSE-Glc medium containing glucose, ammonium, and glutamate as carbon and nitrogen sources, respectively. In this situation, the expression of the *gltAB* genes is induced though RocG is present. RocG continuously degrades glutamate, even though no arginine is present to increase the level of glutamate. This might lead to a very low pool of glutamate and a high pool of α -ketoglutarate inducing the expression of the *gltAB* genes. Red gene: repressed, green gene: expressed.

medium in the presence of GudB (Fig. 3.27). In contrast to RocG, GudB was shown to be regulated on the protein level and a low glutamate concentration in CSE-Glc medium might decrease the stability of the GudB hexamer leading to dissociation and metabolically inactive GudB monomers (Noda-Garcia *et al.*, 2017). The situation in cells carrying the plasmid based *gudB* gene is not that different from the native situation with a chromosomal based *gudB* gene, because both are constitutively expressed. In general, in CSE-Glc medium only low enzymatic activity of GudB is detectable as the *gltAB* genes are only slightly repressed compared to the empty vector control, but no such increase as observed for the overexpressed *rocG* gene was detected (Fig. 3.27). Interestingly, in the presence of arginine, high levels of RocG or GudB did not lead to a detrimental situation for *B. subtilis* (Fig. 4.3 B). Arginine seems to buffer the fast degradation of the co-factor glutamate, resulting in a nearly abolished *gltAB* gene expression.

4.2.5. The importance of untagged proteins

All enzymes used in this work were shown to lose functions due to protein fusion to a tag. The group of Noda-Garcia *et al.*, used for their experiments N-terminal Strep-tagged RocG and GudB variants, though they stated the N-terminus not being involved in the metabolic reactions of RocG and GudB it is questionable whether an impact of this tag on hexamer stability can be excluded (Noda-Garcia *et al.*, 2017). *In vivo* an N-terminal tag is deleterious for

B. subtilis, because it prevents the interaction with GltC (Commichau *et al.*, 2007a).

Working with tag-free proteins is also important for GltC, because in a *B. subtilis* strain harboring a GltC with a C-terminal His₆-tag the *gltAB* gene expression was less reduced upon the addition of ornithine to the medium compared to the WT (Picossi *et al.*, 2007). Whereas an N-terminal His₆-tag inactivated the GltC protein and led *in vivo* to a *B. subtilis* strain auxotroph for glutamate (Picossi *et al.*, 2007). Which makes perfectly sense, because the HTH domain important for DNA binding is present at the N-terminus in LysR-type regulators as GltC. In contrast, the C-terminus seems to be important for interaction with RocG or GudB. Interestingly, an overproduced C-terminal Strep-tagged GltC was used to co-purify RocG, indicating an intact interaction between GltC and RocG. The alteration of the C-terminus with a Strep-tag does not impact the interaction between GltC and RocG (Commichau, 2006; Commichau *et al.*, 2007a). Additionally, only a moderate reduction of *gltAB* gene expression could be observed for overproduced GltC-Strep compared to overproduced native GltC in CSE-Glc, whereas no difference was observed in CSER-Glc. Both the Strep- (WSHPQFEK) and the His₆-tag (HHHHHH) are small protein-tags, but either the Strep-tag interferes less severely with the RocG-GltC interaction or the amount of tagged protein (overexpressed vs single genomic copy) leads to the differences in *gltAB* gene expression. However, this clearly indicates an impact of tags on the function of GltC, RocG and GudB.

In this work, it was tried to fish RocG *in vitro* using entirely tag-free versions of RocG and GltC and biotinylated DNA fragments harboring the promoter region of the *gltAB* genes. However, this was not possible as the complex of RocG and GltC is of highly transient nature depending strongly on the availability of glutamate, which is important for the cell to fast react to changing glutamate levels. Though it is assumed, it is not shown, whether the GDHs are metabolically active when they are present in complex with GltC and the DNA. The use of super repressor variants of RocG could support this experiment. Comparable to a strain entirely lacking RocG, the super repressor variants of RocG cannot grow on arginine as sole carbon source anymore, as they have lost their catabolic activity due to mutations within the active center of the GDH (Gunka *et al.*, 2010). However, in the absence of glutamate, there is activity of the *gltAB* promoter detectable. Hence, in the presence of glutamate the super repressor variants of RocG might be stucked to GltC (Gunka, 2010) comparable to the state of an feedback inhibited GS (Ch. 1.3.1). The super repressor variants of RocG used in the *in vitro* fishing experiment would not alter the glutamate pool, but could show *in vitro*, whether a complex of RocG and GltC can bind to the DNA. Furthermore, it would be interesting to investigate whether the effect of the super repressor variants of RocG can be reversed *in vivo* by a decrease of the glutamate pool. Therefore, an inducible promoter in front of the *ansAB* operon could be used. It was shown that overexpression of the aspartase AnsB allows the utilization of glutamate as carbon source (Flórez *et al.*, 2011). In theory, the resulting decrease of the glutamate concentration should release the binding of the super repressor variant of RocG to GltC allowing the expression of the *gltAB* genes *in vivo*.

4.3. Two GDHs, one GltC, two evolutionary routes?

4.3.1. Different regulation of GltC variants via RocG and GudB

In a recent study, a promoter-enzyme co-evolution was suggested for RocG and GudB, but this study did not consider that both GDHs have a moonlighting function in binding to GltC (Noda-Garcia *et al.*, 2017). Therefore, different GltC variants and their regulation by RocG and GudB were investigated. The GltC variants were isolated in a screen for suppressor mutants compensating for mutations inactivating box II (Belitsky and Sonenshein, 1995). The box II mutations were T-48C and T-48A, of which T-48C was also investigated in this study and shown to cause complete loss of *gltAB* gene expression independent of RocG or GudB and independent of the present co-factors (Fig. 3.25). The GltC variants I160K and T99A were isolated compensating for the T-48C promoter variant and the GltC variant P88L was isolated compensating for the T-48A promoter variant (Belitsky and Sonenshein, 1995). Though they were all isolated as suppressor mutants compensating for the loss of box II, none of them compensated only for a specific mutation within the boxes I or II of the *gltA* promoter. A general slight reduction of the *gltAB* gene expression in the presence of proline compared to the native GltC was observed (Belitsky and Sonenshein, 1995). It is known that overexpressed GltC can be completely inhibited by the native RocG, but the activity of an overexpressed T99A variant of GltC could not be completely inhibited by the native RocG. However, it was possible, to co-purify low levels of RocG using the overexpressed T99A variant of GltC (Commichau *et al.*, 2007a). This low level of interaction between RocG and the T99A variant of GltC in comparison to the native GltC was reflected by the slightly decreased level

of *gltAB* promoter activity (Fig. 3.28). Interestingly, the low interaction completely abolished in presence of the other GDH GudB (Fig. 3.28). This was also the case for the GltC variant P88L also harboring the mutation quite close to the dimerization site of GltC. However, the GltC variant I160K was still inhibited by GudB but not by RocG. It seems that there are two different interaction sites between RocG-GltC and GudB-GltC present. However, GudB and RocG share 74 % of amino acid sequence identity indicating that 26 % of the proteins differ from each other (Belitsky and Sonenshein, 1998). Imagining, there is only one general GDH interaction surface present, it cannot be excluded that the differences in *gltAB* expression result from a conformational change of GltC altering the general structure of GltC around the interaction surface and allowing only, for instance, the smaller GDH to access. Moreover, the different regulation of the GltC variants by either RocG or GudB can also be explained by the complex formation of GltC monomers. All mutations are close to or even in between GltC dimerization sites (Fig. 3.28), so they may enhance or strengthen the formation of dimers or tetramers (Belitsky and Sonenshein, 1995). Presumably, RocG and GudB have different potential to break existing GltC dimeric or tetrameric structures bound to the DNA. Moreover, the DNA binding ability could be enhanced in the GltC variants. Albeit, this is less likely as the mutations are not within the helix-turn-helix motif, which is important for DNA binding (Fig. 3.28).

In any case further GltC variants must be investigated to unravel the real reason for the different regulation of the GltC variants via RocG and GudB, as the presence of two different interaction sites for RocG and GudB would change the view of their evolution. To achieve this, a GltC mutant library derived from a random

mutagenesis approach could be transformed into *B. subtilis* strains harboring similar amounts of either RocG or GudB under conditions where both GDHs are active. Besides the immense number of GltC variants to be investigated simultaneously, this approach lead to the advantage of having comparable amounts of the different GltC variants present in the cell. The GltC variants used in this study were shown to differently autoregulate their expression, leading to different GltC levels within the cell (Belitsky and Sonenshein, 1995). As a result, the *gltAB* gene expression levels between the different GltC variants are not comparable as the amount of enzyme is not known. However, the different impacts of RocG and GudB are definitively there, because exclusively the presence of either RocG or GudB led to different *gltAB* gene expression levels.

4.3.2. The physiological aspect of GltC regulation via RocG and GudB

The overall aim of the moonlighting function of RocG and GltC is to bind and inhibit the GltC activity. Assuming there are different interaction surfaces for RocG-GltC and GudB-GltC, what is the advantage of this for the cell? In nature, different interaction sites are present to avoid competitive binding of two co-factors or two proteins, and to allow simultaneous regulation. It is unlikely that binding of two different GDHs to GltC results in an additive effect, because once GltC is inhibited it cannot be more inhibited. Maybe, the different interaction sites are required to allow regulation under different conditions. *In vitro* studies showed that GDHs need to be present in their hexameric form to be metabolically active, however it is not known whether already monomers or only hexamers can bind to and inhibit GltC (Noda-Garcia *et al.*, 2017). When GudB is continuously present in the cell in its monomeric form and fulfills its

regulatory function, GltC would be continuously inhibited. An alternative binding site that only allows binding under specific conditions might help to avoid the continuous inhibition of GltC. However, as the interaction between a GDH and GltC requires a certain level of glutamate to be present in the cell, these levels are most likely also sufficient for GudB to form hexamers (Picossi *et al.*, 2007; Stannek *et al.*, 2015b).

Another very speculative idea supporting the presence of two different interaction sites is the following: RocG and GudB were shown to interact *in vivo* in the native context via SPINE and in a heterologous system via a bacterial-two-hybrid experiment based in *E. coli* (Stannek *et al.*, 2015b). Assuming, resulting hetero hexamers exist in *B. subtilis in vivo*, the symmetry and orientation of the GltC interaction sites within the hetero hexameric GDHs might be altered. Either this does not allow the formation of a complex with GltC or the resulting complex exhibits an altered conformation preventing the regulatory binding to the *gltAB* promoter compared to the highly balanced complex consisting of native homo hexameric GDHs and GltC that spans exactly the distance between box I and box III of the *gltAB* promoter. However, the result is when high amounts of RocG and GltC are present in the cell forming hetero hexamers, the activity of GltC is not properly inhibited. Albeit this results in a vicious cycle of glutamate biosynthesis and degradation, GltC could counteract the enormous degradation of glutamate and thereby preventing the glutamate pool from depletion.

Certainly, it is also possible that due to the differences between RocG and GudB only different interaction sites of RocG-GltC and GudB-GltC allow the binding of GltC in a heterologous hexamer of RocG and GudB.

To investigate the general problem whether monomers or intact hexamers are required for GltC regulation, super repressor and monofunctional versions of RocG, only able to repress GltC or to degrade glutamate, respectively, could be investigated regarding their ability to form hexamers (Gunka *et al.*, 2010). It would be interesting to see whether monofunctional RocG variants have acquired the ability to degrade glutamate without the formation of an intact hexamer or whether they simply lost their ability to interact with GltC.

4.3.3. The evolutionary aspect of GltC regulation via RocG and GudB

The divergence and convergence of functions are central tools for evolution. Accordingly, the different promoters, enzyme properties, and putative different interaction sites for GltC could result from the divergence of a common ancestor. However, in turn could the common ancestor also be lacking the moonlighting function and this property was developed later in RocG and GudB in a convergent manner, explaining the presence of putative different interaction sites. The question of the evolutionary origin of the RocG and GudB GDHs remains elusive. However, how important is the regulatory function in comparison to the metabolic function of the GDH?

4.3.3.1. The importance of glutamate synthesis regulation

It was observed that the *E. coli* the GDH GdhA is not able to trigger the repressor function of GltC at all (Fig. 3.27). In *E. coli*, the *gltBD* genes encoding for the GOGAT are regulated by many global and local TFs (van Heeswijk *et al.*, 2013). Some of these TF are also involved in the regulation of the genes encoding for the GS and the GDH in *E. coli* (van Heeswijk *et al.*, 2013). A vicious cycle of simultaneous glutamate

biosynthesis and degradation is not observed until now. This might be because the GDH in *E. coli* is anabolically active. However, under conditions favoring the anabolic reaction of the GDH, still 85 % of ammonium assimilation and glutamate synthesis occurs via the energetically unfavorable GS-GOGAT cycle (Yuan *et al.*, 2006; van Heeswijk *et al.*, 2013). However, there are first hints showing that GdhA is also catabolically active under high levels of glutamate (van Heeswijk *et al.*, 2013). Maybe the GdhA lost its catabolic activity, because the prevention of the emergence of a vicious cycle is more important for the cell than the advantage of having a catabolically active GDH. Especially, because the GDH is not needed in *E. coli* for arginine degradation. Arginine catabolism is mediated by the *astCADBE* operon encoding for enzymes of the AST pathway that degrades arginine to succinate and glutamate and thereby generates ammonium serving as nitrogen source for the cell (Schneider *et al.*, 1998).

In *Rhizobium etli*, which lives in a mutually beneficial relationship with legumes, the nitrogen assimilation is of such high importance that a GDH is entirely missing (Bravo and Mora, 1988). *R. etli* lives in nodules of legumes, fixes atmospheric nitrogen, and ensures a proper organic nitrogen supply for the plant, which in turn supplies the bacterium with nutrients. *R. etli* relies solely on the GS-GOGAT cycle for nitrogen fixation (Bravo and Mora, 1988; Castillo *et al.*, 2000). The heterologous expression of the *E. coli* derived GdhA leads to a strong negative effect in symbiosis, as no or only ineffective nodules are formed (Mendoza *et al.*, 1998). This is a very special situation, but shows nicely that GDH has a crucial impact on the nitrogen metabolism.

Moreover, in *B. subtilis* the regulatory function of the GDHs seems to be more important compared to their metabolic function. When the *B. subtilis* strain 168, that harbors an inactivated *gudB^{CR}*

gene, is additionally deficient of the *rocG* gene and is streaked on SP medium containing high levels of glutamate and arginine, rapidly *gudB⁺* suppressor mutants emerged compensating for the loss of the *rocG* gene (Ch. 1.3.3 and 1.4). However, this was not observed in a *B. subtilis* strain deficient of the *rocG* and the *gltC* gene. In a *rocG* deficient *B. subtilis* strain high levels of glutamate accumulate, which presumably lead to detrimental conditions for the cell. The additional loss of the *gltC* gene might partly compensate for the loss of the *rocG* gene, as no additional glutamate can be synthesized in the absence of the GOGAT. Interestingly, the SP medium does not contain glucose and the use of secondary carbon sources is important for the survival of the cell. Another GDH making glutamate accessible as carbon source would be beneficial for the cell, however *gudB⁺* suppressor mutants do not emerge. This observation might be a first hint for the importance of the regulatory function of RocG & GudB in inhibiting GltC compared to their actual metabolic function. Corroborating this assumption, a study searching of monofunctional and super repressor variants of RocG, only one monofunctional exclusively metabolically active variant was found in contrast to ten GltC super repressor variants (Gunka *et al.*, 2010).

In all examples presented here, the metabolic function either anabolic or catabolic is not as important as it is to precisely control the activity of the GOGAT. The GDH is in some cases a means to an end. It might be important under specific nutrient conditions, but it solely enables the use of secondary carbon sources.

4.3.3.2. Evolution of moonlighting proteins

The metabolically active site consists in most cases only of a few relevant residues though many proteins have sizes between 30 and 50 kDa (Srere, 1984). So why are proteins so big? This

question was already discussed in a paper from 1984 and many ideas were presented. For instance, the size could serve as scaffold, for localization or to ensure proper protein-protein interactions (Srere, 1984). However, in large scale proteomics many proteins were found exhibiting post translational modifications (PTMs) for an unknown reason (Jeffery, 2016). PTMs can switch the function of an enzyme and taken together, this could indicate an enormous number of proteins having moonlighting function yet undiscovered (Jeffery, 2016). Of course, many moonlighting enzymes were found to have homologs. However, the moonlighting function is not always maintained (Jeffery, 2016). For instance, in duck eyes there are the delta 1 and delta 2 homologs of crystallins present. Though they only differ in 27 aa, exclusively the delta 2 crystallin has an arginosuccinate lyase function (Chiou *et al.*, 1991).

As expected two redundant enzymes are evolutionary instable, but in *B. subtilis* they are stable for some reason. As recently reported, the GDHs underwent a promoter-enzyme co-evolution: The *gudB* gene is continuously expressed and the resulting GudB is regulated, whereas the *rocG* gene is highly regulated and the resulting RocG is stably active (Noda-Garcia *et al.*, 2017). In this study, the function of RocG and GudB as moonlighting enzymes are neglected. But as both GDHs can inhibit GltC there must be also a co-evolution of the interaction sites of RocG-GltC and GudB-GltC.

The co-evolution of regulatory functions is extensively studied for two-component systems and phosphorelay systems (Salazar and Laub, 2015). Two-component systems consist of a histidine kinase recognizing a signal and subsequently phosphorylating a response regulator that in turn regulates gene expression. One essential aspect in the evolution of novel two-component systems is that the connection

between a histidine kinase and its response regulator must be stable and must not interfere with the novel system. To prevent interconnections between novel and existing two-component systems, duplicated histidine kinases and response regulators only arise under non-selective conditions and diverge fast to eliminate cross-talk between the systems (Capra *et al.*, 2012). In two-component systems the recognition site consists only of four residues and it was shown that these residues could be exchanged with those of another two-component system resulting in accurate recognition *in vitro* (Podgornaia *et al.*, 2013). Investigating the interaction surfaces of RocG-GltC and GudB-GltC the binding sites might be also exchangeable. Another explanation for functional evolution of interaction surfaces was investigated in toxin-antitoxin systems where the toxin-antitoxin system was also shown to co-evolve without ever disrupting their interaction (Aakre *et al.*, 2015), which would be detrimental for the cell. In the toxin-antitoxin system promiscuous enzymes with broadened substrate specificity served as mutational intermediates to allow specific mutations in the opposite gene and subsequent adaptive mutations that restrict substrate specificity (Aakre *et al.*, 2015). This might also be the case for the evolution of the GDHs, as the loss of GltC regulation might be detrimental for the cell. The general problem in continuously maintaining the connection between two proteins is the reduction of possible mutations allowing the general evolution of the system.

One model describing the evolution of enzymes in general is the innovation-amplification-divergence (IAD) model (Näsvall *et al.*, 2012). In the innovation state of the IAD model an enzyme acquires a weak secondary function and subsequently its copy number is increased via duplication and amplification, which is the major

source of novel proteins (Andersson and Hughes, 2009; Näsvall *et al.*, 2012). One study in 1985 even suggested that *B. subtilis* will do gene amplification whenever it is possible (Jannièrè *et al.*, 1985) and for *Salmonella typhimurium* it was estimated that 10 % of all cells growing in non-selective medium contain a gene duplication somewhere in their genome (Roth *et al.*, 1996; Andersson and Hughes, 2009). During the divergence state, beneficial mutations accumulate and finally copies of non-beneficial enzyme versions are lost during segregation. The final outcome is either a novel generalist having its original and the novel secondary function or two specialized enzymes (Näsvall *et al.*, 2012).

In conclusion, there is a promoter-enzyme co-evolution for RocG and GudB and simultaneously a co-evolution of the interaction sites of RocG-GltC and GudB-GltC. Regarding, all these evolutionary aspects the successful co-evolution of enzymes, promoters, and interaction sites appears to be a miracle. But what if this evolution could only take place because these proteins are so highly interconnected?

4.3.3.3. The hypothetical evolution of GudB and RocG

Similar as the paradigm one gene, one protein, one function from Garrod, Beadle and Tatum is not state of the art anymore, it might be time to reevaluate Darwins paradigm of survival of the fittest (Darwin, 1859; Garrod, 1923; Beadle and Tatum, 1941). In a recent review, the evolution of moonlighting proteins was discussed (Fares, 2014). It is postulated that genetical robustness is the key for evolution. In harsh contrast to the general term that redundancy is genetically instable, redundancy might support evolution. Moreover, genetical robustness can be achieved by the accumulation of different silent mutations within a bacterial community, because these mutations increase the genetic variability and

might be precursors for different novel phenotypes (Fares, 2014). As a result, a genetically diverse bacterial culture might faster react to challenging conditions, because the genetical repertoire and the concomitant possibilities for novel functions will increase the statistical chance of a beneficial mutation to occur. Evolution is not a single step method that either fails or wins. It is a gradual process of many small steps (Fares, 2014).

Hypothetically, the ancestor GDH of RocG and GudB acquired the ability to weakly inhibit GltC. This leads to a growth advantage in the presence of glutamate. According to the IAD model the respective gene of the ancestor GDH duplicated or even amplified. Along with the growth advantage occurred the problem that the ancestor GDH was a very stable enzyme encoded by a constitutively expressed gene. The presence of several enzymes with overlapping functions enabled the fast and complex promoter-enzyme co-evolution, because once one enzyme weakened the connection to GltC the other GDH could buffer that loss. Silent mutations might contribute to gradual stepwise evolution of a highly regulated promoter or a protein that is only stable under certain conditions. Of course, this evolution does not exclude the emergence of better or different binding sites of RocG-GltC or GudB-GltC. For sure, the buffering effect and the acceptance of silent mutations contributed to a fast evolution as they allowed many more possibilities leading to improved binding sites for GltC and the respective GDH (Podgornaia and Laub, 2015).

This shows how restricted our view of nature is and that there are always possibilities we do not consider because of our self-made paradigms. A first step is to erase fixed paradigms from our memory, regard them as general rules and to broaden our point of view.

4.4. TR mutagenesis, several machineries?

During evolution, the *rocG* gene was lost in *Bacillus altitudinis*, *Bacillus safensis*, and *Bacillus tequilensis* (Noda-Garcia *et al.*, 2017). In *B. subtilis* 168 the *rocG* gene is present, but the *gudB* gene is inactivated with a TR (Ch. 1.4). Why is the *gudB* gene not lost? In the previous chapters the advantages of having two functional GDHs were discussed, but in the *B. subtilis* 168 a constitutively expressed gene leading to a rapidly degraded, non-functional GDH is stably inherited (Stannek *et al.*, 2015a). This procedure is not economical for the cell, but there must be some advantage of keeping the *gudB^{CR}* gene. In a *rocG* deficient strain rapidly suppressor mutants emerge on selective medium that have activated the *gudB^{CR}* gene by a precise excision of the first TR unit (Ch. 1.4) (Gunka *et al.*, 2012). Due to the high frequency accumulation of *gudB⁺* suppressor mutants, a mutation machinery favoring TR mutations is expected to exist. TRs are known to be mutational hot spots in all organisms, because they can easily recombine (Bichara *et al.*, 2006; Vences *et al.*, 2009; Zhou *et al.*, 2014).

In this work, the machinery of the TR mutagenesis was investigated. Ectopically introduced constructs having the TR either intragenic as the native *gudB^{CR}* gene or having the TR intergenic within the spacer region of the promoter were used to investigate the TR mutagenesis of the *gudB^{CR}* gene. An intergenic TR encounters only the replication machinery, whereas an intragenic TR encounters both, the replication and transcription machinery. In the ectopic locus, orientation of the *gudB* gene was changed, leading to a head-on collision of the transcription and replication machineries instead of a co-directional collision as it happens at the native *gudB^{CR}* locus (Fig. 3.5). The importance of

this becomes obvious when investigating different factors putatively involved in TR mutagenesis in the native and the ectopic locus. For instance, the lack of RNase HIII encoded by the *rnhC* gene, led to an increased amount of emerging SMs for intragenic TR encountering head-on collisions but not for intragenic TR encountering co-directional collisions (Fig. 3.6 and Fig. 3.7). However, there are also factors as the RecA loading proteins RecO and RecR, that substantially contribute to the TR mutagenesis of intragenic TR encountering either head-on or co-directional conflicts, as in their absence a general decrease of SMs was observed.

This observation, was a hint for different mutation machineries being involved in the intra- and intergenic TR mutagenesis upon head-on or co-directional collisions. It was found that the mutation frequency depends on several factors, as the location of the TR as well as the orientation and the temperature (Ch. 3.1). Intergenic TR exhibit in general a low mutation frequency, whereas intragenic TR exhibit in general a high mutation frequency, which is apparently coupled to transcription (Fig. 3.2, Fig. 3.3). A dependence of promoter strength and mutation rate was shown in various examples for somatic hypermutation (Fukita *et al.*, 1998; Bachl *et al.*, 2001; Yoshikawa *et al.*, 2002) and for single base pair substitutions leading to premature stop codons in *E. coli* (Schmidt *et al.*, 2006). Moreover, this is in perfect agreement with the finding of RecO and RecR being involved in TR mutagenesis, because both are important for repair of transcription replication collisions (Million-Weaver *et al.*, 2015). Further analyses corroborated the theory of different mutation machineries. For intergenic TRs the second TR unit in the direction of replication is roughly excised whereas for intragenic TR the first TR in the direction of transcription is precisely excised. Moreover, intragenic TRs exhibit the highest

mutation frequencies under an optimal growth temperature of 37 °C, whereas intergenic TRs exhibit the highest mutation frequencies under a higher temperature of 42 °C, suggesting also a dependence on transcription and division rates (Berger *et al.*, 2009).

This temperature dependence was also observed in a study investigating a TR inactivating a kanamycin resistance gene (Kn^S) that becomes an active Kn^R gene when one TR unit is excised (Bruand *et al.*, 2001a). This gene was located next to the native $gudB^{CR}$ gene (Fig. 3.5), thus the observations are most likely transferable, but not confirmed yet. Some of the investigated factors were only shown to be involved in TR mutagenesis at higher temperatures of 42 °C. Below 42 °C their influence on TR mutagenesis was not obvious. Comparable to this work, no influence of RecA on the TR mutagenesis was detected (Fig. 3.7) (Bruand *et al.*, 2001a). However, many proteins involved in replication are involved in TR mutagenesis, as for instance DnaB, DnaD, DnaG, PolC, DnaN, DnaX and DnaE (Ch. 1.4). Interestingly, the investigation of double mutants having also a $\Delta recA$ deletion divided the proteins into two groups: DnaE, DnaN and DnaX act in a RecA dependent pathway, and DnaG and DnaD act in a RecA independent pathway. Indicating, that an investigation of $\Delta recA$ double mutants could also shed more light on the TR mutagenesis of the $gudB^{CR}$ gene.

As of now, there are several mechanisms possible, but it seems that intragenic TR mutagenesis results mainly from precise mechanisms involving collisions of the transcription and the replication machinery. Intergenic TRs mainly result from a replication-coupled mechanism, which is less efficient and less specific. Moreover, regarding the findings from the kanamycin resistance gene, it is not known whether both mechanisms are truly RecA

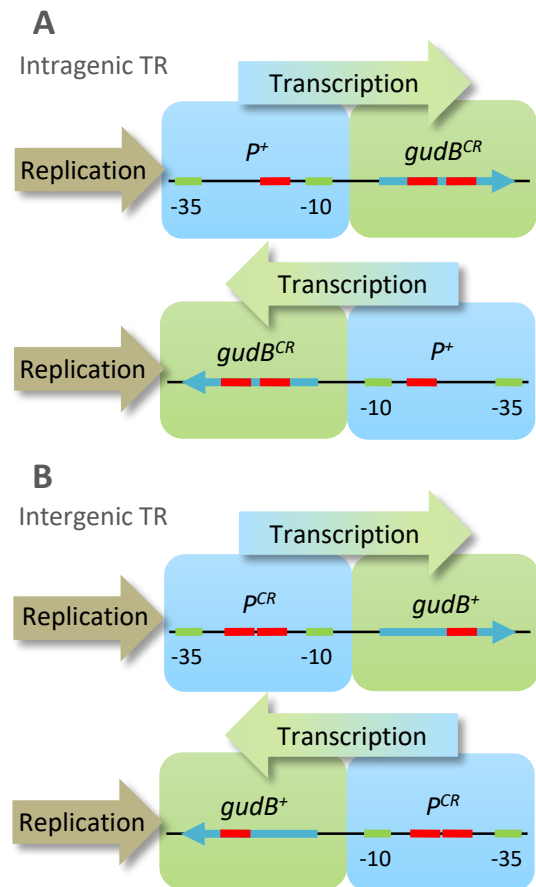


Fig. 4.4 Head-on and co-directional collisions of intra- and intergenic TRs

A: Intragenic TR encountering co-directional and head-on collision. **B:** Intergenic TR encountering co-directional and head-on collision.

independent (Bruand *et al.*, 2001a). With this knowledge, the only approach to unravel the different mutation machineries is a systematic investigation of intra- and intergenic TR in the $gudB$ gene ectopically introduced in the *B. subtilis* genome encountering head-on and co-directional collisions (Fig. 4.4), visualizing the influence of putative factors simultaneously in all situations at different temperatures. Regarding the high mutation rate of the native $gudB^{CR}$ gene, there must be more involved in TR mutagenesis than just the collision of transcription and replication machinery. The native $gudB^{CR}$ gene encounters co-directional collisions, which are not as detrimental as head-on collisions, but can also lead to replication restart (Merrikh *et al.*, 2011; Merrikh, 2017). Recently, the interaction of $GudB^{CR}$ GDH and

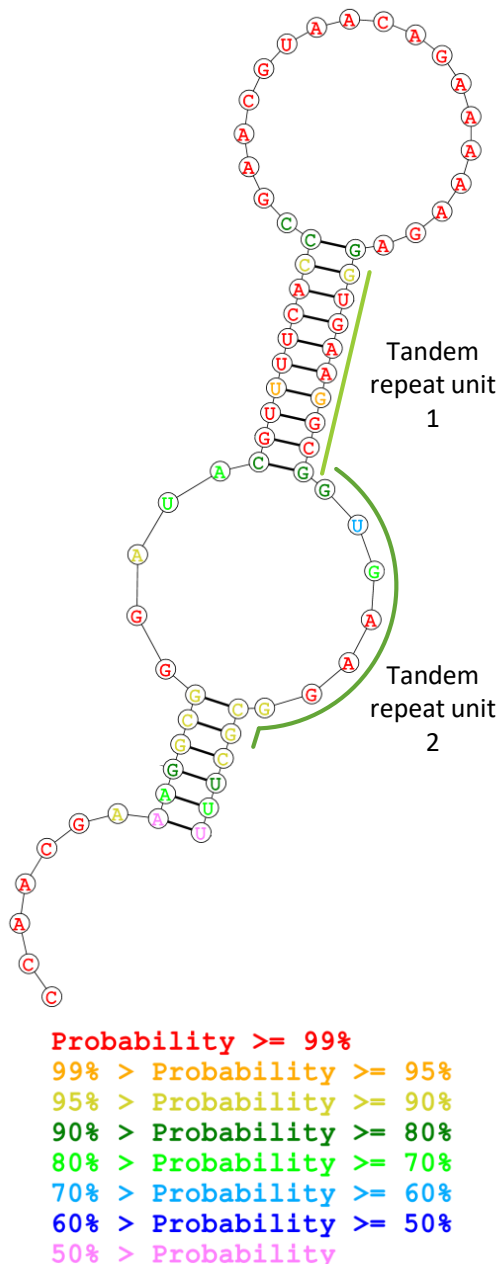


Fig. 4.5 RNA secondary structure of *gudB^{CR}*
 Secondary structure of the bases 232-301 of the 1284 bp coding sequence of the *gudB^{CR}* gene mRNA calculated by the online tool RNAstructure (Reuter and Mathews, 2010). The probabilities are indicated.

NusA was shown (de Jong *et al.*, 2017), leading to the question why does NusA interact with GudB^{CR}? NusA is known in *E. coli* to associate with Rho and NusG to the replisome in order to mediate the Rho-dependent transcription termination and prevent the formation of DSB putatively by translocating the transcription complex when encountering the replication machinery (Washburn and Gottesman, 2011). Furthermore, NusA was shown to be involved in

R-loop removal, in transcription coupled repair and stress induced mutagenesis (Cohen and Walker, 2010; Cohen *et al.*, 2010; Leela *et al.*, 2013) in *E. coli*. In *B. subtilis* NusA is assumed to directly promote the formation of RNA hairpin structures, thereby it directly controls about 16 % of all genes and is in total involved either directly or indirectly in the regulation of >50 % of all genes by controlling transcription read through (Mondal *et al.*, 2016). Especially genes involved in DNA metabolism and repair are under control of NusA. Regarding *gudB^{CR}* mutagenesis the most important function of NusA is most likely the stabilization of emerging R-loops which can cause a simple pausing of the transcription machinery or also promote DNA or RNA strand slippage (Ma *et al.*, 2015; Zhang and Landick, 2016). In the *gudB^{CR}* gene an R-loop including one of the TRs is likely to form (Fig. 4.5), also other DNA secondary structures were predicted previously (Gunka, 2010). This formation could be promoted by NusA and followed by a strand slippage leading to a TR excision as in Streisingers DNA-strand slippage model (Streisinger *et al.*, 1966). However, this might explain an involvement of NusA in *gudB^{CR}* mutation, but not why the highly unstable GudB^{CR} GDH and NusA interact. Hence, there might be another role for the unstable GudB^{CR}, which might explain why the *gudB^{CR}* gene is stably inherited though it was assumed to be non-functional.

5. References

- Aakre, C.D., Herrou, J., Phung, T.N., Perchuk, B.S., Crosson, S., and Laub, M.T. (2015) Evolving new protein-protein interaction specificity through promiscuous intermediates. *Cell* **163**: 594–606.
- Aghajanian, S., Hovsepian, M., Geoghegan, K.F., Chrnyk, B.A., and Engel, P.C. (2003) A thermally sensitive loop in clostridial glutamate dehydrogenase detected by limited proteolysis. *J Biol Chem* **278**: 1067–74.
- Ali, N.O., Jeusset, J., Larquet, E., Le Cam, E., Belitsky, B.R., Sonenshein, A.L., et al. (2003) Specificity of the interaction of RocR with the *rocG-rocA* intergenic region in *Bacillus subtilis*. *Microbiology* **149**: 739–50.
- Anderson, D.G., and Kowalczykowski, S.C. (1997) The translocating RecBCD enzyme stimulates recombination by directing RecA protein onto ssDNA in a χ -regulated manner. *Cell* **90**: 77–86.
- Andersson, D.I., and Hughes, D. (2009) Gene amplification and adaptive evolution in bacteria. *Annu Rev Genet* **43**: 167–95.
- Atkinson, M.R., and Fisher, S.H. (1991) Identification of genes and gene products whose expression is activated during nitrogen-limited growth in *Bacillus subtilis*. *J Bacteriol* **173**: 23–7.
- Ayora, S., Rojo, F., Ogasawara, N., Nakai, S., and Alonso, J.C. (1996) The Mfd protein of *Bacillus subtilis* 168 is involved in both transcription-coupled DNA repair and DNA recombination. *J Mol Biol* **256**: 301–18.
- Bachl, J., Carlson, C., Gray-Schopfer, V., Dessing, M., and Olsson, C. (2001) Increased transcription levels induce higher mutation rates in a hypermutating cell line. *J Immunol* **166**: 5051–7.
- Ballin, P. (2012) Control of PrfA, a transcription activator controlling virulence of *Listeria monocytogenes*. *Master Thesis*.
- Barat, M., Anagnostopoulos, C., and Schneider, A.M. (1965) Linkage relationships of genes controlling isoleucine, valine, and leucine biosynthesis in *Bacillus subtilis*. *J Bacteriol* **90**: 357–69.
- Beadle, G.W., and Tatum, E.L. (1941) Genetic control of biochemical reactions in *Neurospora*. *Proc Natl Acad Sci USA* **27**: 499–506.
- Belitsky, B.R. (2004) Physical and enzymological interaction of *Bacillus subtilis* proteins required for *de novo* pyridoxal 5'-phosphate biosynthesis. *J Bacteriol* **186**: 1191–6.
- Belitsky, B.R., Janssen, P.J., and Sonenshein, A.L. (1995) Sites required for GltC-dependent regulation of *Bacillus subtilis* glutamate synthase expression. *J Bacteriol* **177**: 5686–95.
- Belitsky, B.R., Kim, H., and Sonenshein, A.L. (2004) CcpA-dependent regulation of *Bacillus subtilis* glutamate dehydrogenase gene expression. *J Bacteriol* **186**: 3392–8.
- Belitsky, B.R., and Sonenshein, A.L. (1995) Mutations in GltC that increase *Bacillus subtilis* *gltA* expression. *J Bacteriol* **177**: 5696–700.
- Belitsky, B.R., and Sonenshein, A.L. (1997) Altered transcription activation specificity of a mutant form of *Bacillus subtilis* GltR, a LysR family member. *J Bacteriol* **179**: 1035–43.
- Belitsky, B.R., and Sonenshein, A.L. (1998) Role and regulation of *Bacillus subtilis* glutamate dehydrogenase genes. *J Bacteriol* **180**: 6298–305.
- Belitsky, B.R., and Sonenshein, A.L. (1999) An enhancer element located downstream of the major glutamate dehydrogenase gene of *Bacillus subtilis*. *Proc Natl Acad Sci USA* **96**: 10290–5.
- Belitsky, B.R., and Sonenshein, A.L. (2004) Modulation of activity of *Bacillus subtilis* regulatory proteins GltC and TnrA by glutamate dehydrogenase. *J Bacteriol* **186**: 3399–407.
- Belitsky, B.R., Wray, L. V., Fisher, S.H., Bohannon, D.E., and Sonenshein, A.L. (2000) Role of TnrA in nitrogen source-dependent repression of *Bacillus subtilis* glutamate synthase gene expression. *J Bacteriol* **182**: 5939–47.
- Bergey, D.H., Whitman, W.B., De Vos, P., Garrity, G.M., and Jones, D. (2009) *Bergey's Manual of Systematic Bacteriology*. Vol 3, New York: Springer.
- Bi, W., and Stambrook, P.J. (1998) Site-directed mutagenesis by combined chain reaction. *Anal Biochem* **256**: 137–40.
- Bichara, M., Wagner, J., and Lambert, I.B. (2006) Mechanisms of tandem repeat instability in bacteria. *Mutat Res* **598**: 144–63.
- Binder, D., Grünberger, A., Loeschcke, A., Probst, C., Bier, C., Pietruszka, J., et al. (2014) Light-responsive control of bacterial gene expression: precise triggering of the *lac* promoter activity using photocaged IPTG. *Integr Biol (Camb)* **6**: 755–65.
- Blencke, H.-M., Homuth, G., Ludwig, H., Mäder, U., Hecker, M., and Stülke, J. (2003) Transcriptional profiling of gene expression in response to glucose in *Bacillus subtilis*: regulation of the central metabolic pathways. *Metab Eng* **5**: 133–49.
- Blötz, C., Commichau, F.M., and Stülke, J. (2017) *Methods in Molecular Biology of Bacteria*. 3rd ed., Georg-August-University Göttingen, Göttingen.

References

- Bohannon, D.E., and Sonenshein, A.L.** (1989) Positive regulation of glutamate biosynthesis in *Bacillus subtilis*. *J Bacteriol* **171**: 4718–27.
- Bradford, M.M.** (1976) A rapid and sensitive method for the quantitation of microgram quantities of protein utilizing the principle of protein-dye binding. *Anal Biochem* **72**: 248–54.
- Bravo, A., and Mora, J.** (1988) Ammonium assimilation in *Rhizobium phaseoli* by the glutamine synthetase-glutamate synthase pathway. *J Bacteriol* **170**: 980–984.
- Brill, J., Hoffmann, T., Bleisteiner, M., and Bremer, E.** (2011) Osmotically controlled synthesis of the compatible solute proline is critical for cellular defense of *Bacillus subtilis* against high osmolarity. *J Bacteriol* **193**: 5335–46.
- Brown, S.W., and Sonenshein, A.L.** (1996) Autogenous regulation of the *Bacillus subtilis* *glnRA* operon. *J Bacteriol* **178**: 2450–54.
- Bruand, C., Bidnenko, V., and Ehrlich, S.D.** (2001a) Replication mutations differentially enhance RecA-dependent and RecA-independent recombination between tandem repeats in *Bacillus subtilis*. *Mol Microbiol* **39**: 1248–58.
- Bruand, C., Farache, M., McGovern, S., Ehrlich, S.D., and Polard, P.** (2001b) DnaB, DnaD and DnaI proteins are components of the *Bacillus subtilis* replication restart primosome. *Mol Microbiol* **42**: 245–55.
- Brunhuber, N.M., and Blanchard, J.S.** (1994) The biochemistry and enzymology of amino acid dehydrogenases. *Crit Rev Biochem Mol Biol* **29**: 415–67.
- Burmeister, A.** (2016) Microfluidic heterogeneity analysis of fluorescence-based gene expression of *Bacillus* strains on single-cell level. *Master Thesis*.
- Burnette, W.N.** (1981) “Western blotting”: electrophoretic transfer of proteins from sodium dodecyl sulfate-polyacrylamide gels to unmodified nitrocellulose and radiographic detection with antibody and radioiodinated protein A. *Anal Biochem* **112**: 195–203.
- Cai, D., He, P., Lu, X., Zhu, C., Zhu, J., Zhan, Y., et al.** (2017) A novel approach to improve poly- γ -glutamic acid production by NADPH regeneration in *Bacillus licheniformis* WX-02. *Sci Rep* **7**: 43404.
- Calogero, S., Gardan, R., Glaser, P., Schweizer, J., Rapoport, G., and Debarbouille, M.** (1994) RocR, a novel regulatory protein controlling arginine utilization in *Bacillus subtilis*, belongs to the NtrC/NifA family of transcriptional activators. *J Bacteriol* **176**: 1234–41.
- Capra, E.J., Perchuk, B.S., Skerker, J.M., and Laub, M.T.** (2012) Adaptive mutations that prevent crosstalk enable the expansion of paralogous signaling protein families. *Cell* **150**: 222–32.
- Cárdenas, P.P., Carrasco, B., Defeu Soufo, C., César, C.E., Herr, K., Kaufenstein, M., et al.** (2012) RecX facilitates homologous recombination by modulating RecA activities. *PLoS Genet* **8**: e1003126.
- Cárdenas, P.P., Carzaniga, T., Zangrossi, S., Briani, F., Garcia-Tirado, E., Dehò, G., and Alonso, J.C.** (2011) Polynucleotide phosphorylase exonuclease and polymerase activities on single-stranded DNA ends are modulated by RecN, SsbA and RecA proteins. *Nucleic Acids Res* **39**: 9250–61.
- Carrasco, B., Ayora, S., Lurz, R., and Alonso, J.C.** (2005) *Bacillus subtilis* RecU Holliday-junction resolvase modulates RecA activities. *Nucleic Acids Res* **33**: 3942–52.
- Carrasco, B., Manfredi, C., Ayora, S., and Alonso, J.C.** (2008) *Bacillus subtilis* SsbA and dATP regulate RecA nucleation onto single-stranded DNA. *DNA Repair* **7**: 990–6.
- Carrasco, B., Yadav, T., Serrano, E., and Alonso, J.C.** (2015) *Bacillus subtilis* RecO and SsbA are crucial for RecA-mediated recombinational DNA repair. *Nucleic Acids Res* **43**: 5984–97.
- Castillo, A., Taboada, H., Mendoza, A., Valderrama, B., Encarnación, S., and Mora, J.** (2000) Role of GOGAT in carbon and nitrogen partitioning in *Rhizobium etli*. *Microbiology* **146**: 1627–37.
- Cerozi, B.d.S., and Fitzsimmons, K.** (2016) Use of *Bacillus* spp. to enhance phosphorus availability and serve as a plant growth promoter in aquaponics systems. *Sci Hortic* **211**: 277–82.
- Chakraborty, T., Leimeister-Wächter, M., Domann, E., Hartl, M., Goebel, W., Nichterlein, T., and Notermans, S.** (1992) Coordinate regulation of virulence genes in *Listeria monocytogenes* requires the product of the *prfA* gene. *J Bacteriol* **174**: 568–74.
- Chédin, F., Handa, N., Dillingham, M.S., and Kowalczykowski, S.C.** (2006) The AddAB helicase/nuclease forms a stable complex with its cognate χ sequence during translocation. *J Biol Chem* **281**: 18610–7.
- Chiou, S.H., Lo, C.H., Chang, C.Y., Itoh, T., Kaji, H., and Samejima, T.** (1991) Ostrich crystallins. structural characterization of delta-crystallin with enzymic activity. *Biochem J* **273**(Pt 2): 295–300.
- Choi, S., and Saier, M.H.** (2005) Regulation of *sigL* expression by the catabolite control protein CcpA involves a roadblock mechanism in *Bacillus subtilis*: potential connection between carbon and nitrogen metabolism. *J Bacteriol* **187**: 6856–

- 61.
- Chu, F., Kearns, D.B., McLoon, A., Chai, Y., Kolter, R., and Losick, R.** (2008) A novel regulatory protein governing biofilm formation in *Bacillus subtilis*. *Mol Microbiol* **68**: 1117–27.
- Chumsakul, O., Takahashi, H., Oshima, T., Hishimoto, T., Kanaya, S., Ogasawara, N., and Ishikawa, S.** (2011) Genome-wide binding profiles of the *Bacillus subtilis* transition state regulator AbrB and its homolog Abh reveals their interactive role in transcriptional regulation. *Nucleic Acids Res* **39**: 414–28.
- Claessen, D., Emmins, R., Hamoen, L.W., Daniel, R.A., Errington, J., and Edwards, D.H.** (2008) Control of the cell elongation-division cycle by shuttling of PBP1 protein in *Bacillus subtilis*. *Mol Microbiol* **68**: 1029–46.
- Cohen, S.E., Lewis, C.A., Mooney, R.A., Kohanski, M.A., Collins, J.J., Landick, R., and Walker, G.C.** (2010) Roles for the transcription elongation factor NusA in both DNA repair and damage tolerance pathways in *Escherichia coli*. *Proc Natl Acad Sci USA* **107**: 15517–22.
- Cohen, S.E., and Walker, G.C.** (2010) The transcription elongation factor NusA is required for stress-induced mutagenesis in *Escherichia coli*. *Curr Biol* **20**: 80–5.
- Commichau, F.M.** (2006) Regulation der Glutamatsynthese in *Bacillus subtilis* durch die Glutamatdehydrogenase RocG und das Aktivatorprotein GltC. *Dissertation*.
- Commichau, F.M., Alzinger, A., Sande, R., Bretzel, W., Meyer, F.M., Chevreux, B., et al.** (2014) Overexpression of a non-native deoxyxylulose-dependent vitamin B6 pathway in *Bacillus subtilis* for the production of pyridoxine. *Metab Eng* **25**: 38–49.
- Commichau, F.M., Alzinger, A., Sande, R., Bretzel, W., Reuß, D.R., Dormeyer, M., et al.** (2015). Engineering *Bacillus subtilis* for the conversion of the antimetabolite 4-hydroxy-L-threonine to pyridoxine. *Metab Eng* **29**: 196-207.
- Commichau, F.M., Gunka, K., Landmann, J.J., and Stülke, J.** (2008) Glutamate metabolism in *Bacillus subtilis*: gene expression and enzyme activities evolved to avoid futile cycles and to allow rapid responses to perturbations of the system. *J Bacteriol* **190**: 3557–64.
- Commichau, F.M., Herzberg, C., Tripal, P., Valerius, O., and Stülke, J.** (2007a) A regulatory protein-protein interaction governs glutamate biosynthesis in *Bacillus subtilis*: the glutamate dehydrogenase RocG moonlights in controlling the transcription factor GltC. *Mol Microbiol* **65**: 642–54.
- Commichau, F.M., and Stülke, J.** (2008) Trigger enzymes: bifunctional proteins active in metabolism and in controlling gene expression. *Mol Microbiol* **67**: 692–702.
- Commichau, F.M., Wacker, I., Schleider, J., Blencke, H.-M., Reif, I., Tripal, P., and Stülke, J.** (2007b) Characterization of *Bacillus subtilis* mutants with carbon source-independent glutamate biosynthesis. *J Mol Microbiol Biotechnol* **12**: 106–13.
- Costes, A., Lecoite, F., McGovern, S., Quevillon-Cheruel, S., and Polard, P.** (2010) The C-terminal domain of the bacterial SSB protein acts as a DNA maintenance hub at active chromosome replication forks. *PLoS Genet* **6**: e1001238.
- Cox, M.M.** (1998) A broadening view of recombinational DNA repair in bacteria. *Genes to Cells* **3**: 65–78.
- Cox, M.M.** (2007) Regulation of bacterial RecA protein function. *Crit Rev Biochem Mol Biol* **42**: 41–63.
- Cox, M.M., and Lehman, I.R.** (1982) RecA protein-promoted DNA strand exchange. Stable complexes of RecA protein and single-stranded DNA formed in the presence of ATP and single-stranded DNA binding protein. *J Biol Chem* **257**: 8523–32.
- Czaplewski, L.G., North, a K., Smith, M.C., Baumberg, S., and Stockley, P.G.** (1992) Purification and initial characterization of AhrC: the regulator of arginine metabolism genes in *Bacillus subtilis*. *Mol Microbiol* **6**: 267–75.
- Darwin, C.** (1859) On the origin of species by means of natural selection, or the preservation of favoured races in the struggle for life. London: J. Murray.
- Detsch, C., and Stülke, J.** (2003) Ammonium utilization in *Bacillus subtilis*: transport and regulatory functions of NrgA and NrgB. *Microbiology* **149**: 3289–97.
- Deutscher, J.** (2008) The mechanisms of carbon catabolite repression in bacteria. *Curr Opin Microbiol* **11**: 87–93.
- Deutscher, J., Francke, C., and Postma, P.W.** (2006) How phosphotransferase system-related protein phosphorylation regulates carbohydrate metabolism in bacteria. *Microbiol Mol Biol Rev* **70**: 939–1031.
- Diethmaier, C.** (2011) Die Rolle von YmdB als Regulator der Zelldifferenzierung in *Bacillus subtilis*. *Dissertation* .
- Diethmaier, C., Pietack, N., Gunka, K., Wrede, C., Lehnik-Habrink, M., Herzberg, C., et al.** (2011) A novel factor controlling bistability in *Bacillus*

References

- subtilis*: The Ymdb protein affects flagellin expression and biofilm formation. *J Bacteriol* **193**: 5997–6007.
- Dillingham, M.S., and Kowalczykowski, S.C.** (2008) RecBCD enzyme and the repair of double-stranded DNA breaks. *Microbiol Mol Biol Rev* **72**: 642–71.
- Domann, E., Leimeister-Wächter, M., Goebel, W., and Chakraborty, T.** (1991) Molecular cloning, sequencing, and identification of a metalloprotease gene from *Listeria monocytogenes* that is species specific and physically linked to the listeriolysin gene. *Infect Immun* **59**: 65–72.
- Dormeyer, M.** (2014) Applications of reporter systems that are based on direct repeat instability in *Bacillus subtilis*.
- Dormeyer, M., Egelkamp, R., Thiele, M.J., Hammer, E., Gunka, K., Stanek, L., et al.** (2014) A novel engineering tool in the *Bacillus subtilis* toolbox: inducer-free activation of gene expression by selection-driven promoter decryptification. *Microbiology* **161**: 354–61.
- Dormeyer, M., Lübke, A.L., Müller, P., Lentjes, S., Reuß, D.R., Thürmer, A., et al.** (2017) Hierarchical mutational events compensate for glutamate auxotrophy of a *Bacillus subtilis* *gltC* mutant. *Environ Microbiol Rep* **3**: 279–89.
- Ducret, A., Quardokus, E.M., and Brun, Y.V.** (2016) MicrobeJ, a tool for high throughput bacterial cell detection and quantitative analysis. *Nat Microbiol* **1**: 16077.
- Elez, M., Murray, A.W., Bi, L.-J., Zhang, X.-E., Matic, I., and Radman, M.** (2010) Seeing mutations in living cells. *Curr Biol* **20**: 1432–7.
- Faires, N., Tobisch, S., Bachem, S., Martin-Verstraete, I., Hecker, M., and Stülke, J.** (1999) The catabolite control protein CcpA controls ammonium assimilation in *Bacillus subtilis*. *J Mol Microbiol Biotechnol* **1**: 141–8.
- Fan, J., Leroux-Coyau, M., Savery, N.J., and Strick, T.R.** (2016) Reconstruction of bacterial transcription-coupled repair at single-molecule resolution. *Nature* **536**:234–7.
- Fares, M.A.** (2014) The evolution of protein moonlighting: adaptive traps and promiscuity in the chaperonins. *Biochem Soc Trans* **42**: 1709–14.
- Feng, J., Gu, Y., Quan, Y., Cao, M., Gao, W., Zhang, W., et al.** (2015) Improved poly- γ -glutamic acid production in *Bacillus amyloliquefaciens* by modular pathway engineering. *Metab Eng* **32**: 106–15.
- Fernández, S., Kobayashi, Y., Ogasawara, N., and Alonso, J.C.** (1999) Analysis of the *Bacillus subtilis* *recO* gene: RecO forms part of the RecFLOR function. *Mol Gen Genet* **261**: 567–73.
- Fisher, S.H.** (1999) Regulation of nitrogen metabolism in *Bacillus subtilis*: vive la différence! *Mol Microbiol* **32**: 223–32.
- Fisher, S.H., and Magasanik, B.** (1984) 2-Ketoglutarate and the regulation of aconitase and histidase formation in *Bacillus subtilis*. *J Bacteriol* **158**: 379–82.
- Fisher, S.H., and Wray, L.V.** (2008) *Bacillus subtilis* glutamine synthetase regulates its own synthesis by acting as a chaperone to stabilize GlnR-DNA complexes. *Proc Natl Acad Sci USA* **105**: 1014–9.
- Flórez, L.A., Gunka, K., Polanía, R., Tholen, S., and Stülke, J.** (2011) SPABBATS: A pathway-discovery method based on Boolean satisfiability that facilitates the characterization of suppressor mutants. *BMC Syst Biol* **5**: 5.
- Franken, K.L., Hiemstra, H.S., Meijgaarden, K.E. van, Subronto, Y., Hartigh, J. den, Ottenhoff, T.H., and Drijfhout, J.W.** (2000) Purification of His-tagged proteins by immobilized chelate affinity chromatography: the benefits from the use of organic solvent. *Protein Expr Purif* **18**: 95–9.
- French, S.** (1992) Consequences of replication fork movement through transcription units *in vivo*. *Science* **258**: 1362–5.
- Fukita, Y., Jacobs, H., and Rajewsky, K.** (1998) Somatic hypermutation in the heavy chain locus correlates with transcription. *Immunity* **9**: 105–14.
- Fukushima, S., Itaya, M., Kato, H., Ogasawara, N., and Yoshikawa, H.** (2007) Reassessment of the *in vivo* functions of DNA polymerase I and RNase H in bacterial cell growth. *J Bacteriol* **189**: 8575–83.
- Gaillard, H., Herrera-Moyano, E., and Aguilera, A.** (2013) Transcription-associated genome instability. *Chem Rev* **113**: 8638–61.
- Gardan, R., Rapoport, G., and Débarbouillé, M.** (1995) Expression of the *rocDEF* operon involved in arginine catabolism in *Bacillus subtilis*. *J Mol Biol* **249**: 843–56.
- Garfin, D.E.** (2009) One-dimensional gel electrophoresis. *Methods Enzymol* **463**: 497–513.
- Garrod, A.E.** (1923) *Inborn Errors of Metabolism*. 2nd ed., London: Hoddor and Stoughton.
- Gerwig, J.** (2011) Novel factors involved in the Mfd-mediated decryptification of the *gudB* gene in *Bacillus subtilis*. *Master Thesis*.
- Gómez-Marroquín, M., Martin, H., Pepper, A., Girard, M., Kidman, A., Vallin, C., et al.** (2016) stationary-phase mutagenesis in stressed *Bacillus*

- subtilis* cells operates by Mfd-dependent mutagenic pathways. *Genes (Basel)* **7**: 33.
- Görke, B., and Stülke, J.** (2008) Carbon catabolite repression in bacteria: many ways to make the most out of nutrients. *Nat Rev Microbiol* **6**: 613–24.
- Graumann, P.L., and Knust, T.** (2009) Dynamics of the bacterial SMC complex and SMC-like proteins involved in DNA repair. *Chromosome Res* **17**: 265–75.
- Grünberger, A., Probst, C., Heyer, A., Wiechert, W., Frunzke, J., and Kohlheyer, D.** (2013) Microfluidic picoliter bioreactor for microbial single-cell analysis: fabrication, system setup, and operation. *J Vis Exp* **82**: e50560.
- Grünberger, A., Probst, C., Helfrich, S., Nanda, A., Stute, B., Wiechert, W., et al.** (2015) Spatiotemporal microbial single-cell analysis using a high-throughput microfluidics cultivation platform. *Cytometry* **87A**: 1101–15.
- Grünberger, A., Wiechert, W., and Kohlheyer, D.** (2014) Single-cell microfluidics: opportunity for bioprocess development. *Curr Opin Biotechnol* **29**: 15–23.
- Guérout-Fleury, A.-M., Shazand, K., Frandsen, N., and Stragier, P.** (1995) Antibiotic-resistance cassettes for *Bacillus subtilis*. *Gene* **167**: 335–6.
- Gundlach, J., Herzberg, C., Kaefer, V., Gunka, K., Hoffmann, T., Weiß, M., et al.** (2017) Control of potassium homeostasis is an essential function of the second messenger cyclic di-AMP in *Bacillus subtilis*. *Sci Signal* **10**: eaal3011.
- Gundlach, J., Mehne, F.M.P., Herzberg, C., Kampf, J., Valerius, O., Kaefer, V., and Stülke, J.** (2015) An essential poison: synthesis and degradation of cyclic di-AMP in *Bacillus subtilis*. *J Bacteriol* **197**: 3265–74.
- Gunka, K.** (2010) Der Einfluss der Glutamatdehydrogenasen auf die Verknüpfung des Kohlenstoff- und Stickstoffstoffwechsels in *Bacillus subtilis*. *Dissertation*.
- Gunka, K., and Commichau, F.M.** (2012) Control of glutamate homeostasis in *Bacillus subtilis*: a complex interplay between ammonium assimilation, glutamate biosynthesis and degradation. *Mol Microbiol* **85**: 213–24.
- Gunka, K., Newman, J.A., Commichau, F.M., Herzberg, C., Rodrigues, C., Hewitt, L., et al.** (2010) Functional dissection of a trigger enzyme: mutations of the *Bacillus subtilis* glutamate dehydrogenase RocG that affect differentially its catalytic activity and regulatory properties. *J Mol Biol* **400**: 815–27.
- Gunka, K., Stanek, L., Care, R.A., and Commichau, F.M.** (2013) Selection-driven accumulation of suppressor mutants in *Bacillus subtilis*: the apparent high mutation frequency of the cryptic *gudB* gene and the rapid clonal expansion of *gudB*⁺ suppressors are due to growth under selection. *PLoS One* **8**: e66120.
- Gunka, K., Tholen, S., Gerwig, J., Herzberg, C., Stülke, J., and Commichau, F.M.** (2012) A high-frequency mutation in *Bacillus subtilis*: requirements for the decryptification of the *gudB* glutamate dehydrogenase gene. *J Bacteriol* **194**: 1036–44.
- Guy, L., and Roten, C.-A.H.** (2004) Genometric analyses of the organization of circular chromosomes: a universal pressure determines the direction of ribosomal RNA genes transcription relative to chromosome replication. *Gene* **340**: 45–52.
- Haber, J.E.** (2002) Uses and abuses of HO endonuclease. *Methods Enzymol* **350**: 141–64.
- Halsey, C.R., Lei, S., Wax, J.K., Lehman, M.K., Nuxoll, A.S., Steinke, L., et al.** (2017) Amino acid catabolism in *Staphylococcus aureus* and the function of carbon catabolite repression. *MBio* **8**: e01434-16.
- Hamoen, L.W., Venema, G., and Kuipers, O.P.** (2003) Controlling competence in *Bacillus subtilis*: shared use of regulators. *Microbiology* **149**: 9–17.
- Hardiman, T., Lemuth, K., Keller, M.A., Reuss, M., and Siemann-Herzberg, M.** (2007) Topology of the global regulatory network of carbon limitation in *Escherichia coli*. *J Biotechnol* **132**: 359–74.
- Haruki, M., Tsunaka, Y., Morikawa, M., and Kanaya, S.** (2002) Cleavage of a DNA-RNA-DNA/DNA chimeric substrate containing a single ribonucleotide at the DNA-RNA junction with prokaryotic RNases HII. *FEBS Lett* **531**: 204–8.
- Hauf, K., Kayumov, A., Gloge, F., and Forchhammer, K.** (2016) The molecular basis of TnrA control by glutamine synthetase in *Bacillus subtilis*. *J Biol Chem* **291**: 3483–95.
- van Heeswijk, W.C., Westerhoff, H.V., and Boogerd, F.C.** (2013) Nitrogen assimilation in *Escherichia coli*: putting molecular data into a systems perspective. *Microbiol Mol Biol Rev* **77**: 628–95.
- Heinrich, A., Woyda, K., Brauburger, K., Meiss, G., Detsch, C., Stülke, J., and Forchhammer, K.** (2006) Interaction of the membrane-bound GlnK-AmtB complex with the master regulator of nitrogen metabolism TnrA in *Bacillus subtilis*. *J Biol Chem* **281**: 34909–17.
- Helmrich, A., Ballarino, M., Nudler, E., and Tora, L.**

References

- (2013) Transcription-replication encounters, consequences and genomic instability. *Nat Struct Mol Biol* **20**: 412–8.
- Helmrich, A., Ballarino, M., and Tora, L.** (2011) Collisions between replication and transcription complexes cause common fragile site instability at the longest human genes. *Mol Cell* **44**: 966–77.
- Herzberg, C., Weidinger, L.A.F., Dörrbecker, B., Hübner, S., Stülke, J., and Commichau, F.M.** (2007) SPINE: a method for the rapid detection and analysis of protein-protein interactions *in vivo*. *Proteomics* **7**: 4032–5.
- van den Heuvel, R.H.H., Ferrari, D., Bossi, R.T., Ravasio, S., Curti, B., Vanoni, M.A., et al.** (2002) Structural studies on the synchronization of catalytic centers in glutamate synthase. *J Biol Chem* **277**: 24579–83.
- Hohmann, H., van Dijk, J.M., Krishnappa, L., and Pragáí, Z.** (2016) Host Organisms: *Bacillus subtilis*. In *Industrial Biotechnology*. Wiley-VCH Verlag GmbH & Co. KGaA, Weinheim, Germany. pp. 221–297.
- Hu, P., Leighton, T., and Ishkhanova, G.** (1999) Sensing of nitrogen limitation by *Bacillus subtilis*: Comparison to enteric bacteria. *J Bacteriol* **181**: 5042–50.
- Jannièrè, L., Niaudet, B., Pierre, E., and Ehrlich, S.D.** (1985) Stable gene amplification in the chromosome of *Bacillus subtilis*. *Gene* **40**: 47–55.
- Jeffery, C.J.** (2016) Protein species and moonlighting proteins: Very small changes in a protein's covalent structure can change its biochemical function. *J Proteomics* **134**: 19–24.
- Jong, L. de, Koning, E.A. de, Roseboom, W., Buncherd, H., Wanner, M.J., Dapic, I., et al.** (2017) In-culture cross-linking of bacterial cells reveals large-scale dynamic protein-protein interactions at the peptide level. *J Proteome Res* **16**: 2457–71.
- Karimova, G., Pidoux, J., Ullmann, A., and Ladant, D.** (1998) A bacterial two-hybrid system based on a reconstituted signal transduction pathway. *Proc Natl Acad Sci USA* **95**: 5752–6.
- Kayumov, A., Heinrich, A., Fedorova, K., Ilinskaya, O., and Forchhammer, K.** (2011) Interaction of the general transcription factor TnrA with the PII-like protein GlnK and glutamine synthetase in *Bacillus subtilis*. *FEBS J* **278**: 1779–89.
- Khan, I.H., Ito, K., Kim, H., Ashida, H., Ishikawa, T., Shibata, H., and Sawa, Y.** (2005a) Molecular properties and enhancement of thermostability by random mutagenesis of glutamate dehydrogenase from *Bacillus subtilis*. *Biosci Biotechnol Biochem* **69**: 1861–70.
- Khan, I.H., Kim, H., Ashida, H., Ishikawa, T., Shibata, H., and Sawa, Y.** (2005b) Altering the substrate specificity of glutamate dehydrogenase from *Bacillus subtilis* by site-directed mutagenesis. *Biosci Biotechnol Biochem* **69**: 1802–5.
- Khasanov, F.K., Zvingila, D.J., Zainullin, A.A., Prozorov, A.A., and Bashkirov, V.I.** (1992) Homologous recombination between plasmid and chromosomal DNA in *Bacillus subtilis* requires approximately 70 bp of homology. *Mol Gen Genet* **234**: 494–7.
- Kidane, D., and Graumann, P.L.** (2005) Dynamic formation of RecA filaments at DNA double strand break repair centers in live cells. *J Cell Biol* **170**: 357–66.
- Kidane, D., Sanchez, H., Alonso, J.C., and Graumann, P.L.** (2004) Visualization of DNA double-strand break repair in live bacteria reveals dynamic recruitment of *Bacillus subtilis* RecF, RecO and RecN proteins to distinct sites on the nucleoids. *Mol Microbiol* **52**: 1627–39.
- Kim, J., Kershner, J.P., Novikov, Y., Shoemaker, R.K., and Copley, S.D.** (2010) Three serendipitous pathways in *E. coli* can bypass a block in pyridoxal-5'-phosphate synthesis. *Mol Syst Biol* **6**: 436.
- Kim, N., and Jinks-Robertson, S.** (2012) Transcription as a source of genome instability. *Nat Rev Genet* **13**: 204–14.
- Klingel, U., Miller, C.M., North, A.K., Stockley, P.G., and Baumberg, S.** (1995) A binding site for activation by the *Bacillus subtilis* AhrC protein, a repressor/activator of arginine metabolism. *Mol Gen Genet* **248**: 329–40.
- Kowalczykowski, S.C., and Krupp, R.A.** (1987) Effects of *Escherichia coli* SSB protein on the single-stranded DNA-dependent ATPase activity of *Escherichia coli* RecA protein. Evidence that SSB protein facilitates the binding of RecA protein to regions of secondary structure within single-stranded DNA. *J Mol Biol* **193**: 97–113.
- Krajewski, W.W., Fu, X., Wilkinson, M., Cronin, N.B., Dillingham, M.S., and Wigley, D.B.** (2014) Structural basis for translocation by AddAB helicase-nuclease and its arrest at χ sites. *Nature* **508**: 416–19.
- Kreuzer, K.N.** (2005) Interplay between DNA replication and recombination in prokaryotes. *Annu Rev Microbiol* **59**: 43–67.
- Krüger, N.J., and Stingl, K.** (2011) Two steps away from novelty - principles of bacterial DNA uptake. *Mol Microbiol* **80**: 860–7.
- Kumpfmüller, J., Kabisch, J., and Schweder, T.** (2013) An optimized technique for rapid genome

- modifications of *Bacillus subtilis*. *J Microbiol Methods* **95**: 350–2.
- Kunkel, T.A.** (2004) DNA replication fidelity. *J Biol Chem* **279**: 16895–8.
- Kunkel, T.A., and Erie, D.A.** (2005) DNA mismatch repair. *Annu Rev Biochem* **74**: 681–710.
- Kunst, F., Ogasawara, N., Moszer, I., Albertini, A.M., Alloni, G., Azevedo, V., et al.** (1997) The complete genome sequence of the Gram-positive bacterium *Bacillus subtilis*. *Nature* **390**: 249–56.
- Kunst, F., and Rapoport, G.** (1995) Salt stress is an environmental signal affecting degradative enzyme synthesis in *Bacillus subtilis*. *J Bacteriol* **177**: 2403–7.
- Laemmli, U.K.** (1970) Cleavage of structural proteins during the assembly of the head of bacteriophage T4. *Nature* **227**: 680–5.
- de las Heras, A., Cain, R.J., Bielecka, M.K., and Vázquez-Boland, J.A.** (2011) Regulation of *Listeria* virulence: PrfA master and commander. *Curr Opin Microbiol* **14**: 118–27.
- Lea, D.E., and Coulson, C.A.** (1949) The distribution of the numbers of mutants in bacterial populations. *J Genet* **49**: 264–85.
- Lecoite, F., Sérèna, C., Velten, M., Costes, A., McGovern, S., Meile, J.-C., et al.** (2007) Anticipating chromosomal replication fork arrest: SSB targets repair DNA helicases to active forks. *EMBO J* **26**: 4239–51.
- Lederberg, E.M., and Cohen, S.N.** (1974) Transformation of *Salmonella typhimurium* by plasmid deoxyribonucleic acid. *J Bacteriol* **119**: 1072–4.
- Leela, J.K., Syeda, A.H., Anupama, K., and Gowrishankar, J.** (2013) Rho-dependent transcription termination is essential to prevent excessive genome-wide R-loops in *Escherichia coli*. *Proc Natl Acad Sci USA* **110**: 258–63.
- Lenhart, J.S., Brandes, E.R., Schroeder, J.W., Sorenson, R.J., Showalter, H.D., and Simmons, L.A.** (2014) RecO and RecR are necessary for RecA loading in response to DNA damage and replication fork stress. *J Bacteriol* **196**: 2851–60.
- Lenhart, J.S., Schroeder, J.W., Walsh, B.W., and Simmons, L.A.** (2012) DNA repair and genome maintenance in *Bacillus subtilis*. *Microbiol Mol Biol Rev* **76**: 530–64.
- Lesterlin, C., Ball, G., Schermelleh, L., and Sherratt, D.J.** (2014) RecA bundles mediate homology pairing between distant sisters during DNA break repair. *Nature* **506**: 249–53.
- Lindner, C., Nijland, R., van Hartskamp, M., Bron, S., Hamoen, L.W., and Kuipers, O.P.** (2004) Differential expression of two paralogous genes of *Bacillus subtilis* encoding single-stranded DNA binding protein. *J Bacteriol* **186**: 1097–105.
- Liu, J., Martinez-Corral, R., Prindle, A., Lee, D.D., Larkin, J., Gabalda-Sagarra, M., et al.** (2017) Coupling between distant biofilms and emergence of nutrient time-sharing. *Science* **356**: 638–42.
- Liu, J., Prindle, A., Humphries, J., Gabalda-Sagarra, M., Asally, M., Lee, D.D., et al.** (2015) Metabolic co-dependence gives rise to collective oscillations within biofilms. *Nature* **523**: 550–4.
- Lobel, L., and Herskovits, A.A.** (2016) Systems level analyses reveal multiple regulatory activities of CodY controlling metabolism, motility and virulence in *Listeria monocytogenes*. *PLoS Genet* **12**: e1005870.
- Lohman, T.M., and Ferrari, M.E.** (1994) *Escherichia coli* single-stranded DNA-binding protein: multiple DNA-binding modes and cooperativities. *Annu Rev Biochem* **63**: 527–70.
- Luria, S.E., and Delbrück, M.** (1943) Mutations of bacteria from virus sensitivity to virus resistance. *Genetics* **28**: 491–511.
- Ma, C., Mobli, M., Yang, X., Keller, A.N., King, G.F., and Lewis, P.J.** (2015) RNA polymerase-induced remodelling of NusA produces a pause enhancement complex. *Nucleic Acids Res* **43**: 2829–40.
- Maddocks, S.E., and Oyston, P.C.F.** (2008) Structure and function of the LysR-type transcriptional regulator (LTTR) family proteins. *Microbiology* **154**: 3609–23.
- Martin-Verstraete, I., Débarbouillé, M., Klier, A., and Rapoport, G.** (1992) Mutagenesis of the *Bacillus subtilis* “–12, –24” promoter of the levanase operon and evidence for the existence of an upstream activating sequence. *J Mol Biol* **226**: 85–99.
- Martin-Verstraete, I., Débarbouillé, M., Klier, A., and Rapoport, G.** (1994) Interactions of wild-type and truncated LevR of *Bacillus subtilis* with the upstream activating sequence of the levanase operon. *J Mol Biol* **241**: 178–92.
- Mehne, F.** (2013) Bildung und Homöostase von c-di-AMP in *Bacillus subtilis*. *Dissertation*.
- Mehne, F.M.P., Gunka, K., Eilers, H., Herzberg, C., Kaefer, V., and Stülke, J.** (2013) Cyclic di-AMP homeostasis in *Bacillus subtilis*: Both lack and high level accumulation of the nucleotide are detrimental for cell growth. *J Biol Chem* **288**: 2004–17.
- Mendoza, A., Valderrama, B., Leija, A., and Mora, J.** (1998) NifA-dependent expression of glutamate

References

- dehydrogenase in *Rhizobium etli* modifies nitrogen partitioning during symbiosis. *Mol Plant Microbe Interact* **11**: 83–90.
- Mengaud, J., Braun-Breton, C., and Cossart, P.** (1991) Identification of phosphatidylinositol-specific phospholipase C activity in *Listeria monocytogenes*: a novel type of virulence factor? *Mol Microbiol* **5**: 367–72.
- Merrick, H.** (2017) Spatial and temporal control of evolution through replication-transcription conflicts. *Trends Microbiol* **25**: 515–21.
- Merrick, H., Machón, C., Grainger, W.H., Grossman, A.D., and Soultanas, P.** (2011) Co-directional replication-transcription conflicts lead to replication restart. *Nature* **470**: 554–7.
- Merrick, H., Zhang, Y., Grossman, A.D., and Wang, J.D.** (2012) Replication-transcription conflicts in bacteria. *Nat Rev Microbiol* **10**: 449–58.
- Meyer, F.M., Gerwig, J., Hammer, E., Herzberg, C., Commichau, F.M., Völker, U., and Stülke, J.** (2011) Physical interactions between tricarboxylic acid cycle enzymes in *Bacillus subtilis*: Evidence for a metabolon. *Metab Eng* **13**: 18–27.
- Meyer, T.S., and Lamberts, B.L.** (1965) Use of coomassie brilliant blue R250 for the electrophoresis of microgram quantities of parotid saliva proteins on acrylamide-gel strips. *Biochim Biophys Acta* **107**: 144–5.
- Michna, R.H., Zhu, B., Mäder, U., and Stülke, J.** (2016) SubtiWiki 2.0 - an integrated database for the model organism *Bacillus subtilis*. *Nucleic Acids Res* **44**: D654–62.
- Miethke, M., Westers, H., Blom, E.-J., Kuipers, O.P., and Marahiel, M.A.** (2006) Iron starvation triggers the stringent response and induces amino acid biosynthesis for bacillibactin production in *Bacillus subtilis*. *J Bacteriol* **188**: 8655–7.
- Miller, J.H.** (1972) *Experiments in molecular genetics*. Cold Spring Harbor Laboratory Press, Cold Spring Harbor, New York.
- Million-Weaver, S., Samadpour, A.N., and Merrick, H.** (2015) Replication restart after replication-transcription conflicts requires RecA in *Bacillus subtilis*. *J Bacteriol* **197**: 2374–82.
- Mirouze, N., Bidnenko, E., Noirot, P., and Auger, S.** (2015) Genome-wide mapping of TnrA-binding sites provides new insights into the TnrA regulon in *Bacillus subtilis*. *MicrobiologyOpen* **4**: 423–35.
- Miwa, Y., Saikawa, M., and Fujita, Y.** (1994) Possible function and some properties of the CcpA protein of *Bacillus subtilis*. *Microbiology* **140**: 2567–75.
- Molle, V., Nakaura, Y., Shivers, R.P., Yamaguchi, H., Losick, R., Fujita, Y., and Sonenshein, A.L.** (2003) Additional targets of the *Bacillus subtilis* global regulator CodY identified by chromatin immunoprecipitation and genome-wide transcript analysis. *J Bacteriol* **185**: 1911–22.
- Mondal, S., Yakhnin, A.V., Sebastian, A., Albert, I., and Babitzke, P.** (2016) NusA-dependent transcription termination prevents misregulation of global gene expression. *Nat Microbiol* **1**: 15007.
- Monedero, V., Poncet, S., Mijakovic, I., Fieulaine, S., Dossonnet, V., Martin-Verstraete, I., et al.** (2001) Mutations lowering the phosphatase activity of HPr kinase/phosphatase switch off carbon metabolism. *EMBO J* **20**: 3928–37.
- Mossessova, E., and Lima, C.D.** (2000) Ulp1-SUMO crystal structure and genetic analysis reveal conserved interactions and a regulatory element essential for cell growth in yeast. *Mol Cell* **5**: 865–76.
- Mukherjee, S., and Kearns, D.B.** (2014) The structure and regulation of flagella in *Bacillus subtilis*. *Annu Rev Genet* **48**: 319–40.
- Müller, J.P., An, Z., Merad, T., Hancock, I.C., and Harwood, C.R.** (1997) Influence of *Bacillus subtilis* *phoR* on cell wall anionic polymers. *Microbiology* **143**: 947–56.
- Murray, D.S., Chinnam, N., Tonthat, N.K., Whitfill, T., Wray, L.V., Fisher, S.H., and Schumacher, M.A.** (2013) Structures of the *Bacillus subtilis* glutamine synthetase dodecamer reveal large intersubunit catalytic conformational changes linked to a unique feedback inhibition mechanism. *J Biol Chem* **288**: 35801–11.
- Näsvall, J., Sun, L., Roth, J.R., and Andersson, D.I.** (2012) Real-time evolution of new genes by innovation, amplification, and divergence. *Science* **338**: 384–7.
- Nessler, S., Fieulaine, S., Poncet, S., Galinier, A., Deutscher, J., and Janin, J.** (2003) HPr kinase/phosphorylase, the sensor enzyme of catabolite repression in Gram-positive bacteria: structural aspects of the enzyme and the complex with its protein substrate. *J Bacteriol* **185**: 4003–10.
- Nicolas, P., Mäder, U., Dervyn, E., Rochat, T., Leduc, A., Pigeonneau, N., et al.** (2012) Condition-dependent transcriptome reveals high-level regulatory architecture in *Bacillus subtilis*. *Science* **335**: 1103–06.
- Noda-Garcia, L., Romero Romero, M.L., Longo, L.M., Kolodkin-Gal, I., and Tawfik, D.S.** (2017) *Bacilli* glutamate dehydrogenases diverged via coevolution of transcription and enzyme regulation. *EMBO Rep* **18**: 1139–49.

- Ogawa, T., and Okazaki, T. (1984) Function of RNase H in DNA replication revealed by RNase H defective mutants of *Escherichia coli*. *Mol Gen Genet* **193**: 231–7.
- Oh, Y.-K., Palsson, B.O., Park, S.M., Schilling, C.H., and Mahadevan, R. (2007) Genome-scale reconstruction of metabolic network in *Bacillus subtilis* based on high-throughput phenotyping and gene essentiality data. *J Biol Chem* **282**: 28791–9.
- Ohtani, N., Haruki, M., Morikawa, M., Crouch, R.J., Itaya, M., and Kanaya, S. (1999) Identification of the genes encoding Mn²⁺-dependent RNase HII and Mg²⁺-dependent RNase HIII from *Bacillus subtilis*: classification of RNases H into three families. *Biochemistry* **38**: 605–18.
- Paul, S., Million-Weaver, S., Chattopadhyay, S., Sokurenko, E., and Merrikh, H. (2013) Accelerated gene evolution through replication-transcription conflicts. *Nature* **495**: 512–5.
- Pérez-Rueda, E., and Collado-Vides, J. (2000) The repertoire of DNA-binding transcriptional regulators in *Escherichia coli* K-12. *Nucleic Acids Res* **28**: 1838–47.
- Picossi, S., Belitsky, B.R., and Sonenshein, A.L. (2007) Molecular mechanism of the regulation of *Bacillus subtilis* *gltAB* expression by GltC. *J Mol Biol* **365**: 1298–313.
- Pietack, N. (2010) Investigation of glycolysis in *Bacillus subtilis*. *Dissertation*.
- Podgornaia, A.I., Casino, P., Marina, A., and Laub, M.T. (2013) Structural basis of a rationally rewired protein-protein interface critical to bacterial signaling. *Structure* **21**: 1636–47.
- Podgornaia, A.I., and Laub, M.T. (2015) Pervasive degeneracy and epistasis in a protein-protein interface. *Science* **347**: 673–7.
- Pomerantz, R.T., and O'Donnell, M. (2008) The replisome uses mRNA as a primer after colliding with RNA polymerase. *Nature* **456**: 762–6.
- Pomerantz, R.T., and O'Donnell, M. (2010a) Direct restart of a replication fork stalled by a head-on RNA polymerase. *Science* **327**: 590–2.
- Pomerantz, R.T., and O'Donnell, M. (2010b) What happens when replication and transcription complexes collide? *Cell Cycle* **9**: 2537–43.
- Probst, C., Grünberger, A., Braun, N., Helfrich, S., Nöh, K., Wiechert, W., and Kohlheyer, D. (2015) Rapid inoculation of single bacteria into parallel picoliter fermentation chambers. *Anal Methods* **7**: 91–8.
- Qin, W., Liu, N.-N., Wang, L., Zhou, M., Ren, H., Bugnard, E., et al. (2014) Characterization of biochemical properties of *Bacillus subtilis* RecQ helicase. *J Bacteriol* **196**: 4216–28.
- Raschle, T., Amrhein, N., and Fitzpatrick, T.B. (2005) On the two components of pyridoxal 5'-phosphate synthase from *Bacillus subtilis*. *J Biol Chem* **280**: 32291–300.
- Ratnayake-Lecamwasam, M., Serror, P., Wong, K.-W., and Sonenshein, A.L. (2001) *Bacillus subtilis* CodY represses early-stationary-phase genes by sensing GTP levels. *Genes Dev* **15**: 1093–103.
- Reams, A.B., Kofoid, E., Kugelberg, E., and Roth, J.R. (2012) Multiple pathways of duplication formation with and without recombination (RecA) in *Salmonella enterica*. *Genetics* **192**: 397–415.
- Reams, A.B., Kofoid, E., Savageau, M., and Roth, J.R. (2010) Duplication frequency in a population of *Salmonella enterica* rapidly approaches steady state with or without recombination. *Genetics* **184**: 1077–94.
- Reitzer, L. (2003) Nitrogen assimilation and global regulation in *Escherichia coli*. *Annu Rev Microbiol* **57**: 155–76.
- Reuß, D.R., Altenbuchner, J., Mäder, U., Rath, H., Ischebeck, T., Sappa, K., et al. (2017) Large-scale reduction of the *Bacillus subtilis* genome: consequences for the transcriptional network, resource allocation, and metabolism. **27**: 289-99.
- Reuter, J.S., and Mathews, D.H. (2010) RNAstructure: software for RNA secondary structure prediction and analysis. *BMC Bioinformatics* **11**: 129.
- Rocha, E.P.C., Cornet, E., and Michel, B. (2005) Comparative and evolutionary analysis of the bacterial homologous recombination systems. *PLoS Genet* **1**: e15.
- Rocha, E.P.C., and Danchin, A. (2003) Essentiality, not expressiveness, drives gene-strand bias in bacteria. *Nat Genet* **34**: 377–8.
- Rosenberg, J., Ischebeck, T., and Commichau, F.M. (2017) Vitamin B6 metabolism in microbes and approaches for fermentative production. *Biotechnol Adv* **35**: 31–40.
- Roth, J.R., Benson, N., Galitski, T., Haack, K., Lawrence, J.G., and Miesel, L. (1996) Rearrangements of the bacterial chromosome: formation and applications. p. 2256–76. In F.C. Neidhardt et al. (ed.), *Escherichia coli and Salmonella: cellular and molecular biology*. ASM Press, Washington, D.C.
- RStudio Team (2016) RStudio: Integrated Development Environment for R. <http://www.rstudio.com/>.
- Sakai, A., and Cox, M.M. (2009) RecFOR and RecOR as distinct RecA loading pathways. *J Biol Chem*

References

- 284: 3264–72.
- Salazar, M.E., and Laub, M.T.** (2015) Temporal and evolutionary dynamics of two-component signaling pathways. *Curr Opin Microbiol* **24**: 7–14.
- Sambrook, J., Fritsch, E.F., and Maniatis, T.** (1989) *Molecular cloning: a laboratory manual*. 2nd ed., Cold Spring Harbor Laboratory Press, Cold Spring Harbor, New York.
- Sanchez, H., Carrasco, B., Cozar, M.C., and Alonso, J.C.** (2007) *Bacillus subtilis* RecG branch migration translocase is required for DNA repair and chromosomal segregation. *Mol Microbiol* **65**: 920–35.
- Sanchez, H., Kidane, D., Cozar, M.C., Graumann, P.L., and Alonso, J.C.** (2006) Recruitment of *Bacillus subtilis* RecN to DNA double-strand breaks in the absence of DNA end processing. *J Bacteriol* **188**: 353–60.
- Sanchez, H., Kidane, D., Reed, P., Curtis, F.A., Cozar, M.C., Graumann, P.L., et al.** (2005) The RuvAB branch migration translocase and RecU Holliday junction resolvase are required for double-stranded DNA break repair in *Bacillus subtilis*. *Genetics* **171**: 873–83.
- Sanger, F., Nicklen, S., and Coulson, A.R.** (1977) DNA sequencing with chain-terminating inhibitors. *Proc Natl Acad Sci USA* **74**: 5463–7.
- Sankar, T.S., Wastuwidyaningtyas, B.D., Dong, Y., Lewis, S.A., and Wang, J.D.** (2016) The nature of mutations induced by replication–transcription collisions. *Nature* **535**: 178–81.
- Sasse, J., and Gallagher, S.R.** (2009) Staining proteins in gels. *Curr Protoc Mol Biol* **85**: 10.6.1–10.6.27.
- Schindelin, J., Arganda-Carreras, I., Frise, E., Kaynig, V., Longair, M., Pietzsch, T., et al.** (2012) Fiji: an open-source platform for biological-image analysis. *Nat Methods* **9**: 676–82.
- Schmidt, K.H., Reimers, J.M., and Wright, B.E.** (2006) The effect of promoter strength, supercoiling and secondary structure on mutation rates in *Escherichia coli*. *Mol Microbiol* **60**: 1251–61.
- Schneider, B.L., Kiupakis, A.K., and Reitzer, L.J.** (1998) Arginine catabolism and the arginine succinyltransferase pathway in *Escherichia coli*. *J Bacteriol* **180**: 4278–86.
- Schofield, M.J., and Hsieh, P.** (2003) DNA mismatch repair: molecular mechanisms and biological function. *Annu Rev Microbiol* **57**: 579–608.
- Schumacher, M.A., Chinnam, N.B., Cuthbert, B., Tonthat, N.K., and Whitfill, T.** (2015) Structures of regulatory machinery reveal novel molecular mechanisms controlling *B. subtilis* nitrogen homeostasis. *Genes Dev* **29**: 451–64.
- Schumacher, M.A., Seidel, G., Hillen, W., and Brennan, R.G.** (2007) Structural mechanism for the fine-tuning of CcpA function by the small molecule effectors glucose 6-phosphate and fructose 1,6-bisphosphate. *J Mol Biol* **368**: 1042–50.
- Sharkey, M.A., and Engel, P.C.** (2008) Apparent negative co-operativity and substrate inhibition in overexpressed glutamate dehydrogenase from *Escherichia coli*. *FEMS Microbiol Lett* **281**: 132–9.
- Sheehan, B., Klarsfeld, A., Msadek, T., and Cossart, P.** (1995) Differential activation of virulence gene expression by PrfA, the *Listeria monocytogenes* virulence regulator. *J Bacteriol* **177**: 6469–76.
- Shivers, R.P., and Sonenshein, A.L.** (2004) Activation of the *Bacillus subtilis* global regulator CodY by direct interaction with branched-chain amino acids. *Mol Microbiol* **53**: 599–611.
- Shyamala, V., Schneider, E., and Ames, G.F.-L.** (1990) Tandem chromosomal duplications: role of REP sequences in the recombination event at the join-point. *EMBO J* **9**: 939–46.
- Smaldone, G.T., Revelles, O., Gaballa, A., Sauer, U., Antelmann, H., and Helmann, J.D.** (2012) A global investigation of the *Bacillus subtilis* iron-sparing response identifies major changes in metabolism. *J Bacteriol* **194**: 2594–2605.
- Sonenshein, A.L.** (2007) Control of key metabolic intersections in *Bacillus subtilis*. *Nat Rev Microbiol* **5**: 917–27.
- Spaans, S.K., Weusthuis, R.A., van der Oost, J., and Kengen, S.W.M.** (2015) NADPH-generating systems in bacteria and archaea. *Front Microbiol* **6**: 742.
- Spies, M., Bianco, P.R., Dillingham, M.S., Handa, N., Baskin, R.J., and Kowalczykowski, S.C.** (2003) A molecular throttle: the recombination hotspot χ controls DNA translocation by the RecBCD helicase. *Cell* **114**: 647–54.
- Srere, P.A.** (1984) Why are enzymes so big? *TIBS* **9**: 387–90.
- Srivatsan, A., Tehranchi, A., MacAlpine, D.M., and Wang, J.D.** (2010) Co-orientation of replication and transcription preserves genome integrity. *PLoS Genet* **6**: e1000810.
- Stannek, L.** (2015) Control of glutamate homeostasis in the Gram-positive model organism *Bacillus subtilis*. *Dissertation*.
- Stannek, L., Gunka, K., Care, R.A., Gerth, U., and Commichau, F.M.** (2015a) Factors that mediate and prevent degradation of the inactive and unstable GudB protein in *Bacillus subtilis*. *Front Microbiol* **5**: 758.

- Stannek, L., Thiele, M.J., Ischebeck, T., Gunka, K., Hammer, E., Völker, U., and Commichau, F.M.** (2015b) Evidence for synergistic control of glutamate biosynthesis by glutamate dehydrogenases and glutamate in *Bacillus subtilis*. *Environ Microbiol* **17**: 3379–90.
- Sterlini, J.M., and Mandelstam, J.** (1969) Commitment to sporulation in *Bacillus subtilis* and its relationship to development of actinomycin resistance. *Biochem J* **113**: 29–37.
- Streisinger, G., Okada, Y., Emrich, J., Newton, J., Tsugita, A., Terzaghi, E., and Inouye, M.** (1966) Frameshift mutations and the genetic code. *Cold Spring Harb Symp Quant Biol* **31**: 77–84.
- Stülke, J., Arnaud, M., Rapoport, G., and Martin-Verstraete, I.** (1998) PRD - a protein domain involved in PTS-dependent induction and carbon catabolite repression of catabolic operons in bacteria. *Mol Microbiol* **28**: 865–74.
- Stülke, J., and Hillen, W.** (2000) Regulation of carbon catabolism in *Bacillus* species. *Annu Rev Microbiol* **54**: 849–80.
- Stülke, J., Martin-Verstraete, I., Zagorec, M., Rose, M., Klier, A., and Rapoport, G.** (1997) Induction of the *Bacillus subtilis ptsGHI* operon by glucose is controlled by a novel antiterminator, GlcT. *Mol Microbiol* **25**: 65–78.
- Sung, H.-M., and Yasbin, R.E.** (2002) Adaptive, or stationary-phase, mutagenesis, a component of bacterial differentiation in *Bacillus subtilis*. *J Bacteriol* **184**: 5641–53.
- Suzuki, A., and Knaff, D.B.** (2005) Glutamate synthase: structural, mechanistic and regulatory properties, and role in the amino acid metabolism. *Photosynth Res* **83**: 191–217.
- Tadokoro, T., and Kanaya, S.** (2009) Ribonuclease H: Molecular diversities, substrate binding domains, and catalytic mechanism of the prokaryotic enzymes. *FEBS J* **276**: 1482–93.
- Thiele, M.** (2013) Role of transcription in the specific activation of the cryptic *gudB^{CR}* glutamate dehydrogenase gene in the Gram-positive model bacterium *Bacillus subtilis*. *Master Thesis* .
- Tholen, S.** (2009) Charakterisierung des *gudB*-Gens aus *Bacillus subtilis*. *Diplomarbeit* .
- Trautinger, B.W., Jaktaji, R.P., Rusakova, E., and Lloyd, R.G.** (2005) RNA polymerase modulators and DNA repair activities resolve conflicts between DNA replication and transcription. *Mol Cell* **19**: 247–58.
- Vavrová, L., Muchová, K., and Barák, I.** (2010) Comparison of different *Bacillus subtilis* expression systems. *Res Microbiol* **161**: 91–797.
- Vinces, M.D., Legendre, M., Caldara, M., Hagihara, M., and Verstrepen, K.J.** (2009) Unstable tandem repeats in promoters confer transcriptional evolvability. *Science* **324**: 1213–6.
- Wach, A.** (1996) PCR-synthesis of marker cassettes with long flanking homology regions for gene disruptions in *S. cerevisiae*. *Yeast* **12**: 259–65.
- Wacker, I., Ludwig, H., Reif, I., Blencke, H.-M., Detsch, C., and Stülke, J.** (2003) The regulatory link between carbon and nitrogen metabolism in *Bacillus subtilis*: regulation of the *gltAB* operon by the catabolite control protein CcpA. *Microbiology* **149**: 3001–9.
- Wang, G., and Vasquez, K.M.** (2017) Effects of replication and transcription on DNA structure-related genetic instability. *Genes* **8**: 17.
- Washburn, R.S., and Gottesman, M.E.** (2011) Transcription termination maintains chromosome integrity. *Proc Natl Acad Sci USA* **108**: 792–7.
- Welsch, N., Homuth, G., and Schweder, T.** (2015) Stepwise optimization of a low-temperature *Bacillus subtilis* expression system for “difficult to express” proteins. *Appl Microbiol Biotechnol* **99**: 6363–76.
- Whatmore, A.M., Chudek, J.A., and Reed, R.H.** (1990) The effects of osmotic upshock on the intracellular solute pools of *Bacillus subtilis*. *J Gen Microbiol* **136**: 2527–35.
- Wigley, D.B.** (2013) Bacterial DNA repair: recent insights into the mechanism of RecBCD, AddAB and AdnAB. *Nat Rev Microbiol* **11**: 9–13.
- Woodcock, D.M., Crowther, P.J., Doherty, J., Jefferson, S., DeCruz, E., Noyer-Weidner, M., et al.** (1989) Quantitative evaluation of *Escherichia coli* host strains for tolerance to cytosine methylation in plasmid and phage recombinants. *Nucleic Acids Res* **17**: 3469–78.
- Wray, L.V., Ferson, A.E., Rohrer, K., and Fisher, S.H.** (1996) TnrA, a transcription factor required for global nitrogen regulation in *Bacillus subtilis*. *Proc Natl Acad Sci USA* **93**: 8841–5.
- Wray, L.V., Zalieckas, J.M., and Fisher, S.H.** (2001) *Bacillus subtilis* glutamine synthetase controls gene expression through a protein-protein interaction with transcription factor TnrA. *Cell* **107**: 427–35.
- Xu, L., and Mariani, K.J.** (2003) PriA mediates DNA replication pathway choice at recombination intermediates. *Mol Cell* **11**: 817–26.
- Yadav, T., Carrasco, B., Serrano, E., and Alonso, J.C.** (2014) Roles of *Bacillus subtilis* DprA and SsbA in RecA-mediated genetic recombination. *J Biol Chem* **289**: 27640–52.
- Yanisch-Perron, C., Vieira, J., and Messing, J.**

References

- (1985) Improved M13 phage cloning vectors and host strains: nucleotide sequences of the M13mp18 and pUC19 vectors. *Gene* **33**: 103–19.
- Yao, N.Y., Schroeder, J.W., Yurieva, O., Simmons, L.A., and O'Donnell, M.E.** (2013) Cost of rNTP/dNTP pool imbalance at the replication fork. *Proc Natl Acad Sci USA* **110**: 12942–7.
- Yeeles, J.T.P., and Dillingham, M.S.** (2010) The processing of double-stranded DNA breaks for recombinational repair by helicase-nuclease complexes. *DNA Repair* **9**: 276–85.
- Yoshikawa, K., Okazaki, I.-M., Eto, T., Kinoshita, K., Muramatsu, M., Nagaoka, H., and Honjo, T.** (2002) AID enzyme-induced hypermutation in an actively transcribed gene in fibroblasts. *Science* **296**: 2033–6.
- Yuan, J., Fowler, W.U., Kimball, E., Lu, W., and Rabinowitz, J.D.** (2006) Kinetic flux profiling of nitrogen assimilation in *Escherichia coli*. *Nat Chem Biol* **2**: 529–30.
- Zeigler, D.R., Prágai, Z., Rodriguez, S., Chevreux, B., Muffler, A., Albert, T., et al.** (2008) The origins of 168, W23, and other *Bacillus subtilis* legacy strains. *J Bacteriol* **190**: 6983–95.
- Zhang, J., and Landick, R.** (2016) A Two-Way Street: Regulatory interplay between RNA polymerase and nascent RNA structure. *Trends Biochem Sci* **41**: 293–310.
- Zhang, W., Gao, W., Feng, J., Zhang, C., He, Y., Cao, M., et al.** (2014) A markerless gene replacement method for *B. amyloliquefaciens* LL3 and its use in genome reduction and improvement of poly- γ -glutamic acid production. *Appl Microbiol Biotechnol* **98**: 8963–73.
- Zhou, K., Aertsen, A., and Michiels, C.W.** (2014) The role of variable DNA tandem repeats in bacterial adaptation. *FEMS Microbiol Rev* **38**: 119–41.

6. Appendix

6.1. Supplementary information

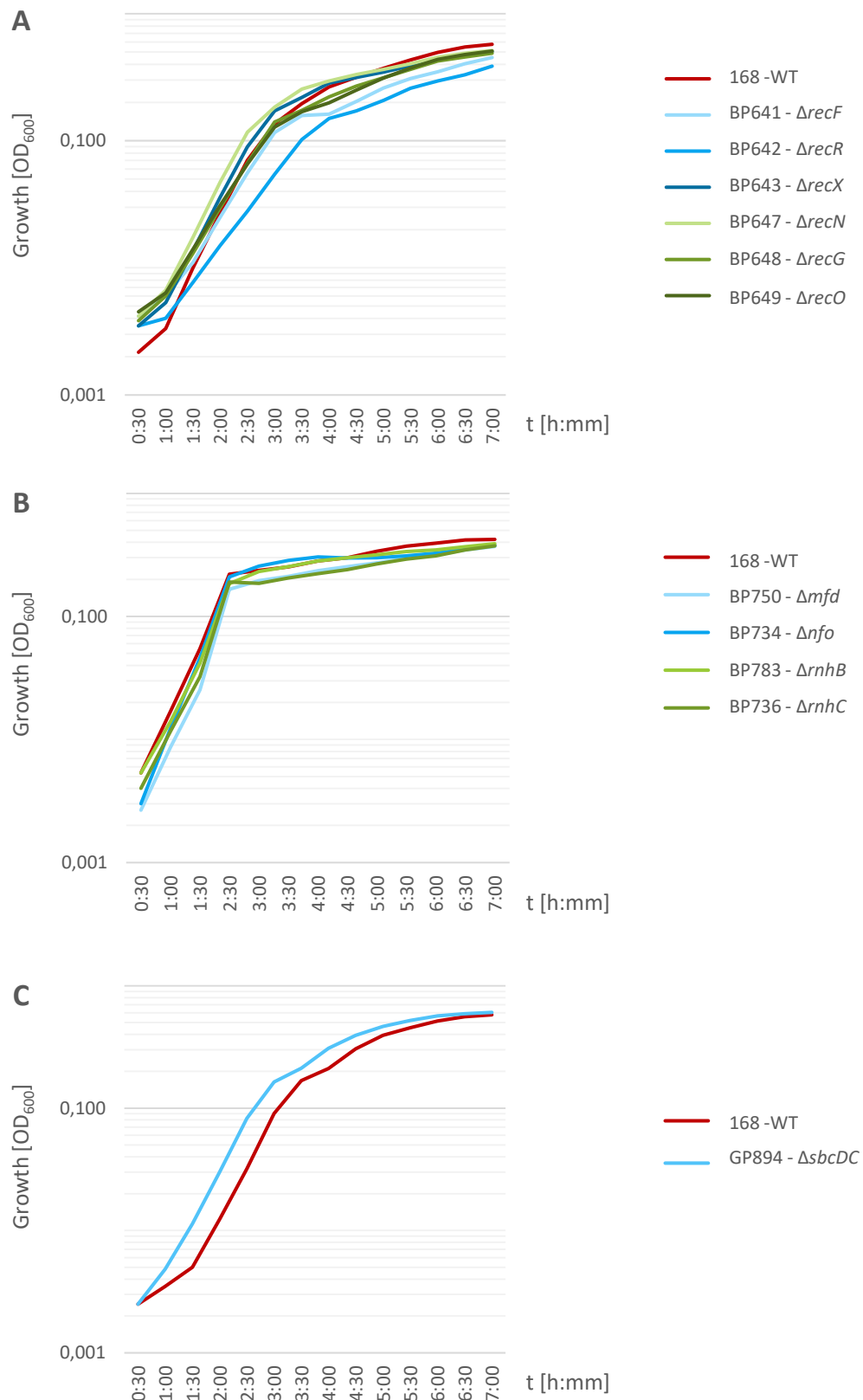


Fig. 6.1 Growth curves of WT and single deletion mutants

Cells were grown in C-Glc medium to an OD₆₀₀ of 0.5 to 0.8, washed twice in 1x C-salts thereby the OD₆₀₀ was adjusted to 0.6. The growth analysis in a microplate reader was performed in SP medium at 37 °C.

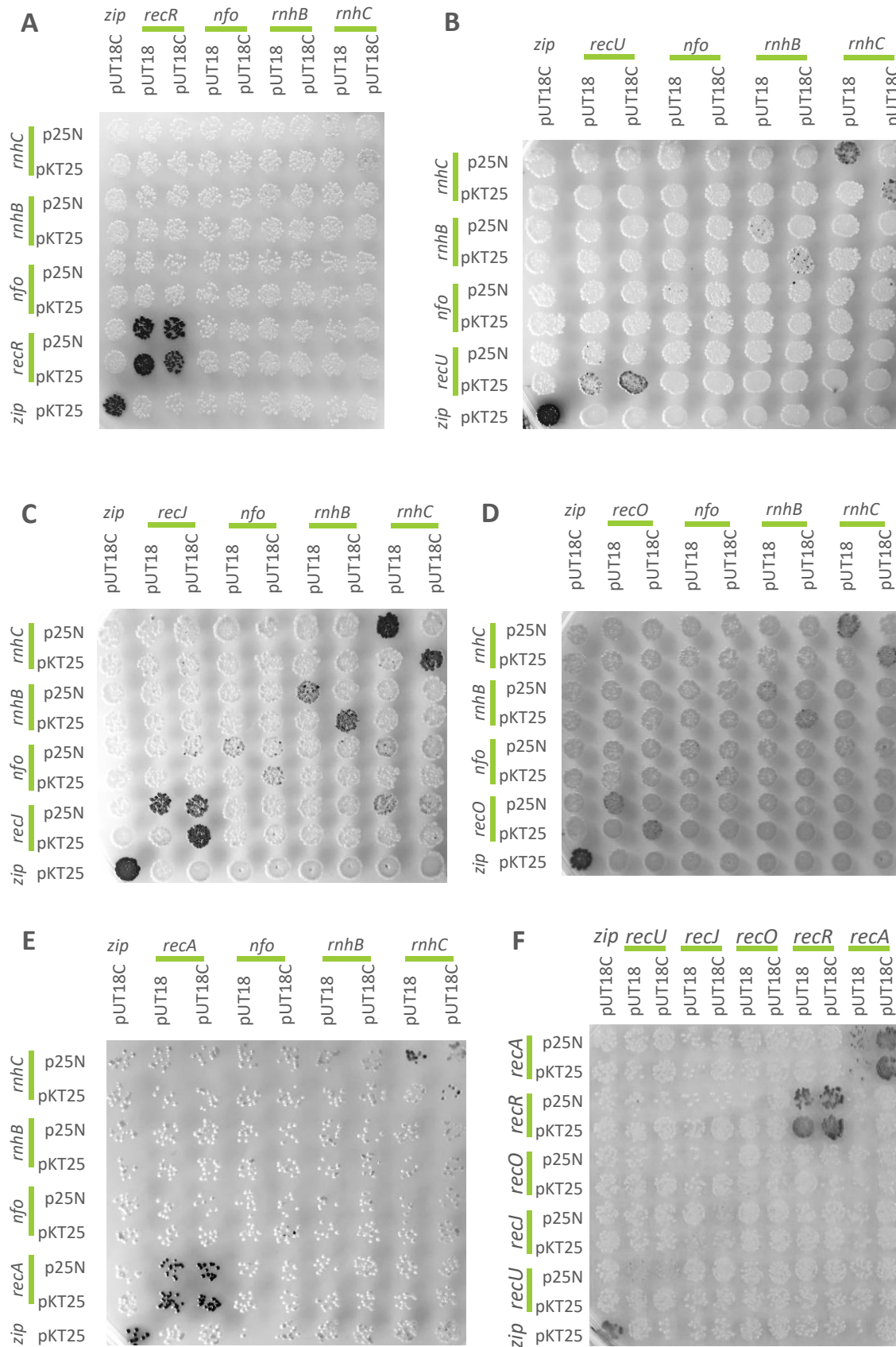


Fig. 6.2 *In vivo* interaction analysis of factors involved in TR mutagenesis
 BACTH of putative factors involved in TR mutagenesis. See 6.5 Plasmids for detailed information about the plasmids cloned into BTH101. The plates were incubated for 2 d and stored at 4 °C for at least two weeks, to stop growth but not metabolism, thereby the blue color was enhanced.

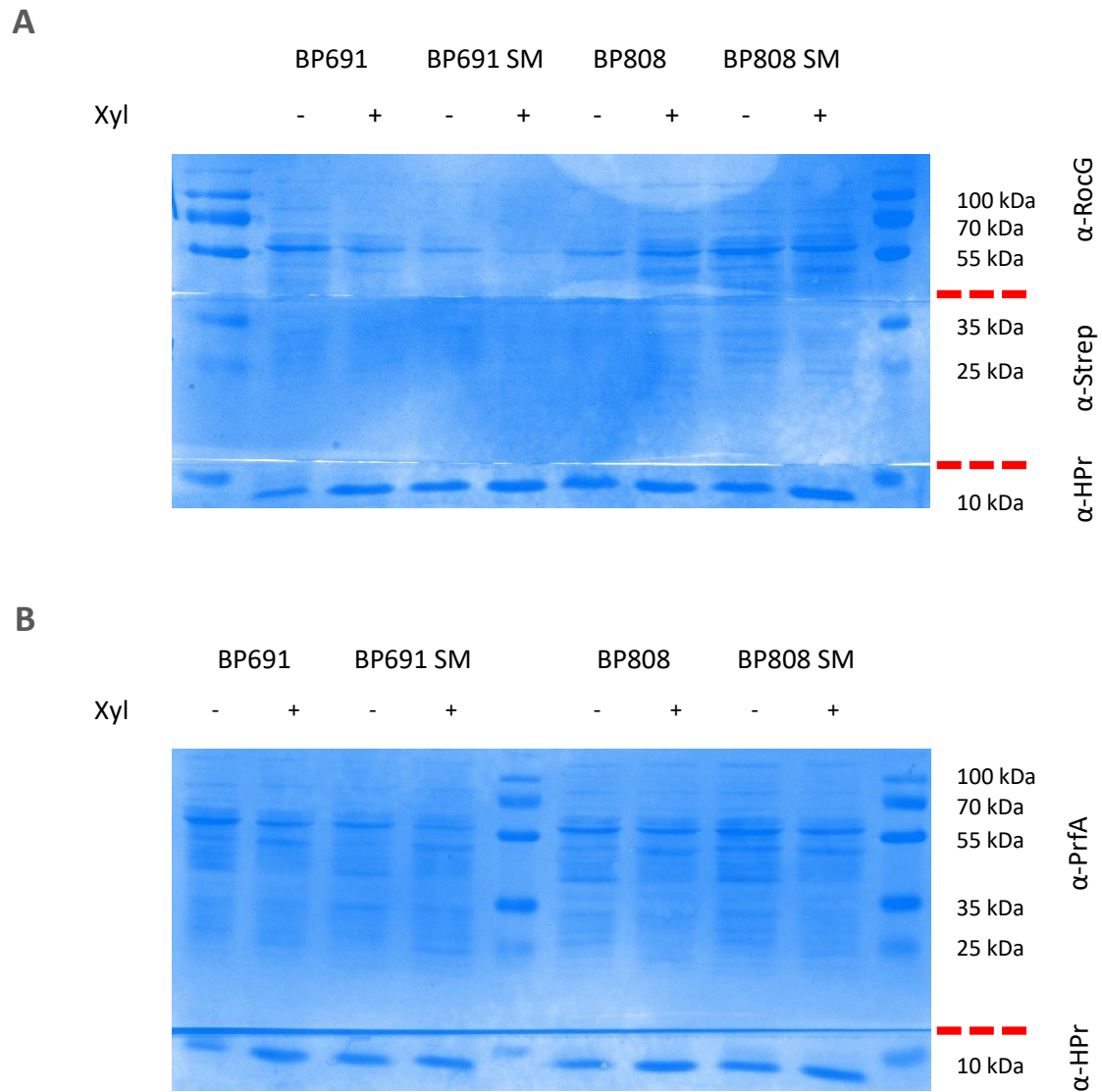


Fig. 6.3 Coomassie stain of the overexpression of heterologous proteins using the activator/reporter system. A fresh colony of BP691, BP808 and respective SMs from an SP pate were used to inoculate 40 ml of SP medium, grown at 37 °C until an OD₆₀₀ of 0.5, split and half of the cultures were supplemented with 0.1 % xylose. After 4 h of growth, the cultures were harvested for microscopic and Western blot analysis. **A:** Coomassie stained Western blot analysis of GudB, PdxST-Strep and HPr (Fig. 3.17 B). The membrane was cut in 3 parts (red lines) to allow the use of different antibodies. The signal of HPr was very strong, therefore a second exposure with only the upper two parts of the Western blot was performed. **B:** Coomassie stained Western blot analysis of PrfA and HPr (Fig. 3.17 C).

6.2. Materials

6.2.1. Chemicals

Acrylamide	Carl Roth, Karlsruhe
Agar	Carl Roth, Karlsruhe
Agarose	Peqlab, Erlangen
Ammonium iron (III) sulfate	Sigma-Aldrich, Taufkirchen
Ammonium peroxydisulfate	Carl Roth, Karlsruhe
Antibiotics	Sigma-Aldrich, Taufkirchen
Bacto agar	Becton, Dickinson and Company, Heidelberg
Blocking reagent	Roche Diagnostics, Mannheim
Bromophenol blue	Serva, Heidelberg
Casein, acidic/hydrolyzed	Sigma-Aldrich, Taufkirchen
CDP*	Roche Diagnostics, Mannheim
Coomassie Brilliant Blue G250	Carl Roth, Karlsruhe
Coomassie Brilliant Blue R350	Amersham, Freiburg
D(+)-Glucose	Merck, Darmstadt
dNTPs	Roche Diagnostics, Mannheim
Imidazole	Sigma-Aldrich, Taufkirchen
Ni ²⁺ -NTA Sepharose	IBA-Göttingen
Skim milk powder, fat-free	Carl Roth, Karlsruhe
TEMED	Carl-Roth, Karlsruhe
Tryptone	Oxoid, Heidelberg
Tween 20	Sigma, München
X-Gal	Peqlab, Erlangen
Yeast Extract	Oxoid, Heidelberg
β-mercaptoethanol	Sigma-Aldrich, Taufkirchen

Other chemicals were also purchased from Merck, Peqlab, Sigma-Aldrich or Carl Roth.

6.2.2. Antibodies

Anti-Digoxigenin-AP, Fab Fragments	Roche Diagnostics, Mannheim
Anti-GudB	Ulf Gerth, Greifswald
Anti-RocG	Commichau <i>et al.</i> , 2007a
Anti-GFP	Medical & Biological Laboratories
Anti-HPr	Monedero <i>et al.</i> , 2001
Anti-Strep	IBA, Göttingen
Anti-Rabbit IgG-AP secondary antibody	Promega, Madison

6.2.3. Enzymes

Ampligase	Epicentre, USA
DNase I	Roche Diagnostics, Mannheim
FastAP™	ThermoFisher, Waltham
Lysozyme	Merck, Darmstadt
Phusion™ DNA polymerase	Biozym, Hessisch Oldendorf
Restriction endonucleases	ThermoFisher, Waltham
RNase A	Roche Diagnostics, Mannheim
T4-DNA ligase	Roche Diagnostics, Mannheim
T7 RNA polymerases	ThermoFisher, Waltham
Taq DNA polymerase	MBI Fermentas, St. Leon-Rot

6.2.4. Commercial systems

HDGreen Plus DNA Stain	Intas, Göttingen
NucleoSpin Plasmid-Kit	Macherey-Nagel, Düren
PageRuler™ Plus Prestained Protein Ladder	ThermoFisher, Waltham

peqGOLD Bacterial DNA Kit	PEQLAB, Erlangen
peqGOLD PCR Purification Kit	PEQLAB, Erlangen
QIAquick PCR Purification Kit	Qiagen, Hilden
DIG RNA Labelling Mix	Roche Diagnostics, Mannheim
Protector RNase Inhibitor	Roche Diagnostics, Mannheim

6.2.5. Equipment

300 W Xenon light source	Sutter Instruments, USA
ANDOR LUCA R DL604 EMCCD camera	Andor Technology plc., Belfast
ChemoCam Imager	Intas, Göttingen
Fluorescence microscope Axioskop 40FL + AxioCam MRm	Zeiss, Göttingen
French pressure cell press	SLM Aminco, Lorch
French pressure cell press	Spectonic Unicam, England
GelDoc™ XR+	Biorad, München
Microplate reader SynergyMx Mini-Protean	BioTek, Bad Friedrichshall
neMESYS pumps	Cetoni, Korbussen
Nikon Eclipse Ti	Nikon Instruments, Inc., New York
OV1 mini hybridization oven	Biometra
Stereo fluorescence microscope Lumar V.12	Zeiss, Göttingen

Ultra centrifuge, Sorvall WX Ultra 80	ThermoFisher, Bonn
VacuGene™ XL	GE Healthcare, Freiburg
YFPHQ (EX 490-550 nm, DM 510 nm, BA 520-560 nm)	Nikon Instruments, Inc., New York

6.2.6. Dispensable equipment

CORNING Cell culture dishes 24.5 x 24.5 cm	Omnilab, Bremen
Nylon membrane, positively charged	Roche Diagnostics, Mannheim
Polyvinylidendifluorid-Membran (PVDF)	Bio-Rad Laboratories GmbH, München
Filtropur S 0.2 µm	Sarstedt, Nümbrecht
Minisart® High Flow Syringe Filter 0.1 µm	Sartorius, Göttingen

6.3. Oligonucleotides

6.3.1. Oligonucleotides constructed in this work

Name	Sequence	Purpose/Reference
MD1	GAATTCTTCTGCTTGAGCGTTTCATTTGAGTTAACCTCCTAG AATCTTCTGTT	<i>P_{gudB}</i> _rev with <i>prfA</i> overhang
MD2	ATGAACGCTCAAGCAGAAGAATTC	<i>prfA</i> _fwd
MD3	AAACTGCAGCATTAGCTTTTCAGAAAGCTTACAGCGAATC	<i>P_{gudB}</i> _fwd [<i>Pst</i> I]
MD4	AAACAATTGGAATTCGGATCCAAAGGAGGAAACAATCAT GAGTAAAGGA	<i>gfp</i> _fwd with SD(<i>gapA</i>) [<i>Bam</i> HI, <i>Eco</i> RI, <i>Mfe</i> I] (pBP9)
MD5	TTTGGATCCATTAGTATATTCCTATCTTAAAGTGACTTTTA TGTT	<i>P_{plcA}</i> _rev without SD(<i>plcA</i>) [<i>Bam</i> HI]
MD6	CAACCATTACCTGTCCACACAATC	<i>gfp</i> _fwd sequencing primer (100 bp)
MD7	GTTTTCCGTATGTTGCATCACCTT	<i>gfp</i> _rev sequencing primer (100 bp)
MD8	TTTCTCGAGCATTAGCTTTTCAGAAAGCTTACAGCGAATC	<i>P_{gudB}</i> _fwd [<i>Xho</i> I]
MD9	AAAGGTACCTTAATTTAATTTTCCCAAGTAGCAGGACAT GC	<i>prfA</i> _rev [<i>Kpn</i> I]
MD10	ATAACTTCGTATAGCATAACATTATACGAACGGTAGTTGAT GATTTGCATAAAAAATAAAAAATCTCCTATG	<i>gudB</i> _downstream region_fwd with <i>lox66</i> overhang (LFH PCR)
MD11	AACACAATTCATTCTCGGTGATTTT	<i>gudB</i> _downstream region_rev (LFH PCR)
MD12	ATAATGTGTTATATGATTTGTGTGCAAGT	<i>gudB</i> _upstream region_fwd (LFH PCR)
MD13	GCATGCTGCTACTTGGGGAAAATTAATTAATTGAGTT AACCTCCTAGAATCTTCTGTT	<i>gudB</i> _upstream region_rev with <i>prfA</i> overhang (LFH PCR)
MD14	ATAACTTCGTATAGCATAACATTATACGAACGGTAGTTGAG AAGCTCCGCAAATAATT	<i>rocG</i> _downstream region_fwd with <i>lox66</i> overhang (LFH PCR)
MD15	CTGTTCCCGCCATAATCGC	<i>rocG</i> _downstream region_rev (LFH PCR)
MD16	CCAAGTGTTAATATTCCTTAAAAACATTTACTT	<i>rocG</i> _upstream region_fwd (LFH PCR)
MD17	GCATGCTGCTACTTGGGGAAAATTAATTAACTTTTCA CCTCATTGTTTTTTGGC	<i>rocG</i> _upstream region_rev with <i>prfA</i> overhang (LFH PCR)
MD18	GTGCTTGTCTTACTAGTGAECTCA	<i>gudB</i> _upstream region_fwd (LFH sequencing)
MD19	CTGTCATGGCAAATACAAAATCATTTT	<i>gudB</i> _downstream region_rev (LFH sequencing)
MD20	CCTTGATAAACAGGAAGGAATTCTCAT	<i>rocG</i> _upstream region_fwd (LFH sequencing)
MD21	GTCAGCCGGTTTTAAGAGAATCG	<i>rocG</i> _downstream region_rev (LFH sequencing)
MD22	CAGTTGAATCTTAATAATTAATCACCAAATAATG	<i>ynaI</i> _upstream region_fwd
MD23	TCTATTTAGAACTCCTTTTCATATGAGAAG	<i>xyIR</i> _downstream region_rev (sequencing primer)
MD24	TTAAAGATTAACAAATGGAGTGGATGAAG	<i>xyIR</i> _upstream region_fwd
MD25	GCCGATTACTTCTTGAGGATTATAATATT	<i>P_{xyIR}</i> _upstream region_fwd (sequencing of the promoter region of <i>xyIR</i>)
MD26	AGCTCCAATTCGCCCTATAGTTGATGATTTGCATAAAAAAT AAAAATCTCCTATG	<i>gudB</i> _downstream region_fwd with overhang to pBP407 (LFH PCR)
MD27	GCATGCTGCTACTTGGGGAAAATTAATTAATTATGAA AAATGAGTTTGTATCGTTTCTACG	<i>P_{gudB}</i> _upstream region_rev with overhang to <i>prfA</i> (LFH PCR)
MD28	AGCTCCAATTCGCCCTATATTTGAGAAGCTCCGCAAAT AATT	<i>rocG</i> _downstream region_fwd with overhang to pBP407 (LFH PCR)
MD29	AAGGATCTGCTTTGATGGGTATC	<i>bpr</i> _upstream region_fwd (LFH PCR)

Name	Sequence	Purpose/Reference
MD30	GCATGTCCTGCTACTTGGGGAAAATTAATTAATTCATC CCCCTTTTTCAACATGC	<i>bpr</i> _upstream region_rev with <i>prfA</i> overhang (LFH PCR)
MD31	AGCTCCAATTCGCCCTATAGTGGAAGGCTGCCGTCA	<i>bpr</i> _downstream region_fwd with overhang to pBP407 (LFH PCR)
MD32	AATGTAATGATCATTACCGGTGTTTTG	<i>bpr</i> _downstream region_rev (LFH PCR)
MD33	GAAACGGTTTGCTGGATGA	<i>xkdE</i> _upstream region_fwd (LFH PCR)
MD34	GCATGTCCTGCTACTTGGGGAAAATTAATTAAGATTTAT GACCTCCTCTTCTCG	<i>xkdE</i> _upstream region_rev with <i>prfA</i> overhang (LFH PCR)
MD35	AGCTCCAATTCGCCCTATAAGGGAGGTGAATCAAGCAGG	<i>xkdE</i> _downstream region_fwd with overhang to pBP407 (LFH PCR)
MD36	TATTGCCGCCGTATCGT	<i>xkdE</i> _downstream region_rev (LFH PCR)
MD37	GATCCACTTTATCCTCATAGCCAAG	<i>sacB</i> _upstream region_fwd (LFH PCR)
MD38	GCATGTCCTGCTACTTGGGGAAAATTAATTAACGTTTCAT GTCTCCTTTTTATGACTG	<i>sacB</i> _upstream region_rev with <i>prfA</i> overhang (LFH PCR)
MD39	AGCTCCAATTCGCCCTATAAAACGCAAAAGAAAATGCCGA T	<i>sacB</i> _downstream region_fwd with overhang to pBP407 (LFH PCR)
MD40	AGGCGTACGTATTTGGTTTGC	<i>sacB</i> _downstream region_rev (LFH PCR)
MD41	GGGGTTCAAGGTATTTCTGACTTG	<i>bpr</i> _upstream region_fwd (LFH sequencing)
MD42	TTTATCTAAAAAGCGAAAGGAATCATCG	<i>bpr</i> _downstream region_rev (LFH sequencing)
MD43	CGCCATCCTGAGCTA	<i>xkdE</i> _upstream region_fwd (LFH sequencing)
MD44	CAATTGATTTCTCCTCCTTGACTG	<i>xkdE</i> _downstream region_rev (LFH sequencing)
MD45	GCAAAAACCATCCCATATAATCAGG	<i>sacB</i> _upstream region_fwd (LFH sequencing)
MD46	AGTCGAAGCCATAGTCAAGCC	<i>sacB</i> _downstream region_rev (LFH sequencing)
MD47	AAACAATTGGATCAGCGGCTTCTGAAACGTG	<i>gltAB</i> _promoter region_fwd [<i>MfeI</i>]
MD48	AAAGTCGACAGATCTGAATTCCTCCCGATCAATTTCC GATAATACC	<i>gltAB</i> _promoter region_rev [<i>EcoRI</i> , <i>BglII</i> , <i>Sall</i>]
MD49	AAACAATTGTTAGGACTTGCAGGCGGAGATGC	<i>plcA</i> _promoter region_fwd [<i>MfeI</i>]
MD50	AAAGTCGACAGATCTGAATTCACCTCCTTTGATTAGTATAT TCCTATCTTAAAGTGAC	<i>plcA</i> _promoter region_rev [<i>EcoRI</i> , <i>BglII</i> , <i>Sall</i>]
MD51	AAAGAATTCATGGTGAGCAAGGGCG	<i>mCherry</i> _fwd [<i>EcoRI</i>]
MD52	AAAGTCGACTTACTTGTACAGCTCGTCCATGCCGC	<i>mCherry</i> _rev [<i>Sall</i>]
MD53	AAAGAATTCGTGGCACAAGGTGAAAAAATTACAGTCTCT AAC	<i>icd</i> _fwd [<i>EcoRI</i>]
MD54	AAAGTCGACTTAGTCCATGTTTTTGATCAGTTCTTCTCCGA AC	<i>icd</i> _rev [<i>Sall</i>]
MD55	AAAGAATTCATGGAGCTGCGCAACTGC	<i>gltC</i> _fwd [<i>EcoRI</i>]
MD56	AAAGTCGACTTATTGATACTGCTCCAGCTTAGAGAAAAAT TGAATG	<i>gltC</i> _rev [<i>Sall</i>]
MD57	GTTATTGTAACATGTAAGCCATAAGCCA	<i>amyE</i> _upstream region_fwd (LFH PCR)
MD58	GAATAACGGCAGTAAAGAGGTTTTGA	<i>amyE</i> _upstream region_rev (LFH PCR)
MD59	TAAATGGTTTATATAATGACTCGGGCTTAAG	<i>amyE</i> _downstream region_fwd (LFH PCR)
MD60	GTTTTCTCAACGAGTTCACTGACC	<i>amyE</i> _downstream region_rev (LFH PCR)
MD61	AGCATAGCGCGCTTCACTTGACAAGAATTCAGCGAACCA TTTGAGGTGATAGGTAAG	<i>aphA3</i> _fwd with parts of <i>P_{alfA}</i> (LFH PCR)

Name	Sequence	Purpose/Reference
MD62	CTTAAGCCCGAGTCATTATATAAACCATTTAATCGATACA AATTCCTCGTAGGCGCTCGGGACC	<i>aphA3_rev</i> with overhang to <i>amyE</i> downstream region (LFH PCR)
MD63	AATTCTTGCAAGTGAAGGCGCGCTATGCTACAATACAGC TTGGAAATGGATCCCTAGGAGGATAATAGATGGAAAAAG AGAAAAAAG	<i>disA_fwd</i> with <i>P_{alf4}</i> (LFH PCR)
MD64	GAATAACGGCAGTAAAGAGGTTTTGATCACAGTTGTCTGT CTAAATAATGCTTC	<i>disA_rev</i> with overhang to <i>amyE</i> upstream region (LFH PCR)
MD65	AATTCTTGCAAGTGAAGGCGCGCTATGCTACAATACAGC TTGGAAATGGATCCCTTGGAGGACGAGGAAATGGC	<i>cdaA_fwd</i> with <i>P_{alf4}</i> (LFH PCR)
MD66	TCAAACCTCTTTACTGCCGTTATTCTTATCCATTTTTCTTG CCCCCCA	<i>cdaA_rev</i> with overhang to <i>amyE</i> upstream region (LFH PCR)
MD67	GAGTCATGATCAATTGGGGGC	<i>amyE_upstream region_fwd</i> (LFH sequencing)
MD68	GTCGCGCCTTTTTCTCAATGATA	<i>amyE_downstream region_rev</i> (LFH sequencing)
MD69	CTATTTTTCAATTTGTTCCGCTGCG	<i>motA_downstream region_rev</i> (LFH)
MD70	CCTATCACCTCAAATGGTTTCGCTGCAAGGAGAGGCGCAA AATGG	<i>motA_downstream region fwd</i> with <i>kan^R</i> tag (LFH)
MD71	CCGAGCGCTACGAGGAATTTGTATCGGCCACAAAAGCA AGAATAATACCGATT	<i>motA_upstream region_rev</i> with <i>kan^R</i> tag (LFH)
MD72	TCGGTTTCAATCAGATGACAGT	<i>motA_upstream region_fwd</i> (LFH)
MD73	TAAAAAGAGTAGGATTAACGCAAAACAGT	<i>motA_downstream region_rev</i> (LFH sequencing)
MD74	CCAAGGCAGAAGTGAAGCTTC	<i>motA_upstream region_fwd</i> (LFH sequencing)
MD75	GAATTCTTGACAAGTTAAGGCTGTGAAGGCGCGCTATGC TATAATACAGCTTGGAAATGGATCTCTAGGAGGTTAACTC AAATGGCAGC	<i>gudB_fwd P^{CR}_{mut1}</i> (for cloning in pAC5) [EcoRI]
MD76	GAATTCTTGACAAGTGAAGGCGGTTAAGGCTCGCTATGC TATAATACAGCTTGGAAATGGATCTCTAGGAGGTTAACTC AAATGGCAGC	<i>gudB_fwd P^{CR}_{mut3}</i> (for cloning in pAC5) [EcoRI]
MD77	GGATCCTTGACAAGTGAAGGCGGTTAAGGCTCGCTATGC TATAATACAGCTTGGAAATGGATCTCTAGGAGGTTAACTC AAATGGCAGC	<i>gudB_fwd P^{CR}_{mut3}</i> (for cloning in pAC5) [BamHI]
MD78	GGATCCTTGACAAGTGAAGGCTGTGAAGGCGCGCTATGC TATAATACAGCTTGGAAATGGATCTCTAGGAGGTTAACTC AAATGGCAGC	<i>gudB_fwd P^{CR}_{mut1}</i> (for cloning in pAC5) [BamHI]
MD79	CAGAACGGGGATCAGAAAACGC	<i>recA_region_fwd</i> (sequencing)
MD80	CAAACCATCACTGCTAAAAGACCA	<i>recA_region_rev</i> (sequencing)
MD81	AAAACAGGCTGGGGTCAACT	<i>ganB_fwd</i>
MD82	CGTCAGCCGTAACGCTTTT	<i>ganA_rev</i>
MD83	ATGGCTGACACACCGGATTT	<i>ganA_fwd</i>
MD84	GCAACCGGTATGCTGATAAGC	<i>ganQ_rev</i>
MD85	TTTGGATCCTTAGGACTTGCAGGCGGAGATGC	<i>P_{plcA_rev}</i> [BamHI]
MD86	AAAGAATTCTCACTATATCCAGCCTCTAAAACGCGAAGCT TC	<i>gudB_rev</i> [EcoRI]
MD87	ATGGAGGGAATAGCACGCAC	<i>hag_upstream region_fwd</i> (LFH sequencing)
MD88	CTGCTGCCTGTATGCTTCCT	<i>hag_downstream region_rev</i> (LFH sequencing)
MD89	CCGAGCGCTACGAGGAATTTGTATCGGGAACCTTTGCC GAACTGTT	<i>recA_upstream region_rev</i> with <i>kan^R</i> tag (LFH)

Name	Sequence	Purpose/Reference
MD90	GCCAAACACGCCGATGAAAA	<i>recA</i> _upstream region_fwd (LFH)
MD91	CCTATCACCTCAAATGGTTCGCTGAGCAAGCTGAAGAGAC ACAAGA	<i>recA</i> _downstream region_fwd with <i>kan</i> ^R tag (LFH)
MD92	GGCTGACGTTTGATTCCCTGA	<i>recA</i> _downstream region_rev (LFH)
MD93	TTTGGCGGCTGATGGAGAG	<i>recA</i> _upstream region_fwd (LFH sequencing)
MD94	CCTGCATGCGTCATTCCCG	<i>recA</i> _downstream region_rev (LFH sequencing)
MD95	CCGAGCGCCTACGAGGAATTTGTATCGTCCAGAAAAATAT TGAAGCGTTCCG	<i>recX</i> _upstream region_rev with <i>kan</i> ^R tag (LFH)
MD96	GCGGTGACATTCATTGGGC	<i>recX</i> _upstream region_fwd (LFH)
MD97	CCTATCACCTCAAATGGTTCGCTGCGCAAAGGATTCTCAC TCGATT	<i>recX</i> _downstream region_fwd with <i>kan</i> ^R tag (LFH)
MD98	GTGCGCTCATCAGGTTGGA	<i>recX</i> _downstream region_rev (LFH)
MD99	CTTACCCGTGCAATCGTTTT	<i>recX</i> _upstream region_fwd (LFH sequencing)
MD100	GAAAGCGCCGTGAATGGAC	<i>recX</i> _downstream region_rev (LFH sequencing)
MD101	CCGAGCGCCTACGAGGAATTTGTATCGTCCGATCCCTGGC AATTCAT	<i>recR</i> _upstream region_rev with <i>kan</i> ^R tag (LFH)
MD102	ACAGTTGGGGCAAGCTTCTT	<i>recR</i> _upstream region_fwd (LFH)
MD103	CCTATCACCTCAAATGGTTCGCTGCGCGGTGATTGGAA TATGC	<i>recR</i> _downstream region_fwd with <i>kan</i> ^R tag (LFH)
MD104	AGAACTTTGTTTACCGCTCGT	<i>recR</i> _downstream region_rev (LFH)
MD105	AAGGAAGCCACAAGACCGG	<i>recR</i> _upstream region_fwd (LFH sequencing)
MD106	AGTTTGACTGACTACGCACATT	<i>recR</i> _downstream region_rev (LFH sequencing)
MD107	CCGAGCGCCTACGAGGAATTTGTATCGTTTCAGCATGGTC GTAGTTGC	<i>recF</i> _upstream region_rev with <i>kan</i> ^R tag (LFH)
MD108	ACACAACCAGCCTGATTCCG	<i>recF</i> _upstream region_fwd (LFH)
MD109	CCTATCACCTCAAATGGTTCGCTGGCATTGATCACGAAAC CTTACGT	<i>recF</i> _downstream region_fwd with <i>kan</i> ^R tag (LFH)
MD110	ACCGTCACATCAAGCTCTGT	<i>recF</i> _downstream region_rev (LFH)
MD111	TTCTTCTCACGGCTTCTGGAC	<i>recF</i> _upstream region_fwd (LFH sequencing)
MD112	CGCGTTTATAGGTTTGGCGG	<i>recF</i> _downstream region_rev (LFH sequencing)
MD113	CCGAGCGCCTACGAGGAATTTGTATCGTTCTGTTCCGGC CCAATACC	<i>recG</i> _upstream region_rev with <i>kan</i> ^R tag (LFH)
MD114	CGGCGGTTCCAGAAAGGACT	<i>recG</i> _upstream region_fwd (LFH)
MD115	CCTATCACCTCAAATGGTTCGCTGACGCTGTGTTAAGAGA TGAATTGC	<i>recG</i> _downstream region_fwd with <i>kan</i> ^R tag (LFH)
MD116	TGGTCTCTCCATTGCATC	<i>recG</i> _downstream region_rev (LFH)
MD117	AGCAGATGGATCATAACCTGTCT	<i>recG</i> _upstream region_fwd (LFH sequencing)
MD118	CTCCGTCAATAACAGCTTTGGG	<i>recG</i> _downstream region_rev (LFH sequencing)
MD119	CCTATCACCTCAAATGGTTCGCTGGACTTAACGAAACGCC ATGC	<i>recN</i> _downstream region_rev with <i>kan</i> ^R tag (LFH)
MD120	ACCCGATTCTGTATTTGCCTTCT	<i>recN</i> _downstream region_fwd (LFH)

Name	Sequence	Purpose/Reference
MD121	CCGAGCGCCTACGAGGAATTTGTATCGCCGCGTTCAAAA GAAACCGT	<i>recN</i> _upstream region_fwd with <i>kan^R</i> tag (LFH)
MD122	AATCACGGGAGGAGACGGA	<i>recN</i> _upstream region_rev (LFH)
MD123	GGTTCATAAAAGGTCATAGTGCCG	<i>recN</i> _downstream region_fwd (LFH sequencing)
MD124	AGGCTATATCTGTAAAGGCTTGTCA	<i>recN</i> _upstream region_rev (LFH sequencing)
MD125	CCTATCACCTCAAATGGTTCGCTGGCGCTTTTTAGATCAAA TGGAAGC	<i>recO</i> _downstream region_rev with <i>kan^R</i> tag (LFH)
MD126	ACACTTAATCCCCGACCT	<i>recO</i> _downstream region_fwd (LFH)
MD127	CCGAGCGCCTACGAGGAATTTGTATCGGTCTCTCCGTAAT CATTTGTGCG	<i>recO</i> _upstream region_fwd with <i>kan^R</i> tag (LFH)
MD128	CATCGAAACCTTGCTCGCG	<i>recO</i> _upstream region_rev (LFH)
MD129	GAGACGCTCAATCCATACGT	<i>recO</i> _downstream region_fwd (LFH sequencing)
MD130	TCATCCCGACCAATTGCTTCT	<i>recO</i> _upstream region_rev (LFH sequencing)
MD131	CCGAGCGCCTACGAGGAATTTGTATCGAACGGGCTGTCA AGATGAAGA	<i>yhaO</i> _upstream region_rev with <i>kan^R</i> tag (LFH)
MD132	TCGGTGATTATGTATGCCAGCA	<i>yhaO</i> _upstream region_fwd (LFH)
MD133	CCTATCACCTCAAATGGTTCGCTGGGAAATAAAGAGCA GGCACAGA	<i>yhaO</i> _downstream region_fwd with <i>kan^R</i> tag (LFH)
MD134	CGCTCCCTCAATCATTGCGGA	<i>yhaO</i> _downstream region_rev (LFH)
MD135	CCAGACGGTAGGGCTTGTTT	<i>yhaO</i> _upstream region_fwd (LFH sequencing)
MD136	CTGCAATCACCTGTTGAGTG	<i>yhaO</i> _downstream region_rev (LFH sequencing)
MD137	AAACTGCAGAGTGAAATATTCAATTTTTGCGTTAGGGA	<i>spIB</i> _rev [<i>Pst</i> I]
MD138	AAAGGATCCTGAAGGCTGGGAAGAAGGATAC	<i>spIB</i> _fwd [<i>Bam</i> HI]
MD139	AAAGTCGACTTAGGACTTGCAGGCGGAGATGC	<i>P_{plcA}</i> _fwd [<i>Sal</i> I]
MD140	AAAAGATCTTCTAGAGGTACCGAATTCGGTTATTATTATT TTGACACCAGACCAACT	<i>lacZ</i> _rev [<i>Bgl</i> II, <i>Xba</i> I, <i>Kpn</i> I, <i>Eco</i> RI]
MD141	AAAGGATCCAAGGAGGAAAACAATCATGAATATTGAGTT GTTACAGGTTTTTC	<i>gltR</i> _fwd SD (<i>gapA</i>) [<i>Bam</i> HI]
MD142	TTTAAGCTTTTACGATTGATCTGGCCTCTTATC	<i>gltR</i> _rev [<i>Hind</i> III]
MD143	TTTAAGCTTCGATTGATCTGGCCTCTTATCTGAA	<i>gltR</i> _rev [<i>Hind</i> III] without stop codon
MD144	TCAGGGGTATTTGAGGCGAA	<i>gltR</i> _rev (sequencing) (Dormeyer <i>et al.</i> , 2017)
MD145	CCCCTTCATTCTGGTGTAGTCA	<i>gltR</i> _fwd (sequencing) (Dormeyer <i>et al.</i> , 2017)
MD146	CTGCCTTGCCCTCCTCTATG	<i>P_{gltAB}</i> _rev (sequencing) (Dormeyer <i>et al.</i> , 2017)
MD147	ACATGCAAATGATCAGCGGC	<i>P_{gltAB}</i> _fwd (sequencing)
MD148	TGGTTCCTGCTGTAAACGCT	<i>rnjB</i> _rev (sequencing)
MD149	GGTGAAATGTCCGGATGCAG	<i>rnjB</i> _rwd (sequencing)
MD150	GCCCGACAAAAGACGTGC	<i>gudB</i> _fwd (Southern blot)
MD151	CTAATACGACTCACTATAGGGAGATTTCAATCGCAGCAGG AACG	<i>gudB</i> _rev with T7 extension (Southern blot)
MD152	GGTCCGTGATGAAAAAGCGC	<i>polC</i> _fwd (Southern blot)

Name	Sequence	Purpose/Reference
MD153	CTAATACGACTCACTATAGGGAGATAACAGCAAATCCGT GGCA	<i>polC_rev</i> with T7 extension (Southern blot)
MD154	AAATCTAGAGATGTTAGCGTCAAAAATGCGATG	<i>recJ_fwd</i> [<i>Xba</i> I] (BACTH)
MD155	AAAGGTACCCGTGTCCTCCTCGTACTTTCATAAGC	<i>recJ_rev</i> [<i>Kpn</i> I] (BACTH)
MD156	AAATCTAGAGATGCTGACAAAATGTGAAGGGATC	<i>recO_fwd</i> [<i>Xba</i> I] (BACTH)
MD157	AAAGGTACCCGACTTTTGTTCACCCATAAGATGTTTC	<i>recO_rev</i> [<i>Kpn</i> I] (BACTH)
MD158	AAATCTAGAGATGCAATATCCTGAACCAATATCAAAGC	<i>recR_fwd</i> [<i>Xba</i> I] (BACTH)
MD159	AAAGGTACCCGCAATTCACGTCTTCCTTCAAGTGC	<i>recR_rev</i> [<i>Kpn</i> I] (BACTH)
MD160	AAATCTAGAGATGGCTATGGATCGGATAGAGGT	<i>uvrA_fwd</i> [<i>Xba</i> I] (BACTH)
MD161	AAAGGTACCCGAGATGTAGCTGTTTCTTTGCTTTCA	<i>uvrA_rev</i> [<i>Kpn</i> I] (BACTH)
MD162	AAATCTAGAGGTGAAAGATCGCTTTGAGTTAGTCTC	<i>uvrB_fwd</i> [<i>Xba</i> I] (BACTH)
MD163	AAAGGTACCCGTCCTTCCGCTTTTAGCTCTAAAA	<i>uvrB_rev</i> [<i>Kpn</i> I] (BACTH)
MD164	AAATCTAGAGTTGCTGAGAATAGGCTCACACG	<i>nfo_fwd</i> [<i>Xba</i> I] (BACTH)
MD165	AAAGGTACCCGTTGCTGTAATAATCTTTCAAGCAATGTAT	<i>nfo_rev</i> [<i>Kpn</i> I] (BACTH)
MD166	AAATCTAGAGGTGATTCGGTATCCTAATGGAAAAACA	<i>recU_fwd</i> [<i>Xba</i> I] (BACTH)
MD167	AAAGGTACCCGACCTTTCGCACCAGATGATG	<i>recU_rev</i> [<i>Kpn</i> I] (BACTH)
MD168	CCGAGCGCCTACGAGGAATTTGTATCGCCATTTAATAGA AGGGATGGGGAT	<i>dprA_upstream region_rev</i> with <i>kan^R</i> tag (LFH)
MD169	GTTCAAACAACCGGCGCTAA	<i>dprA_upstream region_fwd</i> (LFH)
MD170	CCTATCACCTCAAATGGTTCGCTGTGGTCAGCAGAGGATA TTTTCGA	<i>dprA_downstream region_fwd</i> with <i>kan^R</i> tag (LFH)
MD171	CACGGTCAATAATCAAACGGAGG	<i>dprA_downstream region_rev</i> (LFH)
MD172	CTGGAAAAGGCGGAACAGAAG	<i>dprA_upstream region_fwd</i> (LFH sequencing)
MD173	AAGCTCGTTCAAAGGTTTCTTG	<i>dprA_downstream region_rev</i> (LFH sequencing)
MD174	CCGAGCGCCTACGAGGAATTTGTATCGTTAAAATAGAGA TAGATGGTGCCGTC	<i>fadR_upstream region_rev</i> with <i>kan^R</i> tag (LFH)
MD175	GCACGCCAACTTTATCTGGG	<i>fadR_upstream region_fwd</i> (LFH)
MD176	CCTATCACCTCAAATGGTTCGCTGTCTCGTTGCGCTTTCAA ACA	<i>fadR_downstream region_fwd</i> with <i>kan^R</i> tag (LFH)
MD177	TCCTCTGACTCAAATGCTTCCC	<i>fadR_downstream region_rev</i> (LFH)
MD178	TGGAAGCTTGTGGAAGGCT	<i>fadR_upstream region_fwd</i> (LFH sequencing)
MD179	TTTCGAGAAATGCCTGGATGC	<i>fadR_downstream region_rev</i> (LFH sequencing)
MD180	AAATCTAGAGATGCGGCTTGAGCGTCTG	<i>yphH_fwd</i> [<i>Xba</i> I] (BACTH)
MD181	AAAGGTACCCGTGAAAAATGAGTTTGTATC	<i>yphH_rev</i> [<i>Kpn</i> I] (BACTH)
MD182	AAAGGATCCGATGAACATTCCTAAACCGGCAGA	<i>addA_fwd</i> [<i>Bam</i> HI] (BACTH)
MD183	AAAGGTACCCGTAATGTCAGAATGTGCCCTCCG	<i>addA_rev</i> [<i>Kpn</i> I] (BACTH)
MD184	AAAGGATCCGTTGGGAGCAGAGTTTTAGTAGGC	<i>addB_fwd</i> [<i>Bam</i> HI] (BACTH)
MD185	AAAGGTACCCGGAATGTTCAATGCCATCCG	<i>addB_rev</i> [<i>Kpn</i> I] (BACTH)
MD186	CCGAGCGCCTACGAGGAATTTGTATCGCCCGGCAATTC ATCCT	<i>addAB_upstream region_rev</i> with <i>kan^R</i> tag (LFH)
MD187	TGCTCCATGGTTGATTCCCC	<i>addAB_upstream region_fwd</i> (LFH)
MD188	CCTATCACCTCAAATGGTTCGCTGCAGCTGTACACGAAGG CAGT	<i>addAB_downstream region_fwd</i> with <i>kan^R</i> tag (LFH)
MD189	GGAGATCCTGAATAACGCGCA	<i>addAB_downstream region_rev</i> (LFH)

Name	Sequence	Purpose/Reference
MD190	TCTTCCAAGCATTTAGTGAAACAATGA	<i>addAB</i> _upstream region_fwd (LFH sequencing)
MD191	CAGGCTTTGCGTCCACAATC	<i>addAB</i> _downstream region_rev (LFH sequencing)
MD192	CGATCTAGTCCCGCTGCATG	<i>recJ</i> _fwd (sequencing BACTH)
MD193	CCTATCACCTCAAATGGTTCGCTGAACTCCATTCGCCAATACGC	<i>rnhC</i> _upstream region_rev with <i>kan^R</i> tag (LFH)
MD194	CCGAGCGCCTACGAGGAATTTGTATCGGCTGTAAGTGAA CCGCTGTAC	<i>rnhC</i> _downstream region_fwd with <i>kan^R</i> tag (LFH)
MD195	GGGGCGAAGGAAAAGCTCT	<i>addA</i> _fwd (sequencing BACTH)
MD196	TTATGACGAGCAGGCTGAGC	<i>addA</i> _fwd (sequencing BACTH)
MD197	GGGCGATGATCTTGGTACGG	<i>addA</i> _fwd (sequencing BACTH)
MD198	CAGCGAACCATTTGAGGTGATAGGCCCTTTTCTGACTGTTTGGGAT	<i>recU</i> _upstream region_rev with <i>kan^R</i> tag (LFH)
MD199	AGGAGATGTTCTTTTTGTAATCCCG	<i>recU</i> _upstream region_fwd (LFH)
MD200	CGATACAAATTCCTCGTAGGCGCTCGGGGATACGCACCCAGAATTGATT	<i>recU</i> _downstream region_fwd with <i>kan^R</i> tag (LFH)
MD201	TTTTGACCGGGTTGTACGCT	<i>recU</i> _downstream region_rev (LFH)
MD202	GCAATTCCTCGCGCTAAAG	<i>recU</i> _upstream region_fwd (LFH sequencing)
MD203	TTCCTTCTGTGACACGACGC	<i>recU</i> _downstream region_rev (LFH sequencing)
MD204	AAATCTAGAGGTGTCCATTCAGTGATAAAAAGTAT	<i>rnhC</i> _fwd [<i>Xba</i> I] (BACTH)
MD205	AAAGGTACCCGTGAACGTTTTTTATCAGCAAGGCG	<i>rnhC</i> _rev [<i>Kpn</i> I] (BACTH)
MD206	CGATTCCAAGAGTACGACGCA	5'UTR <i>abrB</i> _rev (Dormeyer <i>et al.</i> , 2017)
MD207	GCGGCGATAAGTGCAAATCA	5'UTR <i>abrB</i> _fwd (Dormeyer <i>et al.</i> , 2017)
MD208	CCTTGACCCTGTAATCGGCA	<i>clpC</i> _fwd (Dormeyer <i>et al.</i> , 2017)
MD209	CTGAATCGGCTGAAAACGGC	<i>clpC</i> _rev (Dormeyer <i>et al.</i> , 2017)
MD210	TCTGGGCGAGCGGAAATATG	<i>glcU</i> _fwd (Dormeyer <i>et al.</i> , 2017)
MD211	CGAGTGTGCCGAACCTCTTA	<i>glcU</i> _rev (Dormeyer <i>et al.</i> , 2017)
MD212	AAGCAACTACGCAAAAGCC	<i>yfhJ</i> _fwd (Dormeyer <i>et al.</i> , 2017)
MD213	TTGGCTCAGTCCGGACATTC	<i>yfhJ</i> _rev (Dormeyer <i>et al.</i> , 2017)
MD214	GCATCCGTCTTAACCCGCTA	<i>yxjO</i> _fwd (Dormeyer <i>et al.</i> , 2017)
MD215	CGATGCAGATACGCCCATTA	<i>yxjO</i> _rev (Dormeyer <i>et al.</i> , 2017)
MD216	CGCCGGATAAACTGTATAC	<i>gltA</i> _fwd (Southern blot) (Dormeyer <i>et al.</i> , 2017)
MD217	CTAATACGACTCACTATAGGGAGACCCTCAGTAATGCTTTTCC	<i>gltA</i> _rev with T7 extension (Southern blot) (Dormeyer <i>et al.</i> , 2017)
MD218	CAAGCGGTGTTTCTTCTGCG	<i>P_{tapA}</i> _fwd (Dormeyer <i>et al.</i> , 2017)
MD219	GCAGCGCTGTATCATCGGA	<i>P_{tapA}</i> _rev (Dormeyer <i>et al.</i> , 2017)
MD220	TTATATATTGTTTATATCGTTTTGAAAAGCTACAATGATTATAGATTGTTAGATTT	<i>P_{gltAB(C-14G)}</i> _fwd (MMR Primer) (Dormeyer <i>et al.</i> , 2017)
MD221	AAAGGATCCATTAGGGGGACCAAGAAATGGCTCAAAC	<i>pdxS</i> _fwd with nat. SD [<i>Bam</i> HI]
MD222	AAAGGATCCTTATTTTTCGAACTGCGGGTGG	<i>pdxT</i> -Strep_rev [<i>Bam</i> HI]
MD223	AAAGCGGCCGCTTAGGACTTGCAGGCGGAGATGC	<i>P_{plcA}</i> _fwd [<i>Not</i> I]
MD224	AAATCTAGATCACTATATCCAGCCTCTAAAACGC	<i>gudB</i> _rev [<i>Xba</i> I]
MD225	AAAGAATTCGCGGCCGCTCTAGACTCGAGGGTACCTTAGGACTTGCAGGCGGAGATGC	<i>P_{plcA}</i> _fwd [<i>Eco</i> RI, <i>Not</i> I, <i>Xba</i> I, <i>Xho</i> I, <i>Kpn</i> I]

Name	Sequence	Purpose/Reference
MD226	CCGAGCGCCTACGAGGAATTTGTATCGGCTGCCTGACGA TCACTCAT	<i>recA</i> _upstream region_rev with <i>kan^R</i> tag (LFH)
MD227	CTTTGGCGGCTGATGGAGA	<i>recA</i> _upstream region_fwd (LFH)
MD228	CCTATCACCTCAAATGGTTCGCTGGCAGCAAGCTGAAGA GACAC	<i>recA</i> _downstream region_fwd with <i>kan^R</i> tag (LFH)
MD229	GGAGTAATGGCGCCGTTTC	<i>recA</i> _downstream region_rev (LFH)
MD230	TCGCTTTTTTCGGTATCGGTGA	<i>recA</i> _upstream region_fwd (LFH sequencing)
MD231	GGCTGACGTTTGATTCCCTG	<i>recA</i> _downstream region_rev (LFH sequencing)
MD232	CCGGTCTCATGGTATGGAGCTGCGCCAACTG	<i>gltC</i> _fwd [<i>Bsa</i> I]
MD233	AAACTCGAGTTATTGATACTGCTCCAGCTTAGAGAAA	<i>gltC</i> _rev [<i>Xho</i> I]
MD234	CCGGTCTCATGGTATGTCAGCAAAGCAAGTCTCGA	<i>rocG</i> _fwd [<i>Bsa</i> I]
MD235	AAACTCGAGTTAGACCCATCCGCGGAAAC	<i>rocG</i> _rev [<i>Xho</i> I]
MD236	TGCAGGAGTTAGGATATTAAGTGGCATCGCACATAGCT	<i>prfA</i> (C530A)_fwd MMR
MD237	TGCAGGAGTTAGGATATTAAGTGGCATCGCACATAGCT	<i>prfA</i> (del C530)_fwd MMR
MD238	ACAATGCAGGAGTTAGGATAATTCAAGTGGCATCGCACA TA	<i>prfA</i> (ins A527)_fwd MMR insertion
MD239	AAAGGATCCTTACTGTACTACCGCTGTTTTTGTG	<i>gltA</i> _rev [<i>Bam</i> HI]
MD240	AAAGAATTCGTTTGTCTCACATCCATCTATCTCATTTT	<i>P_{gltA}</i> _fwd [<i>Eco</i> RI]
MD241	TTCTTTTGATCTAAATTATATATTGTTAAATCGTTTTGAAA ACCTACAATGATTATAG	<i>P_{gltA(T-28A)}</i> _fwd MMR
MD242	ATCTATCTCATTTTGTAGATTCTTTTGACCTAAATTATATATT GTTTATATCGTTT	<i>P_{gltA(T-48C)}</i> _fwd MMR
MD243	ATTCAGGACGGTAGAGACCTT	Primer Extension <i>gltA</i> (Dormeyer <i>et al.</i> , 2017)
MD244	CCGGTCTCATGGTATGGCAGCCGATCGAAACACCG	<i>gudB</i> _fwd [<i>Bsa</i> I]
MD245	AAACTCGAGTTATATCCAGCCTCTAAAACGCGA	<i>gudB</i> _rev [<i>Xho</i> I]
MD246	AAAGGATCCCTGAAAGGGAGCATGTGAGAAAC	<i>gudB</i> _fwd [<i>Bam</i> HI]
MD247	AAACTGCAGTTATATCCAGCCTCTAAAACGCGA	<i>gudB</i> _rev [<i>Pst</i> I]
MD248	TTTCAGCTGAGCTATGTGCGATGCCACTTGAATTTATCCTA ACTCCTGCAT	<i>prfA</i> (ins (2xA)527)_rev [<i>Pvu</i> II] MMR
MD249	TTTCAGCTGAGCTATGTGCGATGCCACTTGAATTTTATCCT AACTCCTGCAT	<i>prfA</i> (ins (3xA)527)_rev [<i>Pvu</i> II] MMR
MD250	TTTCAGCTGAGCTATGTGCGATGCCACTTGAATTTTATCC TAACTCCTGCAT	<i>prfA</i> (ins (4xA)527)_rev [<i>Pvu</i> II] MMR
MD251	TTTCAGCTGAGCTATGTGCGATGCCACTTGAATTTTTTATC CTAACTCCTGCAT	<i>prfA</i> (ins (5xA)527)_rev [<i>Pvu</i> II] MMR
MD252	TTTCAGCTGAGCTATGTGCGATGCCACTTGAATTTTTTTTT TTATCCTAACTCCTGCATTGTTAAATTATCCAGTGT	<i>prfA</i> (ins (10xA)527)_rev [<i>Pvu</i> II] MMR
MD253	TTTCAGCTGAGCTATGTGCGATGCCACTTGAATTTTTTTTT TTTTTTTTATCCTAACTCCTGCATTGTTAAATTATCCAGTGT	<i>prfA</i> (ins (15xA)527)_rev [<i>Pvu</i> II] MMR
MD254	TTTCAGCTGAGCTATGTGCGATGCCACTTGAATTTTTTTTT TTTTTTTTTTTTATCCTAACTCCTGCATTGTTAAATTATCCA GTGT	<i>prfA</i> (ins (20xA)527)_rev [<i>Pvu</i> II] MMR
MD255	TTTCAGCTGAGCTATGTGCGATGCCACTTGAATTTTTTTTT TTTTTTTTTTTTTTTTTTTTATCCTAACTCCTGCATTGTTA AATTATCCAGTGT	<i>prfA</i> (ins (30xA)527)_rev [<i>Pvu</i> II] MMR
MD256	GAGATTCTTTGATCTAAATTATATATTGTTTCGCATTAAA ATCTTAGTACAATGATTATAGAGTTGTTAGATTTTATGAC CGGTATTATC	<i>P_{gltA}</i> _fwd Shuffle I

Name	Sequence	Purpose/Reference
MD257	TAAATCTAACAACTCTATAATCATTGTAATAAGATTTA ATGCGAAACAATATATAATTTAGATCAAAGAATCTCAA ATGAGATAGATGG	<i>P_{gltA}</i> _rev Shuffle I
MD258	GAGATTCTTTGATCTAAATTATATATTGTTGATCAAGAC CATTTTATACAATGATTATAGAGTTGTTAGATTTTATGAC CGGTATTATC	<i>P_{gltA}</i> _fwd Shuffle II
MD259	TAAATCTAACAACTCTATAATCATTGTATAAAATGGTCT TGATCAAACAATATATAATTTAGATCAAAGAATCTCAA ATGAGATAGATGG	<i>P_{gltA}</i> _rev Shuffle II
MD260	GAGATTCTTTGATCTAAATTATATATTGTTTATAGCAAG ATTCTCATTACAATGATTATAGAGTTGTTAGATTTTATGAC CGGTATTATC	<i>P_{gltA}</i> _fwd Shuffle III
MD261	TAAATCTAACAACTCTATAATCATTGTAATGAGAATCTTG CTATAAAACAATATATAATTTAGATCAAAGAATCTCAA ATGAGATAGATGG	<i>P_{gltA}</i> _rev Shuffle III

6.3.2. Other oligonucleotides used in this work

Name	Sequence	Purpose/Reference
DR361	ATCGGCAAATCTGTTTAAGTCCTC	<i>gltC</i> _upstream region_fwd (LFH) (Dormeyer <i>et al.</i> , 2017)
DR362	GTTTGTCTCACATCCATCTATCTC	<i>gltC</i> _upstream region_rev with <i>kan^R</i> tag (LFH) (Dormeyer <i>et al.</i> , 2017)
DR363	TCTATATAGAAGCTTCGGGTTTTTTTC	<i>gltC</i> _downstream region_fwd with <i>kan^R</i> tag (LFH) (Dormeyer <i>et al.</i> , 2017)
DR364	TGGTTTCTCAGGCGCAGT	<i>gltC</i> _downstream region_rev (LFH) (Dormeyer <i>et al.</i> , 2017)
DR365	TATGCGTATTTCCGTCCAAGGC	<i>gltC</i> _upstream region_fwd (LFH sequencing) (Dormeyer <i>et al.</i> , 2017)
DR366	AGTTCATTAACAAGCCTTCATGGAG	<i>gltC</i> _upstream region_rev (LFH sequencing) (Dormeyer <i>et al.</i> , 2017)
FC191	AAAGAATTCTTAGACTTGACGGCGGAGATGC	<i>P_{plcA}</i> _fwd [<i>EcoRI</i>]
FC192	TTTGATCCAACAAAATGGCCCCCTCTTGATTAGTA TATTCC	<i>P_{plcA}</i> _rev [<i>BamHI</i>]
FC196	TTTCAATTGTTAATTTAATTTCCCAAGTAGCAGGAC ATGC	<i>prfA</i> _rev [<i>MfeI</i>]
FC305	AAACAGCTGTTAGCAGAATTATTTCAAATTAAGCA AGAG	<i>prfA</i> _fwd [<i>PvuII</i>]
FC306	TTTCAGCTGAGCTATGTGCGATGCCTGCGATGCCACT TGAATATCCTAACTCCTGCAT	<i>prfA</i> _rev [<i>PvuII</i>]
iGEM95	GAAGTAACTTTGATTCCATTCTTTTG	<i>gfp</i> _rev
IW1	AAAGAATTCGATCAGCGGCTTCTGAAACGTG	<i>P_{gltA}</i> _fwd (Dormeyer <i>et al.</i> , 2017)
IW2	AAAGGATCCTGAGCTTTTGGCATTGATTGTACGC	<i>P_{gltA}</i> _rev (Dormeyer <i>et al.</i> , 2017)
JG29	GCCGCATCTGTTGTCGGTACAC	<i>nfo</i> _upstream region_fwd (LFH)
JG30	CCTATCACCTCAAATGGTTCGCTGGACTGCTTCCTGGC TTGCAGCC	<i>nfo</i> _upstream region_rev with <i>kan^R</i> tag (LFH)
JG31	CGAGCGCTACGAGGAATTTGTATCGCCGCATACCG TTTTGAGATTGAAATGC	<i>nfo</i> _downstream region_fwd with <i>kan^R</i> tag (LFH)
JG32	AGTACATCGCTTGCTCAGGACCG	<i>nfo</i> _downstream region_rev (LFH)
JG35	CGATCCTGCTAAGGATGTCGTTACG	<i>nfo</i> _fwd (LFH sequencing)

Name	Sequence	Purpose/Reference
JG36	GTTGTGCCCCGACCGAGACG	<i>nfo_rev</i> (LFH sequencing)
JG43a	AGAGCGATCAGCCAAATTGTC	<i>gudB_fwd</i>
JN127	CGGTGATTGAACTGCAAACCAA	<i>accA_fwd</i> (Southern blot) (Dormeyer <i>et al.</i> , 2017)
JN128	CTAATACGACTCACTATAGGGAGATTAGTTTACCC CGATATATTGATCTTCAAC	<i>accA_rev</i> with T7 extension (Southern blot) (Dormeyer <i>et al.</i> , 2017)
JN133	TTGTAAAGGATATATTCACGAAAAAGAAAAAGTAT	<i>accD_fwd</i> (Southern blot)
JN134	CTAATACGACTCACTATAGGGAGAACCTCTGTTTGA TGCATATCCAG	<i>accD_rev</i> with T7 extension (Southern blot)
kan-check-fwd	CATCCGCAACTGTCCATACTCTG	<i>aphA3_fwd</i> (sequencing)
kan-check-rev	CTGCCTCCTCATCTCTTCATCC	<i>aphA3_rev</i> (sequencing)
kan-fwd	CAGCGAACCATTTGAGGTGATAGG	<i>aphA3_fwd</i> (LFH)
kan-rev	CGATACAAATTCCTCGTAGGCGCTCGG	<i>aphA3_rev</i> (LFH)
KG100	GCAGCAATAACACCGGCAATAA	<i>gudB^{CR}_downstream region_rev</i> (LFH)
KG101	CCTATCACCTCAAATGGTTCGCTGGCTGGATATAAGT TGATGATTTGCAT	<i>gudB^{CR}_downstream region_fwd</i> with <i>kan^R</i> tag (LFH)
KG103	GCCATAATCCGGAGATTCATG	<i>gudB^{CR}_upstream region_fwd</i> (LFH)
KG184	AAAGAATTCTCATTATATCCAGCCTCTAAAACGCG	<i>gudB^{CR}_rev</i>
KG185	TTTGGATCCCATTACGCTTTCAGAAAGCTTACAGCGA ATC	<i>P_{gudB}_fwd</i>
KG92	TTTGGATCCTCATTATATCCAGCCTCTAAAACGCG	<i>gudB^{CR}_rev</i> [<i>Bam</i> HI]
LS11	TTTAGATCTTCACTATATCCAGCCTCTAAAACGCGAAG CTTC	<i>gudB^{CR}_rev</i> [<i>Bgl</i> II]
LS32	AAACTGCAGTTGACAAGTGAAGGCGGTGAAGGC	<i>P^{CR}_fwd</i> (pBP302) [<i>Pst</i> I]
LS33	AAACAATTGGAATTCTCTAGATTATATCCAGCCTCTAA AACGCGAAGCTTCA	<i>gudB_rev</i> with stop codon [<i>Mfe</i> I, <i>Eco</i> RI, <i>Xba</i> I]
LS34	AAATCTAGAGTCGACCTCGAGAGATCTAAGGAGGAA ACAATCATGAGTAAAGGAGAAGAAGCTTTTACTGGA GTTG	<i>gfp_fwd</i> with SD (<i>gapA</i>) [<i>Xba</i> I, <i>Sal</i> I, <i>Xho</i> I, <i>Bgl</i> II]
LS35	TTTGAATTCTTATTTGTATAGTTCATCCATGCCATGTG TAATCC	<i>gfp_rev</i> [<i>Eco</i> RI]
LS52	AAACTGCAGAAAATCAAGGAGATTAAGAATCTTTTCTC AATTCAGCAC	<i>P_{degQ36}_fwd</i> [<i>Eco</i> RI]
ML103	CTCTTGCCAGTCACGTTAC	<i>spc</i> check up fragment (sequencing)
ML104	TCTTGGAGAGAATATTGAATGGAC	<i>spc</i> check down fragment (sequencing)
ML107	GCTTCATAGAGTAATTCTGTAAAGG	<i>aphA3</i> check up fragment (sequencing)
ML108	GACATCTAATCTTTTCTGAAGTACATCC	<i>aphA3</i> check down fragment (sequencing)
ML109	GTCTAGTGTGTAGACTTTATGAAATC	<i>ermC</i> check up fragment (sequencing)
ML84	CTAATGGGTGCTTTAGTTGAAGA	<i>cat</i> check up fragment (sequencing)
ML85	CTCTATTCAGGAATTGTCAGATAG	<i>cat</i> check down fragment (sequencing)
Mls-check-fwd	CCTTAAAACATGCAGGAATTGACG	<i>ermC</i> check down fragment
mIs-fwd	CAGCGAACCATTTGAGGTGATAGGGATCCTTTAACTC TGCAACCCCTC	<i>ermC_fwd</i> with <i>kan^R</i> tag (LFH)
mIs-rev	CGATACAAATTCCTCGTAGGCGCTCGGGCCGACTGCG CAAAAGACATAATCG	<i>ermC_fwd</i> with <i>kan^R</i> tag (LFH)
MT7	GAAGAACTGATCAGCATTTATAAACGTCTCG	<i>rnhC_upstream region_fwd</i> (LFH)
MT10	TGTTTCCATCATACTTGAAAAAACTTCTCCG	<i>rnhC_downstream region_rev</i> (LFH)
MT11	CACCTGACAATCGAAGCAAATAACATTCACG	<i>rnhC_fwd</i> (LFH sequencing)
MT12	CCCTTTGAGTTCATATAGACTGCAATGGTT	<i>rnhC_rev</i> (LFH sequencing)

Name	Sequence	Purpose/Reference
MT13	CCGAGCGCCTACGAGGAATTTGTATCGGAATTGATAT ATGATGTCCGCGCTTTCATCAAG	<i>gudB^{CR}</i> _upstream region_rev with <i>kan^R</i> tag (LFH)
PAC5F	GCGTAGCGAAAAATCCTTTTC	Check primer fwd for pAC5
PAC5R	CTGCAAGCGATAAGTTGG	Check primer rev for pAC5
Tc-check-fwd	CGGCTACATTGGTGGGATACTTGTG	<i>tet</i> check down fragment
Tc-check-rev	CATCGGTCAATAAATCCGTAATGC	<i>tet</i> check up fragment
Tc-fwd2	CAGCGAACCATTGAGGTGATAGGGCTTATCAACGTA GTAAGCGTGG	<i>tet</i> _fwd with <i>kan^R</i> tag (LFH)
Tc-rev	CGATACAAATTCCTCGTAGCGCTCGGGAACTCTCTC CCAAAGTTGATCCC	<i>tet</i> _fwd with <i>kan^R</i> tag

6.4. Bacterial strains

6.4.1. *B. subtilis* strains constructed in this work

Strain	Genotype	Reference/Construction
BP158	<i>trpC2 ΔgudB^{CR}::aphA3 rocG::Tn10 spc amyE::(gudB^{CR} orientation changed lacZ cat) Δmf::ermC</i>	cDNA GP1167 → BP19
BP159	<i>trpC2 ΔgudB^{CR}::aphA3 rocG::Tn10 spc amyE::(gudB^{CR} lacZ cat) Δmf::ermC</i>	cDNA GP1167 → GP1163
BP200	<i>trpC2 ΔgudB^{CR}::cat</i>	cDNA GP27 → 168
BP201	<i>trpC2 ΔgudB^{CR}::cat lacA::aphA3</i>	pBP106 → BP200
BP202	<i>trpC2 ΔgudB^{CR}::cat lacA::(P^{CR}-gudB⁺ aphA3)</i>	pBP168 → BP200
BP203	<i>trpC2 ΔgudB^{CR}::cat lacA::(P^{CR}-gudB⁺ gfp aphA3)</i>	pBP169 → BP200
BP204	<i>trpC2 ΔgudB^{CR}::cat lacA::aphA3 ΔrocG::Tn10 spc</i>	cDNA GP747 → BP201
BP205	<i>trpC2 ΔgudB^{CR}::cat lacA::(P^{CR}-gudB⁺ aphA3) rocG::Tn10 spc</i>	cDNA GP747 → BP202
BP206	<i>trpC2 ΔgudB^{CR}::cat lacA::(P^{CR}-gudB⁺ gfp aphA3) rocG::Tn10 spc</i>	cDNA GP747 → BP203
BP207	<i>trpC2 ΔgudB^{CR}::cat lacA::(P⁺-gudB⁺ aphA3) rocG::Tn10 spc</i>	BP205 spontaneous on SP
BP208	<i>trpC2 ΔgudB^{CR}::cat lacA::(P⁺-gudB⁺ gfp aphA3) rocG::Tn10 spc</i>	BP206 spontaneous on SP
BP209	<i>trpC2 ΔgudB^{CR}::cat lacA::(terminator P^{CR}-gudB⁺ gfp aphA3)</i>	pBP173 → BP200
BP210	<i>trpC2 lacA::(P_{gudB}-prfA^{CR} ermC)</i>	pBP404 → 168
BP212	<i>trpC2 ΔgudB^{CR}::cat lacA::(P^{CR}-gudB⁺ phy gfp aphA3)</i>	pBP171 → BP200
BP213	<i>trpC2 ΔgudB^{CR}::cat lacA::(P^{CR}-gudB⁺ pdxST gfp aphA3)</i>	pBP172 → BP200
BP215	<i>trpC2 ΔgudB^{CR}::cat lacA::(P^{CR}-gudB⁺ phy gfp aphA3) rocG::Tn10 spc</i>	cDNA GP747 → BP212
BP216	<i>trpC2 ΔgudB^{CR}::cat lacA::(P^{CR}-gudB⁺ pdxST gfp aphA3) rocG::Tn10 spc</i>	cDNA GP747 → BP213
BP218	<i>trpC2 ΔgudB^{CR}::cat lacA::(P⁺-gudB⁺ phy gfp aphA3) rocG::Tn10 spc</i>	BP215 spontaneous on SP
BP219	<i>trpC2 ΔgudB^{CR}::cat lacA::(P⁺-gudB⁺ pdxST gfp aphA3) rocG::Tn10 spc</i>	BP216 spontaneous on SP
BP511	<i>trpC2 ΔgudB^{CR}::aphA3 rocG::Tn10 spc</i>	cDNA GP747 → BP442
BP513	<i>trpC2 ΔgudB^{CR}::aphA3 rocG::Tn10 spc amyE::(P_{plcA}-gfp-gudB cat)</i>	cDNA BP518 → BP511

Strain	Genotype	Reference/Construction
BP514	<i>trpC2 ΔgudB^{CR}::aphA3 rocG::Tn10 spc lacA::(P_{degQ36}-prfA^{CR} ermC)</i>	pBP402 → BP511
BP515	<i>trpC2 ΔgudB^{CR}::aphA3 rocG::Tn10 spc lacA::(P_{gudB}-prfA^{CR} ermC)</i>	pBP404 → BP511
BP516	<i>trpC2 Δdxs::ermC</i>	cDNA BV568 → 168
BP517	<i>trpC2 Δdxs ΔxylR::aphA3</i>	cDNA GP1302 → BP516
BP518	<i>trpC2 amyE::(P_{plcA}-gfp-gudB⁺ cat)</i>	pBP406 → 168
BP519	<i>trpC2 ΔgudB^{CR}::aphA3 rocG::Tn10 spc lacA::(P_{degQ36}-prfA^{CR} ermC) amyE::(P_{plcA}-gfp-gudB⁺ cat)</i>	pBP406 → BP514
BP520	<i>trpC2 ΔgudB^{CR}::aphA3 rocG::Tn10 spc lacA::(P_{gudB}-prfA^{CR} ermC) amyE::(P_{plcA}-gfp-gudB⁺ cat)</i>	pBP406 → BP515
BP521	<i>trpC2 Δdxs::ermC ΔxylAB::aphA3</i>	cDNA GP1151 → BP516
BP522	<i>trpC2 ΔgudB^{CR}::aphA3 rocG::Tn10 spc lacA::(P_{degQ36}-prfA⁺ ermC) amyE::(P_{plcA}-gfp-gudB⁺ cat)</i>	BP519 spontaneous on SP
BP523	<i>trpC2 ΔgudB^{CR}::aphA3 rocG::Tn10 spc lacA::(P_{gudB}-prfA⁺ ermC) amyE::(P_{plcA}-gfp-gudB⁺ cat)</i>	BP520 spontaneous on SP
BP524	<i>trpC2 amyE::(P_{plcA}-gfp-gudB⁺ cat) lacA::(P_{degQ36}-prfA^{CR} ermC)</i>	pBP402 → BP518
BP525	<i>trpC2 amyE::(P_{plcA}-gfp-gudB⁺ cat) lacA::(P_{gudB}-prfA^{CR} ermC)</i>	pBP404 → BP518
BP526	<i>trpC2 amyE::(P_{plcA}-gfp-gudB⁺ cat) lacA::(P_{gudB}-prfA^{CR} ermC) sacA::(phl P_{xylA}-cre)</i>	cDNA JK27 → BP525
BP527	<i>trpC2 amyE::(P_{plcA}-gfp-gudB⁺ cat) sacA::(phl P_{xylA}-cre)</i>	cDNA JK27 → BP518
BP529	<i>trpC2 rocG::(P_{gudB}-prfA^{CR} loxkanlox)</i>	LFH (MD14/MD15, pBP407, MD16/MD17) → 168
BP531	<i>trpC2 amyE::(P_{plcA}-gfp-gudB⁺ cat) sacA::(phl P_{xylA}-cre) rocG::(P_{gudB}-prfA^{CR} loxkanlox)</i>	cDNA BP529 → BP527
BP533	<i>trpC2 addAB::spc rocG::cat</i>	cDNA GP1107 → GP1157
BP534	<i>trpC2 ΔrocG::cat ymcB::Tn10 spc</i>	cDNA GP1109 → GP1157
BP535	<i>trpC2 ΔrocG::cat dppE::Tn10 spc</i>	cDNA GP1110 → GP1157
BP536	<i>trpC2 ΔrocG::cat poly1::Tn10 spc</i>	cDNA GP1111 → GP1157
BP537	<i>trpC2 ΔrocG::cat yxjF::Tn10 spc</i>	cDNA GP1112 → GP1157
BP538	<i>trpC2 ΔrocG::cat ymfA::Tn10 spc</i>	cDNA GP1113 → GP1157
BP539	<i>trpC2 ΔrocG::cat hutH::Tn10 spc</i>	cDNA GP1114 → GP1157
BP540	<i>trpC2 ΔrocG::cat yusO::Tn10 spc</i>	cDNA GP1115 → GP1157
BP541	<i>trpC2 ΔrocG::cat yxiM::Tn10 spc</i>	cDNA GP1116 → GP1157
BP542	<i>trpC2 ΔrocG::cat yxkF::Tn10 spc</i>	cDNA GP1117 → GP1157
BP543	<i>trpC2 ΔrocG::cat treA::Tn10 spc</i>	cDNA GP1118 → GP1157
BP544	<i>trpC2 ΔrocG::cat yeaC::Tn10 spc</i>	cDNA GP1119 → GP1157
BP545	<i>trpC2 ΔrocG::cat tepA::Tn10 spc</i>	cDNA GP1120 → GP1157
BP546	<i>trpC2 ΔrocG::cat deaD::tet</i>	cDNA GP1121 → GP1157
BP547	<i>trpC2 Δicd::ermC</i>	cDNA GP682 → 168
BP548	<i>trpC2 ilvA2 P_{hom(C46T)} ybxG::ermC</i>	cDNA BKE02060 → GP349
BP549	<i>trpC2 ilvA2 P_{hom(C46T)} bacP::ermC</i>	cDNA BKE09460 → GP349
BP550	<i>trpC2 gudB^{CR}::aphA3 amyE::P_{gudB}-gudB^{CR} cat</i>	pGP900 → BP442
BP610	<i>trpC2 disA-strep spc</i>	pBP599 → 168
BP623	<i>trpC2 ΔgudB^{CR}::aphA3 rocG::Tn10 spc lacA::(P_{degQ36}-prfA^{CR} ermC) amyE::(P_{plcA}-gfp-gudB⁺ cat) Δhag::tet</i>	cDNA GP902 → BP519

Strain	Genotype	Reference/Construction
BP624	<i>trpC2 ΔgudB^{CR}::aphA3 rocG::Tn10 spc lacA::(P_{gudB}⁻prfA^{CR} ermC) amyE::(P_{plcA}⁻gfp-gudB⁺ cat) Δhag::tet</i>	cDNA GP902 → BP520
BP625	<i>trpC2 amyE::(P_{plcA}⁻gfp-gudB⁺ cat) rocG::(P_{gudB}⁻prfA^{CR} loxscar) sacA::(phl P_{xyIA}⁻cre) ΔgudB^{CR}::aphA3 Δhag::tet</i>	cDNA GP902 → BP692
BP626	<i>trpC2 amyE::(P_{gudB}⁻lacZ cat)</i>	pGP900 → 168
BP627	<i>trpC2 amyE::(P_{plcA}⁻gfp-gudB⁺ P_{plcA}⁻lacZ cat)</i>	pBP416 → 168
BP628	<i>trpC2 ΔrocG::(P_{gudB}⁻prfA^{CR} loxScar) sacA::(phl P_{xyIA}⁻cre) gudB^{CR}::aphA3 amyE::(P_{plcA}⁻gfp-gudB⁺ P_{plcA}⁻lacZ cat)</i>	cDNA BP627 → BP670
BP629	<i>trpC2 ΔrecN::ermC rocG::Tn10 spc</i>	cDNA BP647 → GP747
BP630	<i>trpC2 ΔrecG::ermC rocG::Tn10 spc</i>	cDNA BP648 → GP747
BP631	<i>trpC2 ΔrecO::ermC rocG::Tn10 spc</i>	cDNA BP649 → GP747
BP632	<i>trpC2 amyE::P_{mut1}^{CR}-gudB⁺ cat</i>	pBP412 → 168
BP633	<i>trpC2 amyE::P_{mut3}^{CR}-gudB⁺ cat</i>	pBP413 → 168
BP634	<i>trpC2 amyE::P_{mut1}^{CR}-gudB⁺ orientation changed cat</i>	pBP414 → 168
BP635	<i>trpC2 amyE::P_{mut3}^{CR}-gudB⁺ orientation changed cat</i>	pBP415 → 168
BP636	<i>trpC2 ΔgudB^{CR}::aphA3 amyE::P_{mut1}^{CR}-gudB⁺ rocG::Tn10 spc</i>	cDNA BP632 → GP1161
BP637	<i>trpC2 ΔgudB^{CR}::aphA3 amyE::P_{mut3}^{CR}-gudB⁺ rocG::Tn10 spc</i>	cDNA BP633 → GP1161
BP638	<i>trpC2 ΔgudB^{CR}::aphA3 amyE::P_{mut1}^{CR}-gudB⁺ orientation changed rocG::Tn10 spc</i>	cDNA BP634 → GP1161
BP639	<i>trpC2 ΔgudB^{CR}::aphA3 (amyE::P_{mut3}^{CR}-gudB⁺ orientation changed rocG::Tn10 spc</i>	cDNA BP635 → GP1161
BP640	<i>trpC2 gltC::aphA3 amyE::P_{gltA}⁻lacZ cat</i>	cDNA GP1904 → GP669 (Dormeyer <i>et al.</i> , 2017)
BP641	<i>trpC2 ΔrecF::ermC</i>	LFH (MD107/MD108, MD109/MD110) → 168
BP642	<i>trpC2 ΔrecR::ermC</i>	LFH (MD101/MD102, MD103/MD104) → 168
BP643	<i>trpC2 ΔrecX::ermC</i>	LFH (MD95/MD96, MD97/MD98) → 168
BP644	<i>trpC2 ΔrecF::ermC rocG::Tn10 spc</i>	cDNA BP641 → GP747
BP645	<i>trpC2 ΔrecR::ermC rocG::Tn10 spc</i>	cDNA BP642 → GP747
BP646	<i>trpC2 ΔrecX::ermC rocG::Tn10 spc</i>	cDNA BP643 → GP747
BP647	<i>trpC2 ΔrecN::ermC</i>	LFH (MD119/MD120, MD121/MD122) → 168
BP648	<i>trpC2 ΔrecG::ermC</i>	LFH (MD113/MD114, MD115/MD116) → 168
BP649	<i>trpC2 ΔrecO::ermC</i>	LFH (MD125/MD126, MD127/MD128) → 168
BP650	<i>trpC2 gudB^{CR}::aphA3 amyE::P_{alf1}⁻-gudB^{CR} cat</i>	pBP301 → BP442
BP651	<i>trpC2 ilvA2 ybxG::ermC</i>	cDNA BKE02060 → 1A231
BP652	<i>trpC2 ilvA2 bacP::ermC</i>	cDNA BKE09460 → 1A231
BP653	<i>trpC2 gudB^{CR}::aphA3 amyE::(P⁻-gudB^{CR} cat)</i>	pBP303 → BP442
BP654	<i>trpC2 gudB^{CR}::aphA3 amyE::(P^{alf2}-gudB^{CR} cat)</i>	pBP166 → BP442
BP655	<i>trpC2 gudB^{CR}::aphA3 amyE::(P^{alf4}-gudB^{CR} cat)</i>	pBP167 → BP442
BP656	<i>trpC2 gudB^{CR}::aphA3 amyE::(P^{CR}-gudB⁺ cat) rocG::spc yqfF::ermC</i>	cDNA BKE25330 → BP404
BP657	<i>trpC2 gudB^{CR}::aphA3 amyE::(P⁺-gudB^{CR} cat) rocG::spc yqfF::ermC</i>	cDNA BKE25330 → BP405
BP658	<i>trpC2 ΔgltC::aphA3 amyE::(P_{gltA}⁻-lacZ cat) ΔrecA::ermC</i>	cDNA BKE16940 → BP640

Strain	Genotype	Reference/Construction
BP659	<i>trpC2 P_{gltA(C-14G)} gltC::aphA3 amyE::(P_{gltA}-lacZ cat)</i>	PCR BP796 → GP669
BP660	<i>trpC2 gudB^{CR}::aphA3 amyE::(P^{CR}-gudB⁺ cat) rocG::spc mfd::ermC</i>	cDNA GP1169 → BP404
BP661	<i>trpC2 gudB^{CR}::aphA3 amyE::(P⁺-gudB^{CR} cat) rocG::Tn10 spc mfd::ermC</i>	cDNA GP1169 → BP405
BP662	<i>trpC2 ΔgudB^{CR}::aphA3 rocG::Tn10 spc lacA::(P_{gudB}-prfA^{CR} ermC) amyE::(P_{plcA}-gfp-gudB⁺ cat) ypeP::tet</i>	cDNA BP444 → BP520
BP663	<i>trpC2 ΔgudB^{CR}::aphA3 rocG::Tn10 spc lacA::(P_{gudB}-prfA^{CR} ermC) amyE::(P_{plcA}-gfp-gudB⁺ cat) disA::tet</i>	cDNA GP987 → BP520
BP664	<i>trpC2 ΔrocG::(P_{gudB}-prfA^{CR} lox aphA3 lox) sacA::(phl P_{xyIA}-cre)</i>	cDNA JK27 → BP529
BP665	<i>trpC2 gudB^{CR}::aphA3 amyE::(P^{CR}-gudB⁺ cat) rocG::spc ypeP::tet</i>	cDNA BP444 → BP404
BP666	<i>trpC2 gudB^{CR}::aphA3 amyE::(P⁺-gudB^{CR} cat) rocG::spc ypeP::tet</i>	cDNA BP444 → BP405
BP667	<i>trpC2 gudB^{CR}::aphA3 amyE::(P^{CR}-gudB⁺ cat) rocG::Tn10 spc disA::tet</i>	cDNA GP987 → BP404
BP668	<i>trpC2 gudB^{CR}::aphA3 amyE::(P⁺-gudB^{CR} cat) rocG::Tn10 spc disA::tet</i>	cDNA GP987 → BP405
BP670	<i>trpC2 ΔrocG::(P_{gudB}-prfA^{CR} loxScar) sacA::(phl P_{xyIA}-cre) gudB^{CR}::aphA3</i>	cDNA BP442 → BP664 after induction of the cre-recombinase
BP671	<i>trpC2 gudB^{CR}::aphA3 amyE::(P_{gudB}-gudB^{CR} cat) rocG::Tn10 spc</i>	cDNA GP747 → BP550
BP672	<i>trpC2 gudB^{CR}::aphA3 amyE::(P_{alf1}-gudB^{CR} cat) rocG::Tn10 spc</i>	cDNA GP747 → BP650
BP673	<i>trpC2 gudB^{CR}::aphA3 amyE::(P⁻-gudB^{CR} cat) rocG::Tn10 spc</i>	cDNA GP747 → BP653
BP674	<i>trpC2 gudB^{CR}::aphA3 amyE::(P_{alf2}-gudB^{CR} cat) rocG::Tn10 spc</i>	cDNA GP747 → BP654
BP675	<i>trpC2 gudB^{CR}::aphA3 amyE::(P_{alf4}-gudB^{CR} cat) rocG::Tn10 spc</i>	cDNA GP747 → BP655
BP676	<i>trpC2 ΔyqfF::ermC ΔrocG::tet</i>	cDNA GP2040 → GP810
BP677	<i>trpC2 ΔyqfF::ermC</i>	cDNA BKE25330 → 168
BP678	<i>trpC2 rocG::Tn10 spc ΔyqfF::ermC</i>	cDNA BKE25330 → GP747
BP679	<i>trpC2 rocG::Tn10 spc ΔyqfF::tet</i>	cDNA GP2033 → GP747
BP680	<i>trpC2 ΔgdpP::spc ΔyqfF::ermC ΔrocG::tet</i>	cDNA GP810 → GP2040
BP681	<i>trpC2 gudB^{CR}::aphA3 amyE::(P_{gudB}-gudB⁺ cat) rocG::Tn10 spc</i>	BP671 spontaneous on SP
BP682	<i>trpC2 gudB^{CR}::aphA3 amyE::(P_{alf1}-gudB⁺ cat) rocG::Tn10 spc</i>	BP672 spontaneous on SP
BP683	<i>trpC2 gudB^{CR}::aphA3 amyE::(P_{alf2}-gudB⁺ cat) rocG::Tn10 spc</i>	BP674 spontaneous on SP
BP684	<i>trpC2 gudB^{CR}::aphA3 amyE::(P_{alf4}-gudB⁺ cat) rocG::Tn10 spc</i>	BP675 spontaneous on SP
BP685	<i>trpC2 ΔgudB^{CR}::ermC</i>	LFH (KG100/KG101, MT13/KG103) → 168
BP686	<i>trpC2 amyE::(P_{plcA}-gfp-gudB⁺ cat) rocG::(P_{gudB}-prfA^{CR} loxkanlox)</i>	cDNA BP529 → BP518
BP687	<i>trpC2 ΔgudB^{CR}::ermC rocG::Tn10 spc</i>	cDNA GP747 → BP685
BP688	<i>trpC2 amyE::(P_{plcA}-gfp-gudB⁺ cat) rocG::(P_{gudB}-prfA^{CR} loxkanlox) sacA::(phl P_{xyIA}-cre)</i>	cDNA JK27 → BP686

Strain	Genotype	Reference/Construction
BP689	<i>trpC2 ΔgudB^{CR}::ermC rocG::Tn10 spc lacA::(P_{xyI}-prfA aphA3 xyIR^{Bme})</i>	pBP105 → BP687
BP690	<i>trpC2 amyE::(P_{plcA}-gfp-gudB⁺ cat) rocG::(P_{gudB}-prfA^{CR} loxscar) sacA::(phI P_{xyIA}-cre)</i>	BP688 after induction of the cre-recombinase
BP691	<i>trpC2 ΔgudB^{CR}::ermC rocG::Tn10 spc lacA::(P_{xyI} prfA aphA3 xyIR^{Bme}) amyE::(P_{plcA}-gfp-gudB⁺ P_{plcA}-lacZ cat codirectional)</i>	cDNA BP627 → BP689
BP692	<i>trpC2 amyE::(P_{plcA}-gfp-gudB⁺ cat) rocG::(P_{gudB}-prfA^{CR} loxscar) sacA::(phI P_{xyIA}-cre) ΔgudB^{CR}::aphA3</i>	cDNA BP442 → BP690
BP693	<i>trpC2 ΔxkdE::P_{plcA}-lacZ ermC</i>	pBP422 → 168
BP694	<i>trpC2 amyE::(P_{plcA}-gfp-gudB⁺ cat) rocG::(P_{gudB}-prfA^{CR} loxscar) sacA::(phI P_{xyIA}-cre) ΔgudB^{CR}::aphA3 xkdE::(P_{plcA}-lacZ ermC)</i>	cDNA BP693 → BP692
BP696	<i>trpC2 amyE::(P_{plcA}-gfp-gudB⁺ cat) rocG::(P_{gudB}-prfA^{CR} loxscar) sacA::(phI P_{xyIA}-cre) ΔgudB^{CR}::aphA3 lacA::(P_{gudB}-prfA^{CR} ermC)</i>	cDNA BP210 → BP692
BP697	<i>trpC2 amyE::(P_{plcA}-gfp-gudB⁺ cat) rocG::(P_{gudB}-prfA^{CR} loxscar) sacA::(phI P_{xyIA}-cre) ΔgudB^{CR}::aphA3 lacA::(P_{gudB}-prfA^{CR} ermC) Δhag::tet</i>	cDNA GP902 → BP696
BP698	<i>trpC2 ΔgudB^{CR}::aphA3 amyE::(gudB^{CR} orientation changed lacZ cat)</i>	pBP4 → GP1160
BP699	<i>trpC2 ΔgudB^{CR}::aphA3 amyE::(gudB^{CR} lacZ cat)</i>	pGP900 → GP1160
BP700	<i>trpC2 ΔgudB^{CR}::cat lacA::(P^{CR}-gudB⁺ pdxST gfp aphA3) rocG::Tn10 spc Δhag::tet</i>	cDNA GP902 → BP216
BP701	<i>trpC2 splB-gfp spc</i>	pBP417 → 168
BP702	<i>trpC2 ΔgudB^{CR}::aphA3 rocG::Tn10 spc amyE::(P^{CR}-gudB⁺ cat) ΔrecN::ermC</i>	cDNA BP647 → BP404
BP703	<i>trpC2 ΔgudB^{CR}::aphA3 rocG::Tn10 spc amyE::(P⁺-gudB^{CR} cat) ΔrecN::ermC</i>	cDNA BP647 → BP405
BP704	<i>trpC2 ΔgudB^{CR}::aphA3 rocG::Tn10 spc amyE::(P^{CR}-gudB⁺ cat) ΔrecG::ermC</i>	cDNA BP648 → BP404
BP705	<i>trpC2 ΔgudB^{CR}::aphA3 rocG::Tn10 spc amyE::(P⁺-gudB^{CR} cat) ΔrecG::ermC</i>	cDNA BP648 → BP405
BP706	<i>trpC2 ΔgudB^{CR}::aphA3 rocG::Tn10 spc amyE::(P^{CR}-gudB⁺ cat) ΔrecO::ermC</i>	cDNA BP649 → BP404
BP707	<i>trpC2 ΔgudB^{CR}::aphA3 rocG::Tn10 spc amyE::(P⁺-gudB^{CR} cat) ΔrecO::ermC</i>	cDNA BP649 → BP405
BP708	<i>trpC2 ΔgudB^{CR}::aphA3 rocG::Tn10 spc amyE::(P^{CR}-gudB⁺ cat) ΔrecF::ermC</i>	cDNA BP641 → BP404
BP709	<i>trpC2 ΔgudB^{CR}::aphA3 rocG::Tn10 spc amyE::(P⁺-gudB^{CR} cat) ΔrecF::ermC</i>	cDNA BP641 → BP405
BP710	<i>trpC2 ΔgudB^{CR}::aphA3 rocG::Tn10 spc amyE::(P^{CR}-gudB⁺ cat) ΔrecR::ermC</i>	cDNA BP642 → BP404
BP711	<i>trpC2 ΔgudB^{CR}::aphA3 rocG::Tn10 spc amyE::(P⁺-gudB^{CR} cat) ΔrecR::ermC</i>	cDNA BP642 → BP405
BP712	<i>trpC2 ΔgudB^{CR}::aphA3 rocG::Tn10 spc amyE::(P^{CR}-gudB⁺ cat) ΔrecX::ermC</i>	cDNA BP643 → BP404
BP713	<i>trpC2 ΔgudB^{CR}::aphA3 rocG::Tn10 spc amyE::(P⁺-gudB^{CR} cat) ΔrecX::ermC</i>	cDNA BP643 → BP405
BP714	<i>trpC2 ΔgudB^{CR}::aphA3 rocG::Tn10 spc amyE::(P^{CR}-gudB⁺ cat) ΔycdB::ermC</i>	cDNA BKE02790 → BP404
BP715	<i>trpC2 ΔgudB^{CR}::aphA3 rocG::Tn10 spc amyE::(P⁺-gudB^{CR} cat) ΔycdB::ermC</i>	cDNA BKE02790 → BP405

Strain	Genotype	Reference/Construction
BP716	<i>trpC2 ΔgudB^{CR}::aphA3 rocG::Tn10 spc amyE::(P^{CR}-gudB⁺ cat) ΔoppA::ermC</i>	cDNA BKE11430 → BP404
BP717	<i>trpC2 ΔgudB^{CR}::aphA3 rocG::Tn10 spc amyE::(P⁺-gudB^{CR} cat) ΔoppA::ermC</i>	cDNA BKE11430 → BP405
BP718	<i>trpC2 ΔgudB^{CR}::aphA3 rocG::Tn10 spc amyE::(P^{CR}-gudB⁺ cat) ΔetfB::ermC</i>	cDNA BKE28530 → BP404
BP719	<i>trpC2 ΔgudB^{CR}::aphA3 rocG::Tn10 spc amyE::(P⁺-gudB^{CR} cat) ΔetfB::ermC</i>	cDNA BKE28530 → BP405
BP720	<i>trpC2 ΔgudB^{CR}::aphA3 rocG::Tn10 spc amyE::(P^{CR}-gudB⁺ cat) ΔsftA::ermC</i>	cDNA BKE29805 → BP404
BP721	<i>trpC2 ΔgudB^{CR}::aphA3 rocG::Tn10 spc amyE::(P⁺-gudBCR cat) ΔsftA::ermC</i>	cDNA BKE29805 → BP405
BP722	<i>trpC2 ΔgudB^{CR}::aphA3 rocG::Tn10 spc amyE::(P^{CR}-gudB⁺ cat) ΔfadE::ermC</i>	cDNA BKE32820 → BP404
BP723	<i>trpC2 ΔgudB^{CR}::aphA3 rocG::Tn10 spc amyE::(P⁺-gudB^{CR} cat) ΔfadE::ermC</i>	cDNA BKE32820 → BP405
BP724	<i>trpC2 ΔdprA::ermC</i>	LFH (MD169/MD168, MD170/MD171) → 168
BP726	<i>trpC2 ΔgudB^{CR}::aphA3 rocG::Tn10 spc amyE::(P^{CR}-gudB⁺ cat) ΔhelD::ermC</i>	cDNA BKE33450 → BP404
BP727	<i>trpC2 ΔgudB^{CR}::aphA3 rocG::Tn10 spc amyE::(P⁺-gudB^{CR} cat) ΔhelD::ermC</i>	cDNA BKE33450 → BP405
BP728	<i>trpC2 ΔgudB^{CR}::aphA3 rocG::Tn10 spc amyE::(P^{CR}-gudB⁺ cat) ΔfadF::ermC</i>	cDNA BKE37180 → BP404
BP729	<i>trpC2 ΔgudB^{CR}::aphA3 rocG::Tn10 spc amyE::(P⁺-gudB^{CR} cat) ΔfadF::ermC</i>	cDNA BKE37180 → BP405
BP730	<i>trpC2 ΔgudB^{CR}::aphA3 rocG::Tn10 spc amyE::(P^{CR}-gudB⁺ cat) ΔyxC::ermC</i>	cDNA BKE39600 → BP404
BP731	<i>trpC2 ΔgudB^{CR}::aphA3 rocG::Tn10 spc amyE::(P⁺-gudB^{CR} cat) ΔyxC::ermC</i>	cDNA BKE39600 → BP405
BP732	<i>trpC2 ΔgudB^{CR}::aphA3 rocG::Tn10 spc amyE::(P^{CR}-gudB⁺ cat) ΔrocR::ermC</i>	cDNA BKE40350 → BP404
BP733	<i>trpC2 ΔgudB^{CR}::aphA3 rocG::Tn10 spc amyE::(P⁺-gudB^{CR} cat) ΔrocR::ermC</i>	cDNA BKE40350 → BP405
BP734	<i>trpC2 Δnfo::ermC</i>	LFH (JG29/JG30, JG31/JG32) → 168
BP736	<i>trpC2 ΔrnhC::ermC</i>	LFH (MT7/MD193, MD194/MT10) → 168
BP738	<i>trpC2 ΔrecO::tet</i>	LFH (MD126/MD125, MD127/MD128) → 168
BP739	<i>trpC2 rocG::Tn10 spc gudB⁺ ΔrecO::ermC</i>	cDNA BP649 → GP753
BP740	<i>trpC2 rocG::Tn10 spc gudB⁺ ΔrecR::ermC</i>	cDNA BP642 → GP753
BP741	<i>trpC2 rocG::Tn10 spc gudB⁺ ΔrocR::ermC</i>	cDNA BKE40350 → GP753
BP742	<i>trpC2 rocG::Tn10 spc gudB⁺ ΔfadF::ermC</i>	cDNA BKE37180 → GP753
BP743	<i>trpC2 rocG::Tn10 spc gudB⁺ ΔoppA::ermC</i>	cDNA BKE11430 → GP753
BP744	<i>trpC2 rocG::Tn10 spc gudB⁺ ΔetfB::ermC</i>	cDNA BKE28530 → GP753
BP745	<i>trpC2 rocG::Tn10 spc gudB⁺ ΔrecJ::ermC</i>	cDNA BKE27620 → GP753
BP746	<i>trpC2 rocG::Tn10 spc gudB⁺ ΔrecA::ermC</i>	cDNA BKE16940 → GP753
BP747	<i>trpC2 rocG::Tn10 spc gudB⁺ Δmfd::ermC</i>	cDNA BKE00550 → GP753
BP748	<i>trpC2 ΔrecJ::ermC</i>	cDNA BKE27620 → 168
BP749	<i>trpC2 ΔrecA::ermC</i>	cDNA BKE16940 → 168
BP750	<i>trpC2 Δmfd::ermC</i>	cDNA BKE00550 → 168

Strain	Genotype	Reference/Construction
BP751	<i>trpC2 ΔgudB^{CR}::aphA3 rocG::Tn10 spc amyE::(P^{CR}-gudB⁺ cat) ΔrecJ::ermC</i>	cDNA BKE27620 → BP404
BP752	<i>trpC2 ΔgudB^{CR}::aphA3 rocG::Tn10 spc amyE::(P⁺-gudB^{CR} cat) ΔrecJ::ermC</i>	cDNA BKE27620 → BP405
BP753	<i>trpC2 ΔgudB^{CR}::aphA3 rocG::Tn10 spc amyE::(P^{CR}-gudB⁺ cat) ΔrecA::ermC</i>	cDNA BKE16940 → BP404
BP754	<i>trpC2 ΔgudB^{CR}::aphA3 rocG::Tn10 spc amyE::(P⁺-gudB^{CR} cat) ΔrecA::ermC</i>	cDNA BKE16940 → BP405
BP755	<i>trpC2 ΔgudB^{CR}::aphA3 rocG::Tn10 spc amyE::(P^{CR}-gudB⁺ cat) Δmfd::ermC</i>	cDNA BKE00550 → BP404
BP756	<i>trpC2 ΔgudB^{CR}::aphA3 rocG::Tn10 spc amyE::(P⁺-gudB^{CR} cat) Δmfd::ermC</i>	cDNA BKE00550 → BP405
BP758	<i>trpC2 ΔgudB^{CR}::aphA3 rocG::Tn10 spc amyE::(P⁺-gudB^{CR} cat) ΔyabT::ermC</i>	cDNA GP577 → BP405
BP759	<i>trpC2 ΔgudB^{CR}::aphA3 rocG::Tn10 spc amyE::(P^{CR}-gudB⁺ cat) ΔyabT::ermC</i>	cDNA GP577 → BP404
BP760	<i>trpC2 ΔgudB^{CR}::aphA3 rocG::Tn10 spc amyE::(P⁺-gudB^{CR} cat) ΔdprA::ermC</i>	cDNA BP724 → BP405
BP761	<i>trpC2 ΔgudB^{CR}::aphA3 rocG::Tn10 spc amyE::(P^{CR}-gudB⁺ cat) ΔdprA::ermC</i>	cDNA BP724 → BP404
BP762	<i>trpC2 ΔgudB^{CR}::aphA3 rocG::Tn10 spc amyE::(P⁺-gudB^{CR} cat) ΔrnhC::ermC</i>	cDNA BP736 → BP405
BP763	<i>trpC2 ΔgudB^{CR}::aphA3 rocG::Tn10 spc amyE::(P^{CR}-gudB⁺ cat) ΔrnhC::ermC</i>	cDNA BP736 → BP404
BP764	<i>trpC2 ΔgudB^{CR}::aphA3 rocG::Tn10 spc amyE::(P⁺-gudB^{CR} cat) Δnfo::ermC</i>	cDNA BP734 → BP405
BP765	<i>trpC2 ΔgudB^{CR}::aphA3 rocG::Tn10 spc amyE::(P^{CR}-gudB⁺ cat) Δnfo::ermC</i>	cDNA BP734 → BP404
BP766	<i>trpC2 ΔgudB^{CR}::ermC rocG::Tn10 spc lacA::(P_{xyI}-prfA aphA3 xylR^{Bme}) amyE::(P_{plcA}-gfp-gudB⁺ P_{plcA}-lacZ cat codirectional) SM Amplification</i>	BP691 spontaneous on SP
BP768	<i>trpC2 ΔgudB^{CR}::aphA3 rocG::Tn10 spc amyE::(P⁺-gudB^{CR} cat) ΔrnhB::ermC</i>	cDNA BKE16060 → BP405
BP769	<i>trpC2 ΔgudB^{CR}::aphA3 rocG::Tn10 spc amyE::(P^{CR}-gudB⁺ cat) ΔrnhB::ermC</i>	cDNA BKE16060 → BP404
BP770	<i>trpC2 ΔgudB^{CR}::aphA3 rocG::Tn10 spc amyE::(P⁺-gudB^{CR} cat) ΔrecU::ermC</i>	cDNA BKE22310 → BP405
BP771	<i>trpC2 ΔgudB^{CR}::aphA3 rocG::Tn10 spc amyE::(P^{CR}-gudB⁺ cat) ΔrecU::ermC</i>	cDNA BKE22310 → BP404
BP772	<i>trpC2 ΔgudB^{CR}::aphA3 rocG::Tn10 spc amyE::(P⁺-gudB^{CR} cat) ΔrecO::ermC</i>	cDNA BKE25280 → BP405
BP773	<i>trpC2 ΔgudB^{CR}::aphA3 rocG::Tn10 spc amyE::(P^{CR}-gudB⁺ cat) ΔrecO::ermC</i>	cDNA BKE25280 → BP404
BP774	<i>trpC2 ΔrecO::ermC</i>	cDNA BKE25280 → 168
BP775	<i>trpC2 rocG::Tn10 spc gudB⁺ ΔrecO::ermC</i>	cDNA BKE25280 → GP753
BP776	<i>trpC2 rocG::Tn10 spc gudB⁺ ΔrecO::tet</i>	cDNA BP738 → GP753
BP777	<i>trpC2 rocG::Tn10 spc gudB⁺ ΔrnhC::ermC</i>	cDNA BP736 → GP753
BP778	<i>trpC2 rocG::Tn10 spc gudB⁺ ΔrecU::ermC</i>	cDNA BKE22310 → GP753
BP779	<i>trpC2 rocG::Tn10 spc gudB⁺ Δnfo::ermC</i>	cDNA BP734 → GP753
BP780	<i>trpC2 rocG::Tn10 spc gudB⁺ ΔrnhB::ermC</i>	cDNA BKE16060 → GP753
BP781	<i>trpC2 rocG::Tn10 spc gudB⁺ ΔdprA::ermC</i>	cDNA BP724 → GP753

Strain	Genotype	Reference/Construction
BP782	<i>trpC2 rocG::Tn10 spc gudB⁺ ΔyabT::ermC</i>	cDNA GP577 → GP753
BP783	<i>trpC2 ΔrnhB::ermC</i>	cDNA BKE16060 → 168
BP784	<i>trpC2 ΔrecU::ermC</i>	cDNA BKE22310 → 168
BP785	<i>trpC2 ΔrecR::ermC recO::tet</i>	cDNA BP738 → BP642
BP786	<i>trpC2 rocG::Tn10 spc gudB⁺ ΔrecO::tet ΔrecR::ermC</i>	cDNA BP738 → BP740
BP787	<i>trpC2 ΔgudB^{CR}::aphA3 rocG::Tn10 spc amyE::(P⁻-gudB^{CR} cat) ΔrecO::tet</i>	cDNA BP738 → BP405
BP788	<i>trpC2 ΔgudB^{CR}::aphA3 rocG::Tn10 spc amyE::(P^{CR}-gudB⁺ cat) ΔrecO::tet</i>	cDNA BP738 → BP404
BP789	<i>trpC2 ΔgudB^{CR}::aphA3 rocG::Tn10 spc amyE::(P^{CR}-gudB⁺ cat) ΔrecR::ermC ΔrecO::tet</i>	cDNA BP738 → BP710
BP790	<i>trpC2 ΔgudB^{CR}::aphA3 rocG::Tn10 spc amyE::(P⁻-gudB^{CR} cat) ΔrecR::ermC ΔrecO::tet</i>	cDNA BP638 → BP711
BP791	<i>trpC2 gltC::aphA3 amyE::(P_{gltA}-lacZ cat) gltR²⁴ SM1</i>	BP640 spontaneous on C-Glc (Dormeyer <i>et al.</i> , 2017)
BP792	<i>trpC2 gltC::aphA3 amyE::(P_{gltA}-lacZ cat) gene amplification of the gltAB locus SM2</i>	BP640 spontaneous on C-Glc (Dormeyer <i>et al.</i> , 2017)
BP793	<i>trpC2 gltC::aphA3 amyE::(P_{gltA}-lacZ cat) gltR²⁴ SM3</i>	BP640 spontaneous on C-Glc (Dormeyer <i>et al.</i> , 2017)
BP794	<i>trpC2 gltC::aphA3 amyE::(P_{gltA}-lacZ cat) gene amplification of the gltAB locus SM4</i>	BP640 spontaneous on C-Glc (Dormeyer <i>et al.</i> , 2017)
BP795	<i>trpC2 gltC::aphA3 amyE::(P_{gltA}-lacZ cat) gltR²⁴ SM5</i>	BP640 spontaneous on C-Glc (Dormeyer <i>et al.</i> , 2017)
BP796	<i>trpC2 gltC::aphA3 amyE::(P_{gltA}-lacZ cat) P_{gltA(C-14G)} SM6</i>	BP640 spontaneous on C-Glc (Dormeyer <i>et al.</i> , 2017)
BP797	<i>trpC2 ΔrocG::(P_{gudB}-prfA^{CR} loxScar) sacA::(phl P_{xyIA}-cre) gudB^{CR}::aphA3 amyE::(P_{plcA}-gfp-gudB⁺ P_{plcA}-lacZ cat codirectional) blue SM 3</i>	BP628 spontaneous on SP X-Gal
BP798	<i>trpC2 ΔrocG::(P_{gudB}-prfA^{CR} loxScar) sacA::(phl P_{xyIA}-cre) gudB^{CR}::aphA3 amyE::(P_{plcA}-gfp-gudB⁺ P_{plcA}-lacZ cat codirectional) blue SM 4</i>	BP628 spontaneous on SP X-Gal
BP799	<i>trpC2 ΔrocG::(P_{gudB}-prfA^{CR} loxScar) sacA::(phl P_{xyIA}-cre) gudB^{CR}::aphA3 amyE::(P_{plcA}-gfp-gudB⁺ P_{plcA}-lacZ cat codirectional) white SM 3</i>	BP628 spontaneous on SP X-Gal
BP800	<i>trpC2 ΔrocG::(P_{gudB}-prfA^{CR} loxScar) sacA::(phl P_{xyIA}-cre) gudB^{CR}::aphA3 amyE::(P_{plcA}-gfp-gudB⁺ P_{plcA}-lacZ cat codirectional) white SM 4</i>	BP628 spontaneous on SP X-Gal
BP801	<i>trpC2 amyE::(P_{gltA(C-14G)}-lacZ cat)</i>	pBP468 → 168 (Dormeyer <i>et al.</i> , 2017)
BP802	<i>trpC2 amyE:: amyE::(P_{gltA(C-14G)}-lacZ cat) ΔgltC::aphA3</i>	cDNA BP801 → GP1904 (Dormeyer <i>et al.</i> , 2017)
BP803	<i>trpC2 amyE::(P_{gltA(C-14G)}-lacZ cat) rocG::Tn10 spc</i>	cDNA GP747 → GP669
BP804	<i>trpC2 amyE:: P_{gltA}-lacZ cat ΔgltC::aphA3 rocG::Tn10 spc</i>	cDNA GP747 → BP640
BP805	<i>trpC2 amyE::(P_{gltA(C-14G)}-lacZ cat) rocG::Tn10 spc</i>	cDNA GP747 → BP801
BP806	<i>trpC2 amyE::(P_{gltA(C-14G)}-lacZ cat) ΔgltC::aphA3 rocG::Tn10 spc</i>	cDNA GP747 → BP802
BP807	<i>trpC2 xylR^{Bme} amyE::(P_{plcA}-pdxST-Strep-gfp-gudB⁺ P_{plcA}-lacZ cat codirectional)</i>	pBP470 → 168
BP808	<i>trpC2 ΔgudB^{CR}::ermC rocG::Tn10 spc lacA::(P_{xyI} prfA aphA3 xylR^{Bme}) amyE::(P_{plcA}-pdxST-Strep-gfp-gudB⁺ P_{plcA}-lacZ cat codirectional)</i>	cDNA BP807 → BP689
BP809	<i>trpC2 amyE::(P_{gltA(pT-32A)}-lacZ aphA3)</i>	cDNA GP689 → 168
BP810	<i>trpC2 amyE::(P_{gltA(pC-10T)}-lacZ aphA3)</i>	cDNA GP692 → 168

Strain	Genotype	Reference/Construction
BP811	<i>trpC2 amyE::(P_{gltA}-lacZ aphA3) ΔrocG::cat</i>	cDNA GP1157 → GP342
BP812	<i>trpC2 amyE::(P_{gltA}-lacZ aphA3) gltC::Tn10 spc ΔrocG::cat</i>	cDNA GP1157 → GP650
BP813	<i>trpC2 amyE::(P_{gltA(pT-32A)}-lacZ aphA3) gltC::Tn10 spc ΔrocG::cat</i>	cDNA GP1157 → GP689
BP814	<i>trpC2 gltC::Tn10 spc amyE::(P_{gltA(pC-107)}-lacZ aphA3) ΔrocG::cat</i>	cDNA GP1157 → GP692
BP815	<i>trpC2 amyE::(P_{gltA(pT-32A)}-lacZ aphA3) ΔrocG::cat</i>	cDNA GP1157 → BP809
BP816	<i>trpC2 amyE::(P_{gltA(pC-107)}-lacZ aphA3) ΔrocG::cat</i>	cDNA GP1157 → BP810
BP817	<i>trpC2 amyE::(P_{gltA}-lacZ aphA3) ΔrocG::cat gudB⁺</i>	BP811 spontaneous on SP
BP818	<i>trpC2 amyE::(P_{gltA}-lacZ aphA3) gltC::Tn10 spc ΔrocG::cat gudB⁺</i>	cDNA GP650 → BP817
BP819	<i>trpC2 amyE::(P_{gltA(pT-32A)}-lacZ aphA3) gltC::Tn10 spc ΔrocG::cat gudB⁺</i>	cDNA GP689 → BP821
BP820	<i>trpC2 amyE::(P_{gltA(pC-107)}-lacZ aphA3) gltC::Tn10 spc ΔrocG::cat gudB⁺</i>	cDNA GP692 → BP822
BP821	<i>trpC2 amyE::(P_{gltA(pT-32A)}-lacZ aphA3) ΔrocG::cat gudB⁺</i>	BP815 spontaneous on SP
BP822	<i>trpC2 amyE::(P_{gltA(pC-107)}-lacZ aphA3) ΔrocG::cat gudB⁺</i>	BP816 spontaneous on SP
BP823	<i>trpC2 ΔgudB^{CR}::ermC ΔrocG::cat</i>	GP1157 → BP685
BP824	<i>trpC2 ΔgudB^{CR}::aphA3 rocG::Tn10 spc amyE::(P_{plcA}-gfp-gudB⁺ cat) lacA::(P_{gudB}-prfA(C530A) ermC)</i>	pBP474 → BP513
BP825	<i>trpC2 ΔgudB^{CR}::aphA3 rocG::Tn10 spc amyE::(P_{plcA}-gfp-gudB⁺ cat) lacA::(P_{gudB}-prfA(del C530) ermC)</i>	pBP475 → BP513
BP826	<i>trpC2 ΔgudB^{CR}::aphA3 rocG::Tn10 spc amyE::(P_{plcA}-gfp-gudB⁺ cat) lacA::(P_{gudB}-prfA(ins A527) ermC)</i>	pBP476 → BP513
BP827	<i>trpC2 ΔgudB^{CR}::aphA3 rocG::Tn10 spc amyE::(P_{plcA}-gfp-gudB⁺ cat) lacA::(P_{gudB}-prfA⁺ ermC)</i>	BP824 spontaneous on SP
BP828	<i>trpC2 amyE::(P_{gltA(T-28A)}-lacZ cat)</i>	pBP479 → 168
BP829	<i>trpC2 amyE::(P_{gltA(T-48C)}-lacZ cat)</i>	pBP480 → 168
BP830	<i>trpC2 amyE::(P_{gltA}-lacZ cat) rocG::Tn10 spc gudB⁺</i>	BP803 spontaneous on SP
BP831	<i>trpC2 rocG::Tn10 spc ΔgltC::aphA3</i>	cDNA GP747 → GP1904
BP832	<i>trpC2 amyE::(P_{gltA(T-28A)}-lacZ cat) ΔgltC::aphA3</i>	cDNA BP828 → GP1904
BP833	<i>trpC2 amyE::(P_{gltA(T-28A)}-lacZ cat) rocG::Tn10 spc</i>	cDNA BP828 → GP747
BP834	<i>trpC2 amyE::(P_{gltA(T-28A)}-lacZ cat) rocG::Tn10 spc ΔgltC::aphA3</i>	cDNA BP828 → BP831
BP835	<i>trpC2 amyE::(P_{gltA(T-48C)}-lacZ cat) ΔgltC::aphA3</i>	cDNA BP829 → GP1904
BP836	<i>trpC2 amyE::(P_{gltA(T-48C)}-lacZ cat) rocG::Tn10 spc</i>	cDNA BP829 → GP747
BP837	<i>trpC2 amyE::(P_{gltA(T-48C)}-lacZ cat) rocG::Tn10 spc ΔgltC::aphA3</i>	cDNA BP829 → BP831
BP838	<i>trpC2 amyE::(P_{gltA(T-28A)}-lacZ cat) rocG::Tn10 spc gudB⁺</i>	BP833 spontaneous on SP
BP839	<i>trpC2 amyE::(P_{gltA(T-48C)}-lacZ cat) rocG::Tn10 spc gudB⁺</i>	BP836 spontaneous on SP
BP840	<i>trpC2 amyE::(P_{gltA(T-28A)}-lacZ cat) rocG::Tn10 spc gudB⁺ ΔgltC::aphA3</i>	cDNA GP1904 → BP838
BP841	<i>trpC2 amyE::(P_{gltA(T-48C)}-lacZ cat) rocG::Tn10 spc gudB⁺ ΔgltC::aphA3</i>	cDNA GP1904 → BP839
BP842	<i>trpC2 amyE::(P_{gltA}-lacZ cat) rocG::Tn10 spc gudB⁺ ΔgltC::aphA3</i>	cDNA GP1904 → BP830
BP843	<i>trpC2 ΔgudB^{CR}::ermC rocG::Tn10 spc lacA::(P_{xyI}-prfA aphA3 xyIR^{Bme}) amyE::(P_{plcA}-pdxST-strep-gfp-gudB⁺ P_{plcA}-lacZ cat) SM Amplification</i>	BP808 spontaneous on SP

Strain	Genotype	Reference/Construction
BP845	<i>trpC2 gltC::Tn10 spc amyE::(P_{gltA}-lacZ cat)</i> <i>ΔrocG::aphA3</i>	cDNA BP848 → BP850
BP846	<i>trpC2 amyE::(P_{plcA}-gfp-gudB⁺ cat) rocG::(P_{gudB}-prfA⁺ loxscar) sacA::(phl P_{xyIA}-cre) ΔgudB^{CR}::aphA3</i>	BP692 spontaneous on SP (SM1)
BP847	<i>trpC2 amyE::(P_{plcA}-gfp-gudB⁺ cat) rocG::(P_{gudB}-prfA^{CR/+} loxscar) sacA::(phl P_{xyIA}-cre) ΔgudB^{CR}::aphA3</i> <i>lacA::(P_{gudB}-prfA^{CR/+} ermC)</i>	BP696 spontaneous on SP (SM1)
BP848	<i>trpC2 ΔrocG::aphA3 gudB⁺</i>	GP726 spontaneous on SP
BP849	<i>trpC2 ΔrocG::aphA3 gudB⁺ gltC::Tn10 spc</i>	cDNA GP738 → BP848
BP850	<i>trpC2 gltC::Tn10 spc amyE::(P_{gltA}-lacZ cat)</i>	cDNA GP738 → GP669
BP851	<i>trpC2 ΔrocG::aphA3 gudB⁺ amyE::(P_{gltA}-lacZ cat)</i>	cDNA GP669 → BP848
BP852	<i>trpC2 ΔrocG::aphA3 gudB⁺ gltC::Tn10 spc amyE::(P_{gltA}- lacZ cat)</i>	cDNA GP669 → BP849
BP853	<i>trpC2 ΔrocG::aphA3 gudB⁺ gltC::Tn10 spc amyE::(gltC P_{gltA}-lacZ cat)</i>	pGP908 → BP849
BP854	<i>trpC2 ΔrocG::aphA3 gudB⁺ gltC::Tn10 spc amyE::(gltC(P88L) P_{gltA}-lacZ cat)</i>	pGP953 → BP849
BP855	<i>trpC2 ΔrocG::aphA3 gudB⁺ gltC::Tn10 spc amyE::(gltC(I160K) P_{gltA}-lacZ cat)</i>	pGP954 → BP849
BP856	<i>trpC2 ΔrocG::aphA3 gudB⁺ gltC::Tn10 spc amyE::(gltC(T99A) P_{gltA}-lacZ cat)</i>	pGP955 → BP849
BP857	<i>trpC2 ΔrocG::(P_{gudB}-prfA^{CR} loxScar) sacA::(phl P_{xyIA}-cre) gudB^{CR}::aphA3 amyE::(P_{plcA}-gfp-gudB⁺ P_{plcA}-lacZ cat)</i> <i>Δhag::tet</i>	cDNA GP902 → BP628
BP858	<i>trpC2 ΔgudB^{CR}::ermC rocG::Tn10 spc lacA::(P_{xyIA}-prfA aphA3 xylR^{Bme}) amyE::(P_{plcA}-gfp-gudB⁺ P_{plcA}-lacZ cat)</i> <i>Δhag::tet</i>	cDNA GP902 → BP691
BP859	<i>trpC2 ΔgudB^{CR}::aphA3 rocG::Tn10 spc amyE::(P_{plcA}-gfp- gudB⁺ cat) lacA::(P_{gudB}-prfA(ins (2xA)527) ermC)</i>	pBP483 → BP513
BP860	<i>trpC2 ΔgudB^{CR}::aphA3 rocG::Tn10 spc amyE::(P_{plcA}-gfp- gudB⁺ cat) lacA::(P_{gudB}-prfA(ins (3xA)527) ermC)</i>	pBP484 → BP513
BP861	<i>trpC2 ΔgudB^{CR}::aphA3 rocG::Tn10 spc amyE::(P_{plcA}-gfp- gudB⁺ cat) lacA::(P_{gudB}-prfA(ins (4xA)527) ermC)</i>	pBP485 → BP513
BP862	<i>trpC2 amyE::(P_{gltA}(Shuffle I BOX III)-lacZ cat)</i>	pBP491 → 168
BP863	<i>trpC2 amyE::(P_{gltA}(Shuffle II BOX III)-lacZ cat)</i>	pBP492 → 168
BP864	<i>trpC2 amyE::(P_{gltA}(Shuffle III BOX III)-lacZ cat)</i>	pBP493 → 168
BP865	<i>trpC2 lacA::(P_{gudB}-prfA⁺ ermC)</i>	cDNA SM BP520 → 168
BP866	<i>trpC2 ΔrocG::aphA3 gudB⁺ amyE::(P_{gltA}(Shuffle I BOX III)-lacZ cat)</i>	cDNA BP862 → BP848
BP867	<i>trpC2 ΔrocG::aphA3 gudB⁺ amyE::(P_{gltA}(Shuffle II BOX III)-lacZ cat)</i>	cDNA BP863 → BP848
BP868	<i>trpC2 ΔrocG::aphA3 gudB⁺ amyE::(P_{gltA}(Shuffle III BOX III)- lacZ cat)</i>	cDNA BP864 → BP848
BP869	<i>trpC2 ΔrocG::aphA3 gudB⁺ gltC::Tn10 spc amyE::(P_{gltA}(Shuffle I BOX III)-lacZ cat)</i>	cDNA BP862 → BP849
BP870	<i>trpC2 ΔrocG::aphA3 gudB⁺ gltC::Tn10 spc amyE::(P_{gltA}(Shuffle II BOX III)-lacZ cat)</i>	cDNA BP863 → BP849
BP871	<i>trpC2 ΔrocG::aphA3 gudB⁺ gltC::Tn10 spc amyE::(P_{gltA}(Shuffle III BOX III)-lacZ cat)</i>	cDNA BP864 → BP849
BP872	<i>trpC2 amyE::(P_{gltA}(Shuffle I BOX III)-lacZ cat) gltC::Tn10 spc</i>	cDNA GP738 → BP862
BP873	<i>trpC2 amyE::(P_{gltA}(Shuffle II BOX III)-lacZ cat) gltC::Tn10 spc</i>	cDNA GP738 → BP863

Strain	Genotype	Reference/Construction
BP874	<i>trpC2 amyE::(P_{gltA}(Shuffle III BOX III)-lacZ cat) gltC::Tn10 spc</i>	cDNA GP738 → BP864
BP875	<i>trpC2 amyE::(P_{gltA}(Shuffle I BOX III)-lacZ cat) ΔrocG::aphA3</i>	cDNA BP848 → BP862
BP876	<i>trpC2 amyE::(P_{gltA}(Shuffle II BOX III)-lacZ cat) ΔrocG::aphA3</i>	cDNA BP848 → BP863
BP877	<i>trpC2 amyE::(P_{gltA}(Shuffle III BOX III)-lacZ cat) ΔrocG::aphA3</i>	cDNA BP848 → BP864
BP878	<i>trpC2 amyE::(P_{gltA}(Shuffle I BOX III)-lacZ cat) ΔrocG::aphA3 gltC::Tn10 spc</i>	cDNA GP738 → BP875
BP879	<i>trpC2 amyE::(P_{gltA}(Shuffle II BOX III)-lacZ cat) ΔrocG::aphA3 gltC::Tn10 spc</i>	cDNA GP738 → BP876
BP880	<i>trpC2 amyE::(P_{gltA}(Shuffle III BOX III)-lacZ cat) ΔrocG::aphA3 gltC::Tn10 spc</i>	cDNA GP738 → BP877
BP883	<i>trpC2 ΔgudB^{CR}::aphA3 rocG::Tn10 spc amyE::(P_{plcA}-gfp-gudB⁺ cat) lacA::(P_{gudB}-prfA(ins (5xA)527) ermC)</i>	pBP486 → BP513
BP884	<i>trpC2 ΔgudB^{CR}::aphA3 rocG::Tn10 spc amyE::(P_{plcA}-gfp-gudB⁺ cat) lacA::(P_{gudB}-prfA(ins (10xA)527) ermC)</i>	pBP487 → BP513
BP885	<i>trpC2 amyE::(P_{gltA}-lacZ cat) ΔrocG::aphA3</i>	cDNA BP848 → GP669
BP886	<i>trpC2 ΔgudB^{CR}::aphA3 rocG::Tn10 spc amyE::(P_{plcA}-gfp-gudB⁺ cat) lacA::(P_{gudB}-prfA(ins (2xA)527) ermC) SM</i>	BP859 Spontaneous on SP
BP887	<i>trpC2 ΔgudB^{CR}::aphA3 rocG::Tn10 spc amyE::(P_{plcA}-gfp-gudB⁺ cat) lacA::(P_{gudB}-prfA(ins (3xA)527) ermC) SM</i>	BP860 Spontaneous on SP
BP888	<i>trpC2 ΔgudB^{CR}::aphA3 rocG::Tn10 spc amyE::(P_{plcA}-gfp-gudB⁺ cat) lacA::(P_{gudB}-prfA(ins (4xA)527) ermC) SM</i>	BP861 Spontaneous on SP
BP889	<i>trpC2 ΔgudB^{CR}::aphA3 rocG::Tn10 spc amyE::(P_{plcA}-gfp-gudB⁺ cat) lacA::(P_{gudB}-prfA(ins (15xA)527) ermC)</i>	pBP488 → BP513

6.4.2. *B. subtilis* strains used in this work

Strain	Genotype	Reference/Construction
1A231	<i>trpC2 ilvA2</i>	Barat <i>et al.</i> , 1965
BKE00550	<i>trpC2 Δmfd::erm</i>	Bacillus Genetic Stock Center
BKE02060	<i>trpC2 ΔybxG::erm</i>	Bacillus Genetic Stock Center
BKE02790	<i>trpC2 ΔycdB::erm</i>	Bacillus Genetic Stock Center
BKE09460	<i>trpC2 ΔbcaP::erm</i>	Bacillus Genetic Stock Center
BKE11430	<i>trpC2 ΔoppA::erm</i>	Bacillus Genetic Stock Center
BKE16060	<i>trpC2 ΔrnhB::erm</i>	Bacillus Genetic Stock Center
BKE16940	<i>trpC2 ΔrecA::erm</i>	Bacillus Genetic Stock Center
BKE22310	<i>trpC2 ΔrecU::erm</i>	Bacillus Genetic Stock Center
BKE25280	<i>trpC2 ΔrecO::erm</i>	Bacillus Genetic Stock Center
BKE25330	<i>trpC2 ΔpgpH::erm</i>	Bacillus Genetic Stock Center
BKE27620	<i>trpC2 ΔrecJ::erm</i>	Bacillus Genetic Stock Center
BKE28530	<i>trpC2 ΔetfB::erm</i>	Bacillus Genetic Stock Center
BKE29805	<i>trpC2 ΔsftA::erm</i>	Bacillus Genetic Stock Center
BKE32820	<i>trpC2 ΔfadE::erm</i>	Bacillus Genetic Stock Center
BKE33430	<i>trpC2 ΔcysI::erm</i>	Bacillus Genetic Stock Center
BKE33450	<i>trpC2 ΔhclD::erm</i>	Bacillus Genetic Stock Center
BKE37180	<i>trpC2 ΔfadF::erm</i>	Bacillus Genetic Stock Center
BKE39600	<i>trpC2 ΔyxeC::erm</i>	Bacillus Genetic Stock Center
BKE40350	<i>trpC2 ΔrocR::erm</i>	Bacillus Genetic Stock Center

Strain	Genotype	Reference/Construction
BP12	<i>trpC2 ΔgudB::aphA3 rocG::Tn10 spc amyE::(gudB^{CR}_{mut1} lacZ cat)</i>	Gunka <i>et al.</i> , 2012
BP13	<i>trpC2 ΔgudB::aphA3 rocG::Tn10 spc amyE::(gudB^{CR}_{mut3} lacZ cat)</i>	Gunka <i>et al.</i> , 2012
BP20	<i>trpC2 ΔgudB::aphA3 rocG::Tn10 spc amyE::(gudB^{CR}_{mut1} orientation changed lacZ cat)</i>	Gunka, 2010
BP21	<i>trpC2 ΔgudB::aphA3 rocG::Tn10 spc amyE::(gudB^{CR}_{mut3} orientation changed lacZ cat)</i>	Gunka, 2010
BP100	<i>trpC2 amyE::(P_{hly}-lacZ cat)</i>	Ballin, 2012
BP101	<i>trpC2 amyE::(P_{mpl}-lacZ cat)</i>	Ballin, 2012
BP102	<i>trpC2 amyE::(P_{plcA}-lacZ cat)</i>	Ballin, 2012
BP404	<i>trpC2 ΔgudB^{CR}::aphA3 rocG::Tn10 spc amyE::(P^{CR}-gudB⁺ cat)</i>	Thiele, 2013
BP405	<i>trpC2 ΔgudB^{CR}::aphA3 rocG::Tn10 spc amyE::(P⁺-gudB^{CR} cat)</i>	Thiele, 2013
BP424	<i>trpC2 ΔrnhB::aphA3 rocG::Tn10 spc</i>	Thiele, 2013
BP431	<i>trpC2 ΔrnhC::cat rocG::Tn10 spc</i>	Thiele, 2013
BP442	<i>trpC2 ΔgudB^{CR}::aphA3</i>	Thiele, 2013
BP444	<i>trpC2 ΔypeP::tet rocG::Tn10 spc</i>	Thiele, 2013
BV568	<i>HT^R-5 [bcaP(Δ1094-1159)] Δdxs::erm ΔtrpEDFCAB::tet P*_{hom}(T63C) pBV601(pdxJ-Sm) neo amyE::pdxA-Ec spc</i>	Commichau <i>et al.</i> , 2015
GP27	<i>trpC2 ΔgudB::cat amyE::(P_{gltA}-lacZ aphA3)</i>	Commichau <i>et al.</i> , 2007b
GP28	<i>trpC2 gudB^{CR}::cat rocG::Tn10 spc amyE::(P_{gltA}-lacZ aphA3)</i>	Commichau <i>et al.</i> , 2007b
GP342	<i>trpC2 amyE::(P_{gltA}-lacZ aphA3)</i>	Wacker <i>et al.</i> , 2003
GP577	<i>trpC2 ΔyabT::ermC</i>	Pietack, 2010
GP650	<i>trpC2 gltC::Tn10 spc amyE::(P_{gltA}-lacZ aphA3)</i>	Commichau <i>et al.</i> , 2007a
GP651	<i>trpC2 gltC::Tn10 spc amyE::(gltC P_{gltA}-lacZ cat)</i>	Commichau, 2006
GP652	<i>trpC2 gltC::Tn10 spc amyE::(gltC(P88L) P_{gltA}-lacZ cat)</i>	Commichau, 2006
GP653	<i>trpC2 gltC::Tn10 spc amyE::(gltC(I160K) P_{gltA}-lacZ cat)</i>	Commichau, 2006
GP654	<i>trpC2 gltC::Tn10 spc amyE::(gltC(T99A) P_{gltA}-lacZ cat)</i>	Commichau, 2006
GP669	<i>trpC2 amyE::(P_{gltA}-lacZ cat)</i>	Commichau <i>et al.</i> , 2007b
GP682	<i>trpC2 Δicd::ermC ΔodhA::cat amyE::(P_{gltA}-lacZ aphA3)</i>	Commichau, 2006
GP689	<i>trpC2 gltC::Tn10 spc amyE::(P_{gltA(T-32A)}-lacZ aphA3)</i>	Commichau, 2006
GP692	<i>trpC2 gltC::Tn10 spc amyE::(P_{gltA(C-10T)}-lacZ aphA3)</i>	Commichau, 2006
GP726	<i>trpC2 ΔrocG::aphA3</i>	Commichau, 2006
GP738	<i>trpC2 gltC::Tn10 spc</i>	Commichau, 2006
GP747	<i>trpC2 rocG::Tn10 spc</i>	Commichau <i>et al.</i> , 2007b
GP753	<i>trpC2 rocG::Tn10 spc gudB⁺</i>	Commichau, 2006
GP810	<i>trpC2 ΔrocG::tet</i>	Gunka, 2010
GP896	<i>trpC2 rocG::Tn10 spc ΔsbcDC::aphA3</i>	Gerwig, 2011
GP892	<i>trpC2 rocG::Tn10 spc ΔrecU::cat</i>	Gerwig, 2011
GP894	<i>trpC2 ΔsbcDC::aphA3</i>	Gerwig, 2011
GP902	<i>trpC2 Δhag::tet</i>	Diethmaier <i>et al.</i> , 2011
GP987	<i>trpC2 ΔdisA::tet</i>	Diethmaier, 2011
GP1107	<i>trpC2 ΔrocG::cat amyE::(P_{gltA}-lacZ aphA3) addAB::spc</i>	Tholen, 2009

Strain	Genotype	Reference/Construction
GP1109	<i>trpC2 ΔrocG::cat amyE::(P_{gltA}-lacZ aphA3) ycmB::Tn10 spc</i>	Tholen, 2009
GP1110	<i>trpC2 ΔrocG::cat amyE::(P_{gltA}-lacZ aphA3) dppE::Tn10 spc</i>	Tholen, 2009
GP1111	<i>trpC2 ΔrocG::cat amyE::(P_{gltA}-lacZ aphA3) polY1::Tn10 spc</i>	Tholen, 2009
GP1112	<i>trpC2 ΔrocG::cat amyE::(P_{gltA}-lacZ aphA3) yxjF::Tn10 spc</i>	Tholen, 2009
GP1113	<i>trpC2 ΔrocG::cat amyE::(P_{gltA}-lacZ aphA3) ymfA::Tn10 spc</i>	Tholen, 2009
GP1114	<i>trpC2 ΔrocG::cat amyE::(P_{gltA}-lacZ aphA3) hutH::Tn10 spc</i>	Tholen, 2009
GP1115	<i>trpC2 ΔrocG::cat amyE::(P_{gltA}-lacZ aphA3) yusO::Tn10 spc</i>	Tholen, 2009
GP1116	<i>trpC2 ΔrocG::cat amyE::(P_{gltA}-lacZ aphA3) yxiM::Tn10 spc</i>	Tholen, 2009
GP1117	<i>trpC2 ΔrocG::cat amyE::(P_{gltA}-lacZ aphA3) yxkF::Tn10 spc</i>	Tholen, 2009
GP1118	<i>trpC2 ΔrocG::cat amyE::(P_{gltA}-lacZ aphA3) treA::Tn10 spc</i>	Tholen, 2009
GP1119	<i>trpC2 ΔrocG::cat amyE::(P_{gltA}-lacZ aphA3) yeaC::Tn10 spc</i>	Tholen, 2009
GP1120	<i>trpC2 ΔrocG::cat amyE::(P_{gltA}-lacZ aphA3) tepA::Tn10 spc</i>	Tholen, 2009
GP1121	<i>trpC2 ΔrocG::cat amyE::(P_{gltA}-lacZ aphA3) deaD::tet</i>	Tholen, 2009
GP1151	<i>trpC2 ΔxylAB::aphA3</i>	Mehne, 2013
GP1157	<i>trpC2 ΔrocG::cat</i>	Gunka, 2010
GP1160	<i>trpC2 ΔgudB^{CR}::aphA3 (P_{gudB} not deleted)</i>	Gunka, 2010
GP1161	<i>trpC2 ΔgudB::aphA3 rocG::Tn10 spc</i>	Gunka, 2010
GP1167	<i>trpC2 Δmfd::ermC</i>	Gunka, 2010
GP1169	<i>trpC2 rocG::Tn10 spc Δmfd::ermC</i>	Gunka, 2010
GP1179	<i>trpC2 ΔgudB::aphA3 rocG::Tn10 spc amyE::(gudB^{CR}_{mut1} lacZ cat)</i>	Gunka, 2010
GP1197	<i>trpC2 ΔgudB::aphA3 rocG::Tn10 spc amyE::(gudB^{CR}_{mut3} lacZ cat)</i>	Gunka, 2010
GP1198	<i>trpC2 ΔgudB::aphA3 rocG::Tn10 spc amyE::(gudB⁺_{mut3} lacZ cat)</i>	Gunka, 2010
GP1302	<i>trpC2 ΔxylR::aphA3</i>	Mehne, 2013
GP1501	<i>trpC2 rocG::Tn10 spc nfo::aphA3</i>	Gerwig, 2011
GP1904	<i>trpC2 ΔgltC::aphA3</i>	Dormeyer <i>et al.</i> , 2017
GP2033	<i>trpC2 ΔpgpH::tet</i>	Jan Gundlach, Promotion
GP2040	<i>trpC2 ΔpgpH::erm</i>	Gundlach <i>et al.</i> , 2015
JK27	<i>pSacA-zeo-Cre</i>	Kumpfmüller <i>et al.</i> , 2013

6.4.3. *E. coli* strains used in this work

Strain	Genotype	Reference
DH5α	<i>recA1 endA1 gyrA96 thi hsdR17rk- mK+relA1 supE44 Φ80ΔlacZΔM15 Δ(lacZYA-argF)U169</i>	Sambrook <i>et al.</i> , 1989

XL1 blue	<i>recA1 endA1 gyrA96 thi-1 hsdR17 supE44 relA1 lac</i> [F' <i>proAB lacIq</i> Δ M15 Tn10 (Tetr)]	Stratagene, Woodcock <i>et al.</i> , 1989
BL21	<i>B(834)-derivate F- lon ompT hsdS(rB mB) gal</i> <i>dcm[DE3]</i>	Novagen, Sambrook <i>et al.</i> , 1989
BTH101	F' <i>cya-99' araD139, galE15 galK16, rpsL1 (str^R) hsdR2</i> <i>mcrA1 mcrB1</i>	EUROMEDEX, Karimova <i>et al.</i> , 1998

6.5. Plasmids

6.5.1. Plasmids constructed in this work

Plasmid	Vector	Reference/Construction
pBP168	pBP106 [<i>PstI/EcoRI</i>]	<i>P_{CR} gudB⁺</i> [<i>MfeI/PstI</i>] with LS32/LS33 (Dormeyer <i>et al.</i> , 2014)
pBP169	pBP168 [<i>XbaI/EcoRI</i>]	<i>gfp_{mono}</i> [<i>XbaI/EcoRI</i>] with LS34/LS35 (Dormeyer <i>et al.</i> , 2014)
pBP173	pBP169 [<i>PstI</i>]	Terminator fragment (Hybridization FC299/FC300) [<i>PstI</i>]
pBP402	pBP107 [<i>PstI/EcoRI</i>]	Fusion PCR <i>P_{degQ36}</i> -Promoter [<i>PstI/PvuII</i>] with LS52/FC306 and <i>prfA^{CR}</i> [<i>PvuII/MfeI</i>] with FC305/FC196
pBP404	pBP107 [<i>PstI/EcoRI</i>]	Fusion PCR <i>P_{gudB}</i> -Promoter [<i>PstI/PvuII</i>] with MD1/MD3 and <i>prfA^{CR}</i> [<i>PstI/MfeI</i>] with MD2/FC196
pBP405	pAC5 [<i>EcoRI/BamHI</i>]	<i>gfp-gudB</i> [<i>MfeI/BglII</i>] with MD4/LS11 (result 1,5 <i>gfp</i> , 0,5 <i>gfp</i> cut via <i>EcoRI</i> and religation)
pBP406	pBP405 [<i>BamHI/EcoRI</i>]	<i>P_{plcA}</i> [<i>BamHI/EcoRI</i>] with MD5/FC191
pBP407	pGP2514 [<i>KpnI/XhoI</i>]	<i>P_{gudB-prfA^{CR}}</i> [<i>KpnI/XhoI</i>] with MD8/MD9
pBP408	pGP2514 [<i>EcoRI/SalI</i>]	<i>P_{plcA}</i> [<i>MfeI/SalI</i>] with MD49/MD50 (<i>MfeI</i> cuts within <i>P_{plcA}</i> , but it's not problematical)
pBP409	pGP2514 [<i>EcoRI/SalI</i>]	<i>P_{gltAB}</i> [<i>MfeI/SalI</i>] with MD47/MD48
pBP410	pBP409 [<i>EcoRI/SalI</i>]	<i>mCherry</i> [<i>EcoRI/SalI</i>] with MD51/MD52
pBP411	pBP408 [<i>EcoRI/SalI</i>]	<i>icd</i> [<i>EcoRI/SalI</i>] with MD53/MD54
pBP412	pAC5 [<i>EcoRI/BamHI</i>]	<i>P_{mut1}^{CR} gudB⁺</i> [<i>EcoRI/BamHI</i>] with MD75/KG92
pBP413	pAC5 [<i>EcoRI/BamHI</i>]	<i>P_{mut3}^{CR} gudB⁺</i> [<i>EcoRI/BamHI</i>] with MD76/KG92
pBP414	pAC5 [<i>EcoRI/BamHI</i>]	<i>P_{mut1}^{CR} gudB⁺</i> orientation changed [<i>EcoRI/BamHI</i>] with MD78/KG184
pBP415	pAC5 [<i>EcoRI/BamHI</i>]	<i>P_{mut3}^{CR} gudB⁺</i> orientation changed [<i>EcoRI/BamHI</i>] with MD77/KG184
pBP416	pBP102 [<i>EcoRI</i>]	<i>P_{plcA}gudB⁺gfp</i> [<i>EcoRI</i>] with MD86/FC191 (same orientation as <i>P_{plcA-lacZ}</i>)
pBP417	pBP43 [<i>PstI/BamHI</i>]	<i>spB</i> [<i>PstI/BamHI</i>] with MD137/MD138
pBP418	pBQ200 [<i>HindIII/BamHI</i>]	<i>gltR</i> [<i>HindIII/BamHI</i>] with MD141/MD142
pBP419	pBQ200 [<i>HindIII/BamHI</i>]	<i>gltR24</i> [<i>HindIII/BamHI</i>] with MD141/MD142
pBP420	pGP382 [<i>HindIII/BamHI</i>]	<i>gltR24</i> [<i>HindIII/BamHI</i>] with MD141/MD143
pBP421	pGP382 [<i>HindIII/BamHI</i>]	<i>gltR</i> [<i>HindIII/BamHI</i>] with MD141/MD143
pBP422	pGP885 [<i>SalI/BamHI</i>]	<i>P_{plcA-lacZ}</i> [<i>SalI/BglII</i>] with MD139/MD140
pBP423	pUT18 [<i>XbaI/KpnI</i>]	<i>recJ</i> [<i>XbaI/KpnI</i>] with MD154/MD155
pBP424	pUT18C [<i>XbaI/KpnI</i>]	<i>recJ</i> [<i>XbaI/KpnI</i>] with MD154/MD155
pBP425	pKT25 [<i>XbaI/KpnI</i>]	<i>recJ</i> [<i>XbaI/KpnI</i>] with MD154/MD155
pBP426	p25-N [<i>XbaI/KpnI</i>]	<i>recJ</i> [<i>XbaI/KpnI</i>] with MD154/MD155
pBP427	pUT18 [<i>XbaI/KpnI</i>]	<i>recO</i> [<i>XbaI/KpnI</i>] with MD156/MD157
pBP428	pUT18C [<i>XbaI/KpnI</i>]	<i>recO</i> [<i>XbaI/KpnI</i>] with MD156/MD157
pBP429	pKT25 [<i>XbaI/KpnI</i>]	<i>recO</i> [<i>XbaI/KpnI</i>] with MD156/MD157
pBP430	p25-N [<i>XbaI/KpnI</i>]	<i>recO</i> [<i>XbaI/KpnI</i>] with MD156/MD157
pBP431	pUT18 [<i>XbaI/KpnI</i>]	<i>recR</i> [<i>XbaI/KpnI</i>] with MD158/MD159
pBP432	pUT18C [<i>XbaI/KpnI</i>]	<i>recR</i> [<i>XbaI/KpnI</i>] with MD158/MD159

Plasmid	Vector	Reference/Construction
pBP433	pKT25 [<i>Xba</i> I/ <i>Kpn</i> I]	<i>recR</i> [<i>Xba</i> I/ <i>Kpn</i> I] with MD158/MD159
pBP434	p25-N [<i>Xba</i> I/ <i>Kpn</i> I]	<i>recR</i> [<i>Xba</i> I/ <i>Kpn</i> I] with MD158/MD159
pBP443	pUT18 [<i>Xba</i> I/ <i>Kpn</i> I]	<i>nfo</i> [<i>Xba</i> I/ <i>Kpn</i> I] with MD158/MD159
pBP444	pUT18C [<i>Xba</i> I/ <i>Kpn</i> I]	<i>nfo</i> [<i>Xba</i> I/ <i>Kpn</i> I] with MD158/MD159
pBP445	pKT25 [<i>Xba</i> I/ <i>Kpn</i> I]	<i>nfo</i> [<i>Xba</i> I/ <i>Kpn</i> I] with MD158/MD159
pBP446	p25-N [<i>Xba</i> I/ <i>Kpn</i> I]	<i>nfo</i> [<i>Xba</i> I/ <i>Kpn</i> I] with MD158/MD159
pBP447	pUT18 [<i>Xba</i> I/ <i>Kpn</i> I]	<i>recU</i> [<i>Xba</i> I/ <i>Kpn</i> I] with MD158/MD159
pBP448	pUT18C [<i>Xba</i> I/ <i>Kpn</i> I]	<i>recU</i> [<i>Xba</i> I/ <i>Kpn</i> I] with MD158/MD159
pBP449	pKT25 [<i>Xba</i> I/ <i>Kpn</i> I]	<i>recU</i> [<i>Xba</i> I/ <i>Kpn</i> I] with MD158/MD159
pBP450	p25-N [<i>Xba</i> I/ <i>Kpn</i> I]	<i>recU</i> [<i>Xba</i> I/ <i>Kpn</i> I] with MD158/MD159
pBP451	pUT18 [<i>Xba</i> I/ <i>Kpn</i> I]	<i>ypbH</i> [<i>Xba</i> I/ <i>Kpn</i> I] with MD180/MD181
pBP452	pUT18C [<i>Xba</i> I/ <i>Kpn</i> I]	<i>ypbH</i> [<i>Xba</i> I/ <i>Kpn</i> I] with MD180/MD181
pBP453	pKT25 [<i>Xba</i> I/ <i>Kpn</i> I]	<i>ypbH</i> [<i>Xba</i> I/ <i>Kpn</i> I] with MD180/MD181
pBP454	p25-N [<i>Xba</i> I/ <i>Kpn</i> I]	<i>ypbH</i> [<i>Xba</i> I/ <i>Kpn</i> I] with MD180/MD181
pBP463	pUT18 [<i>Xba</i> I/ <i>Kpn</i> I]	<i>rnhC</i> [<i>Xba</i> I/ <i>Kpn</i> I] with MD180/MD181
pBP464	pUT18C [<i>Xba</i> I/ <i>Kpn</i> I]	<i>rnhC</i> [<i>Xba</i> I/ <i>Kpn</i> I] with MD180/MD181
pBP465	pKT25 [<i>Xba</i> I/ <i>Kpn</i> I]	<i>rnhC</i> [<i>Xba</i> I/ <i>Kpn</i> I] with MD180/MD181
pBP466	p25-N [<i>Xba</i> I/ <i>Kpn</i> I]	<i>rnhC</i> [<i>Xba</i> I/ <i>Kpn</i> I] with MD180/MD181
pBP467	pBP406 [<i>Bam</i> HI]	<i>pdxST</i> with nat. SD and Strep [<i>Bam</i> HI] with MD221/MD222 (from pBP172)
pBP468	pAC5 [<i>Eco</i> RI/ <i>Bam</i> HI]	<i>P_{gltA(C-14G)}</i> [<i>Bam</i> HI/ <i>Eco</i> RI] with IW1/IW2/MD220 CCR (Dormeyer <i>et al.</i> , 2017)
pBP469	pAC5 [<i>Eco</i> RI/ <i>Bam</i> HI]	<i>P_{plcA}</i> [<i>Eco</i> RI/ <i>Bam</i> HI] with FC192/MD225
pBP470	pBP469 [<i>Not</i> I/ <i>Xba</i> I]	<i>P_{plcA}-pdxST-strep-gfp-gudB⁺</i> [<i>Not</i> I/ <i>Xba</i> I] with MD223/MD224
pBP471	pET SUMOadapt [<i>Bsa</i> I/ <i>Xho</i> I]	<i>gltC</i> [<i>Bsa</i> I/ <i>Xho</i> I] with MD232/MD233
pBP472	pET SUMOadapt [<i>Bsa</i> I/ <i>Xho</i> I]	<i>rocG</i> [<i>Bsa</i> I/ <i>Xho</i> I] with MD234/MD235
pBP473	pBP107 [<i>Pst</i> I/ <i>Eco</i> RI]	<i>P_{gudB-prfA}</i> [<i>Pst</i> I/ <i>Eco</i> RI] with MD3/FC196
pBP474	pBP107 [<i>Pst</i> I/ <i>Eco</i> RI]	<i>P_{gudB-prfA}</i> (C530A) [<i>Pst</i> I/ <i>Mfe</i> I] with MD3/FC196/MD236 MMR
pBP475	pBP107 [<i>Pst</i> I/ <i>Eco</i> RI]	<i>P_{gudB-prfA}</i> (del C530) [<i>Pst</i> I/ <i>Mfe</i> I] with MD3/FC196/MD237 MMR
pBP476	pBP107 [<i>Pst</i> I/ <i>Eco</i> RI]	<i>P_{gudB-prfA}</i> (ins A527) [<i>Pst</i> I/ <i>Mfe</i> I] with MD3/FC196/MD238 MMR
pBP477	pBQ200 [<i>Bam</i> HI/ <i>Eco</i> RI]	<i>P_{gltA-gltA}</i> [<i>Bam</i> HI/ <i>Eco</i> RI] with MD239/MD240
pBP478	pBQ200 [<i>Bam</i> HI/ <i>Eco</i> RI]	<i>P_{gltA(C-14G)-gltA}</i> [<i>Bam</i> HI/ <i>Eco</i> RI] with MD239/MD240
pBP479	pAC5 [<i>Eco</i> RI/ <i>Bam</i> HI]	<i>P_{gltA(T-28A)}</i> [<i>Eco</i> RI/ <i>Bam</i> HI] with IW1/IW2/MD241 CCR
pBP480	pAC5 [<i>Eco</i> RI/ <i>Bam</i> HI]	<i>P_{gltA(T-48C)}</i> [<i>Eco</i> RI/ <i>Bam</i> HI] with IW1/IW2/MD242 CCR
pBP481	pET SUMOadapt [<i>Bsa</i> I/ <i>Xho</i> I]	<i>gudB⁺</i> [<i>Bsa</i> I/ <i>Xho</i> I] with MD244/MD245
pBP482	pBQ200 [<i>Bam</i> HI/ <i>Pst</i> I]	<i>gudB⁺</i> [<i>Bam</i> HI/ <i>Pst</i> I] with MD246/MD247
pBP483	pBP107 [<i>Eco</i> RI/ <i>Pst</i> I]	<i>P_{gudB-prfA}</i> (ins (2xA)527) [<i>Pst</i> I/ <i>Pvu</i> II] with MD3/FC196/MD248
pBP484	pBP107 [<i>Eco</i> RI/ <i>Pst</i> I]	<i>P_{gudB-prfA}</i> (ins (3xA)527) [<i>Pst</i> I/ <i>Pvu</i> II] with MD3/FC196/MD249
pBP485	pBP107 [<i>Eco</i> RI/ <i>Pst</i> I]	<i>P_{gudB-prfA}</i> (ins (4xA)527) [<i>Pst</i> I/ <i>Pvu</i> II] with MD3/FC196/MD250
pBP486	pBP107 [<i>Eco</i> RI/ <i>Pst</i> I]	<i>P_{gudB-prfA}</i> (ins (5xA)527) [<i>Pst</i> I/ <i>Pvu</i> II] with MD3/FC196/MD251
pBP487	pBP107 [<i>Eco</i> RI/ <i>Pst</i> I]	<i>P_{gudB-prfA}</i> (ins (10xA)527) [<i>Pst</i> I/ <i>Pvu</i> II] with MD3/FC196/MD252
pBP488	pBP107 [<i>Eco</i> RI/ <i>Pst</i> I]	<i>P_{gudB-prfA}</i> (ins (15xA)527) [<i>Pst</i> I/ <i>Pvu</i> II] with MD3/FC196/MD253
pBP491	pAC5 [<i>Eco</i> RI/ <i>Bam</i> HI]	<i>P_{gltA(Shuffle I BOX III)}</i> [<i>Eco</i> RI/ <i>Bam</i> HI] fusion PCR with IW1/MD257, IW2/MD256
pBP492	pAC5 [<i>Eco</i> RI/ <i>Bam</i> HI]	<i>P_{gltA(Shuffle II BOX III)}</i> [<i>Eco</i> RI/ <i>Bam</i> HI] fusion PCR with IW1/MD259, IW2/MD258
pBP493	pAC5 [<i>Eco</i> RI/ <i>Bam</i> HI]	<i>P_{gltA(Shuffle III BOX III)}</i> [<i>Eco</i> RI/ <i>Bam</i> HI] fusion PCR with IW1/MD261, IW2/MD260

6.5.2. Plasmids used in this work

Plasmid	Function	Reference
p25-N	BACTH, fusion of T25 domain of <i>B. pertussis</i> adenylate cyclase to C-terminus of the protein of interest	Claessen <i>et al.</i> , 2008
pAC5	Translational promoter- <i>lacZ</i> fusions	Martin-Verstraete <i>et al.</i> , 1992
pAC6	Transcriptional promoter- <i>lacZ</i> fusions	Stülke <i>et al.</i> , 1997
pBP4	pAC5:: <i>gudB^{CR}</i> (inverted) with KG184/KG185 [<i>EcoRI/BamHI</i>]	Rachel Care, AG Commichau
pBP103	pBQ200:: <i>prfA</i>	Ballin, 2012
pBP105	Integration plasmid <i>lacA</i> :: <i>P_{xyI}-prfA</i>	Ballin, 2012
pBP106	Integration plasmid <i>lacA</i> with <i>aphA3</i>	Ballin, 2012
pBP107	Integration plasmid <i>lacA</i> with <i>ermC</i>	Ballin, 2012
pBP166	pAC5:: <i>P_{alf2}-gudB^{CR}</i>	Stannek, 2015
pBP167	pAC5:: <i>P_{alf4}-gudB^{CR}</i>	Stannek, 2015
pBP301	pAC6:: <i>P_{alf1}-gudB^{CR}</i>	Thiele, 2013
pBP303	pAC6:: <i>P⁻-gudB^{CR}</i> (no promoter)	Thiele, 2013
pBP599	Overexpression of <i>disA-strep</i>	Anika Klewing, AG Commichau
pBQ200	Overexpression of proteins under the <i>P_{degQ36}</i> promoter	Martin-Verstraete <i>et al.</i> , 1994
pDG1513	Template for <i>tet</i> resistance cassette	Guérout-Fleury <i>et al.</i> , 1995
pDG646	Template for <i>ermC</i> resistance cassette	Guérout-Fleury <i>et al.</i> , 1995
pDG780	Template for <i>aphA3</i> resistance cassette	Guérout-Fleury <i>et al.</i> , 1995
pET SUMOadapt	Overexpression of N-terminally SUMO-His ₆ -tagged proteins, the tac can be completely removed with SUMO protease	Mossessova and Lima, 2000
pGEM-cat	Template for <i>cat</i> resistance cassette	Guérout-Fleury <i>et al.</i> , 1995
pGP382	Overexpression of C-terminally Strep-tagged proteins	Herzberg <i>et al.</i> , 2007
pGP529	pBQ200:: <i>rocG</i>	Commichau <i>et al.</i> , 2008
pGP885	Vector encoding a promoter for xylose inducible expression and the respective <i>xyIR</i> repressor gene	Mehne <i>et al.</i> , 2013
pGP900	pAC5:: <i>gudB</i>	Gunka <i>et al.</i> , 2012
pGP907	pBQ200:: <i>gltC</i>	Commichau <i>et al.</i> , 2007a
pGP908	pAC5:: <i>gltC</i>	Commichau <i>et al.</i> , 2007a
pGP934	pBQ200:: <i>gdhA</i>	Commichau <i>et al.</i> , 2008
pGP953	pAC5:: <i>gltC</i> (P88L)	Commichau, 2006
pGP954	pAC5:: <i>gltC</i> (I160K)	Commichau, 2006
pGP955	pAC5:: <i>gltC</i> (T99A)	Commichau, 2006
pKT25	BACTH, fusion of T25 domain of <i>B. pertussis</i> adenylate cyclase to N-terminus of the protein of interest	Karimova <i>et al.</i> , 1998
pUC19	Primer extension	Yanisch-Perron <i>et al.</i> , 1985
pUT18	BACTH, fusion of T18 domain of <i>B. pertussis</i> adenylate cyclase to C-terminus of the protein of interest	Karimova <i>et al.</i> , 1998
pUT18C	BACTH, fusion of T18 domain of <i>B. pertussis</i> adenylate cyclase to N-terminus of the protein of interest	Karimova <i>et al.</i> , 1998

6.6. Bioinformatic software

Program	Provider	Application
AxioVision	Zeiss	Image acquisition and processing
ChemoStar Imager	Intas	Image acquisition and processing
FIJI	Schindelin <i>et al.</i> , 2012	Image processing
Gen5™ Data analysis software	BioTek®	Reader control and data analysis
Geneious 10.1.2	Biomatters	DNA analysis
ImageLab™ Software	BioRad	Image acquisition and processing of gel and blot images
Mendeley Desktop	PDFTron™ Systems Inc.	PDF Manager (References)
Microsoft Office 365	Microsoft Inc.	Data processing, writing
R Studio	RStudio Team, 2016	Statistical analysis
SubtiWiki 2.0	Michna <i>et al.</i> , 2016	<i>Bacillus subtilis</i> database
Zen	Zeiss	Image processing

7. Curriculum vitae



7.1.1.1. Personal information

Name	Miriam Dormeyer
Date of birth	13 th of October 1989 (Hildesheim, Germany)
Nationality	German
Contact	Mahlumer Straße 33 31167 Bockenem
Mail	miriam.dormeyer@outlook.com

7.1.1.2. Education

2014-2017	<p>Doctorate Georg-August-Universität Göttingen Göttingen Graduate School for Neurosciences, Biophysics, and Molecular Biosciences (GGNB) within the Georg-August School of Science (GAUSS) Dissertation Dept. of General Microbiology, PD Dr. Fabian M. Commichau Maintenance of glutamate homeostasis in <i>Bacillus subtilis</i> by complex regulatory systems and genomic adaptation</p>
2012-2014	<p>Master of Science Microbiology & Biochemistry Georg-August-Universität Göttingen Master Thesis Dept. of General Microbiology, PD Dr. Fabian M. Commichau Applications of reporter systems that are based on direct repeat instability in <i>Bacillus subtilis</i></p>
2009-2012	<p>Bachelor of Science Biology Area of specialization: Molecular life sciences Bachelor Thesis Dept. of Plant Molecular Biology and Physiology, Prof. Dr. Christiane Gatz Analysis of <i>Verticillium longisporum</i>-infected <i>Arabidopsis thaliana</i> mutants</p>
2002-2009	<p>Jacobson Gymnasium Seesen</p>